TWDB CONTRACT NO. 1800012226
FINAL REPORT
RECEIVED JANUARY 18, 2022

Evaluation of Adopted Flow Standards for the Trinity River, Phase 3

"PURSUANT TO HOUSE BILL 1 AS APPROVED BY THE 85TH TEXAS LEGISLATURE, THIS STUDY REPORT WAS FUNDED FOR THE PURPOSE OF STUDYING ENVIRONMENTAL FLOW NEEDS FOR TEXAS RIVERS AND ESTUARIES AS PART OF THE ADAPTIVE MANAGEMENT PHASE OF THE SENATE BILL 3 PROCESS FOR ENVIRONMENTAL FLOWS ESTABLISHED BY THE 80TH TEXAS LEGISLATURE. THE VIEWS AND CONCLUSIONS EXPRESSED HEREIN ARE THOSE OF THE AUTHOR(S) AND DO NOT NECESSARILY REFLECT THE VIEWS OF THE TEXAS WATER DEVELOPMENT BOARD."

Contract No. 1800012226
FINAL REPORT – January 18, 2022

This page intentionally left blank

Evaluation of Adopted Flow Standards for the Trinity River, Phase 3

By
Webster Mangham
Kelly McKnight
Trinity River Authority of Texas

Tim Osting, P.E.
Paul Southard, P.G.
Aqua Strategies, Inc.

David Flores
Arroyo Environmental Consultants, Inc.

Acknowledgements
This work could not have been completed without the hard work, blood, sweat, drive shafts and grit given up by TRA's dedicated field staff, Kelly McKnight and Addison Stucky, who persevere so we can all get to know the Trinity River a little better.

Also, thank you to Dr. Peter Allen for advice, training, and the use of the Baylor sediment laboratory.

Table of Contents

Table of Figures

List of Tables

Table of Appendices

1 Background and Methodology

1.1 Background

In 2007, the 80th Texas Legislature passed Senate Bill 3 (SB3) which created a stakeholder driven process designed to establish environmental flow standards for all of the major river basins in Texas. For the Trinity River, the Trinity and San Jacinto and Galveston Bay Basin and Bay Area Stakeholder Committee (BBASC) and Expert Science Team (BBEST) were created and tasked with recommending environmental flow standards to the Texas Commission on Environmental Quality (TCEQ). On April 20, 2011, the TCEQ adopted flow standards for the Trinity River at the four measurement points (30 TAC § 298.225, 2011) shown below in Table 1-1 and in Figure 1-1. These locations were selected to coincide with Untied States Geological Survey (USGS) stream gages.

Table 1-1. Trinity River Senate Bill 3 Measurement Points and the accompanying study site location as described by the Trinity River basin number (08) and river mile.

Measurement Point USGS Gage Number	Measurement Point USGS Gage Name	Representative Site (Basin Number and River Mile)
08049500	West Fork Trinity River near Grand Prairie	080486
08057000	Trinity River at Dallas	080444
08065000	Trinity River at Oakwood	080295
08066500	Trinity River at Romayor	080075

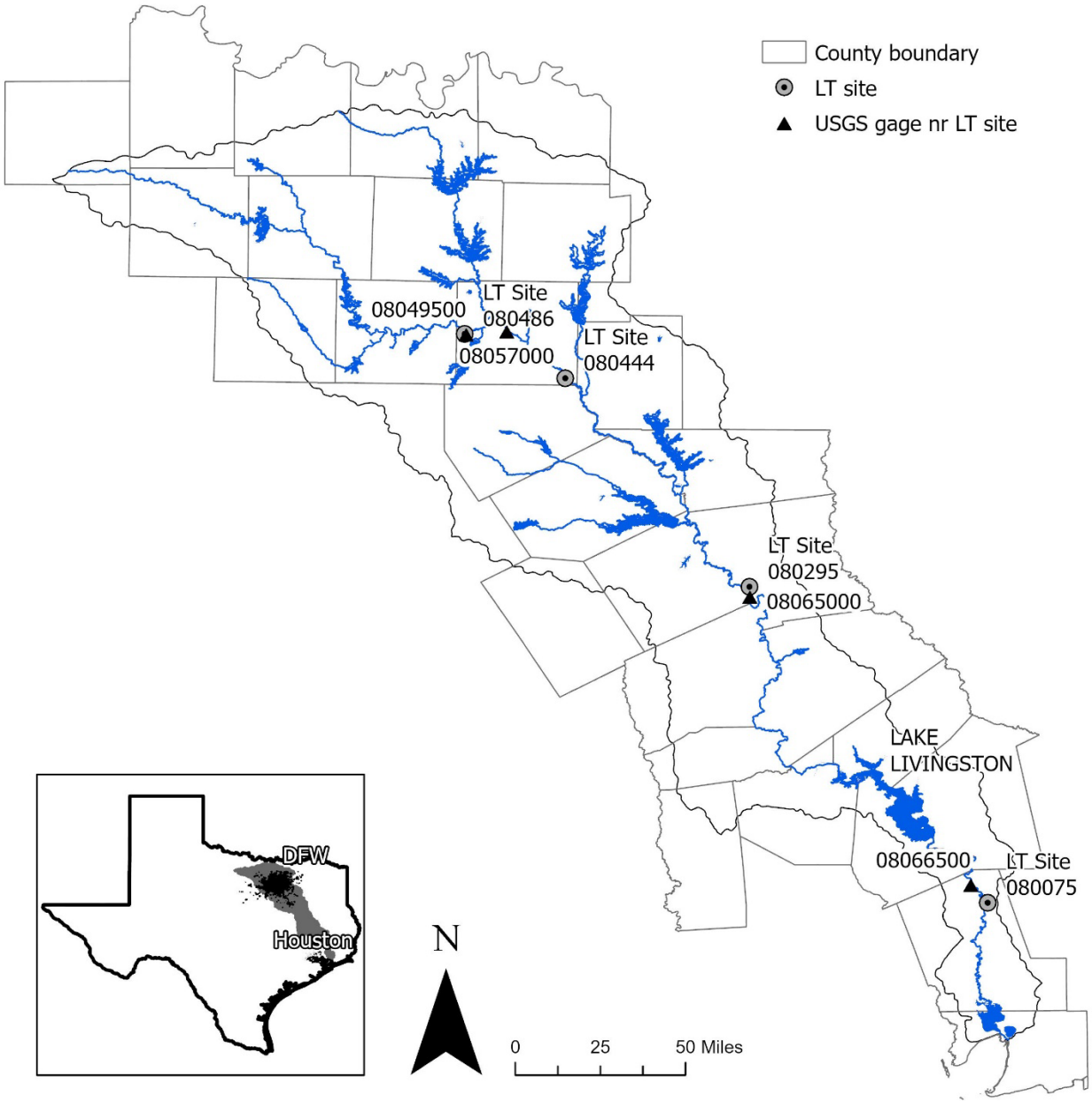

Figure 1-1. Map of the Trinity River basin, long-term monitoring sites, and USGS gages.

During the SB3 process, instream habitat, hydraulics, geomorphology, and ecological data gaps were identified. In response, the BBASC and the BBEST created a Work Plan Report that outlined the additional data needs for the adaptive management provisions of the SB3 legislation (TSJ, 2012). The adaptive management phase is designed to provide for a periodic review of the standards at a maximum interval of every ten years. This is the third phase of a project designed to provide data and tools to the BBASC and BBEST to use during this process. It is important to reiterate that this project is designed to provide information and data, *not* to recommend flows or "validate" existing flows. This phase of the project provides information on the following topics:

1. Channel adjustment: Resurveyed cross-sections at all four measurement points;
2. Water quality: Results for both grab samples and diurnal sonde deployments;
3. Geotechnical: Grain size and erodibility;
4. Riparian trees: Tree growth analysis;
5. Water quality modeling: Dissolved oxygen and temperature; and
6. Sediment transport modeling: Sediment transport and Bank Stability and Toe Erosion Modeling (BSTEM) at sites 080295 and 080075.

1.2 Previous Work

Based on the SB3 environmental flow designated measurement points, TRA selected four long-term representative study sites. Each site is between 1 and 2 river miles and was selected to best represent that reach and SB3 measurement point. While it is beyond the scope of this report to review the previous studies associate with this report, it is important to note that this project is built on the knowledge and results gained during three previous studies:

1. [TRA & RPS] Trinity River Authority of Texas & RPS Espey. 2013. Trinity River Reconnaissance Survey, 2011. Arlington, Texas.
2. Mangham, W., Osting, T.D., and Flores, D.F. 2015. LiDAR Acquisition and Flow Assessment for the Middle Trinity River. Arlington, Texas.
3. Mangham, W., Osting, T.D., and Flores, D.F. 2017. Evaluation of Adopted Flow Standards for the Trinity River, Phase 2. Arlington, Texas.

2 Methods and Results

Many of the methods used for this project have been developed and described in detail in previous reports (Section 1.2). Only methods that were modified from previous phases of this project are described in detail in this report. Multiple field events were completed during this project (Table 2-1) and are detailed below.

Table 2-1. Table describing field data collection events and the date completed.

Site Name(s)	Data Type	Dates
5 Trinity River Mainstem TCEQ Sites	Water Quality Grab	June - September 2018
10919-Trinity River at US Hwy 79		6/29/2018, 8/8/2018, 9/17/2018
10920-Trinity River at US 287		6/29/2018, 8/8/2018, 9/17/2018
16998-Trinty River at FM 3278		7/18/2018, 8/13/2018, 9/25/2018
10896-Trinity River US of FM 787		7/19/2018, 8/13/2018, 9/25/2018
10895-Trinity River at SH 105		7/19/2018, 8/13/2018, 9/25/2018
080846	Long-term XS Resurvey	1/31/2019

080444	Long-term XS Resurvey	2/5/2019
080295	Long-term XS Resurvey	1/6/2020
	Benchmark Survey	2/1/2018
	Sediment Collection	6/28/2018
	WQ Sonde Deployment	6/26/2018 - 07/12/20018
	Pressure Transducer Deployment	6/26/2018 - 07/12/20018
	Riparian Data Collection	2/1/2018
080075	Sediment Collection	7/11/2018
	WQ Sonde Deployment	7/11/2018 - 7/27/2018
	Pressure Transducer Deployment	7/11/2018 - 7/27/2018
	Long-term XS Resurvey	12/03/2020-12/04/2020

2.1 Water Quality

Empirical water quality data provides important calibration data for modeling. Not only do these results provide the variables for the analysis, the results also can help to set the boundaries of the parameters that are adjusted during the calibration process. For this effort, two calibrated multiparameter datasondes were deployed to help capture the daily variability of temperature and dissolved oxygen at one site above (080295) and one site below (080075) Lake Livingston (Figure 2-1). Additionally, grab samples were taken at two sites above Lake Livingston and three sites below Lake Livingston (Figure 2-1) to provide calibration data for the model.

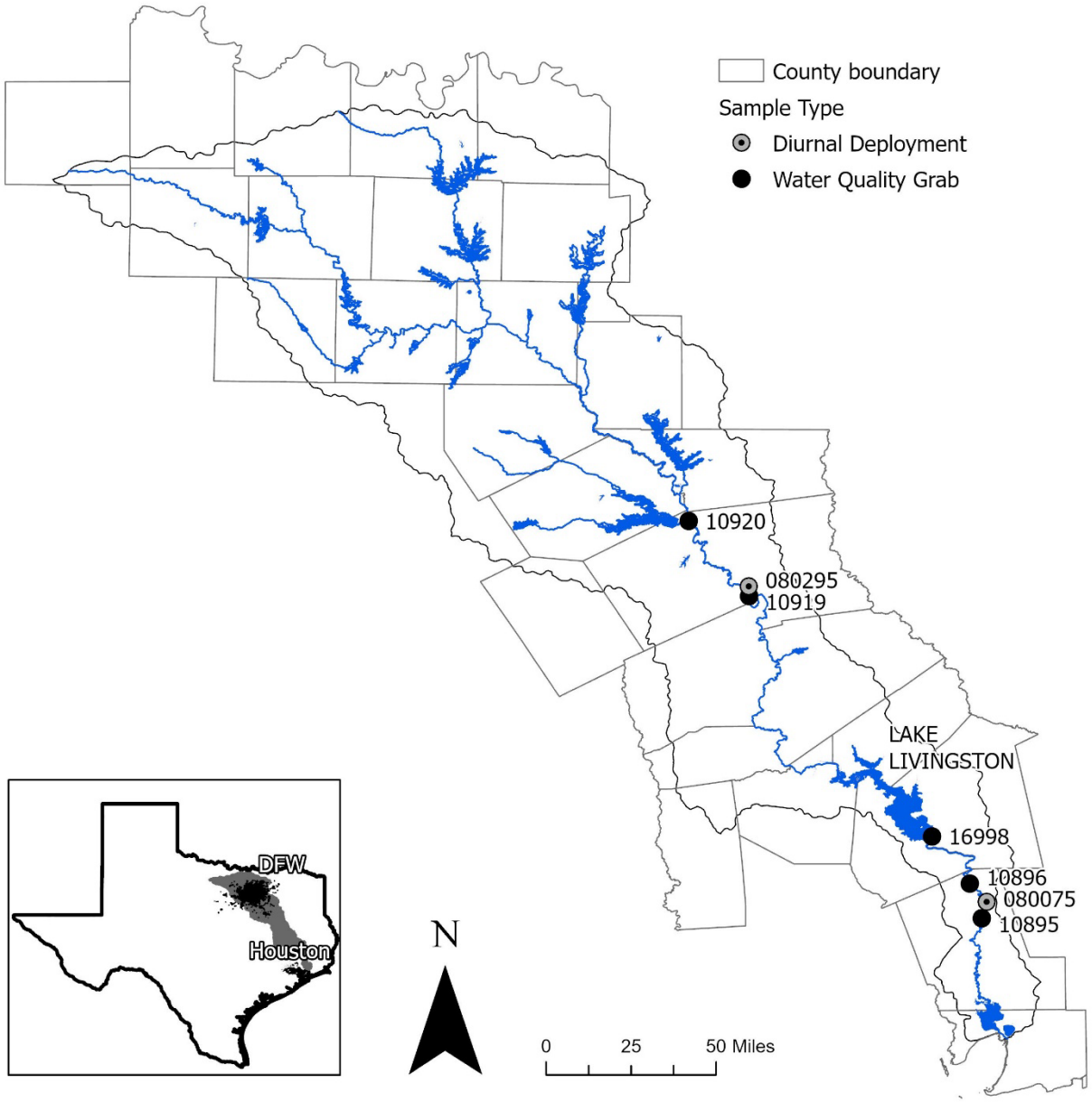

Figure 2-1. Map showing water quality sample locations. Note: The solid black dots represent TCEQ surface water quality monitoring site numbers and the grey dots represent the study sites and begin with a "080" designation.

2.1.1 Water Quality Diurnal Sonde Deployments

The sondes deployed above (080295) and below (080075) Lake Livingston were deployed during the TCEQ designated critical period for fifteen and twenty-one days, respectively (Figure 2-2). Ideally, each sonde would have been deployed for thirty days, but weather forecasts required that the sondes be removed sooner than planned due to the risk of losing the equipment

during potential high flows. During both deployments, the flows remained relatively unchanged (except for a minor pulse at the 080075 site); average daily flows during the deployment periods for 080295 and 080075 were 767 cfs and 901 cfs, respectively.

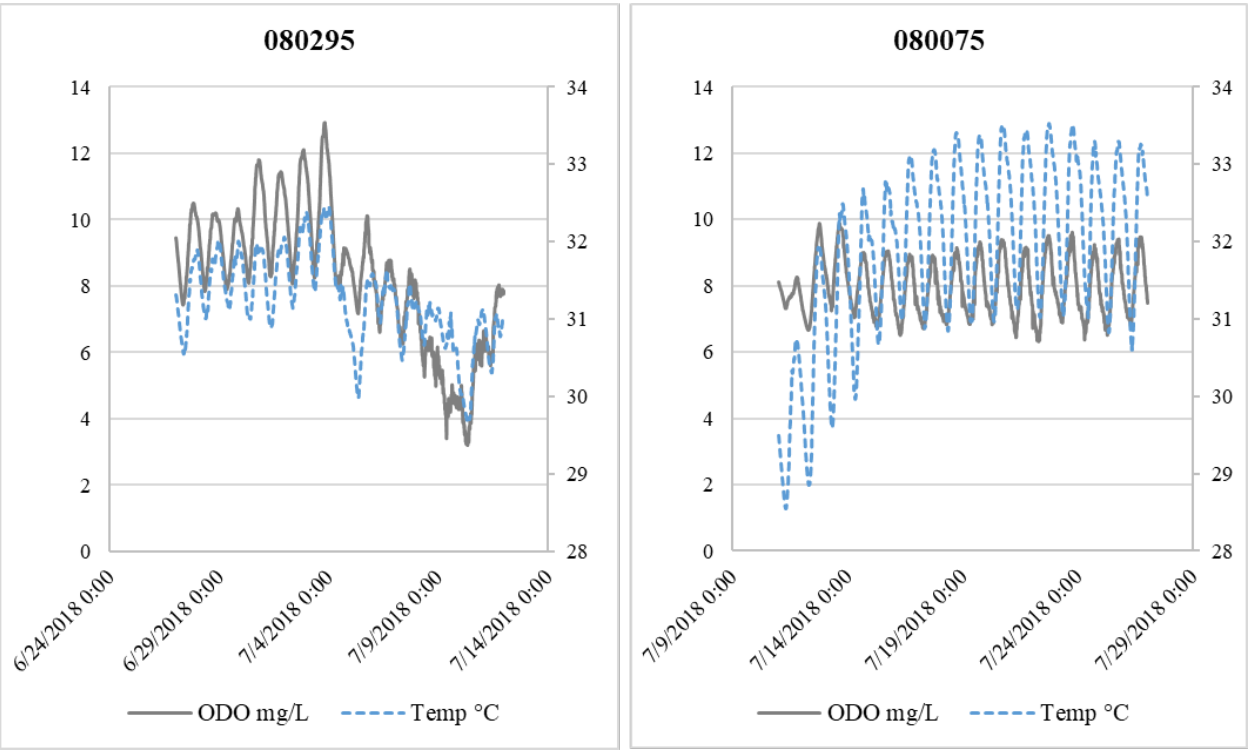

Figure 2-2. Graphs showing sonde deployment data for dissolved oxygen and water temperature at sites 080295 and 080075. Note: Optical Dissolved Oxygen (ODO) is in mg/L and Temperature is degrees Celsius.

2.1.2 Water Quality Grab Samples

Grab samples were collected between June and September 2018 at five sites (Figure 2-1). Thirty parameters were collected at each site and no results exceeded any TCEQ designated water quality criteria. However, several samples for nitrate, total phosphorus, and chlorophyll-a exceeded the TCEQ designated screening level. These results were used to calibrate a HEC-RAS water quality model discussed later in this report. All water quality grab results are shown in Appendix 1. Water Quality Grab Sample Results.

2.2 Topographic and Bathymetric Surveying

Each of the four long-term monitoring sites were resurveyed to better understand how the channel changes between surveys. River channels are naturally dynamic and change based on conditions, e.g. hydrology, drought, development, erosion, etc. Stable river channels are in a state of dynamic equilibrium, meaning that although the river channel changes event to event, it is stable over time in its pattern, plan, and profile (Rosgen, 1996).

During this survey, all topography and bathymetry data were collected with survey-grade, real-time kinematic (RTK) GPS equipment, or a Trimble S6 robotic total station with RTK control. These methods result in highly accurate northing, easting, and elevation data, far exceeding the minimum < 1.0-foot accuracy goal for this project. Data were collected in United States survey feet in the appropriate Texas State Plane Zone coordinates and reference the North American Vertical Datum 1988 (NAVD88).

2.2.1 Long-term Monitoring Cross-section Resurvey

With the exception of cross-section XS1 at site 080444 and cross-sections XS1 and XS4 at site 080075, very little change in cross-section geometry was observed between the Phase II survey in 2017 and Phase III in 2019 (Figure 2-3, Figure 2-4, Figure 2-5, Figure 2-6).

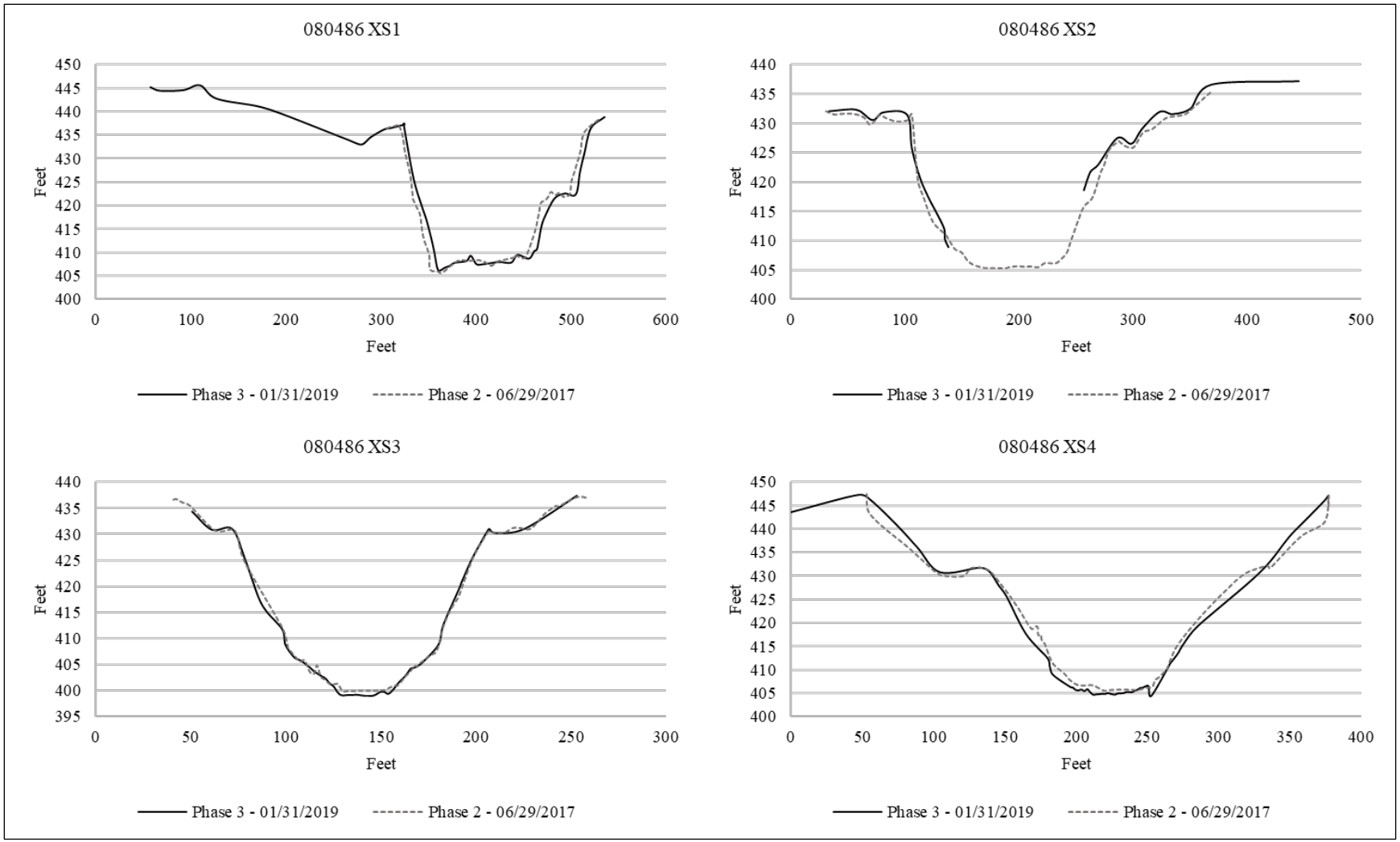

Figure 2-3. Cross-section comparisons for site 080486.

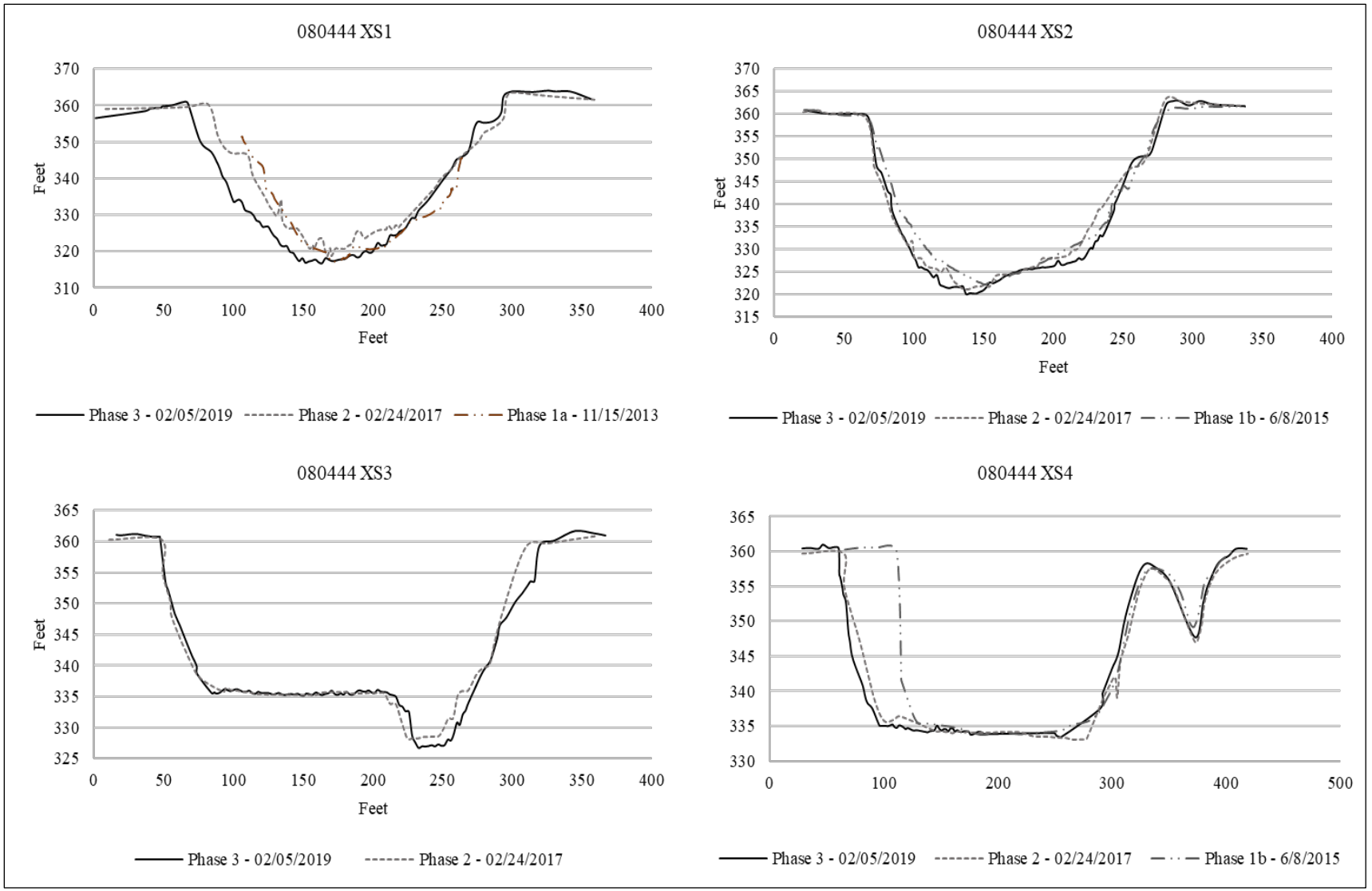

Figure 2-4. Cross-section comparison for site 080444.

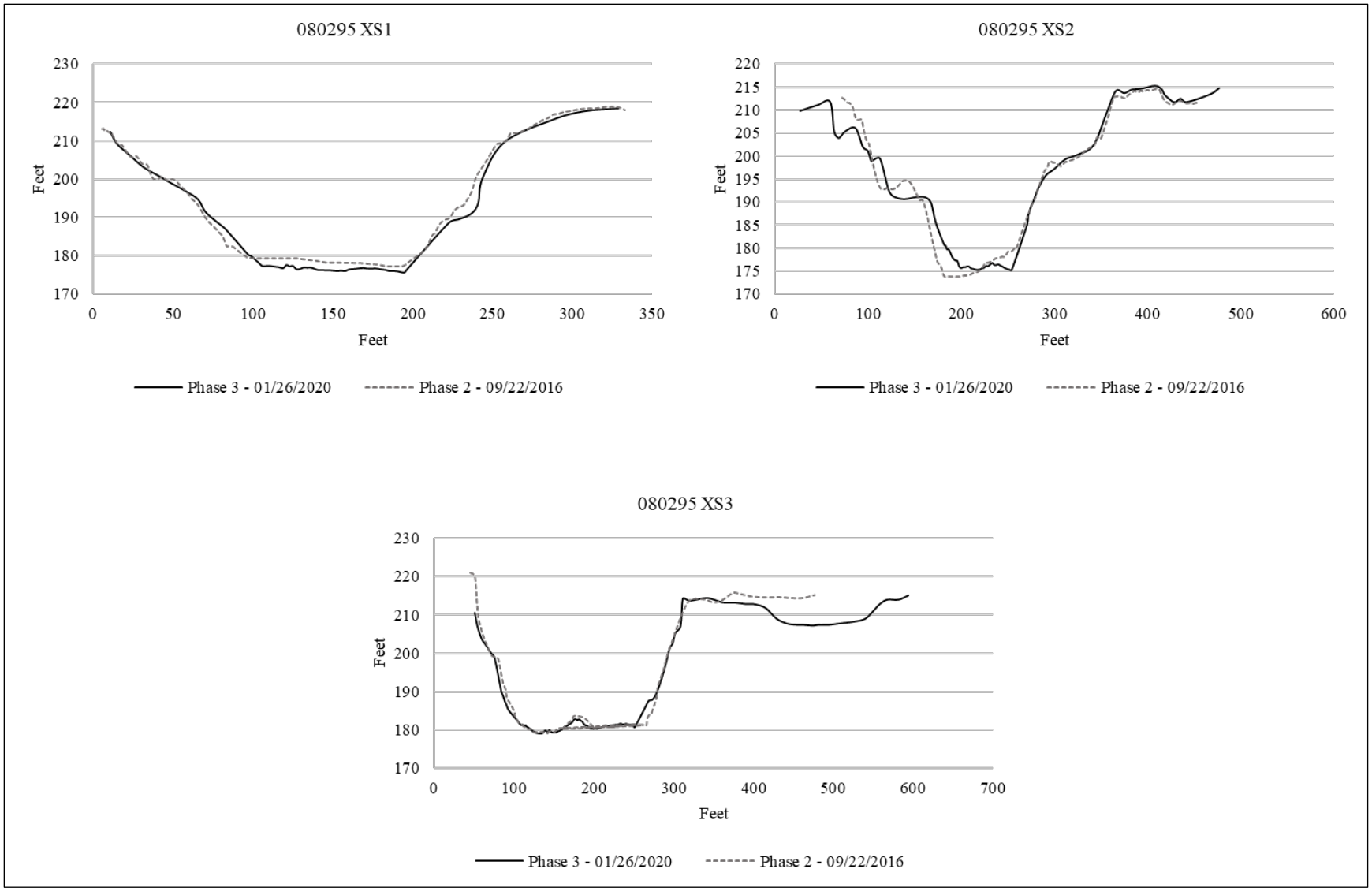

Figure 2-5. Cross-section comparison for site 080295.

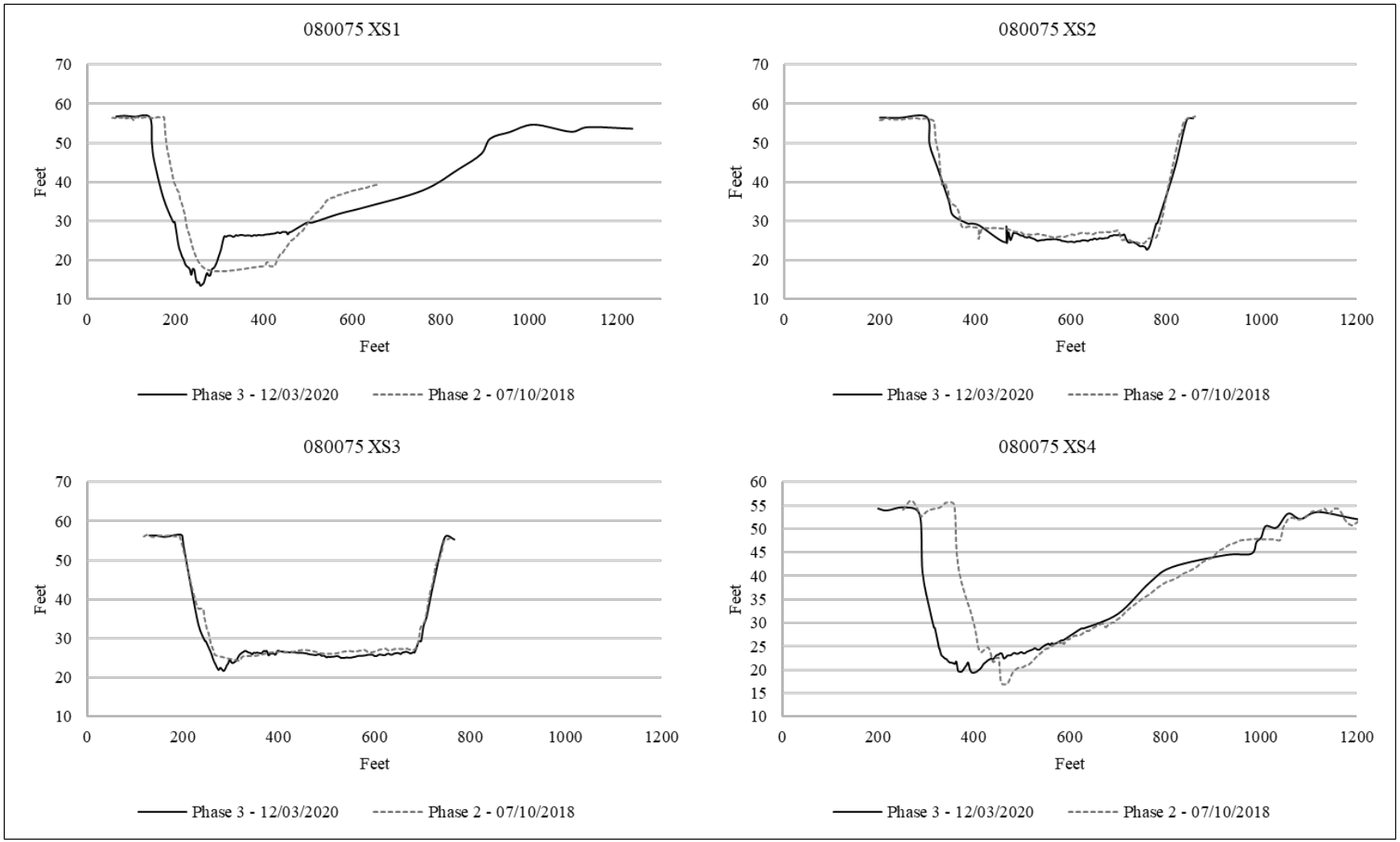

Figure 2-6. Cross-section comparisons for site 080075.

2.3 Riparian Trees

As a continuation of the 2017 tree coring survey (Mangham, Osting & Flores, 2017), additional data collection, analysis and literature research were completed to improve our understanding of riparian forest ecosystems within the Trinity River Basin and to continue identifying and evaluating relationships between river flow regime and riparian tree recruitment.

One hundred three tree cores were collected at site 080295 within and near (within 530 feet) all three cross-sections for three years: 2017, 2018 and 2019 (Figure 2-7). Of those, seventy-six tree cores were analyzed to determine tree age and associated estimated date of germination (Appendix 3). Twenty-six of the 103 cores were of too poor quality to analyze as a result of oversaturation, rotting black willow trees and delicate boxelder cores that broke off inside the tree. Only individual trees having a DBH of greater than 2 inches were sampled for this study.

Figure 2-7. Photograph showing a tree core taken from the riparian area at site 080295.

Aging of individual tree cores from the three core sample years (2017, 2018, 2019) was standardized to year 2019 numbers to take into account the aging done in each year (e.g. 2017 age 10 = 2019 age 12). Age class intervals were consequentially changed to account for this standardization. The overall period of record for the estimated tree germination year was 1957 to 2009. The youngest trees sampled were from the 10-year age class (2.5-inch DBH) with an estimated germination date of 2009.

As previously described in Mangham et al. (2017), river systems are complex and dynamic, and are in a constant state of disturbance from various artificial and natural processes such as flood

inundation, drought, sediment deposition and erosion, etc. This idea of constant disturbance is supported by riparian forest inventories completed by Hayes (2018) and Mangham et al. (2017), which document a high diversity of riparian species ranging from "Obligate" to "Upland" type species, with most of the species (and individuals) being Facultative (+-), generally meaning they are likely to occur in wet or dry habitats. Riparian forest inventories along a stretch of the Trinity River completed by Hayes (2018) were similar in species composition and included an abundance of Facultative (+-) species as expected, which coincided with results presented in Mangham, Osting & Flores (2017).

Biological and river geomorphic processes continue to be active at this long-term study site. Evidence of channel alterations, such as large bank sluffs, were observed, which continue to result in the relocation of larger/older riparian trees and the creation of potential germination sites for more hydric species like black willow. Those active conditions appeared to be ideal for black willow recruitment as a high density of black willow (*Salix nigra*) seedlings and saplings were documented during the 2017 riparian tree survey documented in Mangham et al. Several stands of large diameter black willow trees were observed adjacent to the riparian cross-section on both banks of the river. However, these sluff banks, which contain larger/older riparian trees from higher bank elevations, have been documented as rotting away because of oversaturation and/or being harvested by beavers.

As reported in the Phase II report's (Mangham et al., 2017) riparian vegetation tables, large quantities of black willow, hackberry, and swamp privet seedlings and saplings were observed during the 2017 riparian surveys. However, no recent riparian surveys have been completed to document if the high germination rates for these species translated into recruitment of mature tree (>2" DBH) individuals.

In this ongoing study and analysis of tree age classification, green ash has become an indicator species for the riparian forest owing to the high percentage of successful tree cores collected compared to other species attempted. Results and conclusions from age classification and recruitment analysis presented in this study may not be the same for every species identified during the forest inventories. However, green ash is classified as a Facultative (and Facultative Wet in the Atlantic and Gulf Coast Plain and Arid West Regions; Lichvar, Melvin, Butterwick & Kirchner, 2012; Lichvar, Banks, Kirchner & Melvin, 2016) and therefore represents a more generalist type of riparian species. It is plausible to assume a decrease in green ash recruitment results in an increase of more hydric or upland species depending on what hydrologic and/or climatic conditions impacted green ash. As study efforts continue over time, additional indicator species (e.g. upland or obligate) should be considered if successful tree cores can be collected and analyzed.

This study continued to collect data and evaluate the importance of a variable hydrology regime and the role it plays in overall riparian forest health and ongoing tree recruitment. Additional tree cores and subsequent tree age classification provide further insight into the potential riparian tree assemblage changes that extended climatic events (e.g. droughts and hurricanes) and hydrologic fluctuations (e.g. high magnitude floods, long duration floods and seasonal timing of floods) can cause.

It has become more apparent after years of riparian forest monitoring that a highly variable flow regime is needed to maintain sufficient diversity and abundance of the riparian forest and to maintain adequate tree recruitment. These riparian ecosystems rely on constant disturbance from both climatic and river hydrology at such a highly variable and random nature that it may not be possible to sufficiently mimic these processes with a structured management plan. A management approach that focuses on setting structured flow requirements risks reducing diversity and shifting riparian forest communities by inadvertently precluding one or more habitat preference(s).

2.3.1 Tree coring at 080295

Mangham et al. (2017) provided data suggesting there was a trend showing hydrologic relationships predicting the strength of riparian tree recruitment. Although there are a variety of factors that can affect riparian tree recruitment (e.g. biotic: wildlife browsing; abiotic: nutrient availability), this continued study effort focuses on the hydrologic conditions present on the site (i.e. flow regime). Data collection and analysis methods can be found in Mangham et al. (2017). Any additional methods of analysis are covered in individual sections.

Estimated Tree Age vs DBH

All trees were arranged in order from youngest to oldest and a two-year interval age class was used to categorize raw age data. The two-year interval was used due to having a small sample size.

Riparian tree age was plotted with DBH to determine if any correlation exists between the two parameters (Figure 2-8). Mangham et al. (2017) found a positive correlation between Age and DBH ($R^2 = 0.7721$). However, combined with additional data from the two successive years (2018 and 2019), this relationship was not as significant ($R^2 = 0.4906$). Additionally, only the most frequently sampled species (green ash) was used in a revised correlation effort but did not result in any significant change in correlation strength. Various studies on a range of tree species in a variety of habitats have shown both a good correlation (Irvine & West, 1979) and a poor correlation (Howe & Knopf, 1991) between age and DBH (Brotherson, Rushforth, Evenson, Johansen & Morden, 1983; Hinchman & Birkeland, 1995). Additionally, models for determining age of trees based on DBH and other factors have been formulated and actively used in forest management plans (Teck and Hilt, 1991); however, they are specific to tree species and take other factors into account (e.g. site quality, tree's competitive position within the tree stand).

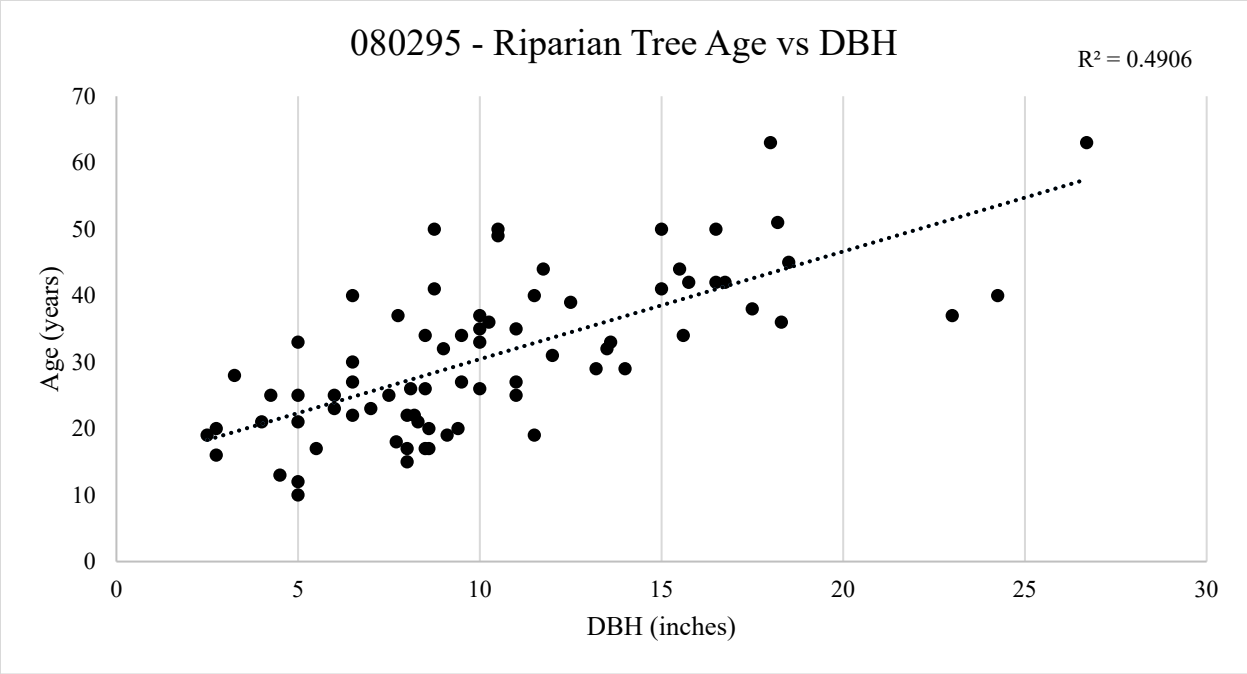

Figure 2-8. Relationship between estimated tree age and DBH for select 080295 riparian trees.

Estimated Tree Age vs Flow

The riparian recruitment (using estimated tree age) versus flow analysis utilized data from 1957 to 2009 (due to estimated tree age). The United States Geologic Survey (USGS, 2020) 08065000 Oakwood gage daily average flows were used to compare riparian recruitment to flow. Recruitment of riparian trees continued throughout the time period, although there was some variability in recruitment consistency and quantity. Tree recruitment appeared greater (>3 trees) during three periods: 1968-1969, 1978-1987 and 1992-2003 (Figure 2-9 and Figure 2-10). Tree age classes for these time periods were 50, 42 to 32 and 28 to 16, respectively. Four lower recruitment periods (<3 trees) were identified (1957-1967, 1970-1977, 1988-1991, 2004-2009) and consisted of 62 to 52, 50 to 42, 32 to 28 and 14 to 10-year-old age class trees, respectively. These trends were similar to those presented in Mangham et al. (2017), although a bit more refined with the additional data. Trinity River flows at the 08065000 gage for these time periods can be seen in Appendix 2.

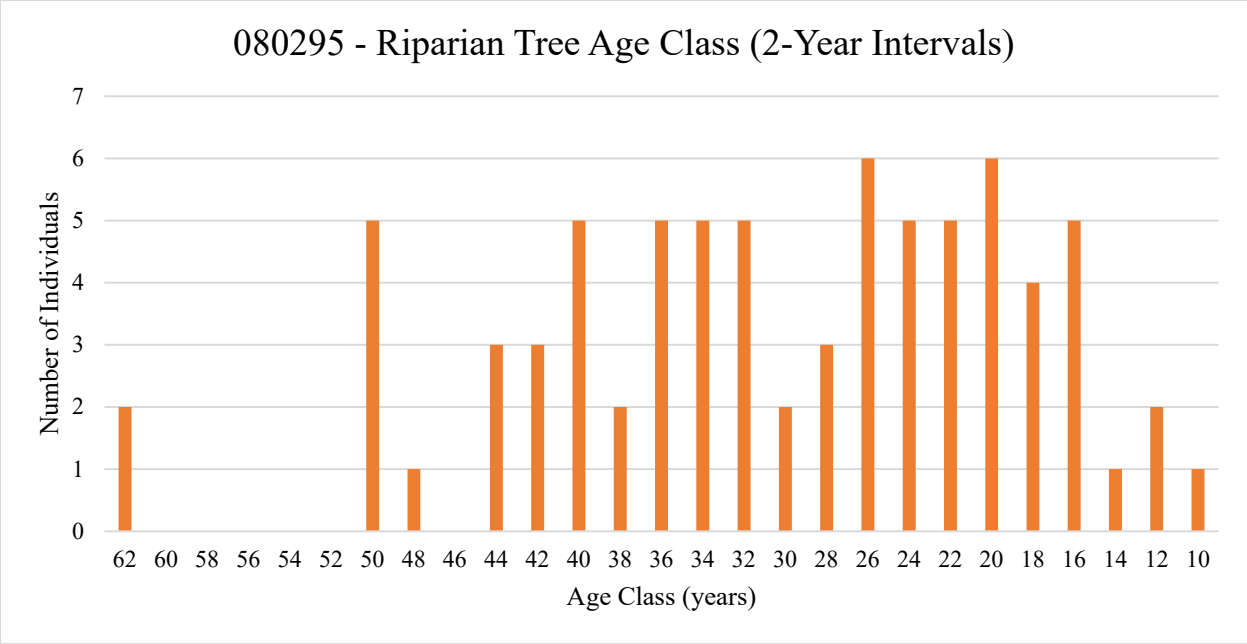

Figure 2-9. 080295 riparian tree age classes. Examples: tree ages 14-15 = 14 age class, tree ages 16-17 = 16 age class, etc.

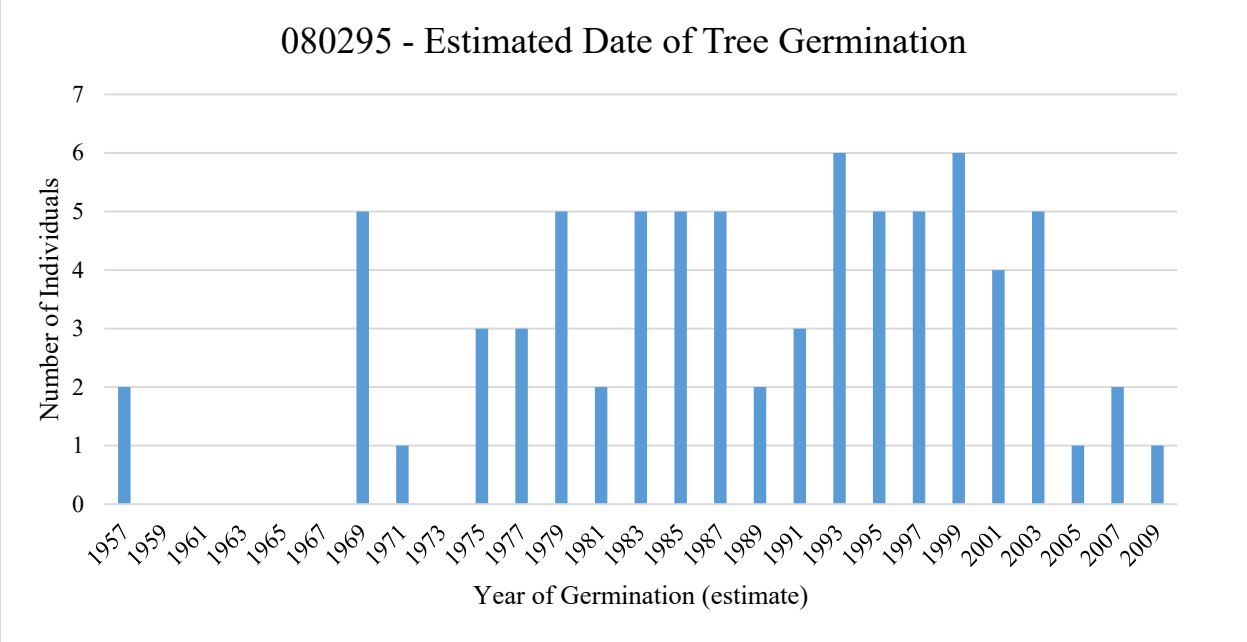

Figure 2-10. 080295 riparian tree estimated date of germination.

During the greater riparian tree recruitment periods, an average of 4.8 tree individuals were recruited in most of the age classes compared to an average of 1.4 trees in the low riparian tree recruitment periods.

For the remainder of this section, refer to Appendix 2 for specific flow data from USGS gage 08065000. Generally, it appears that lower recruiting numbers occur after a long period of drought followed by an extremely high flow event (>80,000cfs). The "50's" drought of record (1949 to 1957) was followed by an extreme high flow event in April 1957 (peak of 90,600cfs), which was then followed by another extreme high flow event in May 1958 (peak of 94,100cfs). After that, two peak flow events in quick succession occurred (61,600cfs in December 1960 and 53,800cfs in January 1961). These events were then followed by lower flows (<20,000cfs) from 1961 through 1964. In 1965 and 1966 two more peaks over 50,000cfs occurred (51,300cfs in May 1965 and 68,100cfs in May 1966). These successive events likely contributed to the recruitment numbers found (effectively zero) from 1958 through 1967 (Figure 2-10). Following this trend, it is likely the site will see the same effects on recruitment in the years following the new drought of record that occurred from May 2010 through July 2015. This new drought of record was succeeded by a sustained flow period (>35,000cfs) from May 15 to June 16, with a peak of 79,000cfs. This was followed by a 17-day flow event (>35,000cfs) in which flow peaked at 99,200cfs within two days of going over 1,000cfs (extreme pulse flow over a short period of time). Mangham et al. reported in 2017 that overbank flow for this site is estimated at 30,000cfs.

Another period of consistently low flow (<13,000cfs from July 1987 through April 1989 [678 days]) appears to be the cause of a large drop in recruitment from 1988 through 1990. A similar pattern is seen from March 2003 through April 2004 (418 days) where flows were consistently well below 10,000cfs with a few spikes into 13,000cfs. See Appendix 2 for USGS flow data from gage 08065000.

Conversely, the data shows that having consistent flow events each Spring (>30,000cfs) followed by shorter periods of low flow stages through the summer, or medium flow events in the fall followed by shorter periods of low flow through the winter, resulted in higher recruitment from year to year, as seen from 1978 through 1987. A similar pattern is seen from 1992 through 2003.

Cored Trees and Inundation Stages

In addition to tree cores, GPS locations of each tree were collected each survey year (Figure 2-11). The GPS locations were mapped for each inundation stage modeled for the area (Mangham, et al, 2015): 6,180, 7,000, 10,000, 11,800, 16,500, 21,000 and 30,000cfs. Trees were mapped by 2-year age class and can be seen in Figure 2-12 through Figure 2-18. Only trees found in each successive floodplain inundation stage (beginning with 6,180cfs) were mapped, not an accumulation of trees (i.e. trees found in first floodplain inundation, 6,180, were not mapped in 7,000, 10,000, etc.). It is important to note that the original (2017 survey) tree core samples were obtained from areas near the three previously established cross-sections (Mangham et al., 2013; Mangham et al., 2015), excluding the area between the upper and middle cross-sections (approximately 0.5 river miles apart). For the 2018 and 2019 data collection effort, the search distance was expanded to include more tree core samples from trees found in between the cross-sections. All study trees and their corresponding ages and floodplain stage can be found in Appendix 3.

Figure 2-11. 080295 - Cored trees for study years 2017, 2018 and 2019.

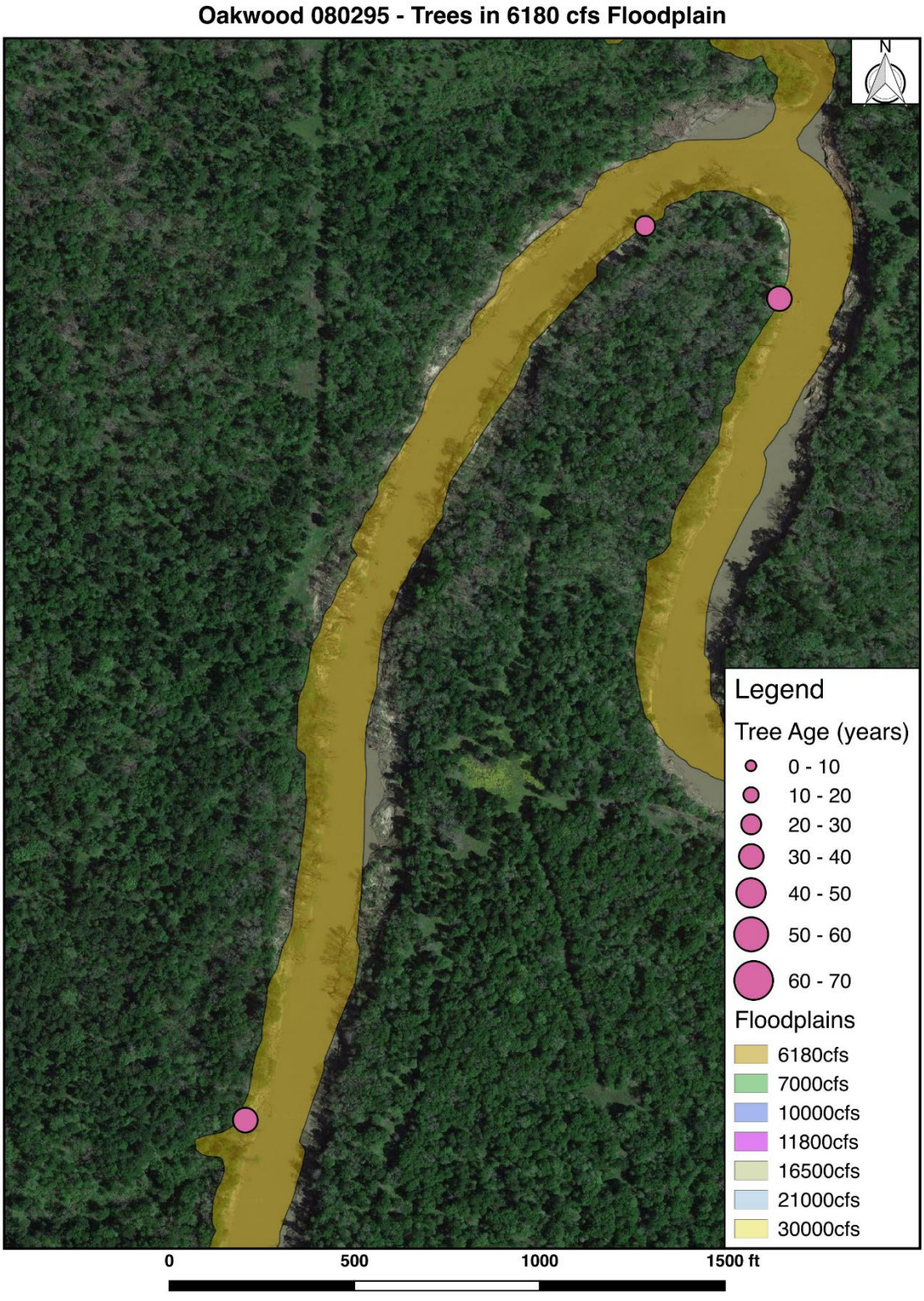

Figure 2-12. 080295 – Cored trees found in 6,180cfs inundation area.

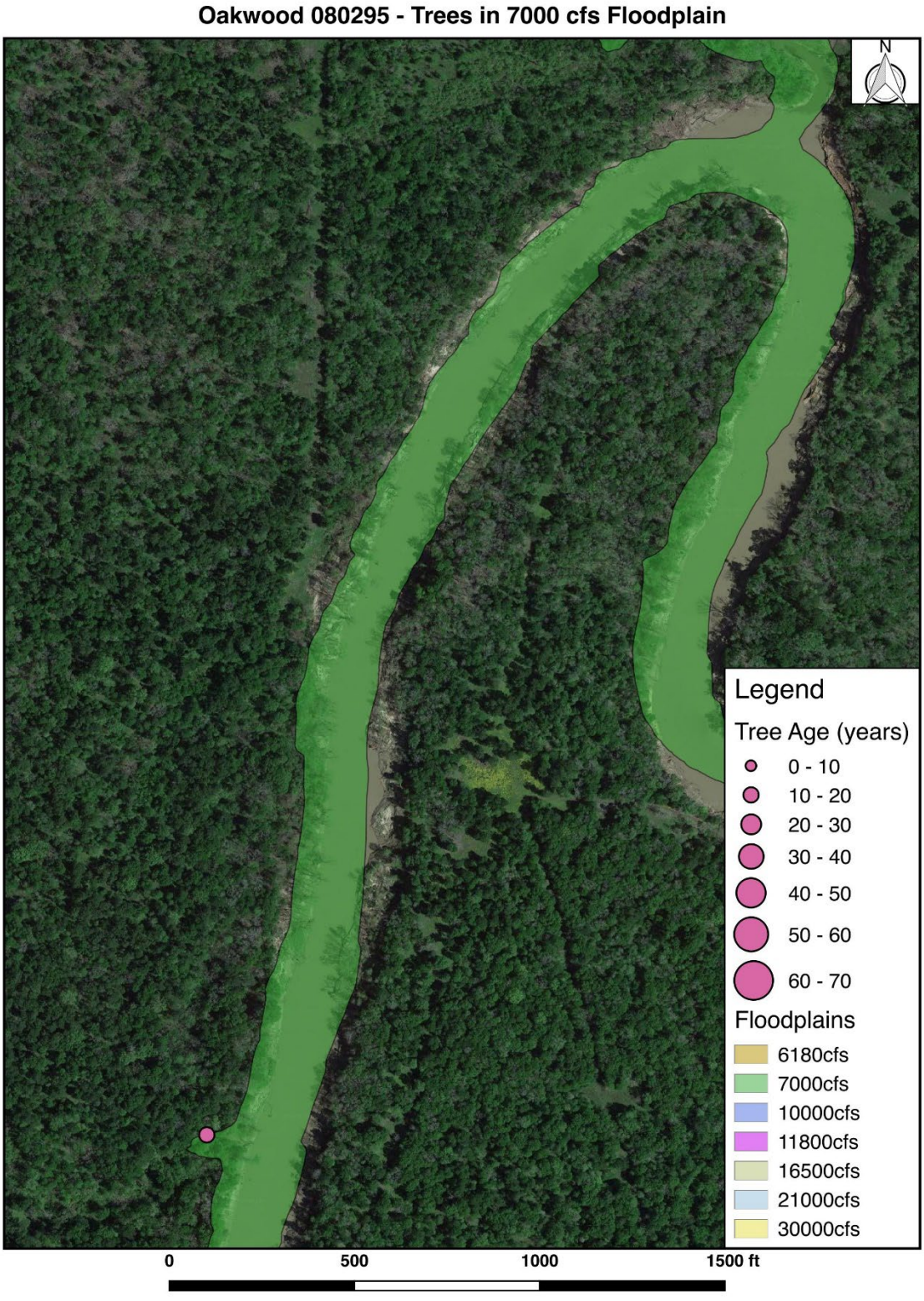

Figure 2-13. 080295 – Cored trees found in 7,000cfs inundation area.

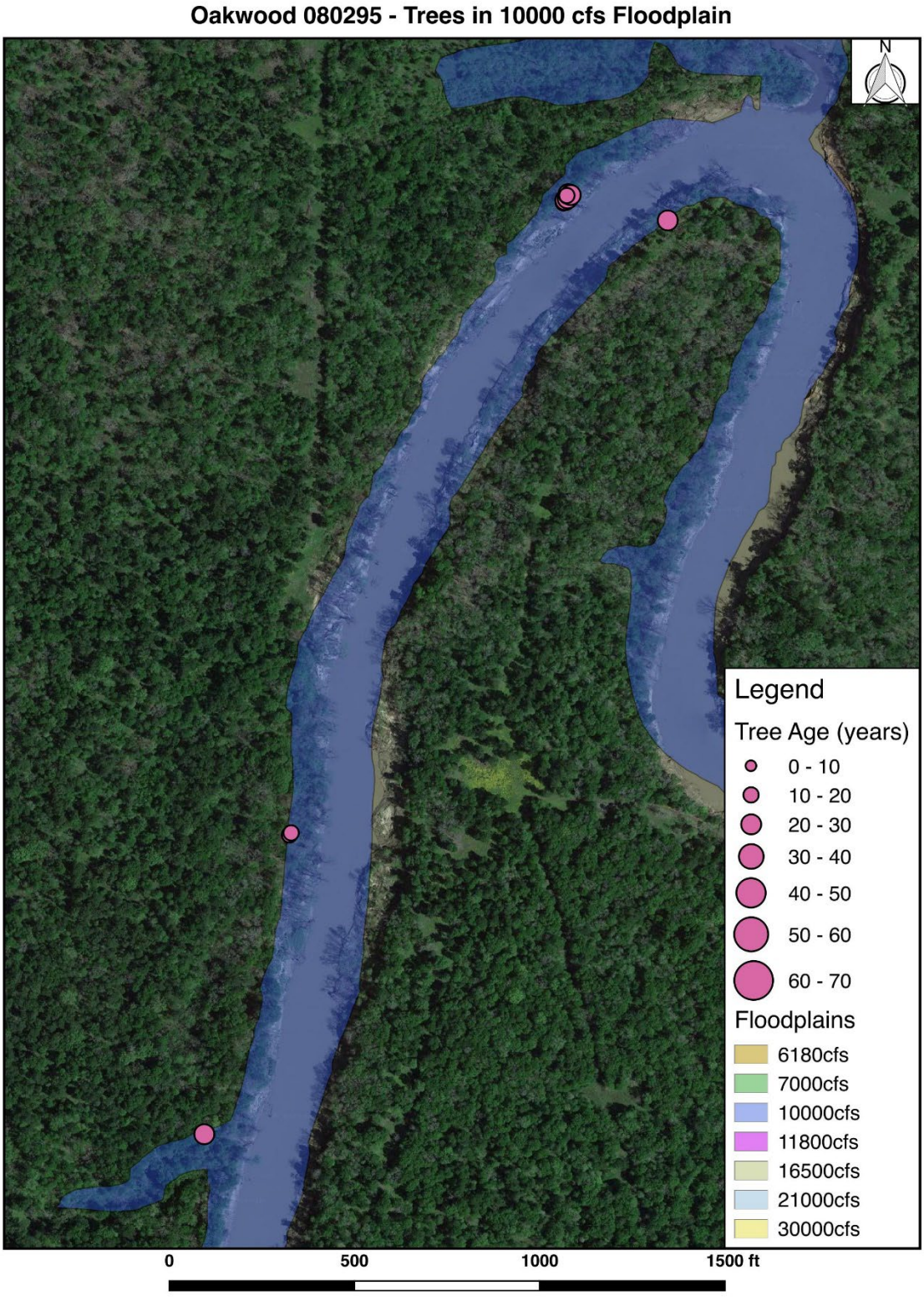

Figure 2-14. 080295 – Cored trees found in 10,000cfs inundation area.

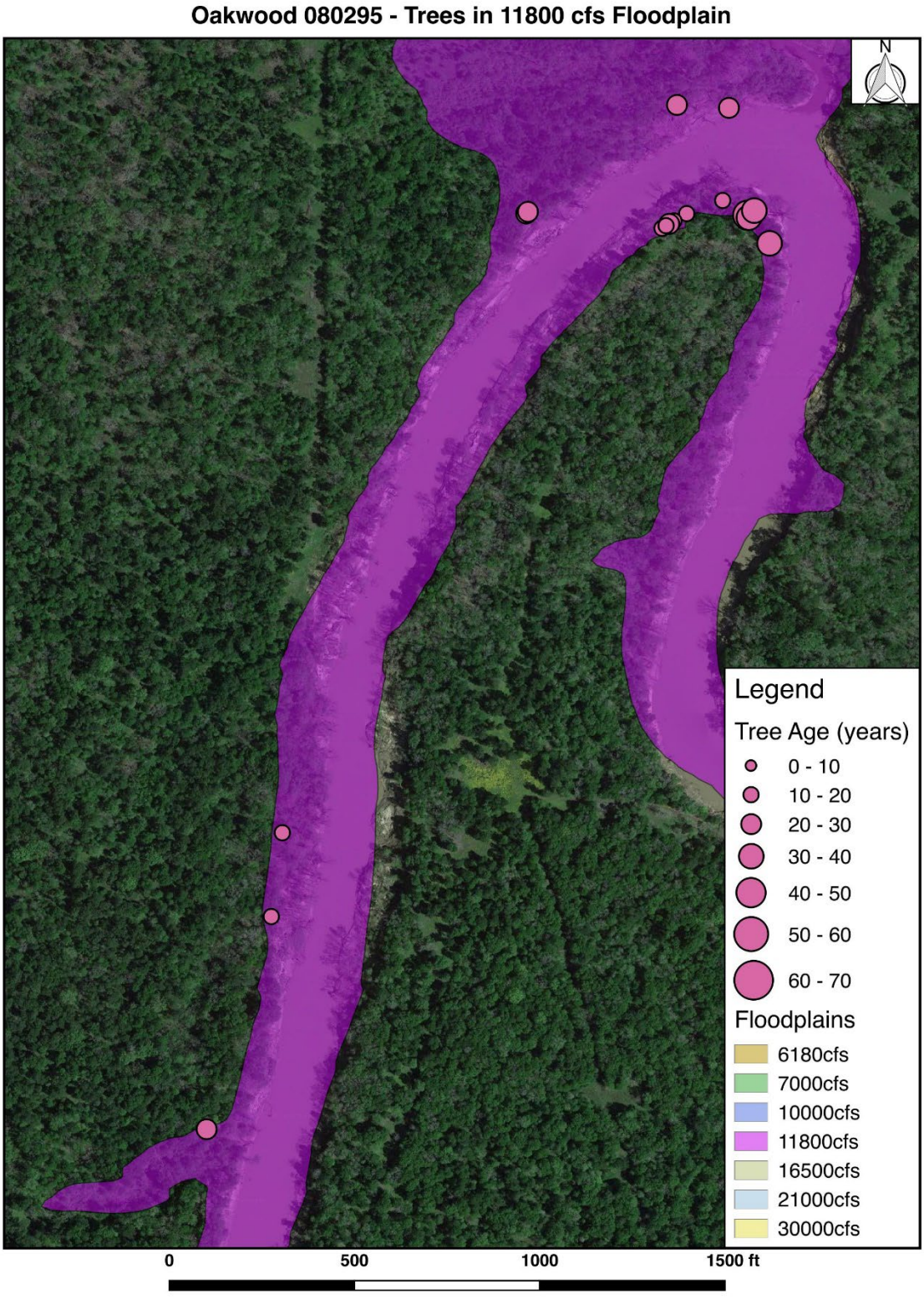

Figure 2-15. 080295 – Cored trees found in 11,800cfs inundation area.

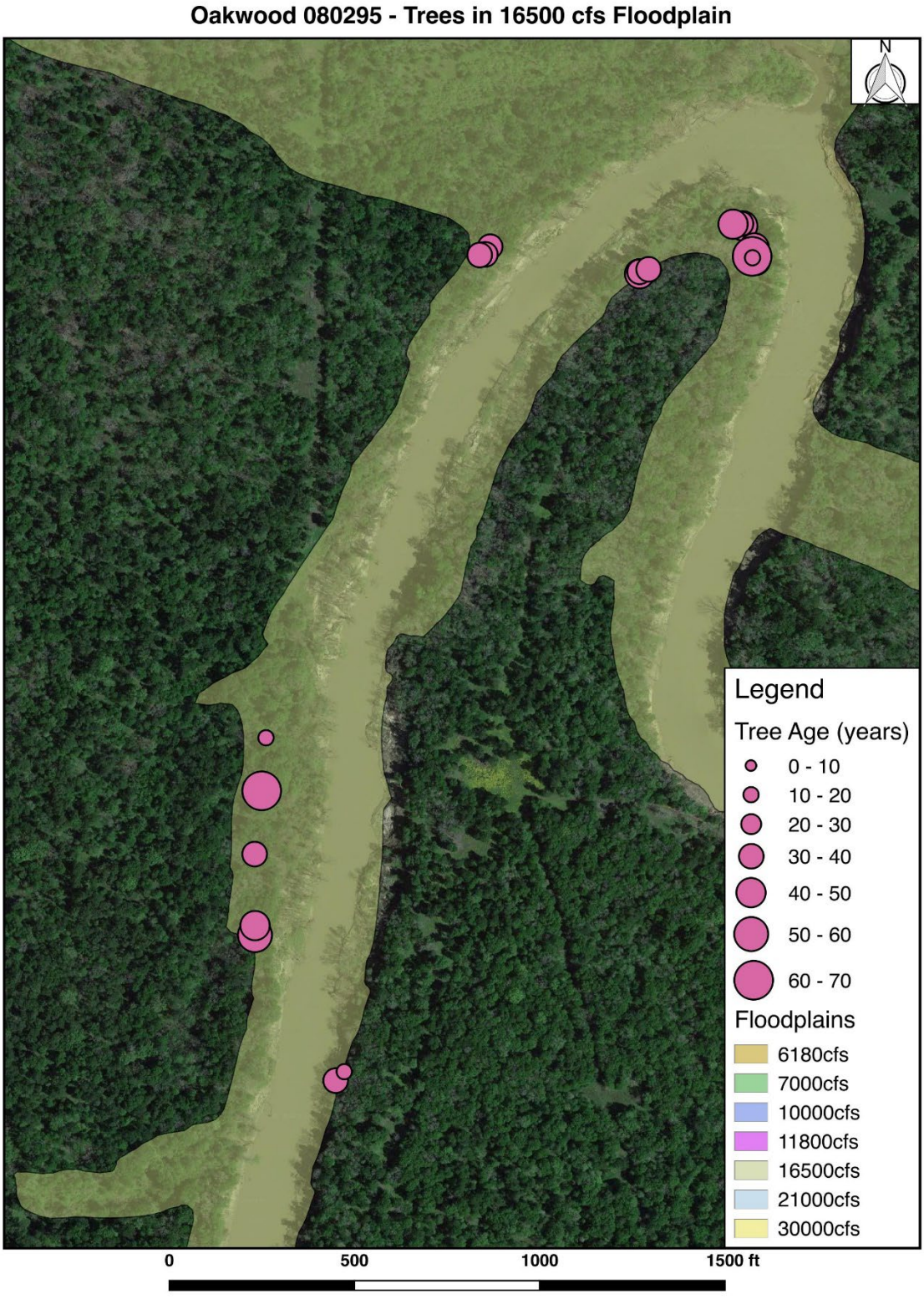

Figure 2-16. 080295 – Cored trees found in 16,500cfs inundation area.

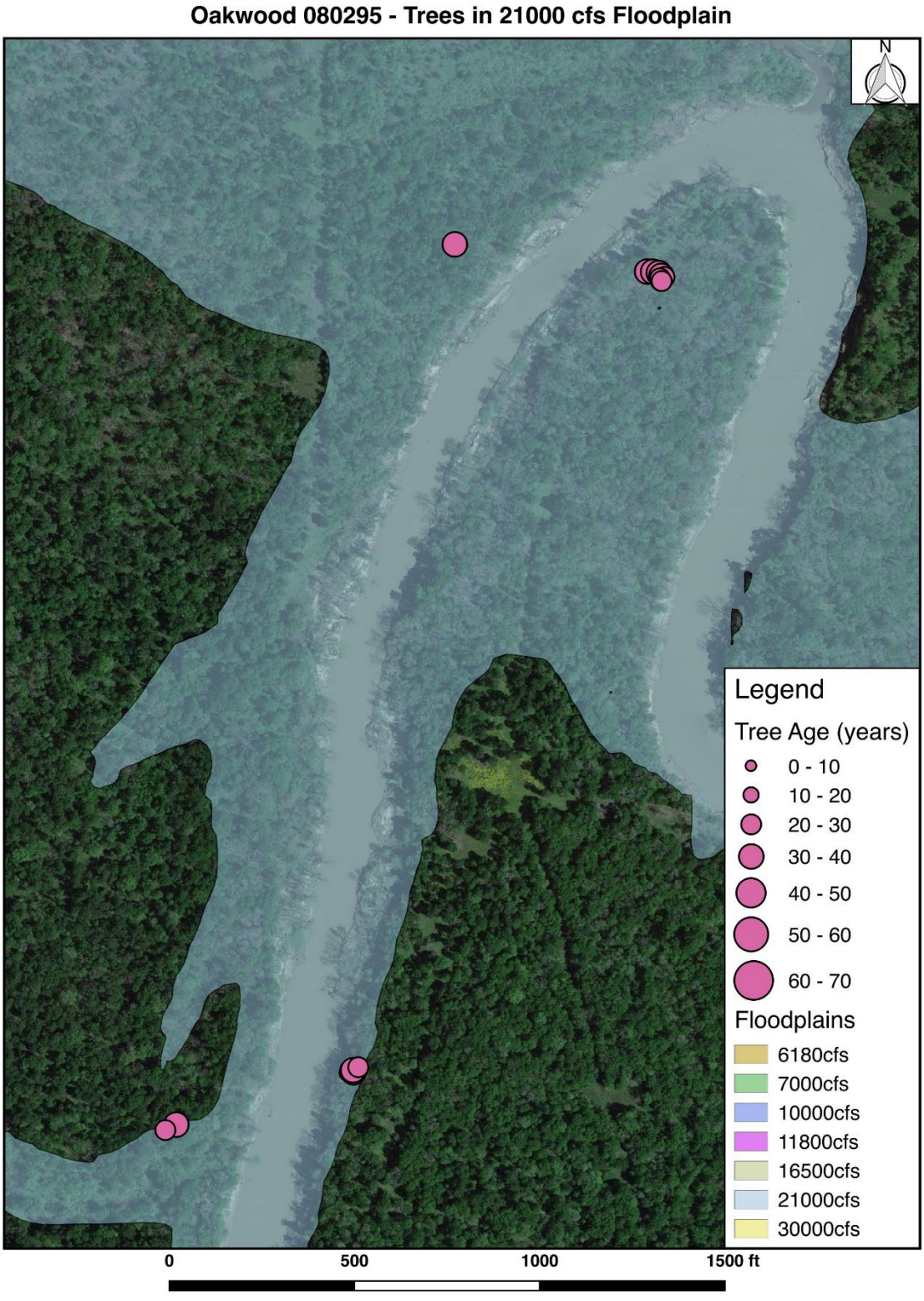

Figure 2-17. 080295 – Cored trees found in 21,000cfs inundation area.

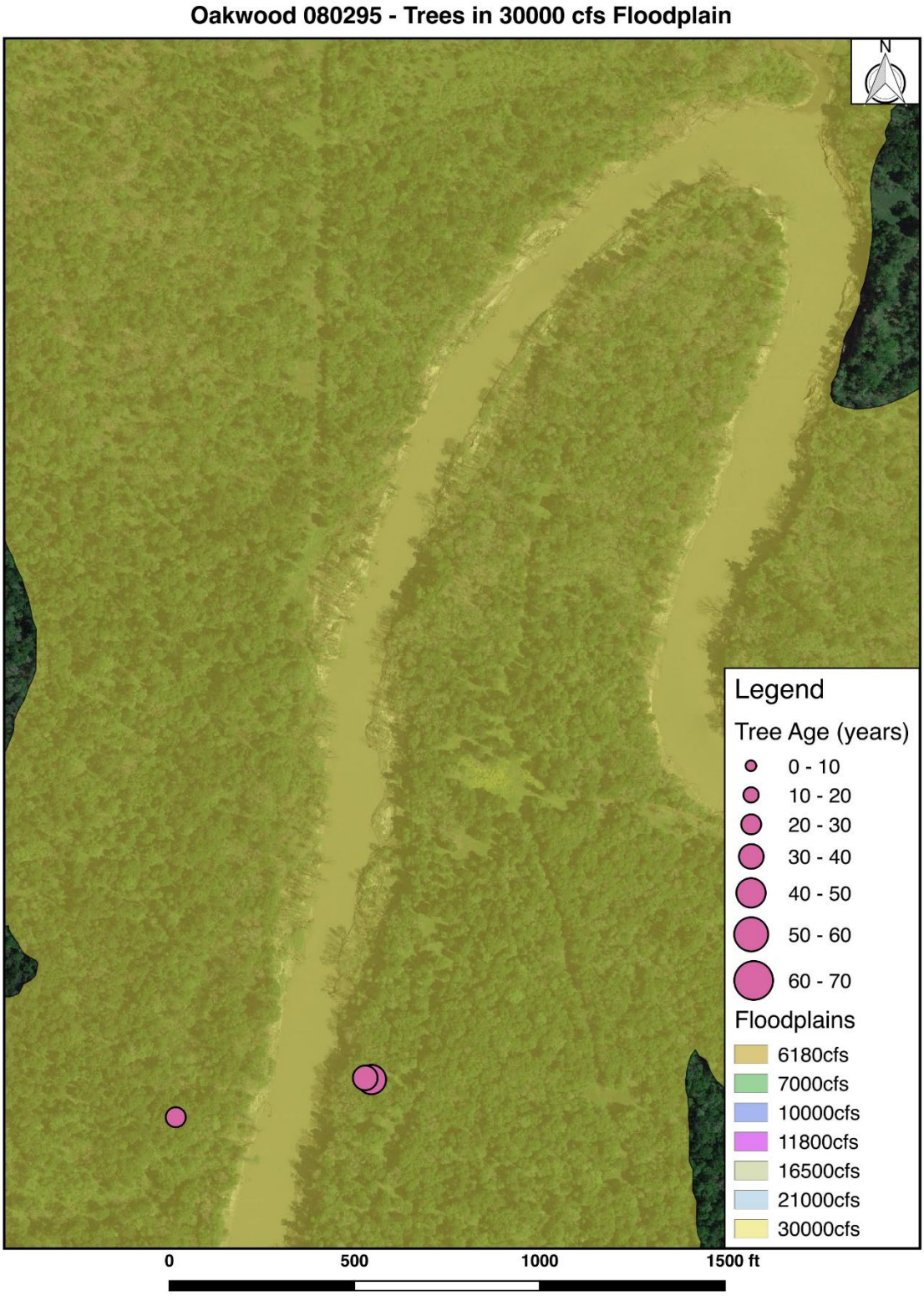

Figure 2-18. 080295 – Cored trees found in 30,000cfs inundation area.

Generally, the lowest and highest floodplain stages have the fewest number of trees (Table 1), with the highest number of trees and age class range found in the 16,500cfs inundation stage. The youngest few age classes of trees (10 – 16) were only represented in the 11,800 and 16,500cfs stages. Additionally, the eight oldest trees were found in the 16,500cfs stage, being the only stage to include age classes 48 to 62. Each of the age classes from 20 to 28 were not found in the 16,500cfs stage but are represented in at least one of the other floodplain stages. The lowest floodplain stage (6,180cfs) contains only middle age range trees (26 to 36 years old), instead of the youngest or oldest.

Table 2-2. Cored trees for each floodplain stage.

Floodplain Stage (cfs)	Number of Trees	Average Age (yr)
6,180	3	31
7,000	1	20
10,000	11	22
11,800	18	23
16,500	24	40
21,000	16	30
30,000	3	37

2.3.2 Discussion

It is important to point out that riparian tree recruitment is a complex biological process consisting of known (e.g., stream flow, predation, disease, extreme temperatures, fire, harvesting, etc.) and unknown factors that are highly variable and can be unpredictable themselves. These factors cumulatively influence the overall riparian recruitment process and the relative significance of each changes on various temporal scales. This report studies only stream flow as the variable for riparian tree recruitment; it is important to consider these results and this discussion within that context. When considering flow as the sole variable, it would appear, overall, that the 10,000cfs to 21,000cfs elevation provide the most consistent optimal conditions for riparian recruitment for the species collected during this ongoing study (Table 2-2). This is consistent with the original study expectations for selecting an indicator species classified as a generalist (Lichvar et al., 2012; Lichvar et al., 2016). Additionally, the results suggest older trees are found at higher flood stages except for the lowest flood stage (6,500cfs; Table 2-2), which had a similar average tree age to higher flood stages. This might be the result of a limited sample size or could be further evidence of natural tree relocation due to channel sluffing.

Analysis of tree age versus gage flow data at the site did seem to present a possible trend. Recruitment appeared to be negatively affected by long periods of drought followed by extreme high flow events (>80,000cfs), resulting in little recruitment in multiple years following such events. Extended periods of drought can lower the local water table and reduce areas and

frequency of inundation within a river's floodplain. This would result in a dynamic shift similarly described in Hayes & Baker (2019) in the overall riparian community with an overall reduction in recruitment habitat for more hydric species. Recruitment would likely be limited to areas near the shoreline and possibly large backwater oxbows. In contrast, during these extended periods of drought, available recruitment habitat for upland species should expand and result in an increase in upland individuals at lower elevations. As mentioned above, it appears significant high flow events that occur after extended drought periods reduce riparian recruitment for two main reasons. First, hydric seedlings/saplings and even smaller (younger trees) will be more abundant at lower elevations making them more susceptible to channel forming processes and long periods of inundation during high flow events. Second, upland species found at lower elevations cannot tolerate saturated soils or long periods of inundation.

Recruitment seemed to be higher as a result of the occurrence of flow events greater than 30,000cfs in the spring or fall, followed by shorter low flow periods (<10,000cfs), with no peak flow events over 20,000cfs throughout the rest of the year.

Determining the floodplain stage at which trees first occur (from lowest to highest stage) provided a visual account of the abundance at each tree age and stage that may correspond to the flow event relationship. The elevation ranges of 11,800cfs, 16,500cfs and 21,000cfs stages, account for 76% of the trees cored. This might indicate these elevations experience moderate disturbances within the floodplains studied and result in ideal conditions more frequently. Middle-age range trees (26 to 36 years old) were the only ages found in the lowest floodplain stage (6,180cfs), which could be a result of active channel forming processes at this stage.

Examining the tree core data to determine trends in hydrologic relationships to predict the strength of riparian tree recruitment is challenging. Due to the complexity of river systems generally, as in all ecological systems, there are many factors that contribute to a river system's success. These dynamic systems usually have inconsistent influences, whether it be natural (e.g. predation, hydrologic and climatic) or anthropogenic (e.g. pesticide use, tree harvest); however, the importance in continuing to study these systems remains an essential task to aid in a better understanding of the effects of flow as a factor for riparian tree recruitment.

2.3.3 Recommendations

The amount of time it takes for a tree along the Trinity River at this study site to mature to tree status (>2 inches DBH) has been documented at ten years. Thus, it is recommended that the study continue through at least 10 years after the end of the drought of record in 2015, to 2025. Gathering more data on tree age, continuing to attempt to add different tree species and expanding the study reach to include more areas between all three established cross-sections, would add valuable data to aid in determining trends. In addition, a more in-depth study of the seedlings counted at each surveyed cross-section (riparian elevation survey, Mangham et al., 2017) and their position relative to distance from water's edge and floodplain stage, will provide valuable insight into the recruitment of seedlings.

Additionally, conducting riparian surveys and tree core sampling during a drought and immediately after an extreme flow event would be an exciting addition to the dataset. This would

provide evidence of tree species (seedling, sapling and tree) reaction to the drought/extreme high flow pattern.

2.4 Geomorphology

At sites 080295 and 080075, geotechnical data was collected to provide data for HEC-RAS sediment transport modeling and Bank Stability and Toe Erosion Modeling (BSTEM). The data collected (Figure 2-21 and Figure 2-22) included in situ field measurements/observations and quadruplicate eight-inch sediment cores that were collected near the waterline along the toe of the slope (Table 2-3). Detailed results are shown in Appendix 4. One of the quadruplicate core samples from each sampling site was sent to the TEAM Consultants, Inc. laboratory for grain size analysis, Atterberg limit testing, and moisture content; the results are shown in Appendix 5. Another one of the quadruplicate core samples were taken to the Sediment Laboratory at the University of Baylor for additional testing (Table 2-3) and the results are shown in Appendix 4.

Table 2-3. Table describing the geotechnical data collected for this project.

Parameter	Sample Type	Instrument/Method
Moisture content	In situ	Pogo Hydraprobe ™
Salinity	In situ	Pogo Hydraprobe™
Soil Temperature	In situ	Pogo Hydraprobe™
Vane shear	In situ	Gilson Pocket Shear Vane (Torvane)
Soil type	Field Observation	Visual and texture
Laboratory Geotechnical Properties	Quadruplicate Core Samples	Baylor University Sediment Laboratory: Jet Testing Vane Shear Strength – Penetrometer Bulk Density
Laboratory Geotechnical Properties	Quadruplicate Core Samples	TEAM Consultants, Inc. Laboratory: Grain Size Atterberg Limits Moisture Content

2.4.1 Geomorphology Results and Discussion

TEAM Consultant, Inc.

Based on the quadruplicate core sample analyzed at the TEAM Consultants, Inc. Laboratory, generally, samples from site 080295 contained equal parts of sand, silt, and clay, while two samples at 080075 contained very little clay and were mostly sand (Table 2-4 and Figure 2-20). The middle sample (080075 RM 74.65) at 080075 was taken from a straight area of the stream with a high, near-vertical bank that is common along these reaches. That sample was found to be almost entirely clay.

Erosion is, in part, dependent upon particle size. The D10, D50, and D90 describe the 10^{th}, 50^{th}, and 90 percent finer grain size diameters for each core sample. For example, the D10 is the grain size diameter in which 10-percent of the sample by weight is finer and 90-percent is larger. Conversely, the D90 is the grain size diameter in which 90-percent of the sample by weight is

finer and 10-percent is larger. The D50 represents the median grain size. By looking at the relationship between these three values, assumptions can be made regarding not only the median particle size, but also the variability of particle sizes within the sample. For example, a sample with similar values of the D10, D50, and D90 would suggest that the sample is fairly homogeneous (Figure 2-19 site 080075 74.65), while a wide range of values suggest a heterogeneous sample consistency (Figure 2-19 site 080075 75.25). Because each type of soil erodes differently, these results helped to drive the inputs for sediment modeling. The D50 for each sample is shown in Figure 2-20, along with the percentages of sand, silt, and clay. These results are consistent with field observations and were used during sediment transport modeling discussed later in this report.

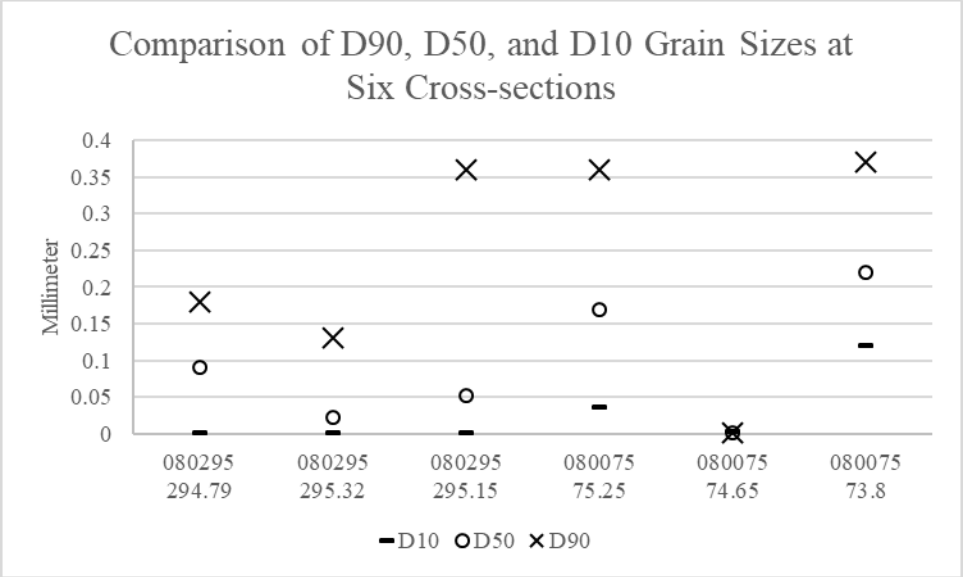

Figure 2-19. Comparison of D90, D50, and D10 at six cross-sections.

Table 2-4. Table showing the TEAM Consultants, Inc. core sample results for the D10, D50, D90 particle sizes and the percentages of sand, silt, and clay for each sample.

Site and Approximate River Mile	Visual Description & Unified Soil Classification	D10	D50	D90	% Sand	% Silt	% Clay
080075 73.8	Tan and gray poorly graded sand with silt	.12	.22	.37	94.5	0.7	4.8
080075 74.65	Gray fat clay	0.0034	0.001	0.001	2.5	7.2	90.3
080075 75.25	Gray silty sand	0.036	0.17	0.36	83.0	9.2	7.8
080295 294.79	Brown clayey sand	0.001	0.090	0.18	62.2	14.8	23.0
080295 295.15	Brown and gray sandy lean clay	0.001	0.053	0.36	45.8	19.6	32.3
080295 295.32	Dark brown and gray fat clay with sand	0.001	0.023	0.13	31.0	32.8	36.2

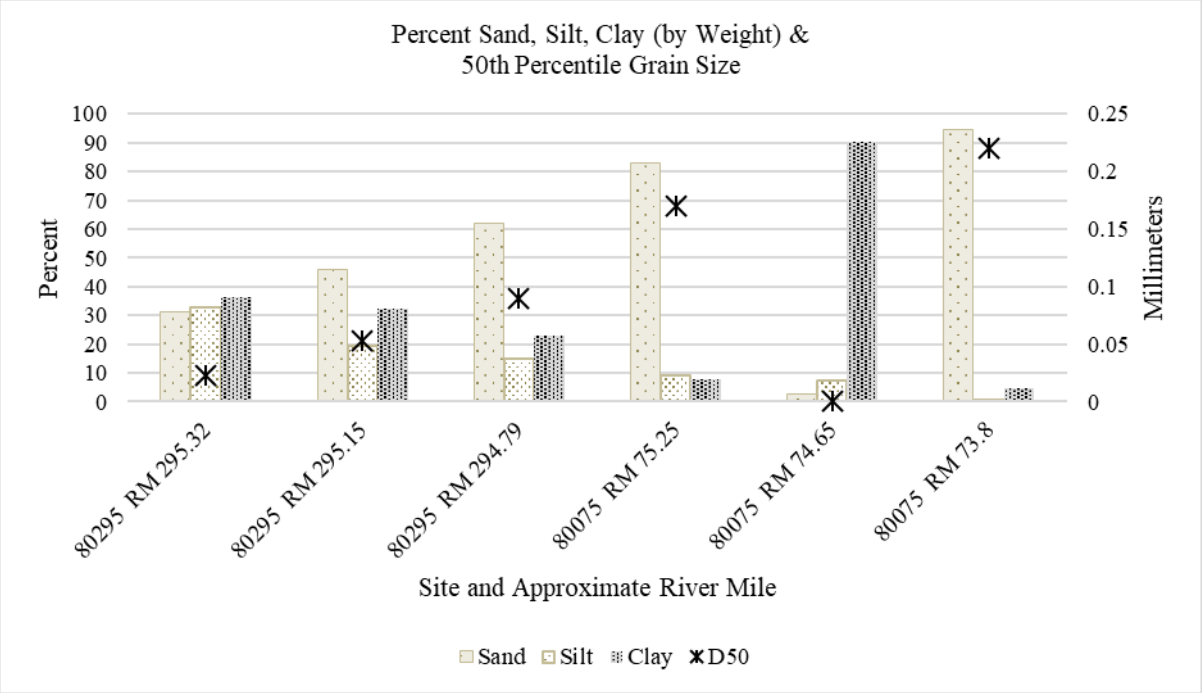

Figure 2-20. Graph showing the TEAM Consultants, Inc. core sample results for the D50 grain size and the percentages of sand, silt, and clay for each sample.

Figure 2-21. Photographs showing how sediment cores were collected and preserved for transportation.

Figure 2-22. Photographs showing (from left to right) field vane, hydrometer, bank RTK GPS surveying, and channel RTK GPS surveying.

Baylor University Sediment Laboratory

Two of the quadruplicate core samples weres taken to the sediment laboratory at Baylor University for further testing. Typically, the excess shear stress equation is used to determine the erosion rate of cohesive soils. This method provides an erodibility coefficient (*K*d) and the critical shear (*Tc*) stress for, in this case, the stream bank. For this project, the core samples were tested using the Submerged Jet Erosion Test (Jet) method which uses the scour depth as the means for developing critical shear and erodibility. A detailed review of the Jet process is beyond the scope of the report, but has been well documented in Hanson, 1990; Hanson and Cook, 1997, Hanson and Simon, 2001, and Daly et al. 2013. The data is available in Appendix 4.

Generally, the Jet method applies water to the core sample at a known velocity for a known period of time, in this case either five or ten minutes. At each time interval, the depth of the hole is measured and associated with the time period (Figure 2-23). These results, along with various pressure, and nozzle readings, were input into the Jet Erosion Test Spreadsheet Tool (Daly, 2014). The spreadsheet calculates various parameters, including the scour depth solution (SD). The SD provides the estimated critical shear and erodibility for that particular core sample.

Additionally, the core samples were tested in the lab with a vane shear and penetrometer and those measurement were compared to the field results (Figure 2-24 and Figure 2-25). There was no correlation between the vane shear taken in the lab and the vane shear taken in the field; however, although the measurements were higher in the lab, the pattern was similar.

Figure 2-23. Photographs showing laboratory processing of core samples using (clockwise from upper left) a penetrometer, vane, jet pressure tester, and a post-jet testing core.

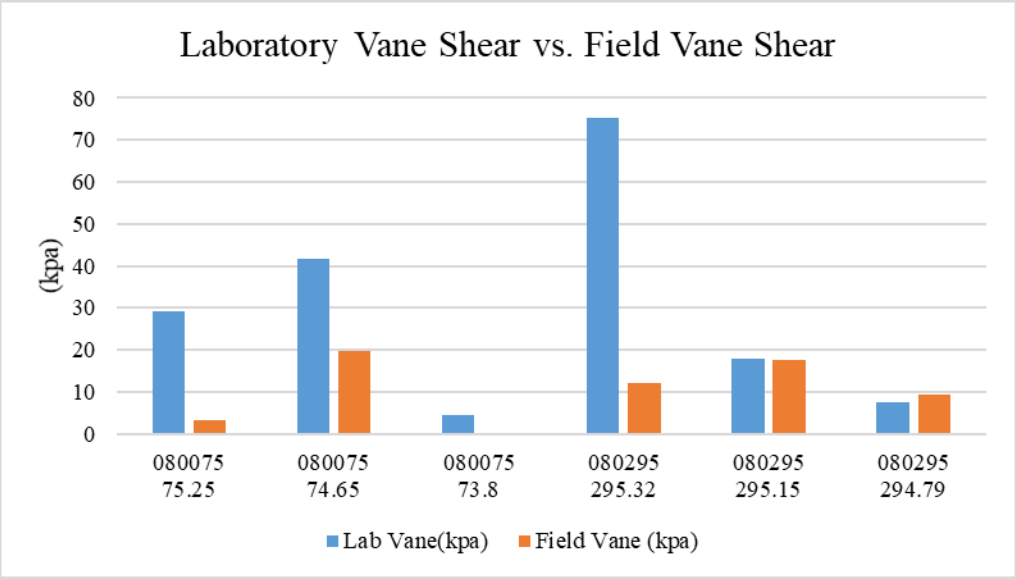

Figure 2-24. Laboratory vane shear vs. field vane shear.

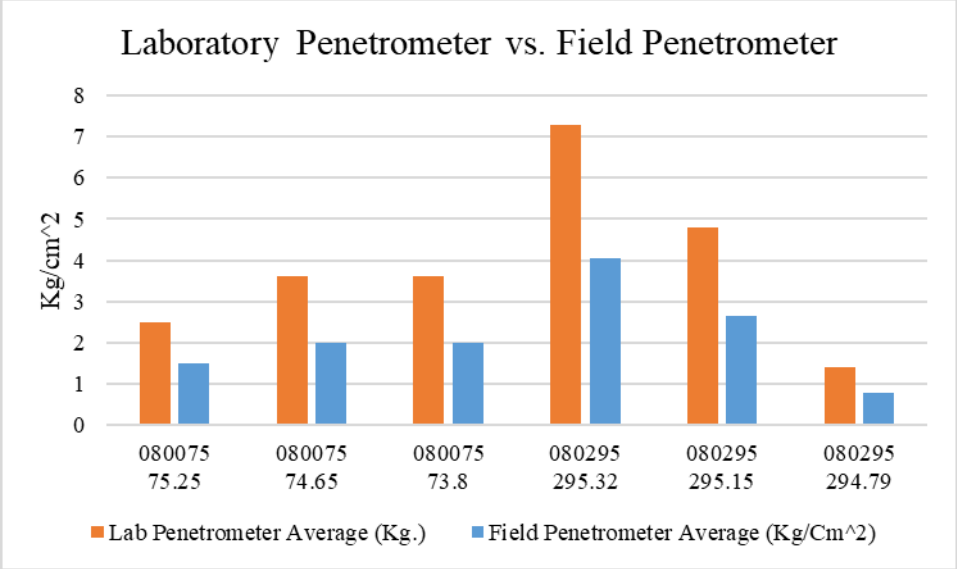

Figure 2-25. Field penetrometer versus laboratory penetrometer.

3 Modeling

In addition to channel monitoring at all sites, empirically gathered data was used to create models that will provide the BBASC a better understanding of the riparian habitat, water quality, and sediment transport dynamics of the Trinity River at the designated SB3 measurement points or their surrogates. The area of modeling includes the Trinity Oakwood and Trinity River Romayor measurement points (Figure 3-1). The water quality modeling component will provide an understanding of the temperature and dissolved oxygen ranges at the mesohabitat level

(riffles, runs, pools, and backwaters) and those values will be compared to thresholds for selected fish and freshwater mussel species identified during SB2 field work.

The HEC-RAS model was used to analyze sediment transport and bank stability. The sediment transport and Bank Stability and Toe Erosion Modeling (BSTEM) component can provide a tool to analyze channel processes like aggradation, degradation, and bank failures using historical hydrology and also using potential SB3 flow regimes. Together, along with continued channel monitoring this study will provide stakeholders a better understanding of the channel sediment conditions in context of flow levels for SB3 subsistence, base and pulse flows.

3.1 HEC-RAS Models

Two HEC-RAS models on the Trinity River were developed for both the water quality and geomorphology portions of this project. The first model (upper model) incorporates site 080295 (Oakwood), and extends from upstream near the USGS Trinity River near Rosser streamgage to the downstream boundary at Lake Livingston. The second model (lower model) incorporates site 080075 (Romayor), and extends from upstream at the USGS Romayor streamgage site to downstream past Highway 105. The upper and lower modeled cross sections are shown in Figure 3-2 and Figure 3-3.

There are a number of existing HEC-RAS models from previous studies on the Trinity River, which are listed in Table 3-1. No previous model was entirely sufficient for this study since none incorporated recent LiDAR-derived elevation data or existing TRA collected in-channel bathymetry data. This project integrates the most up-to-date data into the HEC-RAS models. Cross sections from previous models were used to fill in data gaps for the two project models (Table 3-1). Details of which previous model cross sections were used are explained and shown in the following section.

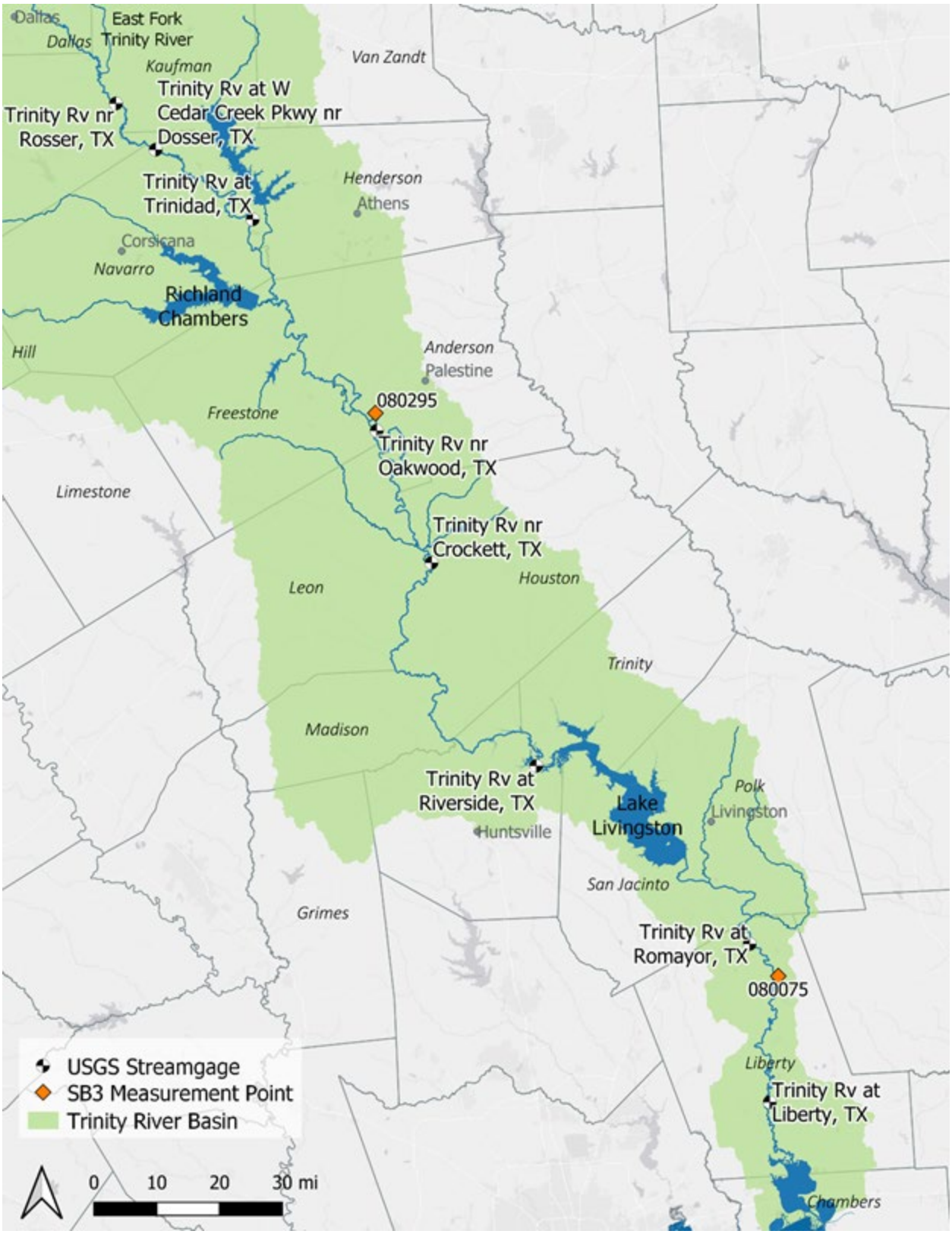

Figure 3-1. Project study site, including major USGS streamgages, and SB3 measurement points.

Table 3-1. Existing HEC-RAS models within the project study area, including cross sections used in the project models.

Model Project Name	TWDB Contract No.	Model Extent	Cross Section Location(s) Used in Project Models
Water Quality Model of the Middle Trinity River (2016)	1348311642	Downstream of USGS streamgage Trinity River near Rosser to headwaters of Lake Livingston	Throughout upper model, including Cedar Creek, Crockett streamgage region, and Lake Livingston region
TRWD PMF (2013)		Trinity River upstream of Dowdy Ferry Road (near Hutchins) to headwaters of Lake Livingston	Upper model, between Rosser and Cedar Creek Pkwy streamgages,
LiDAR Acquisition and Flow Assessment for the Middle Trinity River (2015)	1400011696	Multiple site models: 080444 (Dallas), 080295 (Oakwood), 080075 (Romayor)	Lower model, downstream of Romayor streamgage

3.2 Terrain and Model Cross Section Generation

The HEC-RAS models developed for this project incorporate LiDAR-derived digital elevation model (DEM) terrains as well as Trinity River in-channel bathymetric survey data collected by TRA.

The DEM terrains, covering the full extent of both models, are composed of available LiDAR-derived DEM tiles obtained from the Texas Natural Resources Information System (TNRIS[1]) for the upper HEC-RAS model, and the LiDAR-derived DEM generated from TRA 2016 for the lower HEC-RAS model. DEM datasets used in the upper HEC-RAS model are presented in Figure 3-4 and in Appendix 6 and Appendix 7.

A mosaic of available LiDAR-derived DEMs was created for the upper HEC-RAS model. If DEM data overlapped, the most recent dataset was prioritized. The only exception was the 2017 Neches Basin LiDAR dataset, which was prioritized over the 2018 Eastern Texas LiDAR dataset. The Eastern LiDAR data were collected when the Trinity River's water surface was elevated due to recent storm events, leaving significantly less elevation data on channel banks compared to the Neches data.

[1] https://tnris.org/

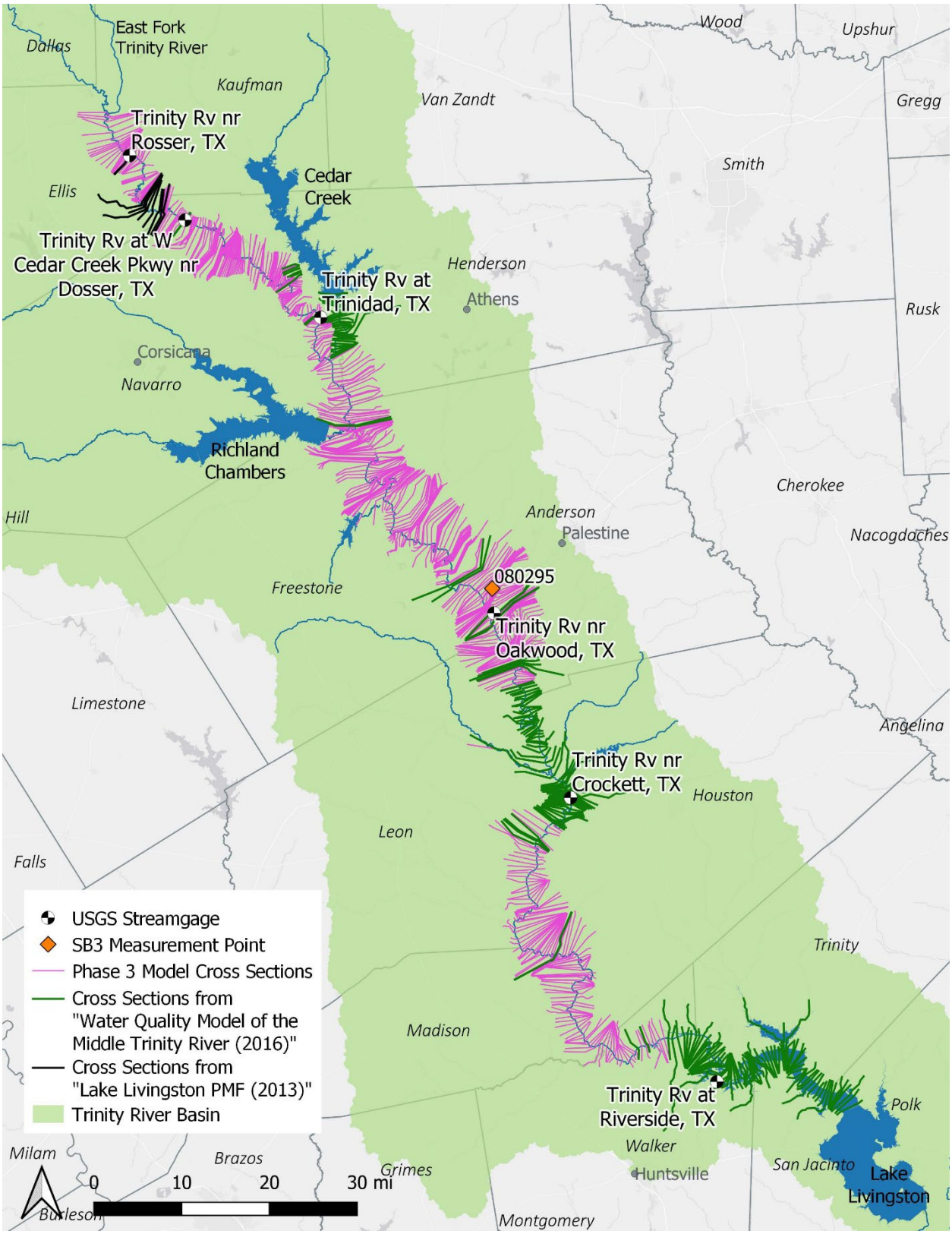

Figure 3-2. Upper model cross sections created in this study and previous model cross sections and their sources.

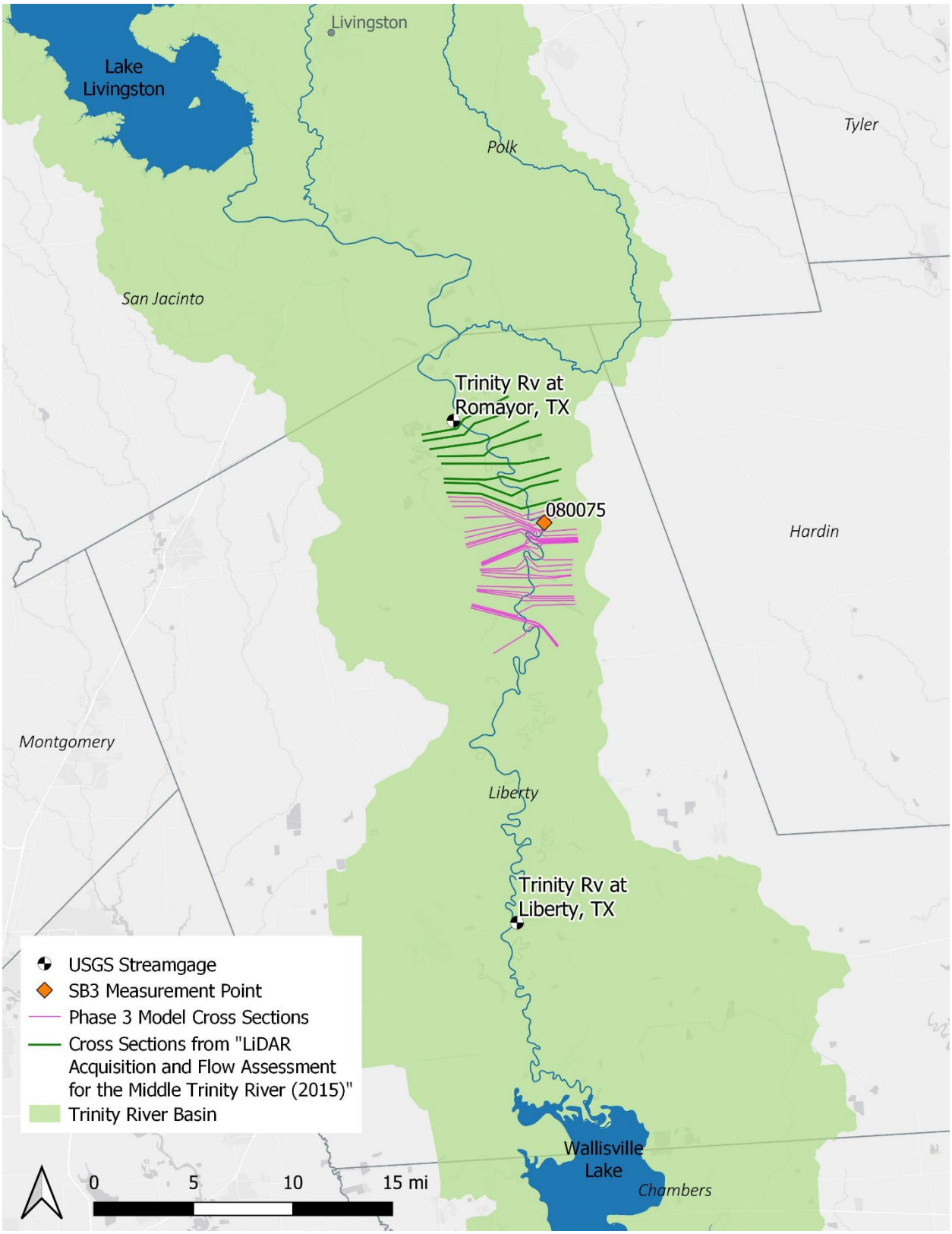

Figure 3-3. Lower model cross sections created in this study and previous model cross sections from the LiDAR Acquisition and Flow Assessment for the Middle Trinity River (2015).

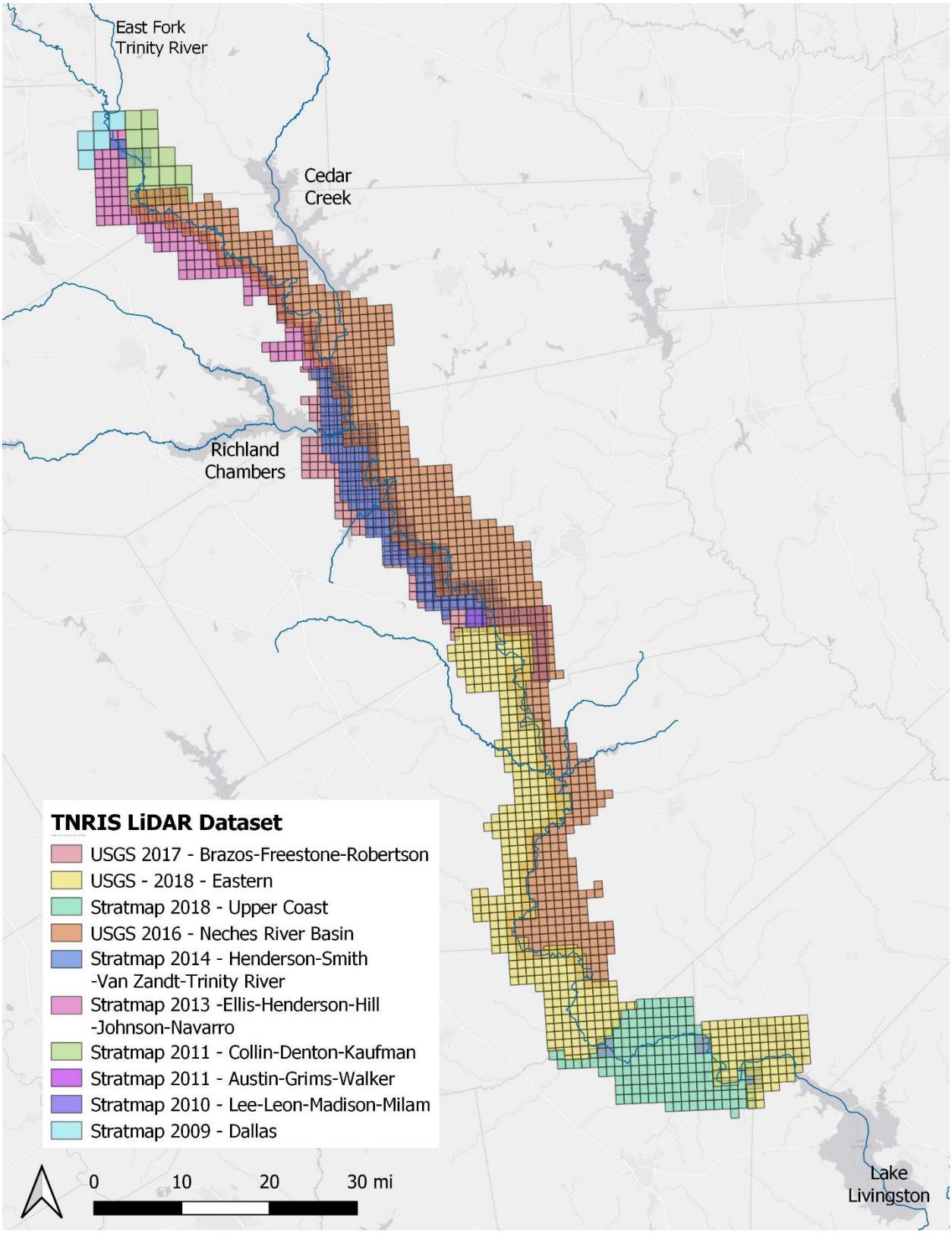

Figure 3-4. LiDAR tiles used to develop upstream RAS model.

TRA bathymetry data were used to represent in-channel bottom elevations within the HEC-RAS upper model. These data were collected perpendicular to the Trinity River at approximately ½ river mile increments, from the USGS Trinity River near Rosser streamgage to the headwaters of Lake Livingston. A gap of approximately 29 river miles upstream and downstream of the USGS Trinity River near Crockett streamgage does not have any in-channel bathymetry data. A gap of approximately 9 river miles between the USGS Trinity River near Rosser and USGS Trinity River at W Cedar Creek Pkwy near Dosser streamgages also does not have any in-channel bathymetry data. The TRA DEM (2016) for the lower model incorporates TRA collected in-channel longitudinal bathymetry data from 2011, and TRA collected site survey data from 2017.

The mosaic LiDAR DEMs and TRA collected bathymetry data were used to create cross sections within RiverGIS[1], a QGIS plugin similar to HEC-GeoRAS. Cross sections were created at approximately ½ river mile increments, aligned with existing TRA in-channel bathymetry data. When data sources overlapped, in-channel bathymetry data were prioritized over LiDAR-derived DEM data, which does not penetrate the water surface.

Any locations in the model without TRA in-channel bathymetry used cross sections from previous HEC-RAS models (Figure 3-2 and Figure 3-3) for the upper and lower models, respectively. These cross sections were unaltered and do not include updates for recent LiDAR DEM data for overbank areas.

For each model (upper and lower), streamlines were manually edited to follow the river channel observable in the most recent LiDAR-based DEM. Channel banks were based on previous model geometries or the underlying terrain, as appropriate. Manning's 'n' values were assigned based on previous model geometries, and updated during model calibration, as described below. Finally, ineffective flow areas were assigned based on previous model geometries and cross section geometry, where appropriate.

3.3 Water Quality Models

Upper and Lower HEC-RAS calibrated 1-D hydraulic models created for this project were used to create HEC-RAS water quality simulations to evaluate temperature and dissolved oxygen and how they relate to stated water quality goals from RPS, 2015. Tier 1 stated water quality goals are used to identify critical instream conditions that would have an adverse effect on native aquatic species, and are based on values identified by the Texas Instream Flow Program. Tier 2 stated water quality goals are used to identify satisfaction of current state water quality standards, as determined by the TCEQ surface water quality assessment program. Table 3-2 details stated water quality goals for the three segments of the Trinity River included in the model. These goals are taken from RPS, 2015 and are extended to Segment 0802 Trinity River Below Lake Livingston using the same criteria. An Upper water quality model was already available from RPS and was refined as part of this project. A Lower water quality model was created for this project. Both models used unsteady hydraulics with a 2-minute computation interval.

[1] http://rivergis.com/

Nine water quality models were run using Upper model hydraulics, representing nine different water quality scenarios. Eight of these scenarios were included in the last iteration of the water quality model for the Middle Trinity River from RPS, 2015. These eight scenarios were refined by using updated model hydraulics, primarily including significantly improved bathymetry collected by TRA as part of this project, and calibrated water quality model coefficients, and new results from these scenarios are presented here. An additional scenario called scenario I was included in this iteration of the model. Scenarios are designed to i) calibrate and validate the model, ii) test the impact of WWTP loadings on instream water quality, and iii) test the impact of SB3 environmental flows on water quality. Model results for temperature and dissolved oxygen were compared to identified water quality thresholds, specifically to appropriate Tier 1 primary priorities (Table 3-2) described in RPS 2015.

Five water quality models were run using Lower Model hydraulics, representing five different water quality scenarios. Model results for temperature and dissolved oxygen were compared to identified water quality thresholds, specifically to appropriate Tier 1 primary priorities and Tier 2 secondary priorities (Table 3-2) described in RPS 2015.

Table 3-2: SB2 Instream Flow water quality goals for Trinity River segments 0802, 0804, and 0805. Items with a * are preliminary indicators identified by SB2 TIFP stakeholders.

Parameter	Instream Flow Goals (Values)		
	Segment 0805 Upper Trinity River Cedar Creek Reservoir	**Segment 0804 Trinity River Above Lake Livingston**	**Segment 0802 Trinity River Below Lake Livingston**
Tier 1 Primary Priority			
DO (EC 2010)	<= 12 hours below 3 mg/L		
	<= 2 hours below 2 mg/L		
	> 1.5 mg/L		
Temperature (EC 2010)	<= 35°C (95°F)		
Tier 2 Secondary Priority			
DO (2014)	>5.0 mg/L daily average		
	=3.0 mg/L minimum for <= 8 hours		
	For Spring Condition:		
	>= 5.5 mg/L daily average		
	=4.5 mg/L minimum for <= 8 hrs		
	>=3.5 mg/L when headwater flow at USGS Gage 0804800 is <80 cfs		
Temperature*	<=27°C (80.6°F) Jan - May		
Temperature (2014)	<= 35°C (95°F)	<= 33.9° C (93°F)	
TSS	90th percentile		
Nitrate (2010b)	<= 1.95 mg/L		

Parameter	Instream Flow Goals (Values)		
	Segment 0805 Upper Trinity River Cedar Creek Reservoir	**Segment 0804 Trinity River Above Lake Livingston**	**Segment 0802 Trinity River Below Lake Livingston**
Ammonia (2010b)	<= 0.33 mg/L		
Orthophosphate (2010b)	<= 0.37 mg/L		
Tier 3 - additional parameters			
E. Coli (2014)	<= 126 org/100 mL geometric mean		
Total Nitrogen*	no value		
Nox* (2004)	<= 2.76 mg/L		
Organic Nitrogen*	no value		
Total Phosphorous (2010b)	<= 0.69 mg/L		
Chlorophyll-a (2010b)	<= 14.1 mg/L		
Salinity*	<= 2 ppt		
Chloride (2014)	<= 175 mg/L	<= 150 mg/L	<= 125 mg/L
Sulfate (2014)	<= 175 mg/L	<= 150 mg/L	
Specific Conductance (2010b)	<= 3077 uS/cm		
pH (2014)	6.5-9.0		
TDS (2014)	<= 850 mg/L	<= 600 mg/L	

3.3.1 Water Quality Data

Numerous sources of water quality data collected over multiple years were incorporated into the upper and lower water quality models. Model inputs were derived from TRA and TCEQ grab samples, USGS flows and TCEQ records for TPDES discharges. Comparison of model predictions to observations at downstream locations are based on observations from TRA grab samples, TRA long-term deployment sondes, TCEQ SWQM records and USGS flow and water quality records. Model inputs at the upstream boundary condition were derived from observation data, interpolated between observation dates, or were calculated from available observed constituents as follows:

- Temp (°C)
- DO (mg/L)
- CBOD (mg/L) = BOD20 (mg/L); (or, = 2.3*BOD5(mg/L)
- Algae (mg/L) = Chl-a (ug/L) / 11.1
- NH4 (mg/L)
- NO2 (mg/L)
- NO3 (mg/L)
- OrgN (mg/L) = TKN – NH4; (or, = TN – NO3 – NH4)
- Orthophosphate (mg/L)
- OrgP (mg/L) = TP – Orthophosphate (mg/L)

Model inputs for each scenario are tabulated in Appendix 6 for the Upper Model and Appendix 7 for the Lower Model.

3.3.2 Wastewater Treatment Plant Inputs

Wastewater Treatment Plant (WWTP) discharge data were included for a number of water quality modeling scenarios, which are defined and discussed further in Section 3.5. The factors that were considered when identifying which WWTPs to include in the model were: 1) distance from the mainstem of the Trinity River, 2) if it was within the model extents, 3) the maximum permitted discharge amount, and 4) the proportion of its nutrient load compared against normal loads in the Trinity River. After reviewing these factors no WWTP discharge data were included in the lower model, while Table 3-3 lists the five WWTPs included in the upper model. All WWTP data were accessed from EPA Environmental and Compliance History Online (Echo) and were available as monthly average data (2020). No temperature data were available for any WWTP, so all WWTP flow input temperatures were estimated to be 30 °C. These data were represented within the water quality model either as lateral inflow locations or combined with the upper boundary condition input data.

Table 3-3. WWTP discharge data and sites included in the upper water quality model.

WWTP Name	TPDES No.	Model Cross Section Location	Maximum Permitted Discharge (cfs)	Incorporated Water Quality Parameters[1]
TRA Ten Mile	TX0022811	Upper boundary condition/headwaters	37.1	Flow, DO, BOD, NH4, TSS
Freestone Power	TX0123935	1009019	1.9	Flow, TSS
TDCJ Coffield	TX0031577	900194.3	4.4	Flow, DO, BOD, NH4, TSS
TDCJ Beto	TX0075388	849825.3	2.2	Flow, DO, BOD, NH4, TSS
TDCJ Ferguson	TX0031615	274701.3	1.5	Flow, DO, BOD, NH4, TSS

[1] Flow = discharge, DO = dissolved oxygen, BOD = 5-day carbonaceous biochemical oxygen demand, NH4 = total ammonia nitrogen, TSS = total suspended solids

3.3.3 Upper Water Quality Model Results

The existing Upper Model water quality simulation has been calibrated and refined, and subsequently used to evaluate water quality for the reach with an upstream boundary near the confluence with East Fork Trinity River and Trinity Falls near Rosser, TX, and a downstream boundary in the headwaters of Lake Livingston.

The Upper Model was calibrated using scenario B, which includes historical flows and historical WWTP inputs for June 1st, 2014 to September 30th, 2014. Scenario I included historical flows and historical WWTP inputs for June 1st, 2018 to September 30th, 2018, and was used as a validation of the model calibration. This validation included new observation data collected by TRA for this project. Calibration and validation results were deemed satisfactory given limitations in input data detailed in Appendix 8. The calibrated water quality was subsequently used, in tandem with the updated model hydraulics, to re-run all scenarios from the original water quality model of the Middle Trinity River. Scenario names, objectives and goals are comparable to RPS 2015. Runs A, B and C model water quality in the Middle Trinity from June

1st, 2014 to September 30th, 2014 with no WWTP loading, existing conditions WWTP loading and fully-permitted WWTP loading, respectively. Runs D, E, F and G simulate Trinity River SB3 environmental flows for "Subsistence Summer", "Subsistence Spring", "Base Summer" and "Base Spring" conditions, respectively, and fully-permitted WWTP loading to evaluate the impact of different SB3 flows on water quality with worst-case scenario WWTP loadings. Run H simulates fully-permitted WWTP loading for historical flows from June 1st, 2011 to September 30th, 2011, a period of drought conditions, to evaluate water quality impacts from fully-permitted WWTP loading during low-flow conditions. The basic details of each run and associated time periods used in analyses are included in Table 3-4. More information about hydraulic and water quality boundary conditions for each run is available in Appendix 6. Upstream boundary flow hydrographs for 2011, 2014 and 2018 are shown in Figure 3-5 with box callouts showing specific time periods used for analyses. Figure 3-6 compares low-flow magnitudes for these periods.

Table 3-4: Run details for Upper water quality model scenarios A-I.

Run/Period	Time	Description	Reason for Scenario
A	Summer 2014	2014 Flow Conditions; No WWTP Discharges	Impact of existing WWTP conditions
B	Summer 2014	2014 Flow Conditions; Current conditions WWTP Discharges; Calibration	Existing Conditions; Calibration of nutrient parameters; Baseline for comparisons
B1	8/23/2014 - 8/31/2014	Ten-day lowest stable flow period	-
B2	8/27/2014 - 9/27/2014	Observation Period	-
C	Summer 2014	2014 Flow Conditions; Fully-permitted WWTP Discharges	Predict impact of fully-permitted WWTP discharges
D	Oakwood Subsistence Summer	Run C with constant headwater at 75 cfs; Fully-permitted WWTP Discharges	Predict impact of coincident fully-permitted WWTP discharges and Subsistence Summer flow conditions
E	Oakwood Subsistence Spring	Run C with constant headwater at 160 cfs; Fully-permitted WWTP Discharges	Predict impact of coincident fully-permitted WWTP discharges and Subsistence Spring flow conditions

Run/Period	Time	Description	Reason for Scenario
F	Oakwood Base Summer	Run C with constant headwater at 250 cfs; Fully-permitted WWTP Discharges	Predict impact of coincident fully-permitted WWTP discharges and Base Summer flow conditions
G	Oakwood Base Spring	Run C with constant headwater at 450 cfs; Fully-permitted WWTP Discharges	Predict impact of coincident fully-permitted WWTP discharges and Base Spring flow conditions
H	Summer 2011	2011 Flow Conditions; Fully-permitted WWTP Discharges	Worst-case scenario (i.e. lowest historical flows) impact of Fully-permitted WWTP discharges
H1	6/1/2011 - 8/31/2011	Entire Simulation Period	-
H2	8/1/2011 - 8/11/2011	Ten-day lowest stable flow period	-
I	Summer 2018	2018 Flow Conditions; Current conditions WWTP Discharges; Validation	Validation of model calibration
I1	6/26/2018 - 7/12/2018	Observation Period	-
I2	6/19/2018 - 9/30/2018	Entire Simulation Period	-

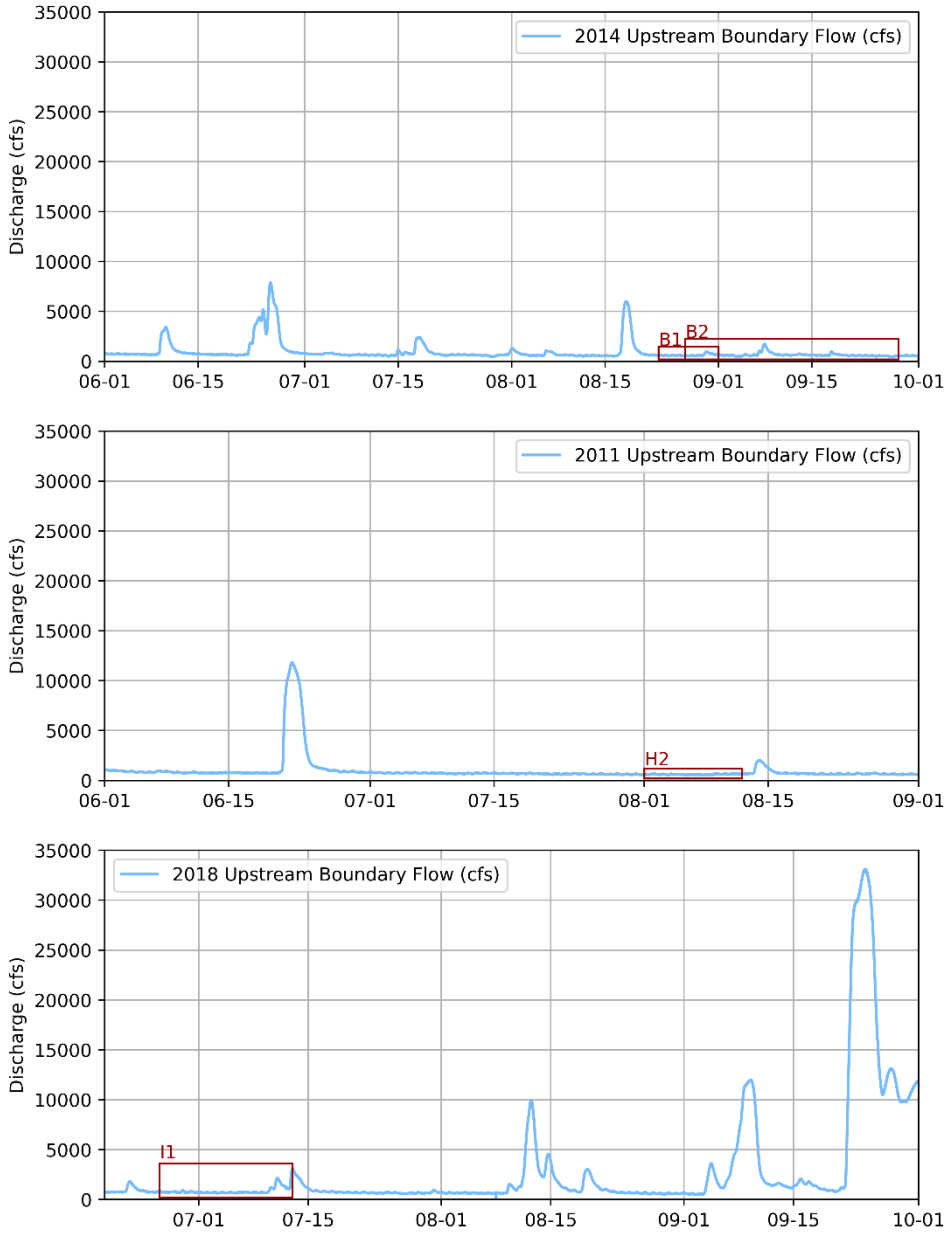

Figure 3-5: Top: 2014 Upstream boundary flow hydrograph, used for Runs A-G, with analysis periods B1 and B2 detailed in red. Middle: 2011 Upstream boundary flow hydrograph, used for Run H, with analysis periods H2 detailed in red. Bottom: 2018 Upstream boundary flow hydrograph, used for Run I, with analysis periods I1 detailed in red.

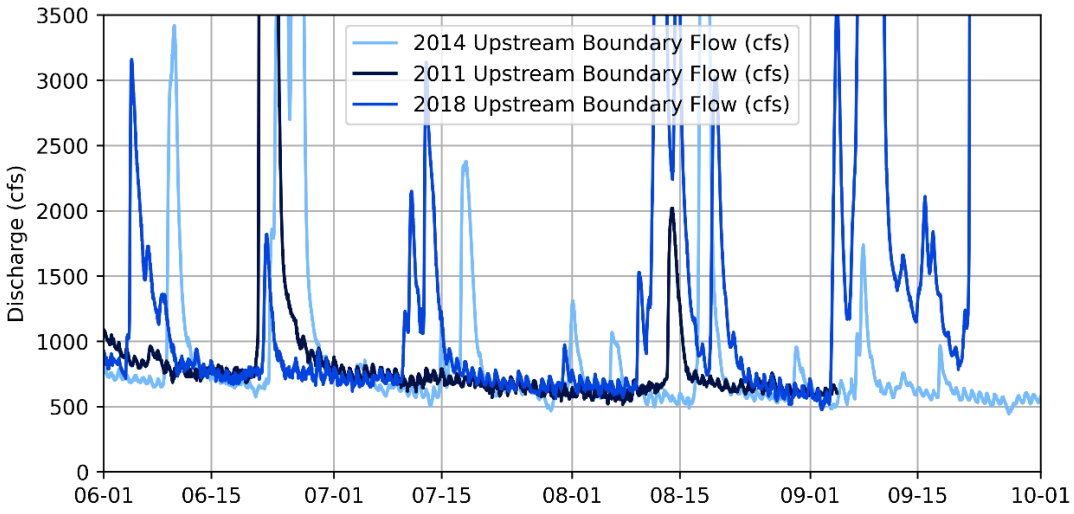

Figure 3-6: 2011, 2014 and 2018 flow conditions used for Runs H, A-G and I, respectively. Axis cut off at 3,500 cfs to compare low flow magnitudes.

Impact of WWTP Loading

Using calibrated nutrient parameters from Run B, Runs A and C were performed to evaluate water quality in a no WWTP loading and a fully-permitted WWTP loading scenario and compare both with existing WWTP loading conditions. Figure 3-7 and Figure 3-8 detail temperature and dissolved oxygen at the Oakwood study site for each of these scenarios and Figure 3-9 and Figure 3-10 detail temperature and dissolved oxygen at the Crockett study site for each of these scenarios. Box and whisker plots of temperature and dissolved oxygen, shown in Figure 3-23 and Figure 3-24, compare the ranges of values for each of these scenarios. It is apparent at both sites that the addition of water from WWTP's does not greatly affect temperature. Dissolved oxygen is <0.1 mg/L lower at both sites for Run C with fully-permitted loadings from WWTP's included, though still far above the Tier 1 and Tier 2 priorities. There is minimal impact to both dissolved oxygen and temperature from existing conditions WWTP loadings. For this time

period, fully-permitted WWTP loadings were not shown to exceed Tier 1 Primary Priority water quality standards for temperature or dissolved oxygen.

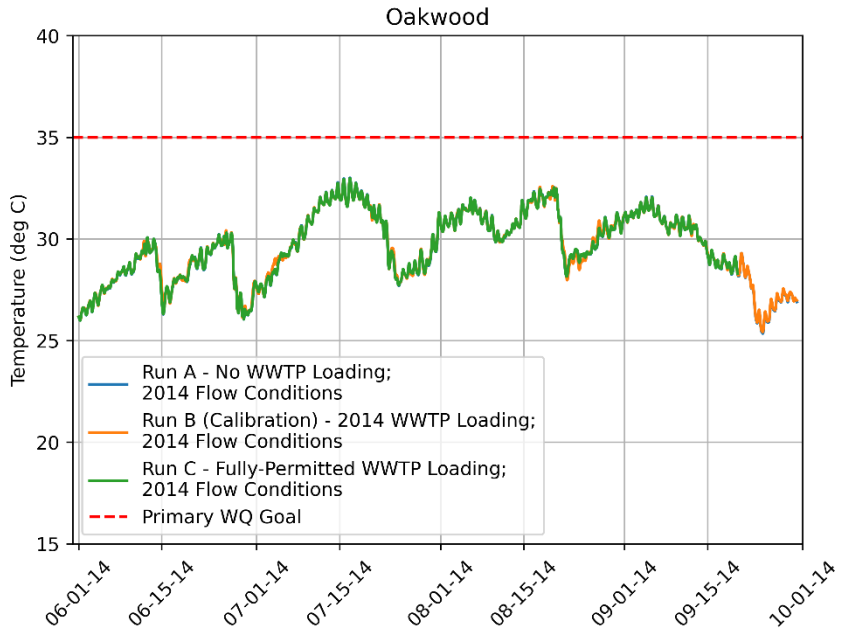

Figure 3-7: Run A, B and C temperature results at Oakwood study site. WWTP loading is shown to have little effect on temperature.

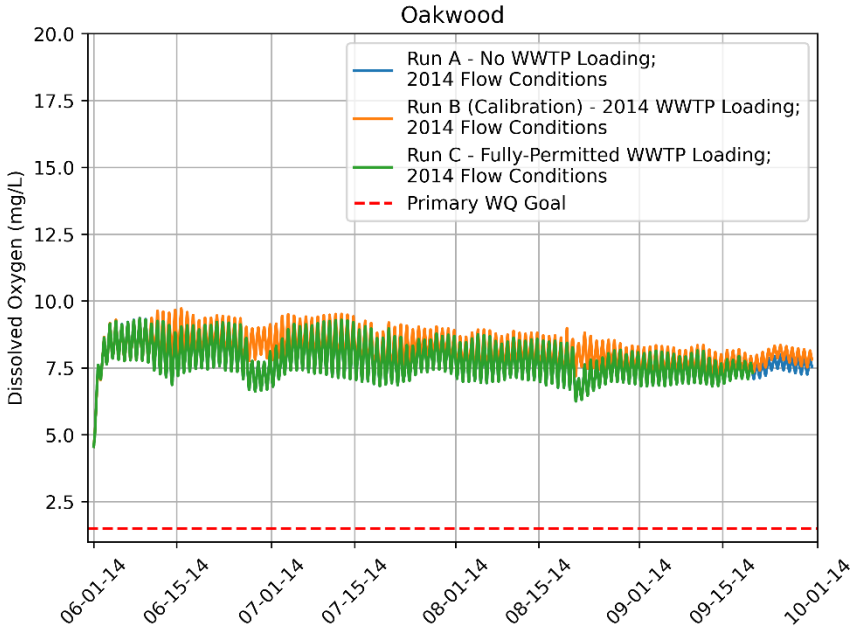

Figure 3-8: Run A, B and C dissolved oxygen results at Oakwood study site. Existing WWTP loading has little effect on dissolved oxygen levels. Fully-permitted WWTP loading causes a decrease of

~1 mg/L in dissolved oxygen. NOTE: The low values at the beginning of the model run are artificial and part of the model spin-up process.

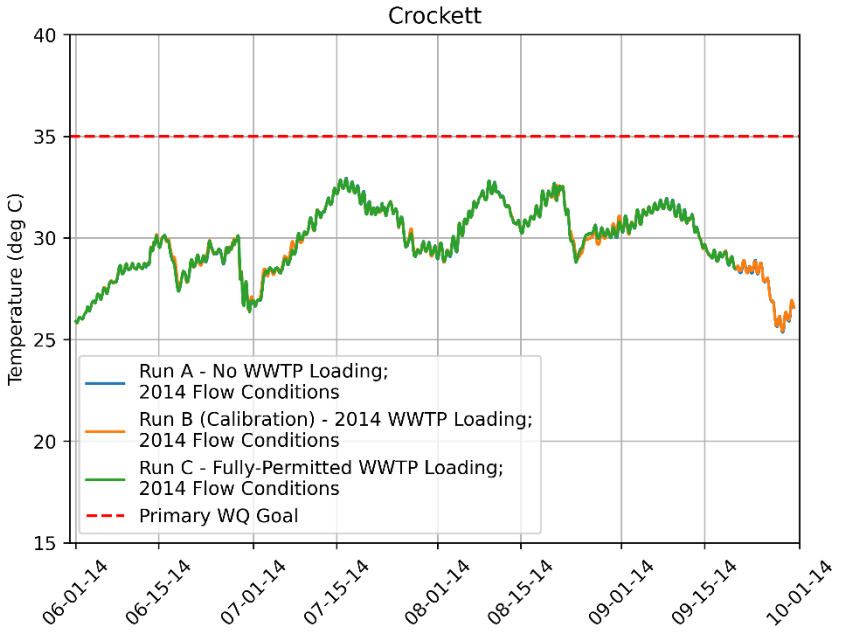

Figure 3-9: Run A, B and C temperature results at Crockett study site. WWTP loading is shown to have little effect on temperature.

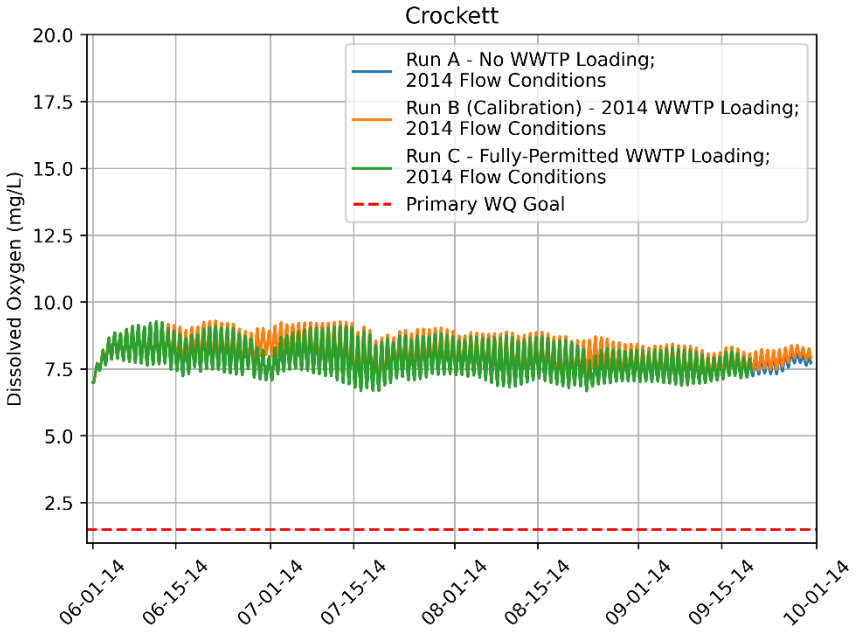

Figure 3-10: Run A, B and C dissolved oxygen results at Crockett study site. Existing WWTP loading has little effect on dissolved oxygen levels. Fully-permitted WWTP loading causes a decrease of

~1 mg/L in dissolved oxygen. NOTE: The low values at the beginning of the model run are artificial and part of the model spin-up process.

Run H was performed for a period in summer 2011 to evaluate water quality in a fully-permitted WWTP loading scenario during low-flow drought conditions, and compare it with a fully-permitted WWTP loading scenario during more normal summer flow conditions in 2014 (Run C). In other words, these scenarios compared identical WWTP loadings at record low flows (2011 - Run H) and a more normal summer low flow period (2014 - Run C). Figure 3-12 and Figure 3-13 detail temperature and dissolved oxygen at the Oakwood study site for each of these scenarios and Figure 3-14 and Figure 3-16 detail temperature and dissolved oxygen at the Crockett study site for each of these scenarios. Box and whisker plots of temperature and dissolved oxygen, shown in Figure 3-17 and Figure 3-18, compare the range of values simulated for the ten-day lowest stable flow period (H1: 8/1/2011 – 8/11/2011) and the full simulation period (H2: 6/1/2011 – 9/30/2011) to that of Run C.

It is apparent at both sites that temperature is typically between 2-4 °C higher and dissolved oxygen is similar at Oakwood and <0.5 mg/L lower at Crockett in the drought conditions scenario (Run H). The highest temperatures experienced in Run H coincide with the ten-day lowest stable flow period. Run H did exceed the identified Tier 1 Primary Priority temperature criteria at both study sites for between 2 and 4 weeks and by <1 °C. Interestingly, real-time, measured USGS temperature data at Crockett (15-minute) did not go above the Tier 1 threshold (35 degrees C) in 2011, which was the hottest and driest single year on record (Figure 3-15). High water temperatures during the Run H 2011 time period are primarily a result of higher air temperature and higher solar radiation model inputs acting on lower flows, as well as higher inflow water temperature at the upstream boundary. It is important to emphasize that this model does not incorporate any intervening flows from the watershed or tributaries between the upstream and downstream end of the model, which could lead to higher predicted flows and lower predicted temperatures. Additional work is needed to refine this model by adding some representation of intervening flows to determine if these results are realistic. As an example of the importance of the effects of intervening flows, seeps were noted along the river during field surveys (Figure 3-11), even during the record drought of 2011.

Figure 3-11: Groundwater contributions to the river observed along the Middle Trinity during the 2011 drought.

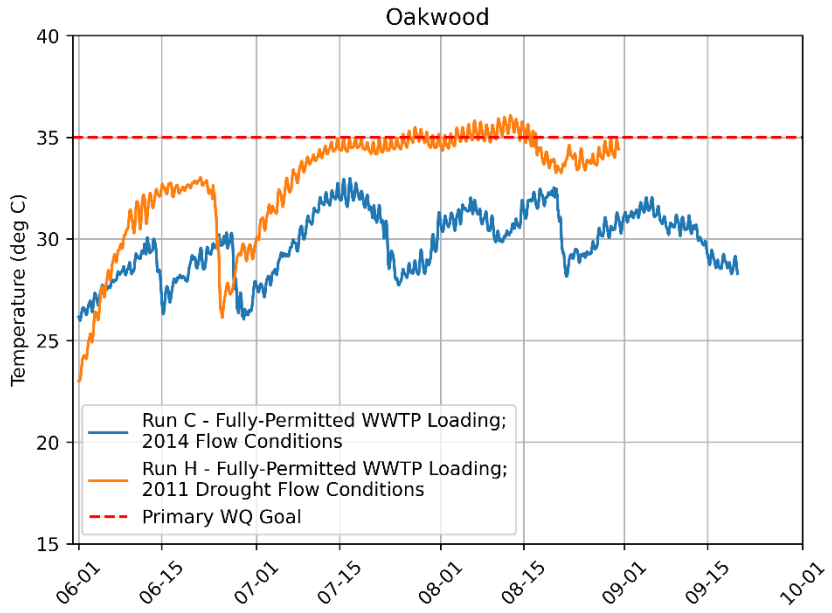

Figure 3-12: Run C and Run H temperature results at Oakwood study site. Water temperature is about 2-4 °C higher during 2011 flow (record drought) conditions.

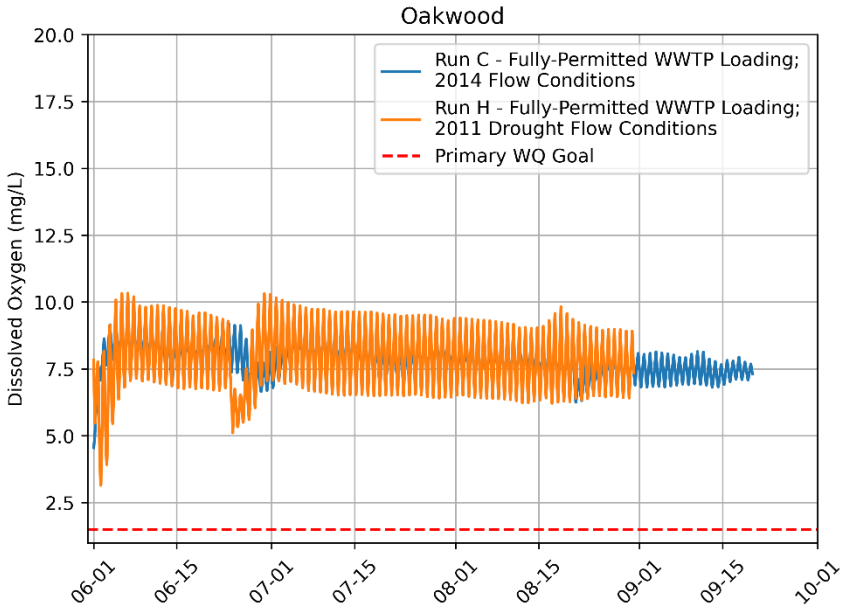

Figure 3-13: Run C and Run H dissolved oxygen results at Oakwood study site. Dissolved oxygen is similar to or, at times, about 1 mg/L lower during 2011 flow conditions. NOTE: The low values at the beginning of the model run are artificial and part of the model spin-up process.

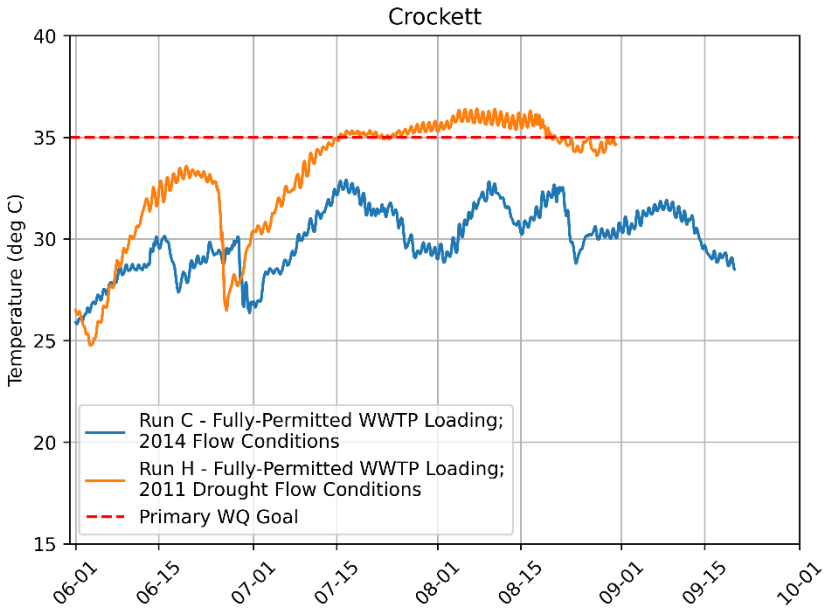

Figure 3-14: Run C and Run H temperature results at Crockett study site. Water temperature is about 2-4 °C higher during 2011 flow conditions.

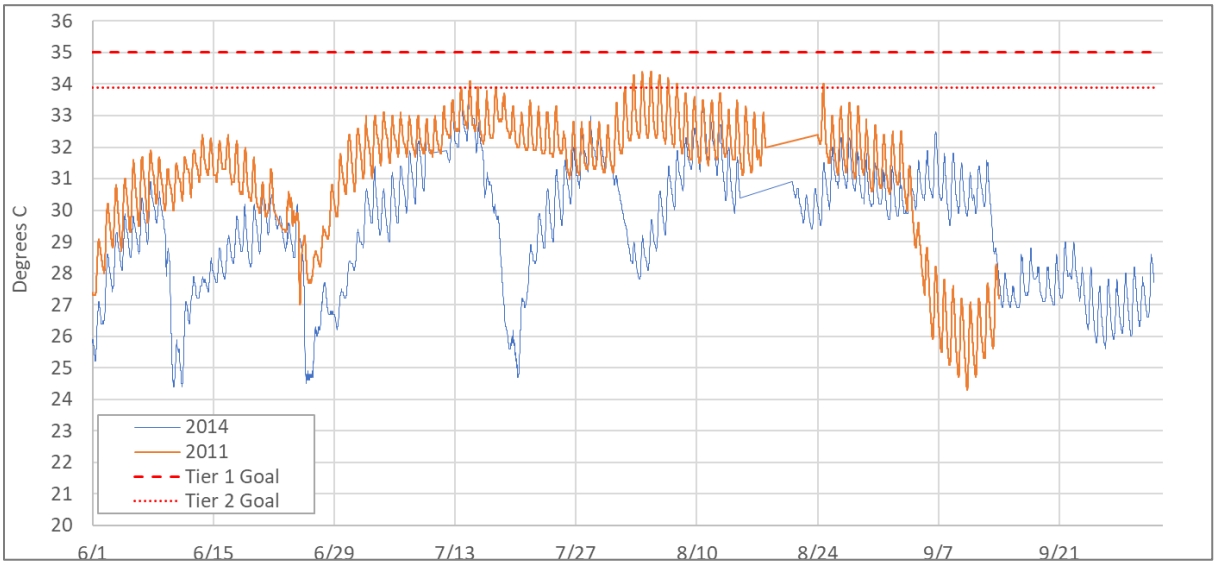

Figure 3-15. Real-time temperature at the USGS gage at Crockett for 2011 and 2014. Note: Even during the record summer of 2011, the measured data did not cross the 35-degree C threshold Tier 1 goal.

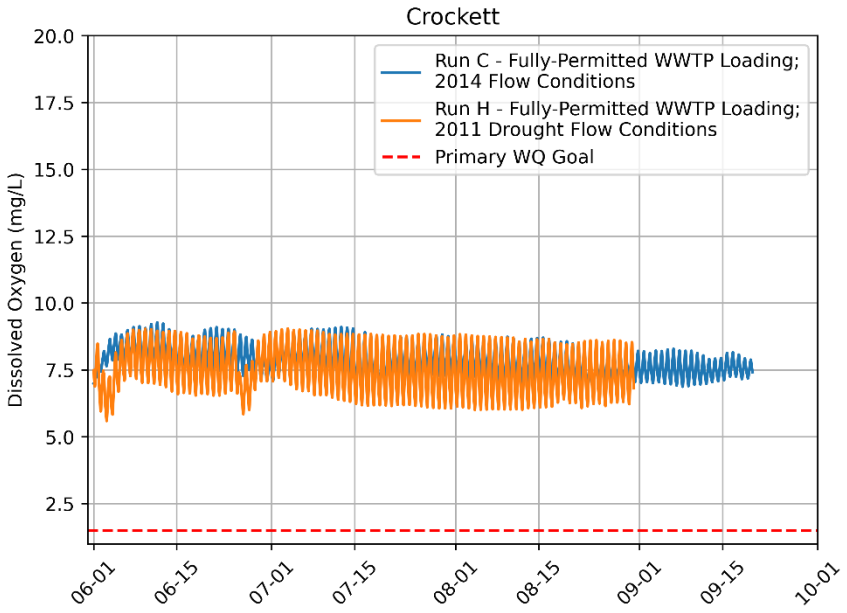

Figure 3-16: Run C and Run H dissolved oxygen results at Crockett study site. Dissolved oxygen is <0.5 mg/L lower during 2011 flow conditions. NOTE: The low values at the beginning of the model run are artificial and part of the model spin-up process.

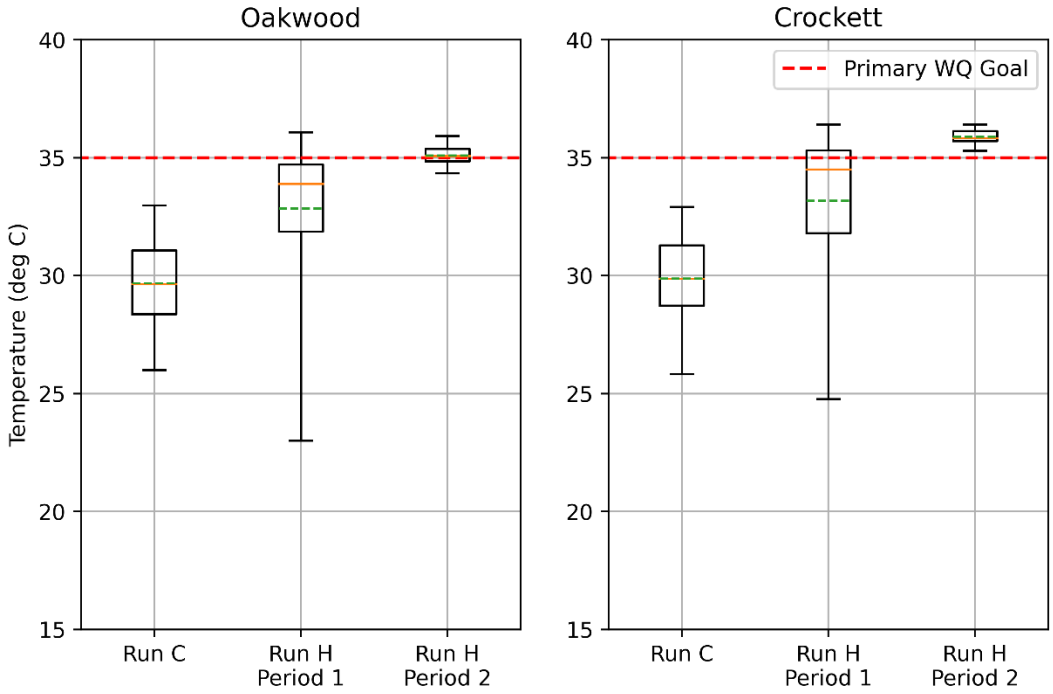

Figure 3-17: Box and whisker plots of Run H temperature results for the ten-day lowest stable flow period (H1) and the full simulation period (H2), and Run C temperature results for the full simulation period. During summer 2011 low-flow conditions, there is a wider range of temperatures experienced and the average temperature is about 3 °C higher at both sites than for summer 2014 flow conditions. The average temperature was 35-36 °C during period H1, the ten-day lowest stable flow period for 2011 conditions – note that period H1 is a sub-period of period H2, and that it represents the most extreme period (lowest flows) of the worst-case scenario Run H. Orange lines represent sample medians, green dashed lines represent sample averages, boxes represent interquartile range (25th percentile – 75th percentile) and whiskers represent sample maximum and minimum.

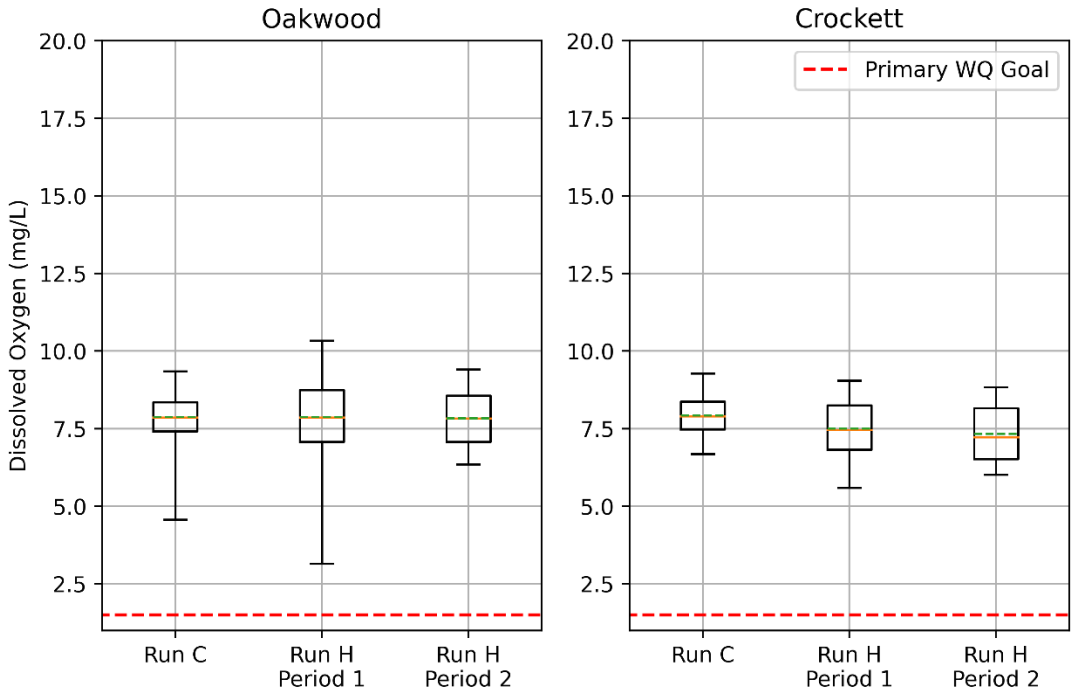

Figure 3-18: Box and whisker plots of Run H dissolved oxygen results for the ten day lowest stable flow period (H1) and the full simulation period (H2), and Run C dissolved oxygen results for the full simulation period. Dissolved oxygen results were similar for summer 2011 and summer 2014 flow conditions at Oakwood and they were <0.5 mg/L lower at Crockett. Dissolved oxygen was not significantly lower in Run H during the ten-day lowest stable flow period for 2011 conditions. Orange lines represent sample medians, green dashed lines represent sample averages, boxes represent interquartile range (25th percentile – 75th percentile) and whiskers represent sample maximum and minimum.

Impact of SB3 Environmental Flows

Model runs D, E, F and G with mainstem flows set to constant headwaters of discharges specified for SB3 “Subsistence Summer”, “Subsistence Spring”, “Base Summer”, and “Base Spring” flow conditions and fully-permitted WWTP loadings were run and are compared with Run C below to assess their impact on water quality in the worst-case WWTP loadings scenario.

Figure 3-19 and Figure 3-20 detail comparisons of temperature and dissolved oxygen for each scenario at the Oakwood study site, and Figure 3-21 and Figure 3-22 detail comparisons of temperature and dissolved oxygen for each scenario at the Crockett study site. Box and whisker plots of temperature and dissolved oxygen, shown in Figure 3-23 and Figure 3-24, compare the ranges of values for all of the Upper Model scenarios.

Temperatures were higher most of the time for all four SB3 runs than they were for Run C (more normal summertime flows). Dissolved oxygen was nearly always 1-1.5 mg/L lower in Runs D and E than it was in Run C at both sites, but minimal impact was observed in Runs F and G. The relative impact of each scenario consistently scaled with the magnitude of the reduction in flow, i.e. impacts were greatest for the "Subsistence Summer" scenario D and least for "Spring Base" scenario G (Figure 3-25). Temperatures approached but did not actually exceed the Tier 1 Primary priority temperature value in any of these scenarios, but did exceed Tier 2 (33.9 C) for Summer Subsistence and Spring Subsistence at both sites (Figure 3-23 and Figure 3-25). Dissolved oxygen values did not drop below the identified Tier 1 criteria in any scenarios.

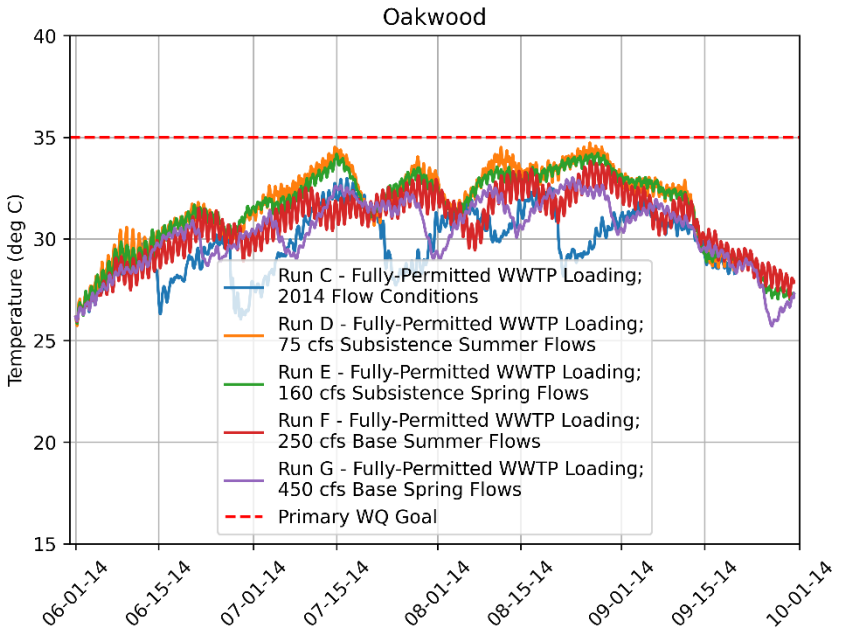

Figure 3-19: Run C, D, E, F and G temperature results at Oakwood study site. As expected, water temperature was consistently higher for SB3 Environmental flows than for summer 2014 flow conditions, and the magnitude of the increase scaled with the magnitude of the reduction in flow.

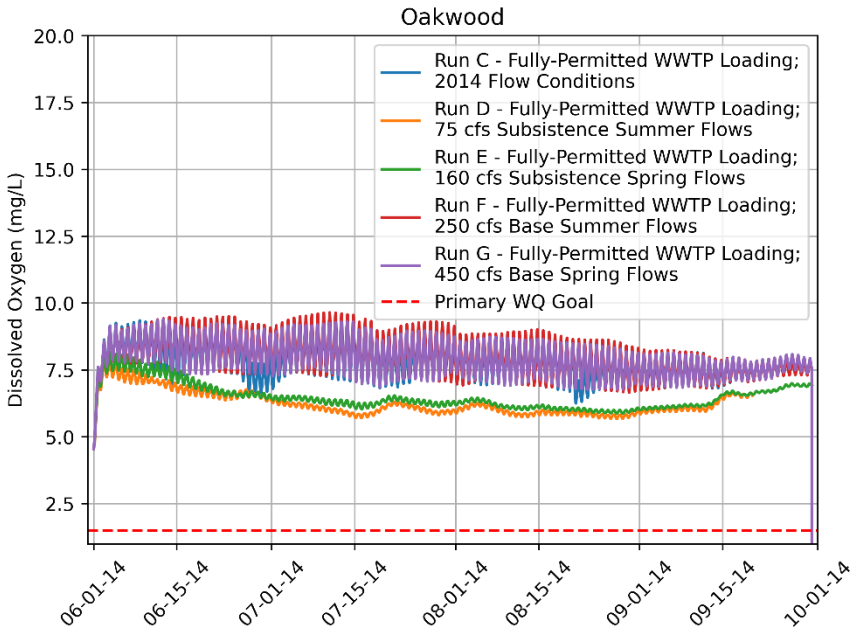

Figure 3-20: Run C, D, E, F and G dissolved oxygen results at Oakwood study site. Dissolved oxygen remained relatively similar for SB3 Base Summer and Base Spring flows compared to summer 2014 flow conditions. Dissolved oxygen was about 2 mg/L lower for Subsistence Summer and Subsistence Spring flows compared to summer 2014 flow conditions, but still above the Tier 1 and Tier 2 targets. NOTE: The low values at the beginning of the model run are artificial and part of the model spin-up process.

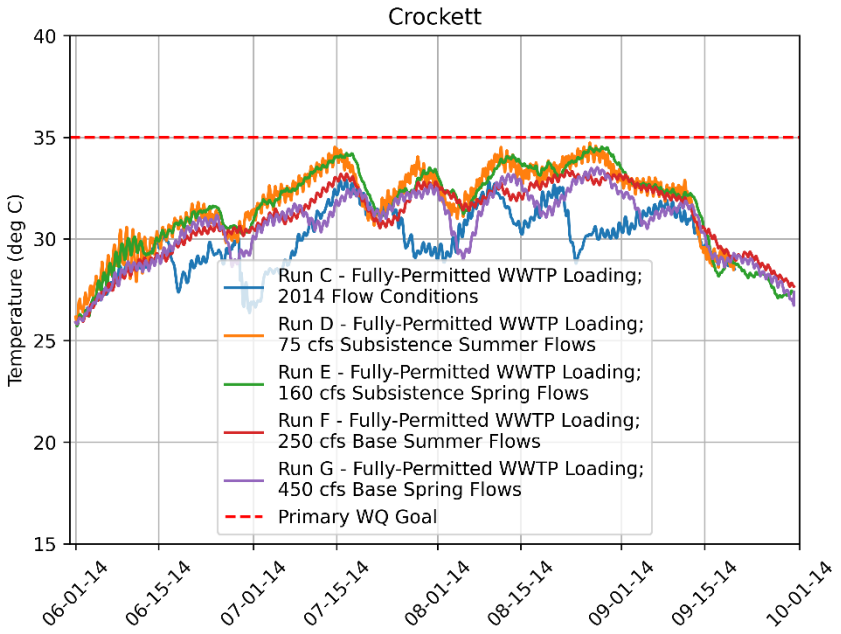

Figure 3-21: Run C, D, E, F and G temperature results at Crockett study site. As expected, water temperature was consistently higher for SB3 Environmental flows than for summer 2014 flow conditions, and the magnitude of the increase scaled with the magnitude of the reduction in flow.

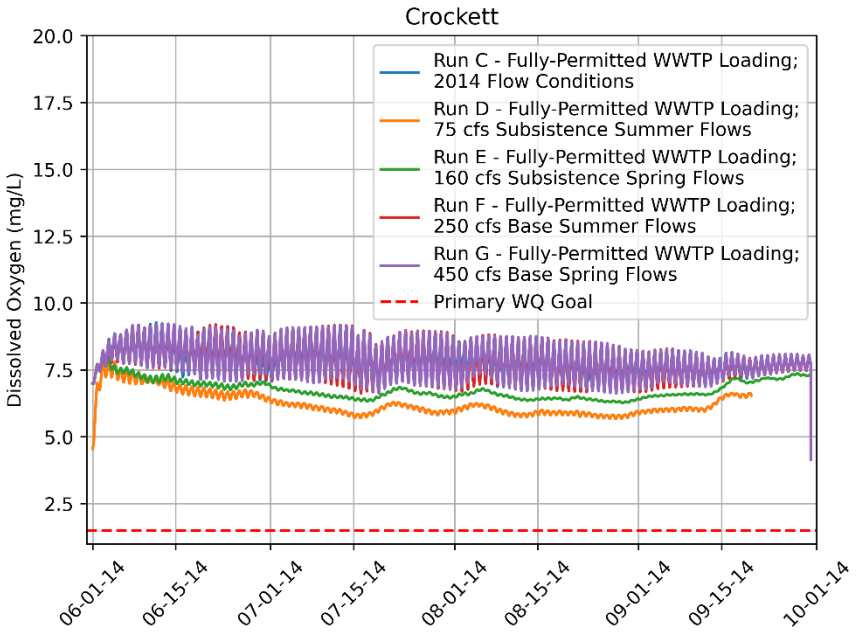

Figure 3-22: Run C, D, E, F and G dissolved oxygen results at Crockett study site. Dissolved oxygen remained relatively similar for SB3 Base Summer and Base Spring flows compared to Summer 2014 flow conditions. Dissolved oxygen was about 1-2 mg/L lower for Subsistence

Summer and Subsistence Spring flows compared to summer 2014 flow conditions. NOTE: The low values at the beginning of the model run are artificial and part of the model spin-up process.

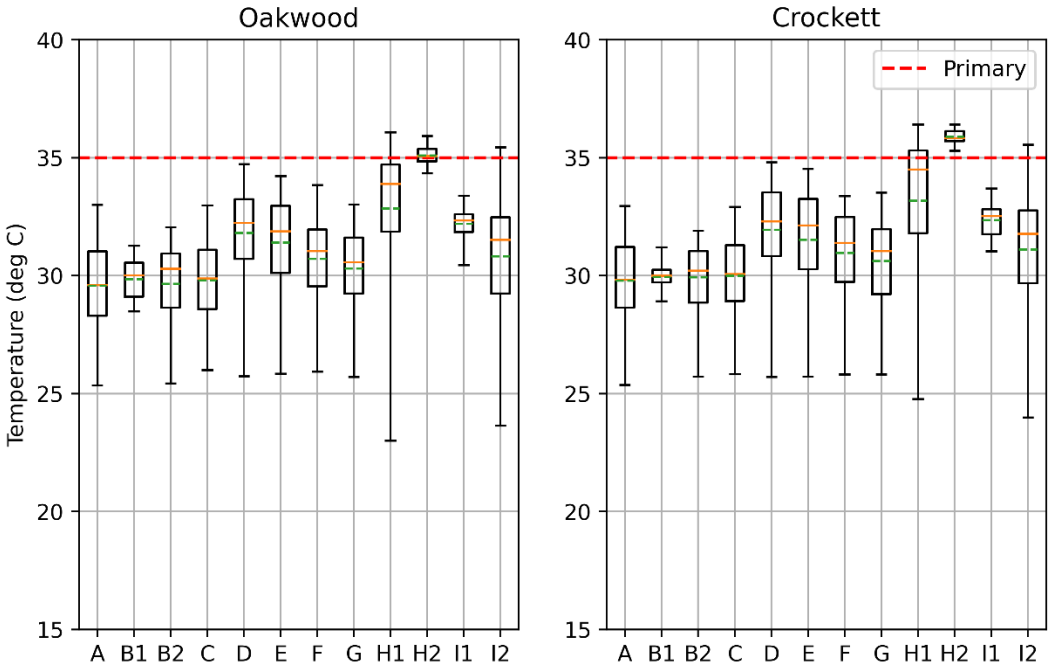

Figure 3-23: Box and whisker plots of temperature results for all scenarios and periods within scenarios. Orange lines represent sample medians, green dashed lines represent sample averages, boxes represent interquartile range (25th percentile – 75th percentile) and whiskers represent sample maximum and minimum. Temperatures were higher for Runs D-G with SB3 Environmental Flows than for Run C with 2014 flow conditions, with the magnitude of the impact scaling with the magnitude of the reduction in flow. The highest temperatures predicted by the model were for Run H with summer 2011 flow conditions, and did cross Tier 1 Primary Priority Water Quality thresholds for temperature during period H1 (which is a sub-period within period H2). Note that the period of Run H during which water temperature exceeded the Tier 1 Primary Priority Water Quality threshold was the ten-day lowest stable flow period of the worst-case scenario run.

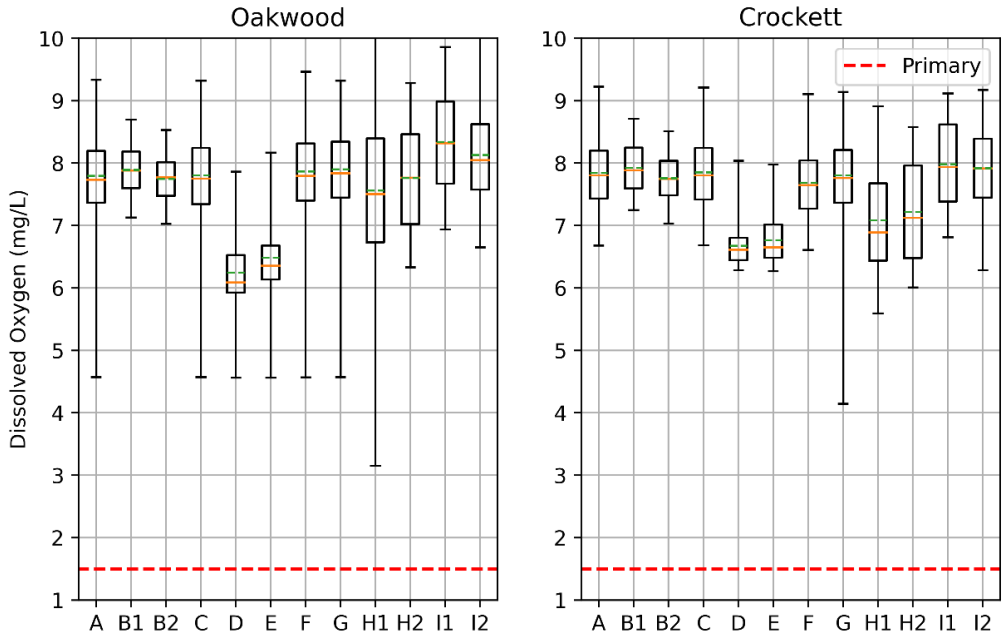

Figure 3-24. Box and whisker plots of dissolved oxygen results for all scenarios and periods within scenarios. Orange lines represent sample medians, green dashed lines represent sample averages, boxes represent interquartile range (25th percentile – 75th percent).

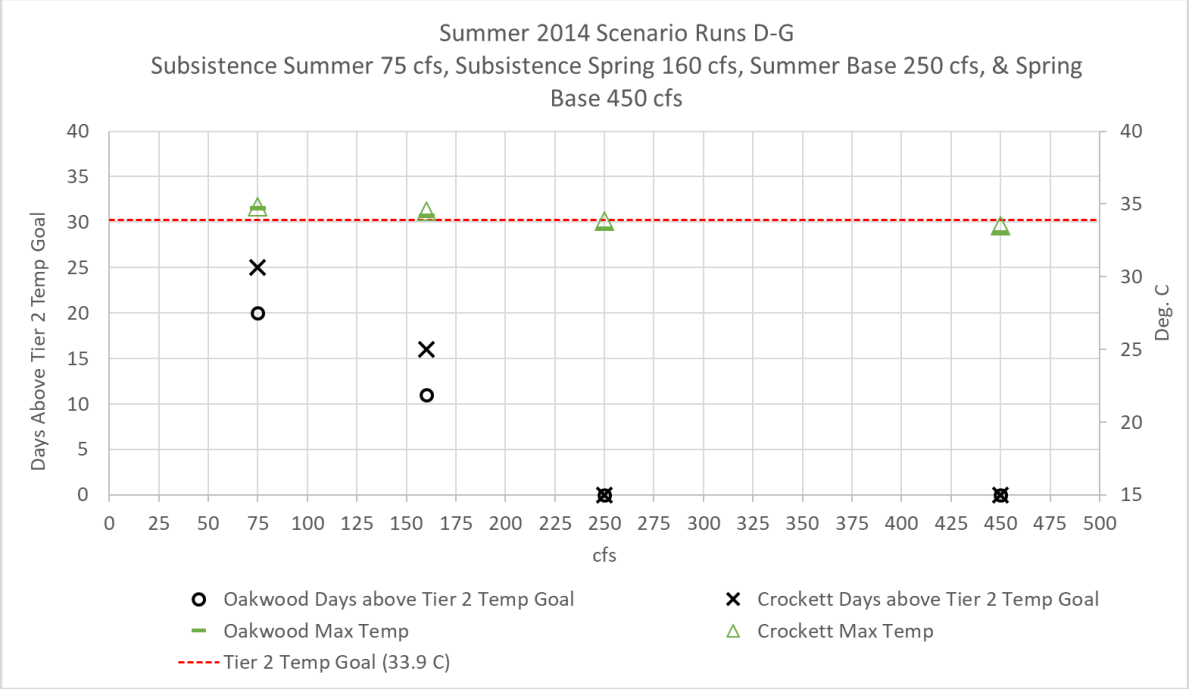

Figure 3-25. Graph comparing days above Tier 2 priority to streamflow and maximum temperature.

3.3.4 Upper Model Discussion

The Upper and Lower Trinity models have some limitations, most of which arise from a sparsity of observational data that can be used 1) as model inputs or 2) as calibration data, that are described elsewhere in this report. This is a common problem in environmental modeling, especially when attempting to represent spatially extensive systems. In the case of these models, the primary limitations are 1) a lack of representation of inflows and associated constituent loadings from intervening watersheds that flow into the Trinity mainstem downstream of the upper model boundary and 2) temporally-sparse data on constituent loadings in Trinity flows at the upper model boundary and in the model domain. Despite these limitations, this model is useful for examining the relative impacts of several different loading and flow scenarios, and, especially, for examining the predicted impact of low-flow conditions during hot, dry, summer conditions. Ultimately the model is in fact well-suited for the latter scenario, when flow is low on the mainstem and inflows from the intervening watershed are minimal, which is also the most critical scenario for high temperatures and low dissolved oxygen. So, while these limitations are pertinent to any consideration of model results, they are less of a concern when discussing model-predicted temperature and dissolved oxygen for low-flow summer condition scenarios.

The model suggests that existing WWTP loadings and fully-permitted WWTP loadings have negligible impact on temperature and dissolved oxygen, as shown by the ranges and average values of each variable for Run A, Run B Period 2 and Run C in Figure 3-23 and Figure 3-24.

As expected, modeled results also show that SB3 flows have an impact on temperature and, to a lesser extent, dissolved oxygen. Temperature was higher for Subsistence Summer, Subsistence Spring, Base Summer and Base Spring flows (Runs D, E, F and G) than it was for summer 2014 flow conditions with fully-permitted WWTP loadings (Run C), and the magnitude of the impact scaled consistently with the amount of the reduction in flow, as shown in Figure 3-23. Importantly, these flows still satisfy the Tier 1 water temperature priority of <35 degrees C. Dissolved oxygen was >10% lower for Subsistence Summer and Subsistence Spring flows (Run D and E) than it was for summer 2014 flow conditions with fully-permitted WWTP loadings (Run C), as shown in Figure 3-23. Dissolved oxygen levels were only slightly diminished for Base Summer and Base Spring flows (Run F and G) compared to summer 2014 flow conditions with fully-permitted WWTP loadings (Run C), as shown in Figure 3-24.
.

A model run with fully-permitted WWTP loadings and summer 2011 flow conditions showed that the impact of low flows, high air temperatures and high solar radiation from a period of record hot, drought conditions in the region had a significantly greater impact on temperature than both fully-permitted WWTP loadings and SB3 Environmental Flows. Average temperatures for fully-permitted WWTP loadings and summer 2011 flow conditions (Run H Period 1) were > 10% higher than for WWTP loadings and summer 2014 flow conditions (Run C) and 3-10% higher than for all of the SB3 Environmental Flows scenarios (Runs D, E, F and G). Unlike the SB3 Environmental Flows runs and the WWTP loading runs with summer 2014 flow conditions, the run with summer 2011 flow conditions does show temperatures exceeding, by about 1-2 °C, the Tier 1 Primary Priority Water Quality goals. This is true despite the fact that the flows are typically higher during this period than the Subsistence Summer flow of 75 cfs.

This result, however, should be interpreted with caution because of the aforementioned lack of watershed inputs in the model and the validation runs indicate that the calibrated model tends to overpredict, rather than underpredict, temperature (Figure 5-8 in Appendix 8. Water Quality Calibration and Modeling). The addition of watershed inputs into the model could significantly change temperature results by, in effect, diluting the flow that has been traveling through the mainstem with cooler water from tributaries and seeps[1].

Taken as a whole, these results suggest that the impacts of flow reductions from SB3 Environmental Flows are significantly more than those of WWTP loadings. They also suggest that temperatures would be higher during the worst-case scenario hot and dry historic conditions than for normal summer conditions at the SB3 Environmental Flows.

The modeling conducted for the Upper water quality model in this project indicates that SB3 environmental flows do have a significant impact on temperature and dissolved oxygen. It also indicates that they may cause water temperatures to cross Tier 1 Primary Priority Water Quality thresholds if they occurred during some of the hottest periods that have historically been observed in Texas. However, as mentioned previously, further refinement of the model is needed before definitive conclusions can be made. Results do not indicate that there is a significant risk from any of the scenarios tested of dissolved oxygen dropping below the Tier 1 Primary Priority Water Quality threshold of 1.5 mg/L.

Further refinement of the model is recommended. The model would benefit from the inclusion of some representation of intervening watershed hydrologic inputs with representative nutrient loadings and temperature information. These could be directly modeled using a watershed model like HEC-HMS or SWMM, or they could utilize existing functionality in HEC-RAS to estimate incremental inflows using internal flow boundaries. If the latter was implemented, refinement would also require some characterization of nutrient loadings and how they vary with input flow hydrographs, time of year, antecedent hydrologic conditions and other factors. Additionally, the model would benefit greatly from a better, more continuous representation of nutrient concentrations at its upstream boundary, as it already has for temperature and dissolved oxygen. This could be accomplished by performing a period of more frequent sampling and creating new model runs to coincide with that period or using some estimation technique to characterize representative nutrient concentrations for different flow magnitudes, different stages of the hydrograph, or different times of year and creating reasonable synthetic time series of nutrient concentrations at the upstream boundary.

[1] In the course of a river survey during the record drought of 2011, Trinity River Authority staff noted active seeps along the Middle Trinity River.

Table 3-5. Water quality modeling summary chart. Note: See text on the following page for additional detail.

				Oakwood							Crockett						
				Tier 1 Instream Flow Goals (RPS, 2015)				Selected Tier 2 Instream Flow Goals*			Tier 1 Instream Flow Goals (RPS, 2015)				Selected Tier 2 Instream Flow Goals*		
Run/Period	Time	Description	Reason for Scenario	<= 12 hours below 3 mg/L	<= 2 hours below 2 mg/L	> 1.5 mg/L	<= 35°C (95°F)	>5.0 mg/L daily average	=3.0 mg/L minimum for <= 8 hours	<= 33.9°C (95°F)	<= 12 hours below 3 mg/L	<= 2 hours below 2 mg/L	> 1.5 mg/L	<= 35°C (95°F)	>5.0 mg/L daily average	=3.0 mg/L minimum for <= 8 hours	<= 33.9°C (95°F)
				DO (mg/L)	DO (mg/L)	DO (mg/L)	Temp (Deg. C)	DO (mg/L)	DO (mg/L)	Temp (Deg. C)	DO (mg/L)	DO (mg/L)	DO (mg/L)	Temp (Deg. C)	DO (mg/L)	DO (mg/L)	Temp (Deg. C)
A	Summer 2014	2014 Flow Conditions; No WWTP Discharges	Impact of existing WWTP conditions	Y	Y	Y	Y	Y	Y	Y	Y	Y	Y	Y	Y	Y	Y
B	Summer 2014	2014 Flow Conditions; Current conditions WWTP Discharges; Calibration	Existing Conditions; Calibration of nutrient parameters; Baseline for comparisons	Y	Y	Y	Y	Y	Y	Y	Y	Y	Y	Y	Y	Y	Y
B1	8/23/2014 - 8/31/2014	Ten-day lowest stable flow period	-	Y	Y	Y	Y	Y	Y	Y	Y	Y	Y	Y	Y	Y	Y
B2	8/27/2014 - 9/27/2014	Observation Period	-	Y	Y	Y	Y	Y	Y	Y	Y	Y	Y	Y	Y	Y	Y
C	Summer 2014	2014 Flow Conditions; Fully-permitted WWTP Discharges	Predict impact of fully-permitted WWTP discharges	Y	Y	Y	Y	Y	Y	Y	Y	Y	Y	Y	Y	Y	Y
D	Oakwood Subsistence Summer	Run C with constant headwater at 75 cfs; Fully-permitted WWTP Discharges	Predict impact of coincident fully-permitted WWTP discharges and Subsistence Summer flow conditions	Y	Y	Y	Y	Y	Y	N	Y	Y	Y	Y	Y	Y	N
E	Oakwood Subsistence Spring	Run C with constant headwater at 160 cfs; Fully-permitted WWTP Discharges	Predict impact of coincident fully-permitted WWTP discharges and Subsistence Spring flow conditions	Y	Y	Y	Y	Y	Y	N	Y	Y	Y	Y	Y	Y	N
F	Oakwood Base Summer	Run C with constant headwater at 250 cfs; Fully-permitted WWTP Discharges	Predict impact of coincident fully-permitted WWTP discharges and Base Summer flow conditions	Y	Y	Y	Y	Y	Y	Y	Y	Y	Y	Y	Y	Y	Y
G	Oakwood Base Spring	Run C with constant headwater at 450 cfs; Fully-permitted WWTP Discharges	Predict impact of coincident fully-permitted WWTP discharges and Base Spring flow conditions	Y	Y	Y	Y	Y	Y	Y	Y	Y	Y	Y	Y	Y	Y
H	Summer 2011	2011 Flow Conditions; Fully-permitted WWTP Discharges	Worst-case scenario (i.e. lowest historical flows) impact of Fully-permitted WWTP discharges	Y	Y	Y	N	Y	Y	N	Y	Y	Y	N	Y	Y	N
H2	8/1/2011 - 8/11/2011	Observation Period	-	Y	Y	Y	N	Y	Y	N	Y	Y	Y	N	Y	Y	N
I	Summer 2018	2018 Flow Conditions; Current conditions WWTP Discharges; Validation	Validation of model calibration	Y	Y	Y	N	Y	Y	N	Y	Y	Y	N	Y	Y	N
I1	6/26/2018 - 7/12/2018	Observation Period	-	Y	Y	Y	Y	Y	Y	Y	Y	Y	Y	Y	Y	Y	Y

Notes for Table Above. :

- Run D - Temperature at Oakwood exceeded the Tier 2 goal on 20 days, with a max temperature of 34.73 degrees C. At Crockett, the Tier 2 temperature goal was exceeded on 25 days, with a max temperature of 34.81 degrees C.
- Run E - Temperature at Oakwood exceeded the goal on 11 days, with a max temperature of 34.2 degrees C. At Crockett, the temperature goal was exceeded on 16 days, with a max temperature of 34.5 degrees C.
- Run H - Temperature at Oakwood exceeded the Tier 1 goal of 35 degrees C for 25 days and the Tier 2 goal for 51 days, with a max temperature of 36.07 degrees C. At Crockett, the Tier 1 temperature goal was exceeded on 39 days and the Tier 2 goal for 53 days, with a max temp of 36.4 degrees C.
- SubRun H2 - Temperature at Oakwood and Crockett both exceeded the Tier 1 and Tier 2 goals on all 10 days of the observation period.
- Run I - Temperature at Oakwood exceeded the Tier 1 goal of 35 degrees C for 4 days and the Tier 2 goal for 12 days, with a max temperature of 35.43 degrees C. At Crockett, the Tier 1 temperature goal was exceeded on 5 days and the Tier 2 goal for 16 days, with a max temp of 35.55 degrees C.

3.3.5 Lower Water Quality Model Results

A Lower Model water quality simulation was created and calibrated, and subsequently used to evaluate water quality for the reach with an upstream boundary just downstream of the USGS gage in Romayor, TX, and a downstream boundary just south of where SH 105 crosses the Trinity River in Franklin, TX. No WWTP's are located along this stretch of the Trinity River.

The Lower Model was calibrated using scenario A, which includes historical flows for June 1st, 2018 to October 15th, 2018. Calibration and validation results were deemed satisfactory given limitations in input data detailed in Appendix 8. The calibrated water quality was subsequently used to run SB3 Environmental Flows scenarios. Runs B, C, D and E simulate Trinity River SB3 environmental flows for "Subsistence Summer", "Subsistence Spring", "Base Summer" and "Base Spring" conditions, respectively, to evaluate the impact of different SB3 flows on water quality. The basic details of each run and associated time periods used in analyses are included in Table 3-6. More information about hydraulic and water quality boundary conditions for each run is available in Appendix 7. An upstream boundary flow hydrograph for 2018 is shown in Figure 3-26. Model results were evaluated for calibration and SB3 simulations at RS 58607, just downstream of the Romayor USGS gage, and at RS 12927, at SH 105 near the downstream boundary of the model.

Table 3-6: Run details for Lower water quality model scenarios A-E.

Run/Period	Time	Description	Reason for Scenario
A	Summer 2018	2018 Flow Conditions; Calibration	Existing Conditions; Calibration of nutrient parameters; Baseline for comparisons
B	Romayor Subsistence Summer	Run A with constant headwater at 200 cfs	Predict impact of Subsistence Summer flow conditions
C	Romayor Subsistence Spring	Run A with constant headwater at 700 cfs	Predict impact of Subsistence Spring flow conditions
D	Romayor Base Summer	Run A with constant headwater at 575 cfs	Predict impact of Base Summer flow conditions
E	Romayor Base Spring	Run A with constant headwater at 1150 cfs	Predict impact of Base Spring flow conditions

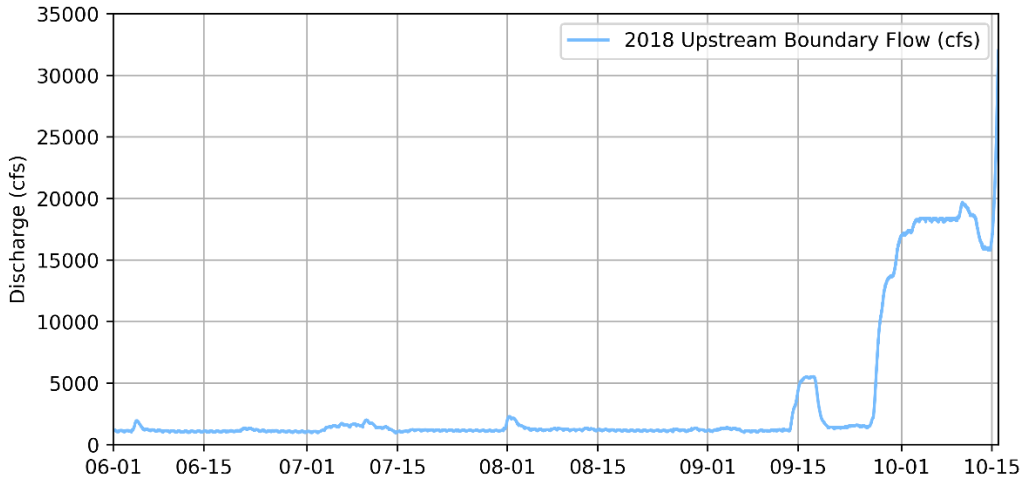

Figure 3-26: 2018 Upstream boundary flow hydrograph, used for Runs A-E.

Impact of SB3 Environmental Flows

Model runs B, C, D, and E with mainstem flows set to constant headwaters of discharges specified for SB3 "Subsistence Summer", "Subsistence Spring", "Base Summer", and "Base Spring" flow conditions were run and are compared with Run A below to assess their impact on water quality. Figure 3-27 and Figure 3-28 detail comparisons of temperature and dissolved oxygen for each scenario at the study site downstream of the Romayor gage, and Figure 3-29 and Figure 3-30 detail comparisons of temperature and dissolved oxygen for each scenario at SH 105 near the downstream end of the model. Box and whisker plots of temperature and dissolved oxygen, shown in Figure 3-31 and Figure 3-32, compare the ranges of values for each of these scenarios. Temperatures were higher for Subsistence Summer flows (Run B) than they were for summer 2018 flow conditions (Run A) by 1-2 °C, as shown in Figure 3-31. Otherwise, SB3 Environmental flows were not seen to have a considerable effect on mean temperature. Dissolved oxygen was 0.5–1.5 mg/L lower for SB3 Environmental Flow scenarios (Runs B - E) than for summer 2018 flow conditions (Run A), as shown in Figure 3-32. In the case of dissolved oxygen, the relative impact of each scenario consistently scaled with the magnitude of the reduction in flow, i.e. impacts were greatest for the "Subsistence Summer" scenario Run B. Temperatures only exceeded the Tier 1 Primary Priority Water Quality threshold for temperature at the SH 105 site for about a week in the Subsistence Summer scenario, by a magnitude of about 1.5 °C, as shown in Figure 3-29. Dissolved oxygen values did not drop below the identified Tier 1 criteria in any scenarios.

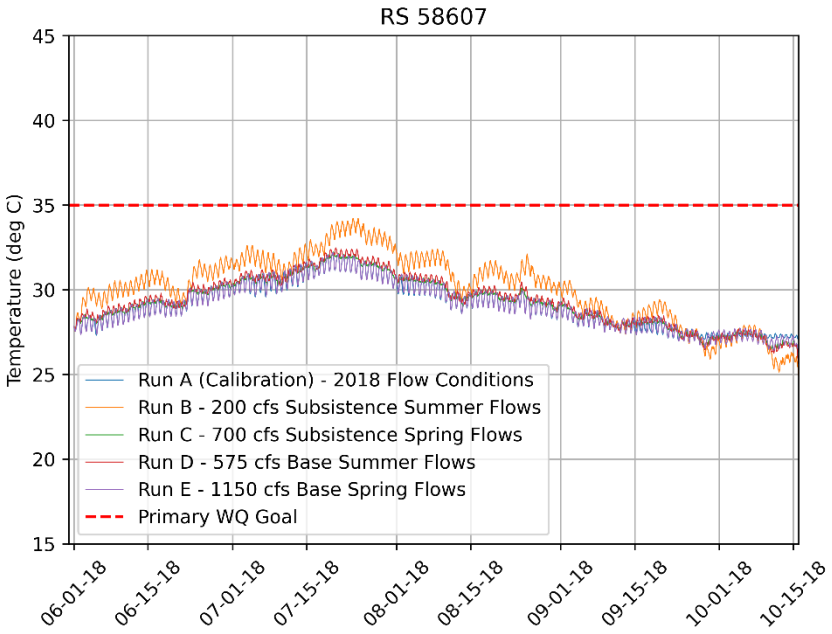

Figure 3-27: Run A, B, C, D, and E temperature results at study site just downstream of Romayor gage. Water temperature was higher for Subsistence Summer flows than for summer 2018 flow conditions, but was below the 35-degree C Tier 1 Goal and not significantly higher for any other SB3 Environmental Flows.

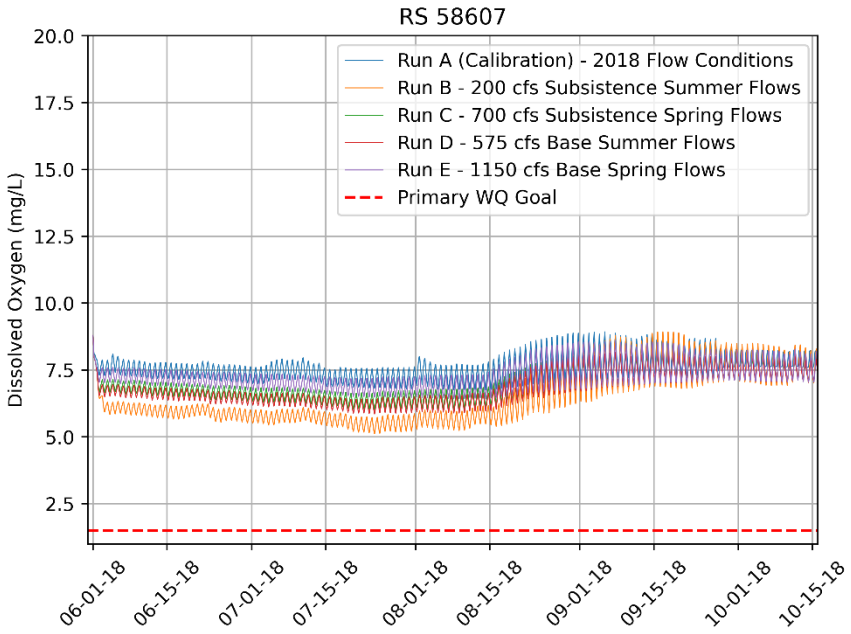

Figure 3-28: Run A, B, C, D, and E dissolved oxygen results at study site just downstream of Romayor gage. Dissolved oxygen was consistently lower for SB3 Environmental flows than for summer 2018 flow conditions, but was still above the 5.0 mg/L Tier 1 goal.

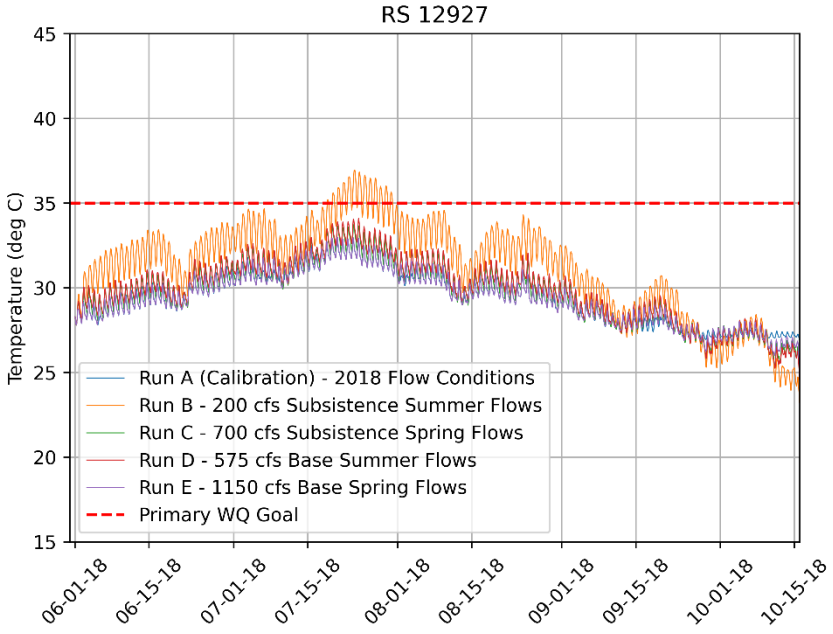

Figure 3-29: Run A, B, C, D, and E temperature results at SH 105 near downstream end of model. Water temperature was substantially higher for Subsistence Summer flows and slightly higher for Base Summer flows than for summer 2018 flow conditions, but was not significantly higher for SB3 Spring Environmental Flows. Subsistence Summer Flows did cause the temperature

to exceed the Tier 1 Primary Priority Water Quality threshold by as much as 1.5 °C for about a week.

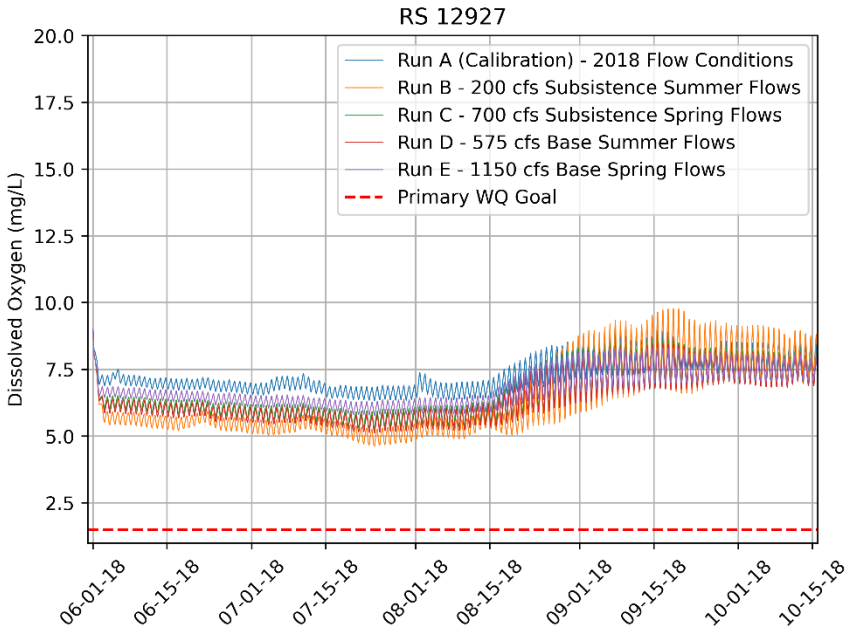

Figure 3-30: Run A, B, C, D, and E dissolved oxygen results at SH 105 near downstream end of model. Dissolved oxygen was consistently lower for SB3 Environmental flows than for summer 2018 flow conditions, with the magnitude of the decrease scaling with the magnitude of the reduction in flow. Note that Tier 1 and 2 goals were still met in all scenarios.

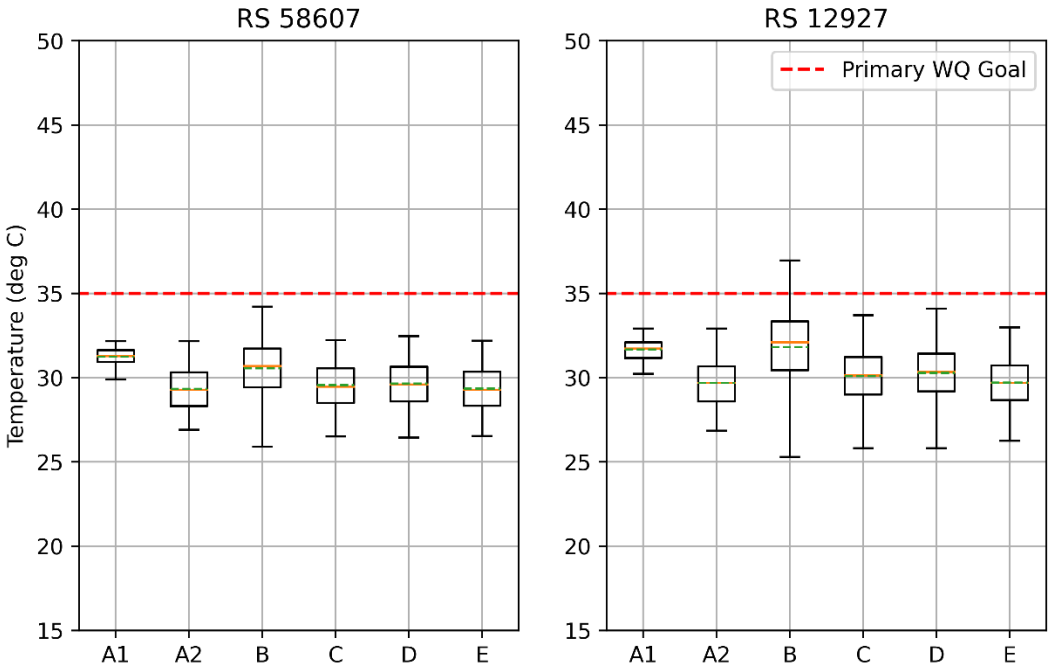

Figure 3-31: Box and whisker plots of temperature results for all scenarios and periods within scenarios. Orange lines represent sample medians, green dashed lines represent sample averages, boxes represent interquartile range (25th percentile – 75th percentile) and whiskers represent sample maximum and minimum. Other than for Subsistence Summer, SB3 Environmental Flows did not have a considerable impact on temperature at either comparison site. Subsistence Summer Flows did cause the temperature to exceed the Tier 1 Primary Priority Water Quality threshold at the site at SH105 near the downstream end of the model.

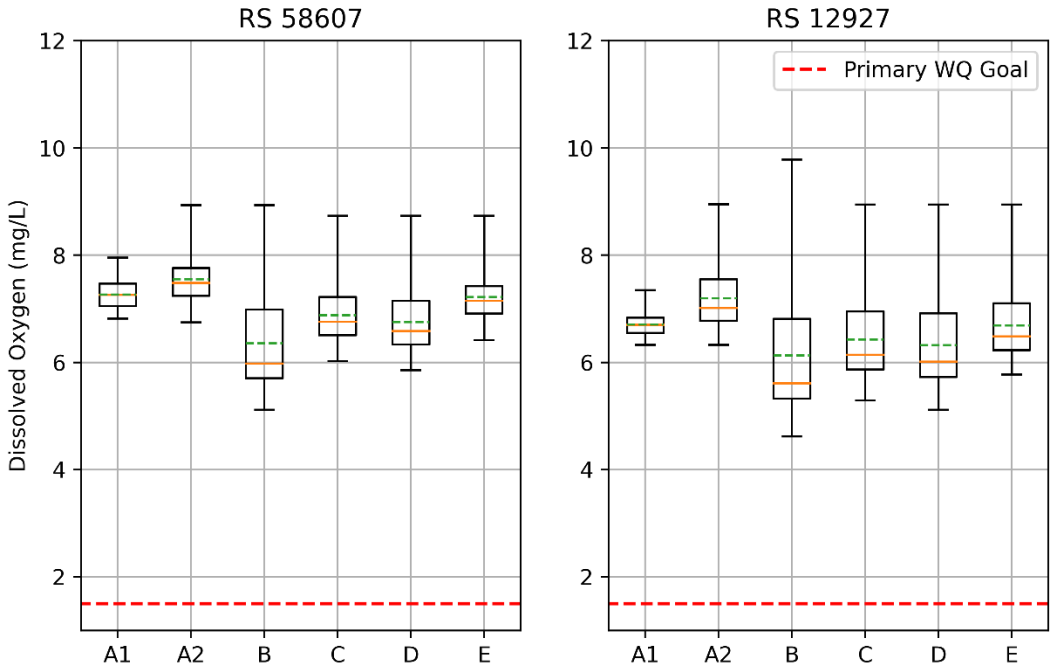

Figure 3-32: Box and whisker plots of dissolved oxygen results for all scenarios and periods within scenarios. Orange lines represent sample medians, green dashed lines represent sample averages, boxes represent interquartile range (25th percentile – 75th percentile) and whiskers represent sample maximum and minimum. Dissolved oxygen was consistently lower for SB3 Environmental flows than for summer 2018 flow conditions by 0.5-1.5 mg/L at both sites, with the magnitude of the decrease scaling with the magnitude of the reduction in flow. Dissolved oxygen did not come close to the Tier 1 Primary Priority Water Quality threshold of 1.5 mg/L.

*3.3.6 **Lower Model Discussion***

The Lower model faces the same limitations as described for the Upper Model (Upper Model Discussion, Section 3.3.4) above in regard to flow conditions, watershed inputs, and discontinuous and interpolated nature of nutrient loading data at the upstream boundary. The Lower model also only covers a short reach of the river downstream of Lake Livingston. As a result, the Lower water quality model is limited by having only a single location with TCEQ SWQM measurements for calibration and that site being located near the downstream boundary where hydraulics are not as well-calibrated. The downstream boundary of the model is not located at a USGS gage, and, accordingly, has to use a less-accurate normal depth boundary condition because no time series of water surface elevation is available.

Results show that, of the SB3 Environmental Flows, only the most severe Subsistence Summer (Run B) flows caused a significant increase (>5%) in temperature compared to summer 2018 flow conditions (Run A), as shown in Figure 3-31. They also show that all of the SB3 Environmental Flows (Runs B, C, D and E) have the effect of decreasing dissolved oxygen by 5-

20% compared to summer 2018 flow conditions (Figure 3-32), but are still above Tier 1 and 2 goals. Temperature exceeded the Tier 1 Primary Priority Water Quality temperature threshold by about 1.5 °C for a period of about one week only at the SH 105 site (Figure 3-29) near the downstream boundary of the model. This result should, however, be interpreted with caution due to the lack of watershed inputs in the model and the site's proximity to the model's downstream boundary. Results do not indicate that there is a significant risk for any of the SB3 Environmental Flow scenarios of dissolved oxygen dropping below the Tier 1 Primary Priority Water Quality threshold of 1.5 mg/L or the Tier 2 threshold of 5.0 mg/L daily average and 3.0 mg/L for <=8 hours.

The impact of SB3 Environmental Flows compared to normal summer flow conditions is different for the Upper and Lower model. Some of this difference may be explained by the fact that SB3 Environmental flows for the Lower model are considerably higher and may come closer to approaching normal summer flow conditions. Additionally, in the Lower model area, Base Summer flows are actually less than Subsistence Spring flows.

In addition to the refinement suggested above for the Upper model, the Lower model would benefit from having its footprint extended well up- and down-stream of the area for which water quality is to be assessed.

Table 3-7. Water quality summary table for the Lower Model. Note: Run A exceeded the Tier 2 temperature goal of 33.9 on 5 days.

		Romayor						
		Teir 1 Instream Flow Goals (RPS, 2015)				Selected Tier 2 Instream Flow		
Description	Reason for Scenario	<= 12 hours below 3 mg/L	<= 2 hours below 2 mg/L	> 1.5 mg/L	<= 35°C (95°F)	>5.0 mg/L daily average	=3.0 mg/L minimum for <= 8 hours	<= 33.9°C (95°F)
		DO (mg/L)	DO (mg/L)	DO (mg/L)	Temp (Deg. C)	DO (mg/L)	DO (mg/L)	Temp (Deg. C)
2018 Flow Conditions; Calibration	Existing Conditions; Calib	Yes	Yes	Yes	Yes	Yes	Yes	Yes
Run A with constant headwater at 200 cfs	Predict impact of Subsist	Yes	Yes	Yes	Yes	Yes	Yes	No
Run A with constant headwater at 700 cfs	Predict impact of Subsist	Yes	Yes	Yes	Yes	Yes	Yes	Yes
Run A with constant headwater at 575 cfs	Predict impact of Base Su	Yes	Yes	Yes	Yes	Yes	Yes	Yes
Run A with constant headwater at 1150 cfs	Predict impact of Base Sp	Yes	Yes	Yes	Yes	Yes	Yes	Yes

3.4 Sediment Transport Modeling and Inputs

Changes in Trinity River planform and cross-section have been observed since 2011, including observed data reported to TWDB as part of Phase 1, 2 and 3. The magnitude of those changes can be evaluated using available historical mapping data and recent detailed observation data. Evaluating those information sources would improve our understanding of what constitutes recent typical migration and cross-section change patterns, or whether atypical conditions are occurring that are indicative of a change in system inputs (e.g., flow, structures, etc.). To date, observed changes appear to be typical and unsurprising for the sediment types and flow rates exhibited between observational events. The main departures from typical region-wide patterns

appear to be in localized areas caused by rapid changes near man-made structures, for example river adjustments following the flanking and failure of relic lock and dam structures.

Available observations of sediment characteristics and morphologic changes caused by sediment transport provide a basis to inform predictive sediment transport models. These models can, in turn, be used to evaluate the impact of hypothetical system changes (e.g. drought conditions, bridge construction, managed flows) on channel morphology and sediment transport. They can also be used to gain additional insight into sediment transport processes in the existing system. Development of sediment transport models using data produced in Phases 1, 2 and 3 provides an excellent opportunity to leverage available field data to enhance our understanding of sediment transport in the Trinity River.

3.4.1 Model Characteristics

Sediment transport models that incorporate BSTEM analysis were prepared in HEC-RAS for the Oakwood and Romayor study sites. HEC-RAS sediment transport analyses require initial conditions and boundary conditions at every cross-section in the model domain, therefore a smaller model with fewer cross-sections was created for the Oakwood study site (Figure 3-33) using the calibrated upper model geometry. By doing so, we avoided simulating sediment transport for long stretches of the upper model with no sediment data available. The lower model is smaller and centered around the Romayor study site (Figure 3-34), so the full geometry was included in the Romayor study site model.

Implementation of a HEC-RAS BSTEM analysis requires that there be an active mobile-bed sediment transport model. A mobile bed extent is defined for the sediment transport analysis, which defines the extent of the cross-section over which erosion and deposition calculated based on hydraulics are applied. Toe and bank locations within each cross-section are identified for BSTEM analysis, with the toe typically located at the edge of the mobile bed extent on each side of the channel. A BSTEM analysis performs bank failure computations. When a failure is identified in the BSTEM analysis, the portion of the bank that failed is removed from the cross-section and deposited evenly on the channel bed. This bank sediment is then available to sediment transport computations.

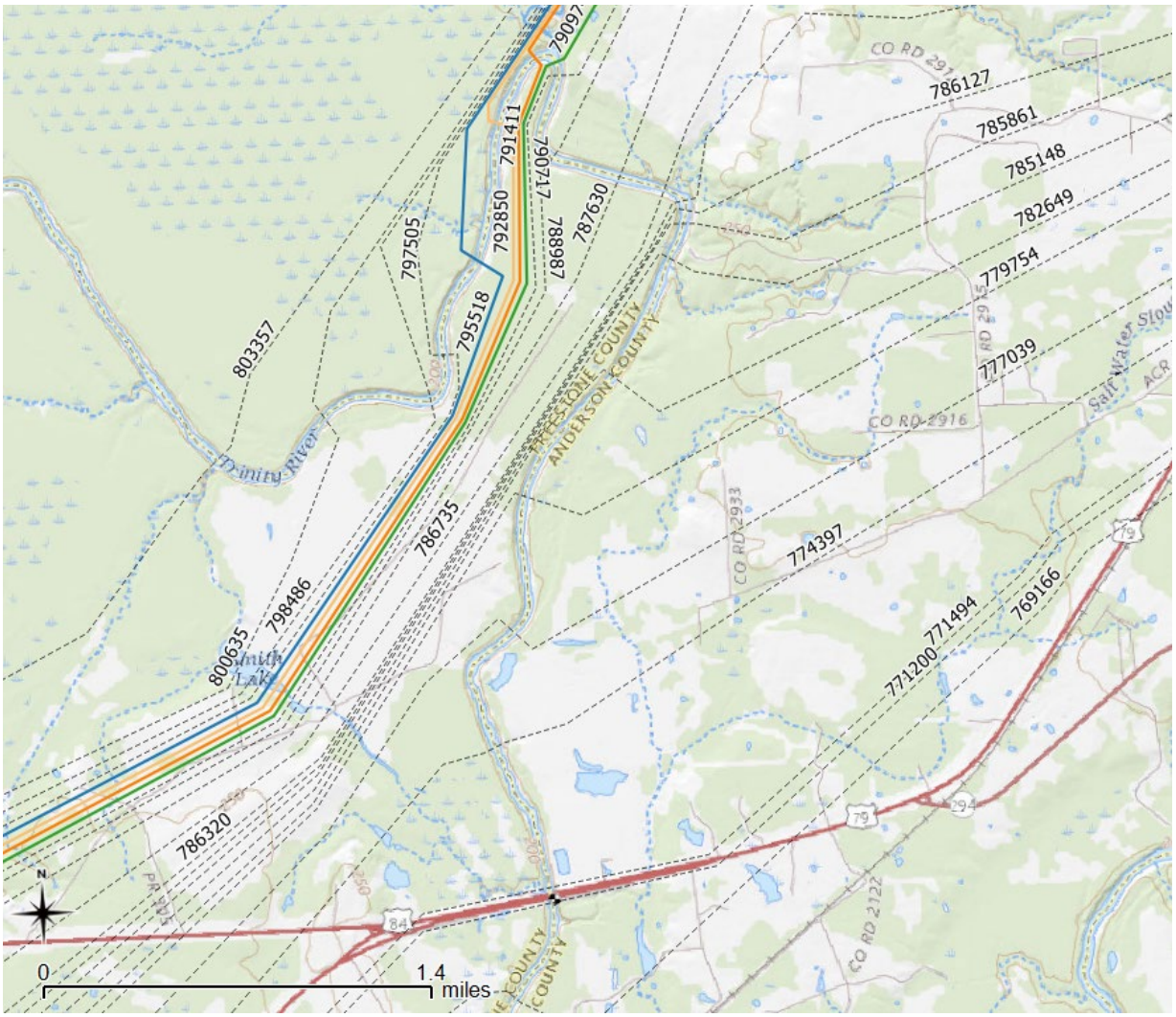
786127
785861
785148
782649
779754
777039
774397
771494
771200
769166
803357
800635
798486
797505
795518
792850
791411
790717
788987
787630
786735
786320
CO RD 2916
CO RD 2933
CO RD 2122
PRESTON COUNTY
ANDERSON COUNTY
Trinity River
Smith Lake
0
1.4
miles
N

Figure 3-33. Oakwood Study Site HEC-RAS model cross-sections and USGS Gage 08065000 at US 79/84.

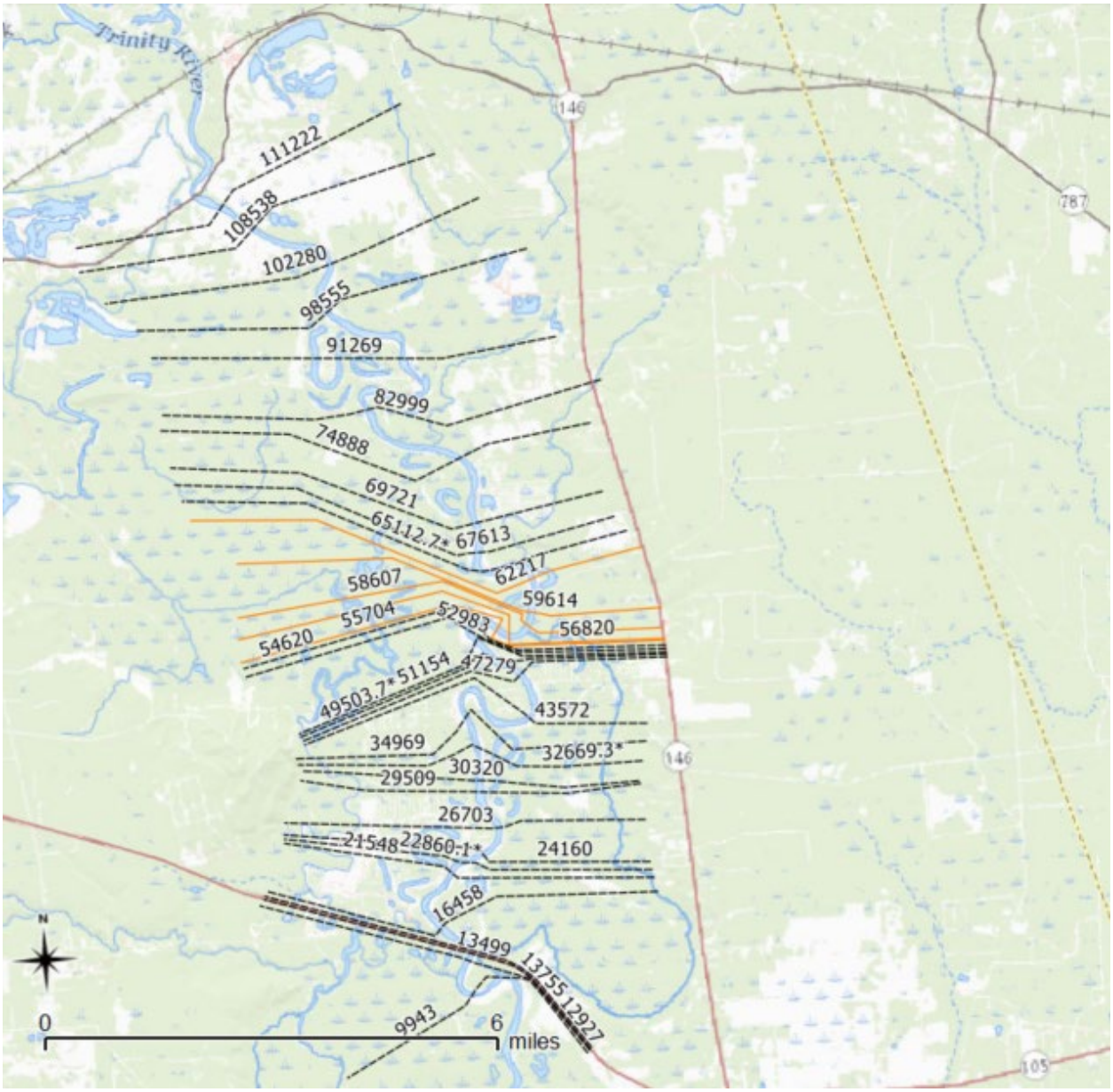

Figure 3-34. Romayor Lower Study Site HEC-RAS model cross-sections and USGS Gage 08066500 at FM787.

3.4.2 Sediment Data

Sediment characteristic data available from previous studies and USGS sediment samples was supplemented with data collected in the field as part of this study. This data was used to inform model initial conditions, boundary conditions and to compare model results to observation data.

3.4.3 Sediment Initial and Boundary Conditions

A sediment transport analysis in HEC-RAS requires an initial condition for each bed location and an upstream boundary condition. Incorporating BSTEM analysis requires an additional set of initial conditions for each cross-section.

Bed gradations were available for select study site cross-sections from the 2015 TRA report. These bed gradations were provided as inputs for their corresponding cross-sections and HEC-RAS used these inputs to interpolate bed gradations for all remaining undefined cross-sections. Table 5 details cross-sections with input bed gradations in each model. The extent of the mobile bed for this analysis was set to the defined bank points from the HEC-RAS geometry. An available sediment depth of 20 feet was also specified for each cross-section.

USGS field measurement data for each study site's respective gage were used to inform an upstream rating curve boundary condition for both models. A selection of total sediment discharge data points with grain size distribution data for the suspended load and bed load portion of the total load was available at each gage. For both gages, samples with total sediment discharge data date back to the 1970's, so an analysis was performed to ensure that they approximately represent modern-day flow load measurements. Visual comparison of total sediment discharge and corresponding suspended sediment discharge for each observation date demonstrated that total sediment discharge and suspended sediment discharge were consistently related across a range of discharge values. Additionally, suspended sediment discharge sampled during the 1970's as part of total sediment discharge measurements showed the same relationship to flow as more recent suspended sediment discharge measurements made after 2015. Determined flow-load relationships for each study site are detailed in Figure 3-35 and Figure 3-36. Representative gradations of the total sediment load were chosen for each study site, and used as the upstream boundary sediment load gradation for all flow values. These representative gradations are detailed in Figure 3-37 and Figure 3-38.

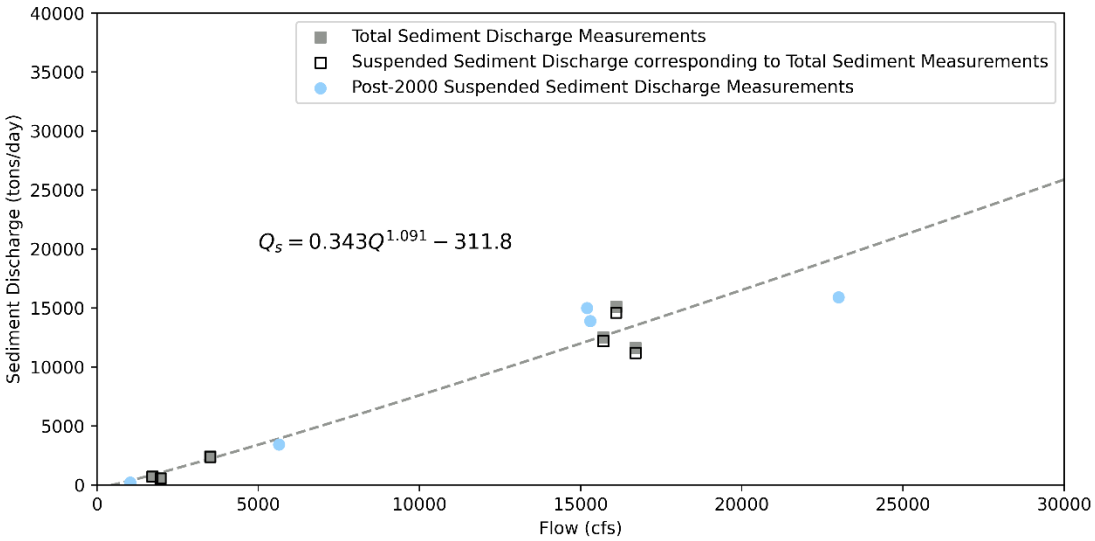

Figure 3-35. Oakwood Study Site Rating Curve established from field measurements from USGS Gage 08065000.

Grain size distributions from bank sediment samples collected as part of this study were input as bank gradations at the cross-sections where they were available. BSTEM computations can be turned on or off at different cross-sections in the model, and in this case were only turned on at cross-sections for which bank sediment grain size distributions were available. Table 3-8 details cross-sections with input bed gradations in each model. Mobile bed extents from sediment transport initial conditions were used as bank toe stations and the top of bank station was identified visually. For each BSTEM cross-section, default BSTEM soil properties (saturated unit weight, friction angle, cohesion, phi b) were used based on the dominant grain size from the grain size distribution. Results from JET test analyses performed in tandem with bank sediment sampling as part of this study were used to inform the critical shear stress and erodibility of the bank material for each BSTEM cross-section. JET test results used in the BSTEM analysis are detailed in (Table 3-9).

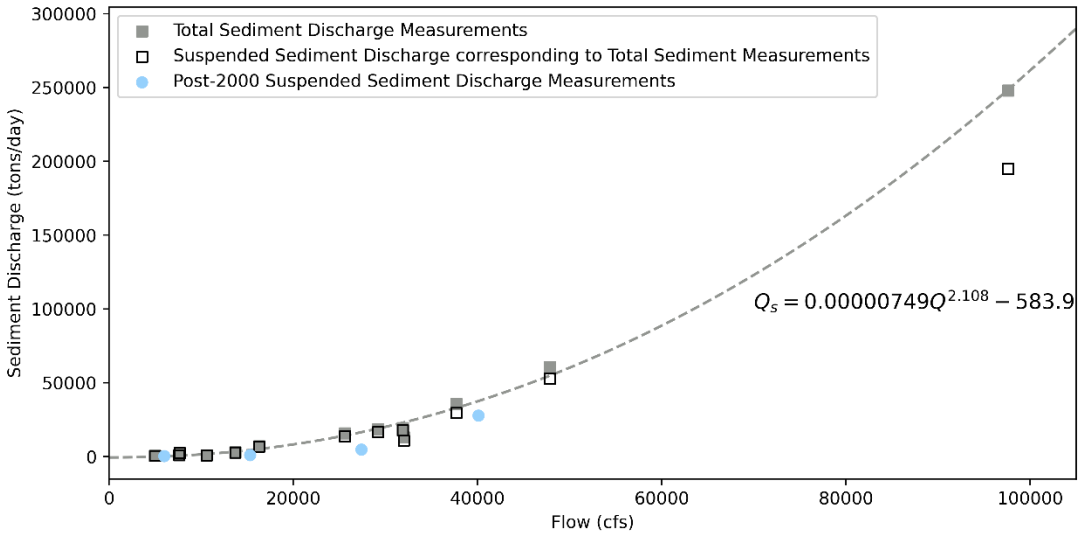

Figure 3-36. Romayor Study Site Rating Curve established from field measurements from USGS Gage 08066500.

Table 3-8. Cross-sections with bed or bank gradation data available in HEC-RAS sediment transport models for Oakwood and Romayor study sites.

Study Site	Bed Gradation Data Available	Bank Gradation Data Available
Oakwood	795518, 791411, 790974	795518, 792850, 791411
Romayor	62217, 59614, 58607, 55704	62217, 59614, 56820

Table 3-9. JET Test results for Oakwood and Romayor study sites used in BSTEM analysis.

	Calculated Values			Values in Model	
Cross-Section	**Critical Shear Stress (lbf/ft2)**	**Erodibility (ft3/lbf/s)**	**Method**	**Critical Shear Stress (lbf/ft2)**	**Erodibility (ft3/lbf/s)**
Oakwood - 795518	0.02	0.00279	Scour Depth Solution	0.02	0.00279
Oakwood - 792850	0.0215	0.00344	Scour Depth Solution	0.0215	0.000344
Oakwood - 791411	0.00159	0.0452	Scour Depth Solution	0.00159	0.00226
Romayor - 62217	0	0.0160	Scour Depth Solution	0	0.0016
Romayor - 59614	0.00209	0.00319	Scour Depth Solution	0.00208	0.000319
Romayor - 56820	0.00125	0.0194	Scour Depth Solution	0.00125	0.00097

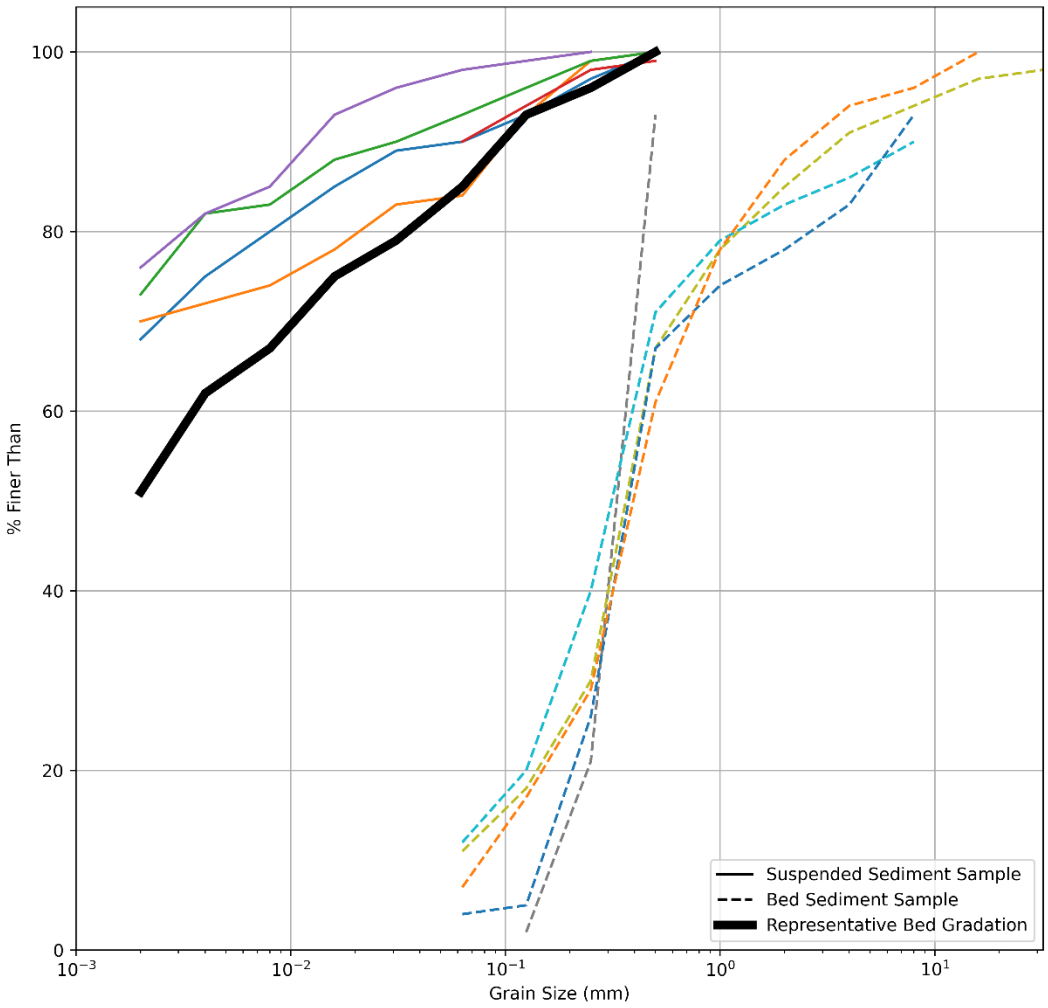

Figure 3-37. Representative gradation for upstream boundary total sediment load at Oakwood Study Site from field measurements at USGS Gage 08065000.

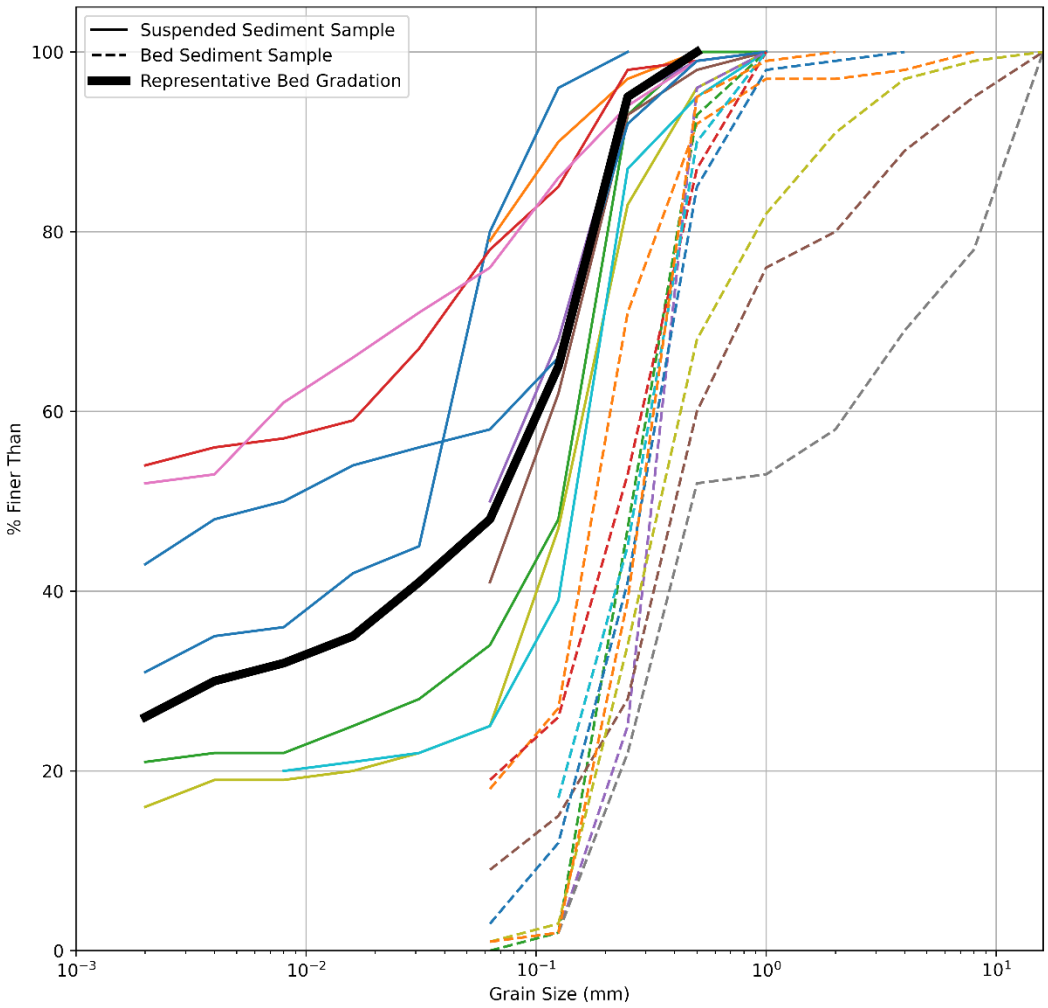

Figure 3-38. Representative gradation for upstream boundary total sediment load at Romayor Study Site from field measurements at USGS Gage 08066500.

3.4.4 Sediment Transport Scenarios

Sediment transport analyses for the period from January 1st, 2015 – December 31st, 2018 were prepared for the Oakwood and Romayor study sites. In addition to the sediment data file described in the section above, this involved the preparation of a quasi-unsteady flow data file. For each, the quasi-unsteady flow analysis consisted of an upstream flow hydrograph boundary condition and a downstream stage hydrograph boundary condition. Both flow and stage values were obtained from 15-minute increment flow and stage observations from each study site's respective USGS gage. The downstream stage hydrograph boundary was deemed appropriate based on the fact that, in both study-site model geometries, the bridge cross-section where the respective gages are located is just upstream (i.e. the next cross-section) of the downstream boundary cross-section.

3.5 Sediment Transport Results

3.5.1 Upper Model Results

Results of sediment transport and BSTEM analysis computations for the period from January 1st, 2015 to December 31st, 2018 are presented below for cross-sections (Figure 3-39) with available bed/bank gradation data and JET test data. Figure 3-40 details invert elevation changes at model cross-sections 795518, 791411, and 790974, respectively. Figure 3-41 details the net change in sediment volume at these same cross sections. Figure 3-42 details the daily volume of bank failures from BSTEM analysis at model cross-sections 795518, 792850, and 791411, respectively. Finally, Figure 3-43, Figure 3-44, Figure 3-45, and Figure 3-46 detail the yearly cross-section change for model cross-sections 795518, 792850, 791411, and 790974, respectively.

Figure 3-39. Oakwood Site HEC RAS Upper Model cross-sections 795518, 791411, and 790974.

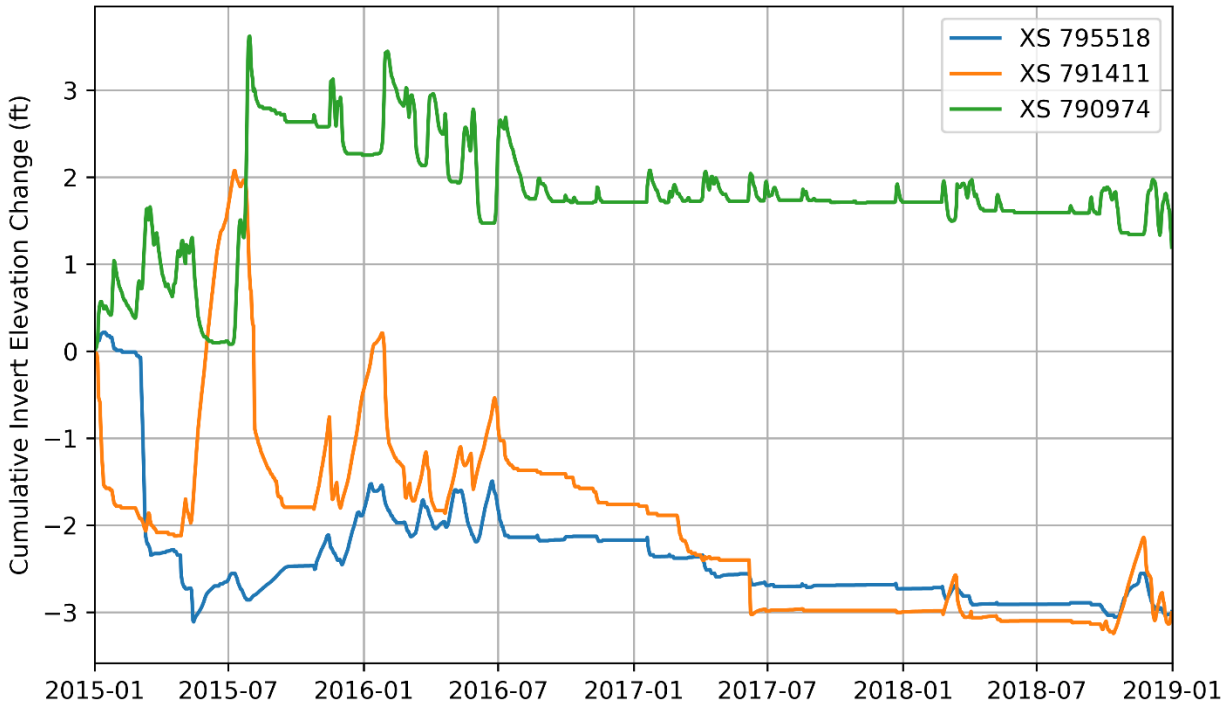

Figure 3-40: Cumulative Invert Elevation Change at Upper Model cross-sections 795518, 791411, and 790974.

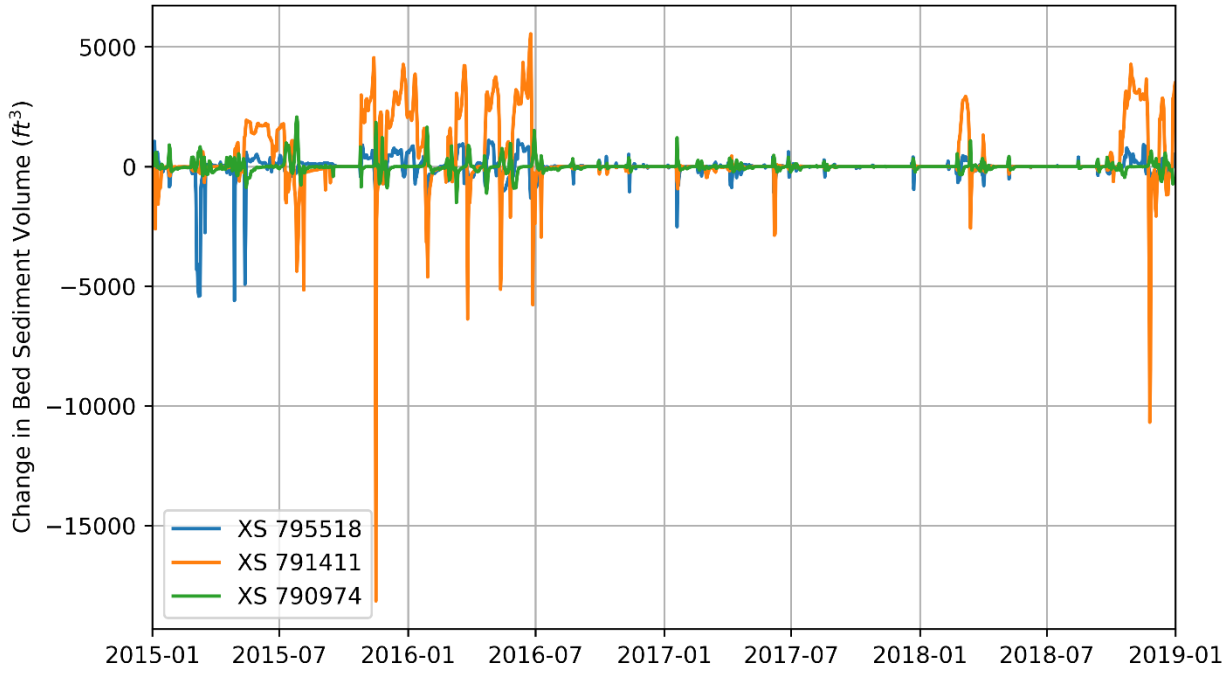

Figure 3-41: Change in Bed Sediment Volume at Upper Model cross-sections 795518, 791411, and 790974.

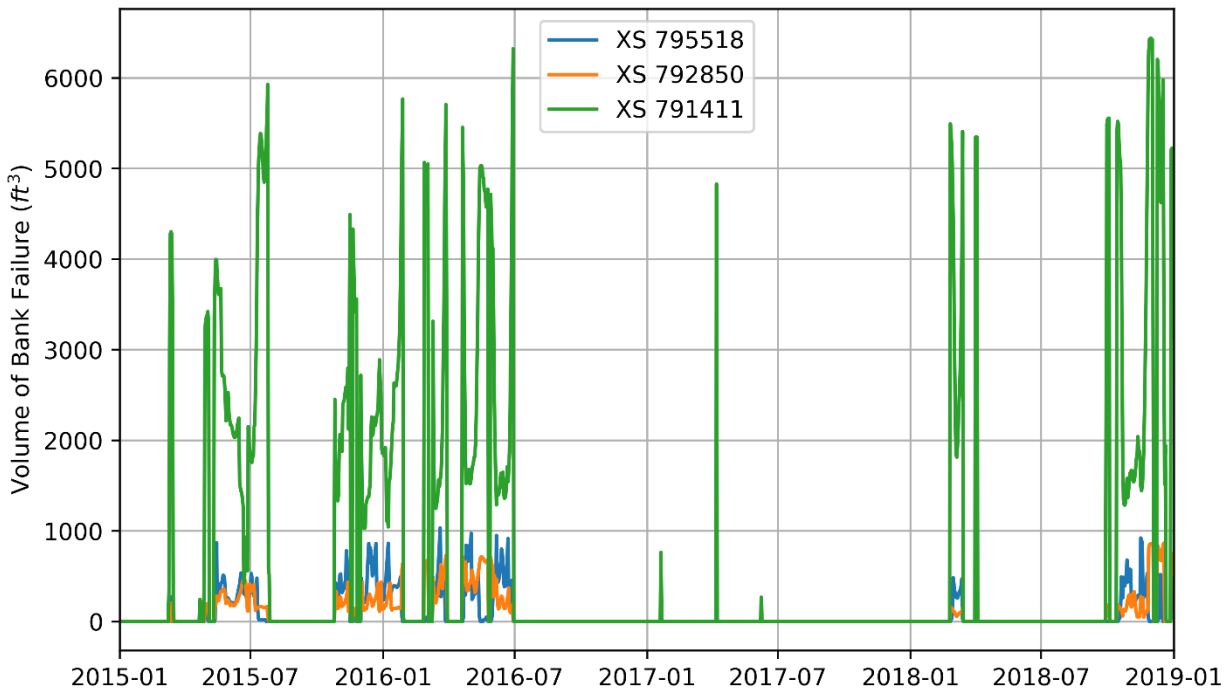

Figure 3-42: Volume of Bank Failure from BSTEM analysis at Upper Model cross-sections 795518, 792850, and 791411.

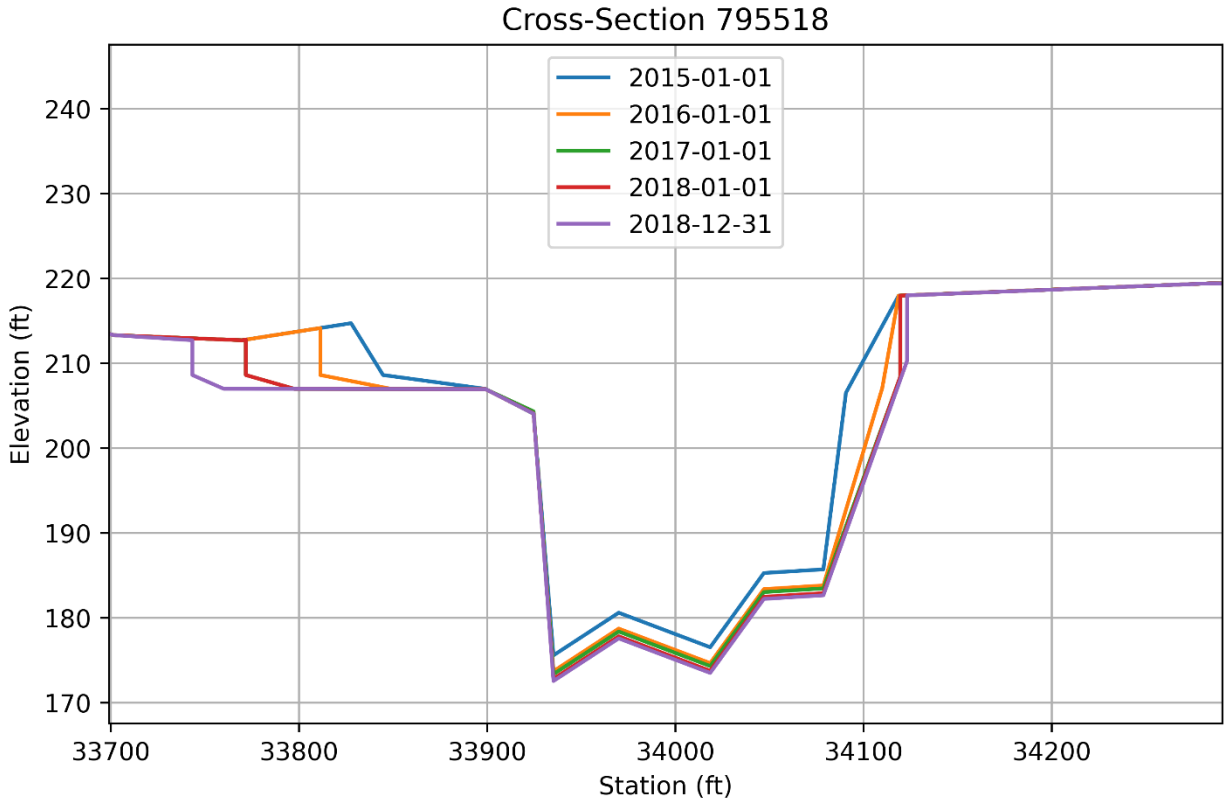

Figure 3-43: Annual change in cross-section form for Upper Model cross-section 795518, with mobile bed sediment transport and BSTEM analysis active.

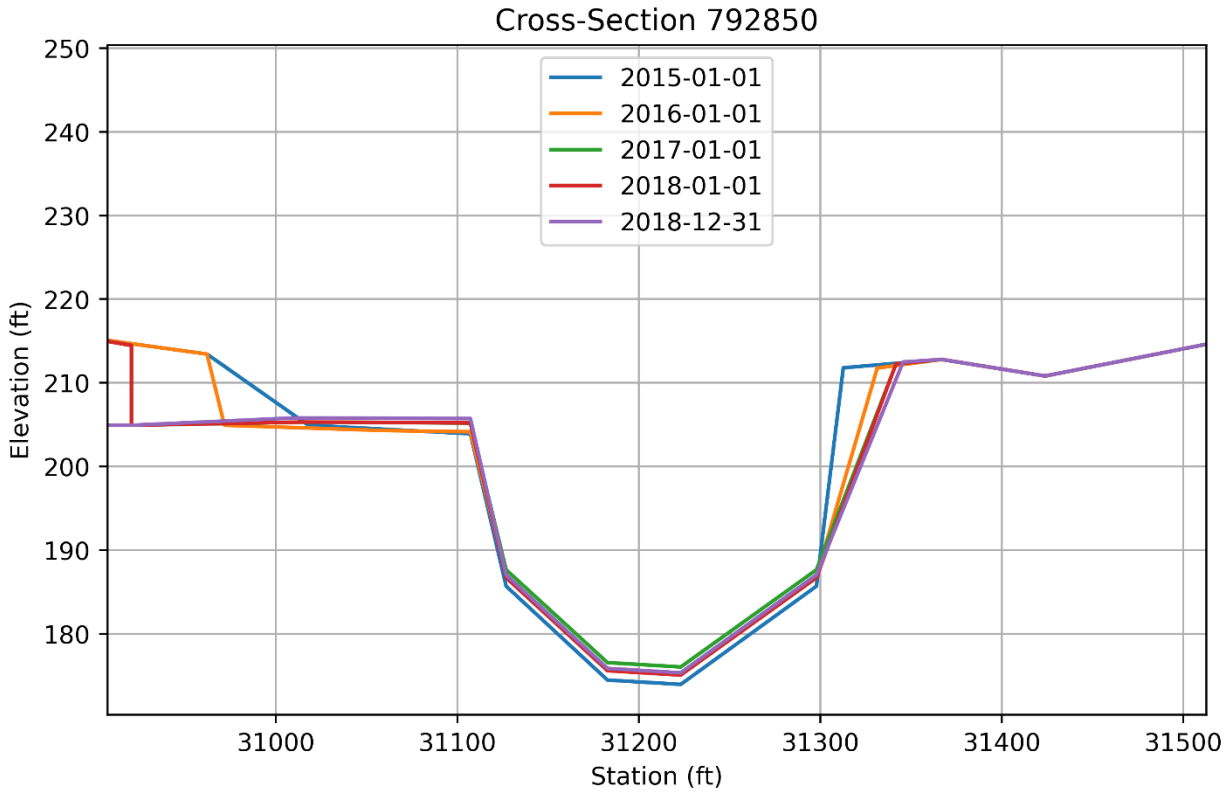

Figure 3-44: Annual change in cross-section form for Upper Model cross-section 792850, with mobile bed sediment transport and BSTEM analysis active.

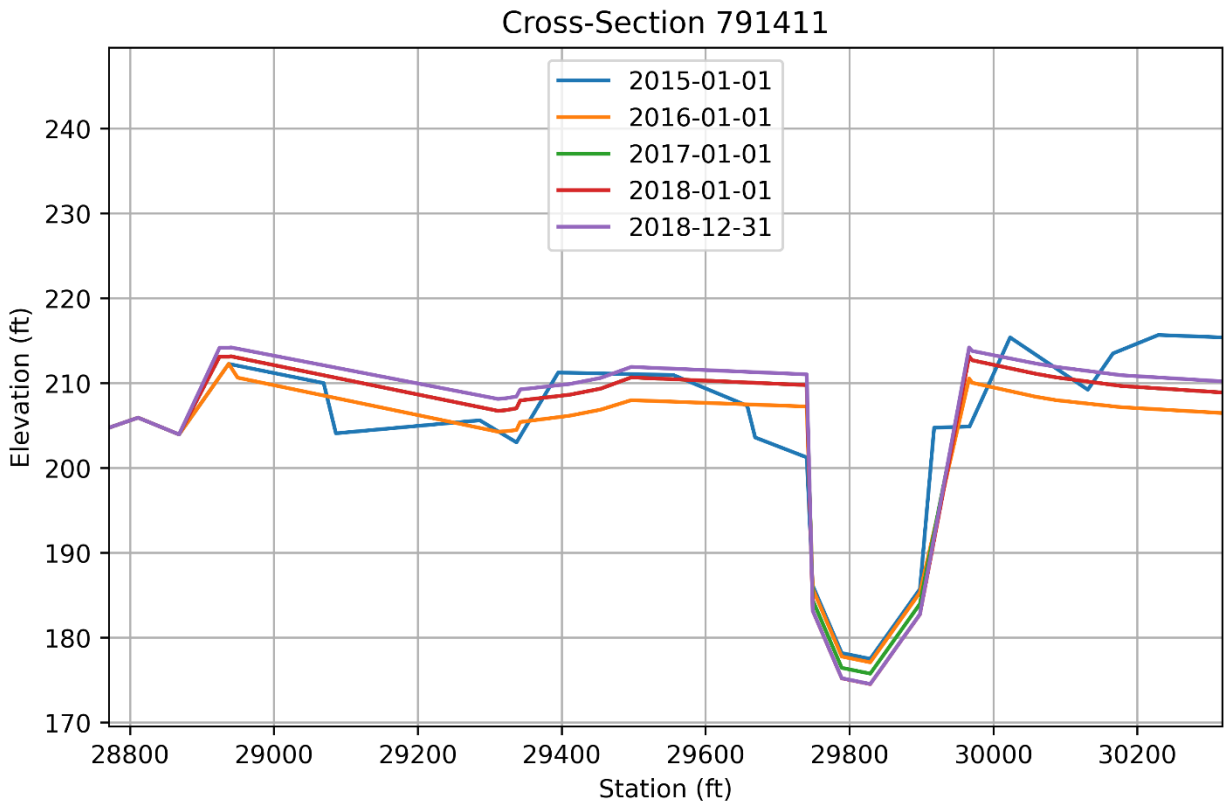

Figure 3-45: Annual change in cross-section form for Upper Model cross-section 791411, with mobile bed sediment transport and BSTEM analysis active.

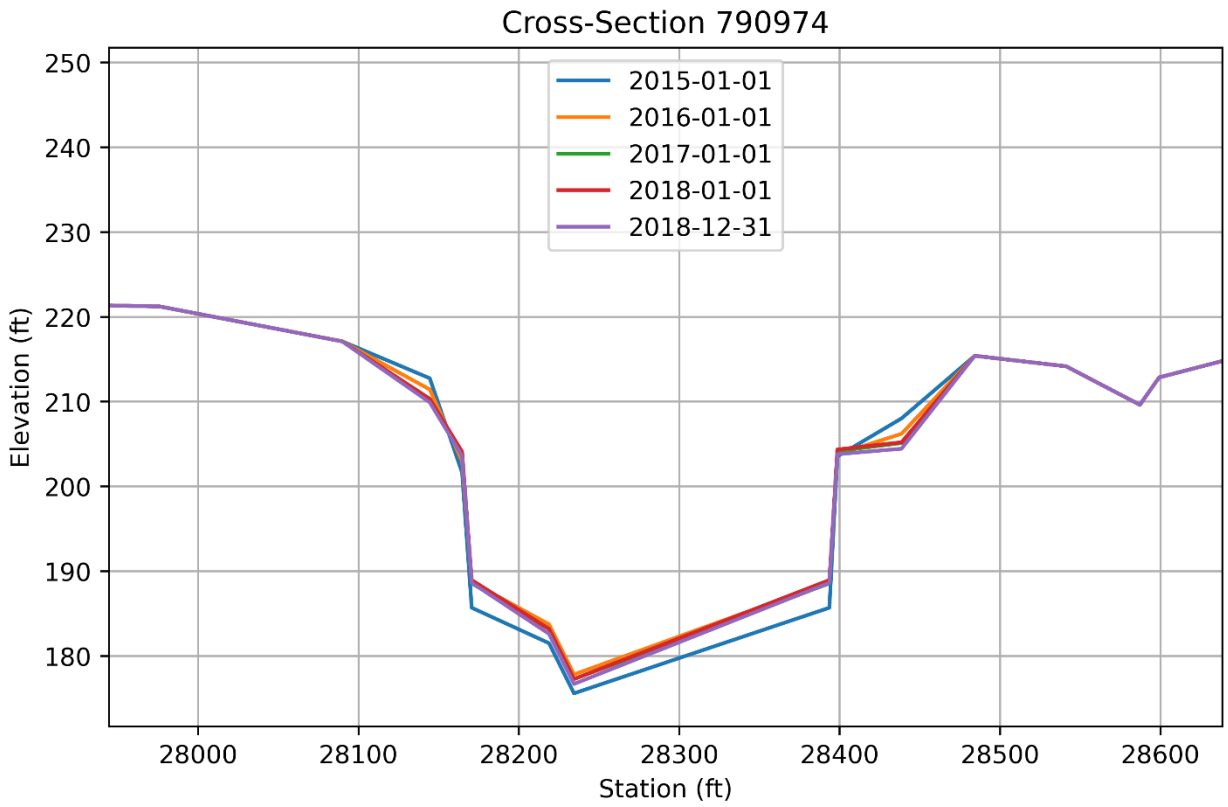

Figure 3-46: Annual change in cross-section form for Upper Model cross-section 790974, with mobile bed sediment transport analysis active.

3.5.2 Lower Model Results

Results of sediment transport and BSTEM analysis computations for the Romayor-area "lower model" for the period from January 1st, 2015 to December 31st, 2018 are presented below for cross-sections (Figure 3-47) with available bed/bank gradation data and JET test data. Figure 3-48 details invert elevation changes at model cross-sections 62217, 59614, 58607, and 55704, respectively. Figure 3-49 details the daily net change in sediment volume at these same cross sections. Figure 3-50 details the daily volume of bank failures from BSTEM analysis at model cross-sections 62217, 59614, and 56820, respectively. Finally, Figure 3-51, Figure 3-52, Figure 3-53, Figure 3-54, and Figure 3-55 detail the yearly cross-section change for model cross-sections 62217, 59614, 58607, 56820, and 55704, respectively.

Figure 3-47: Romayor Site HEC RAS Lower Model cross-sections 62217, 59614, 58607, 56820, and 55704.

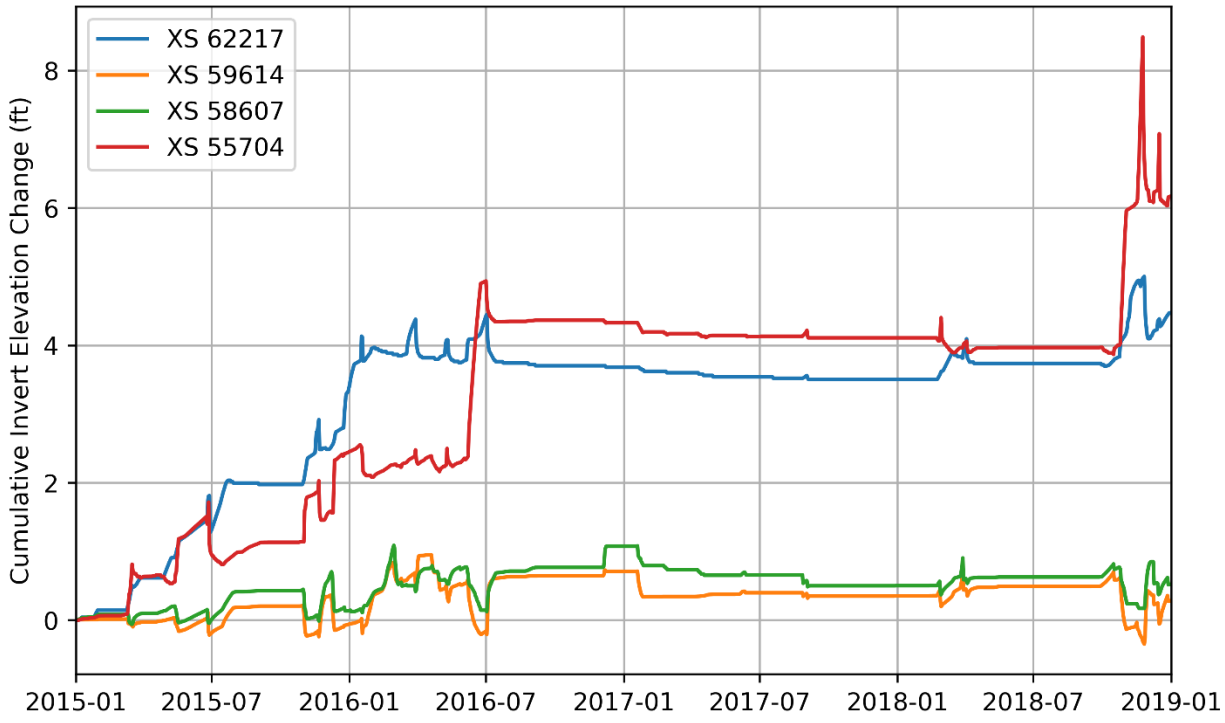

Figure 3-48: Cumulative Invert Elevation Change at Lower Model cross-sections 62217, 59614, 58607, and 55704.

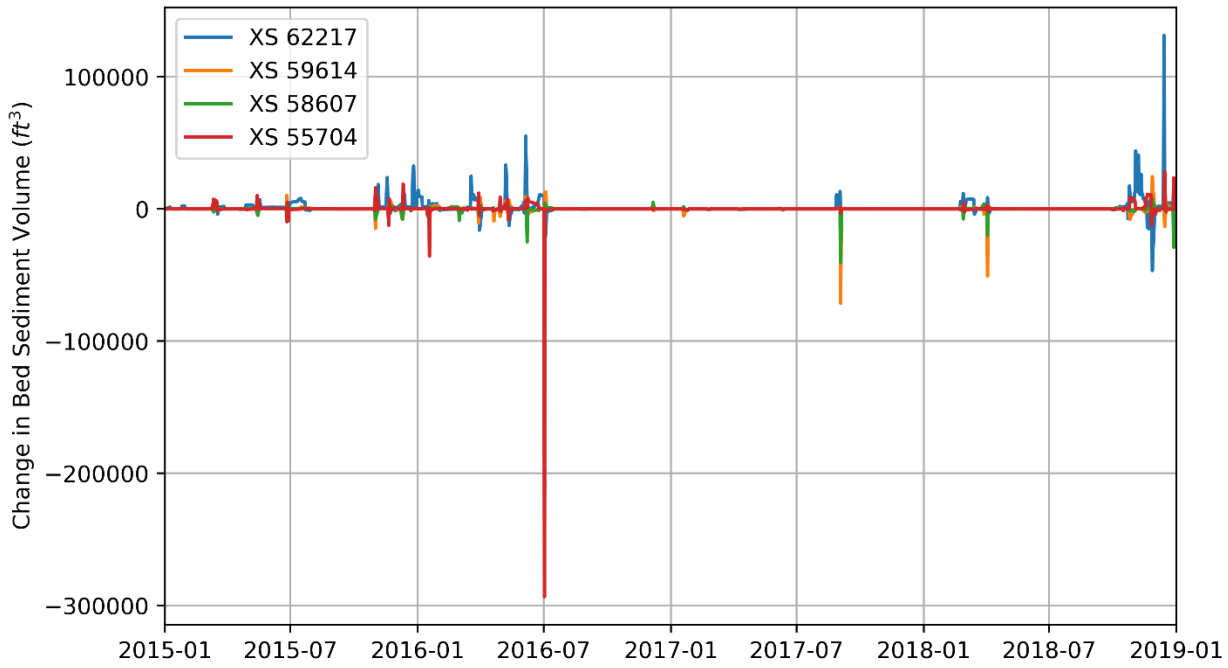

Figure 3-49: Change in Bed Sediment Volume at Lower Model cross-sections 62217, 59614, 58607, and 55704.

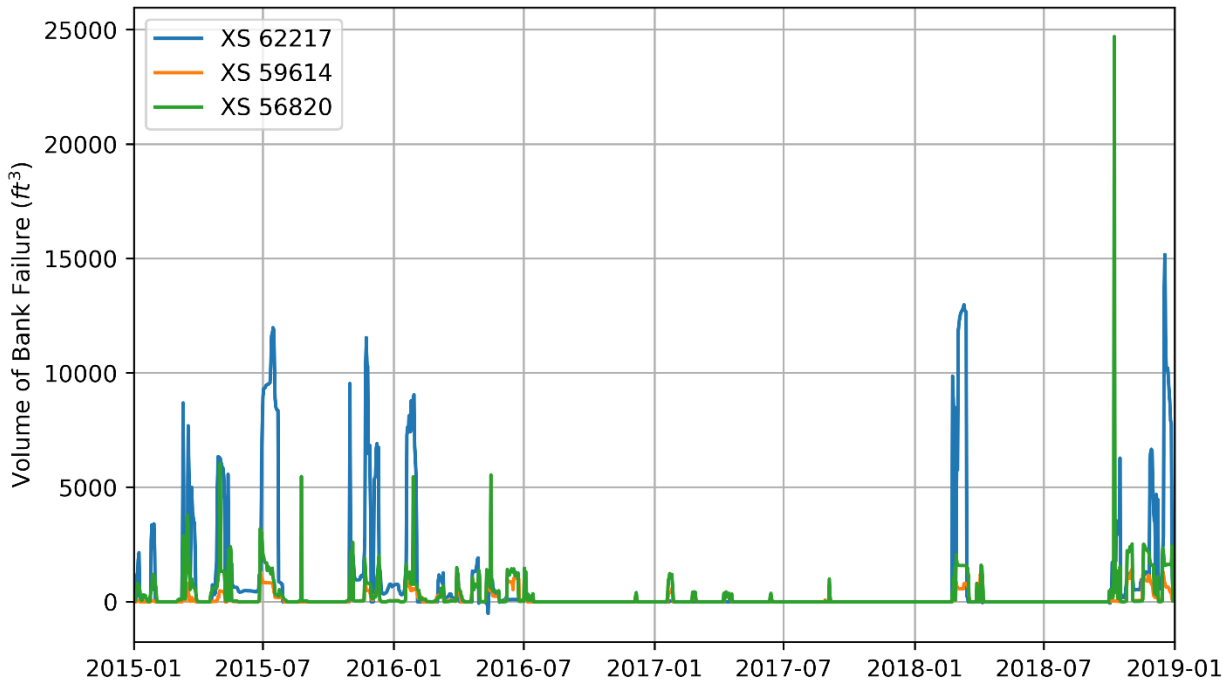

Figure 3-50: Volume of Bank Failure from BSTEM analysis at Lower Model cross-sections 62217, 59614, and 56820.

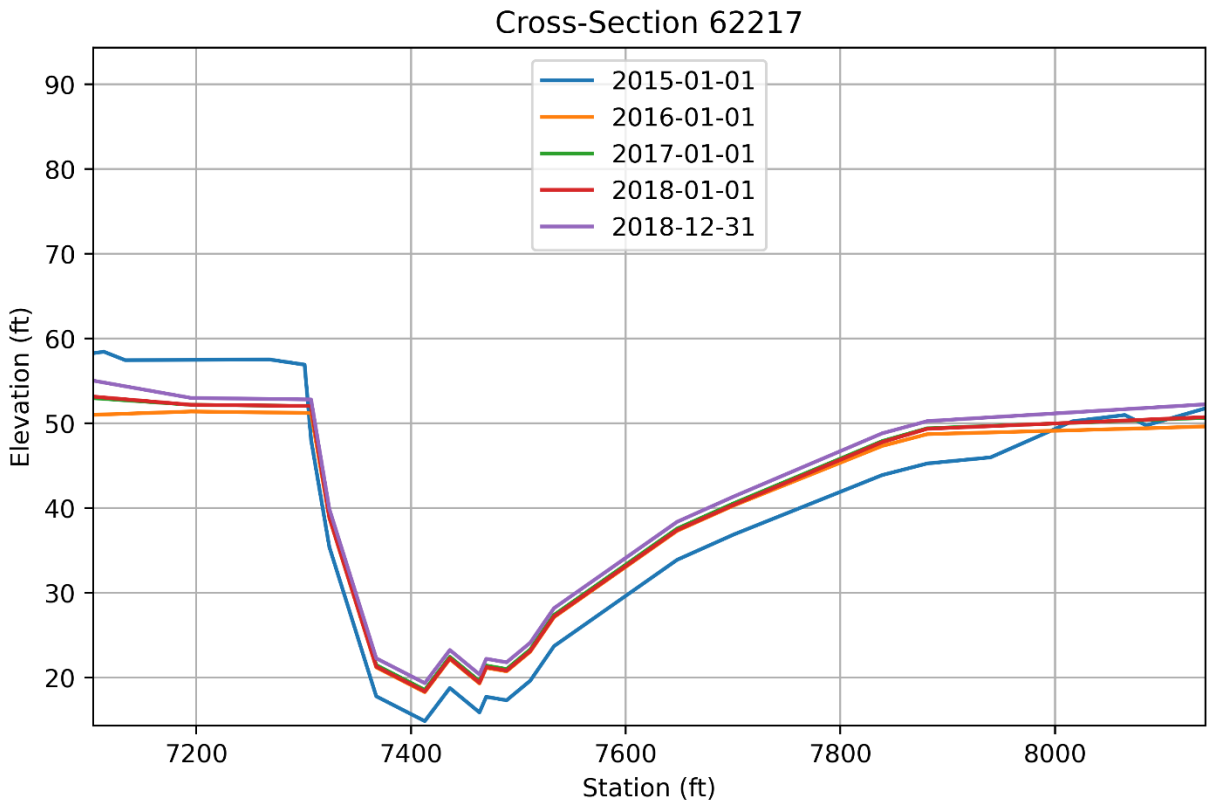

Figure 3-51: Annual change in cross-section form for Lower Model cross-section 62217, with mobile bed sediment transport and BSTEM analysis active.

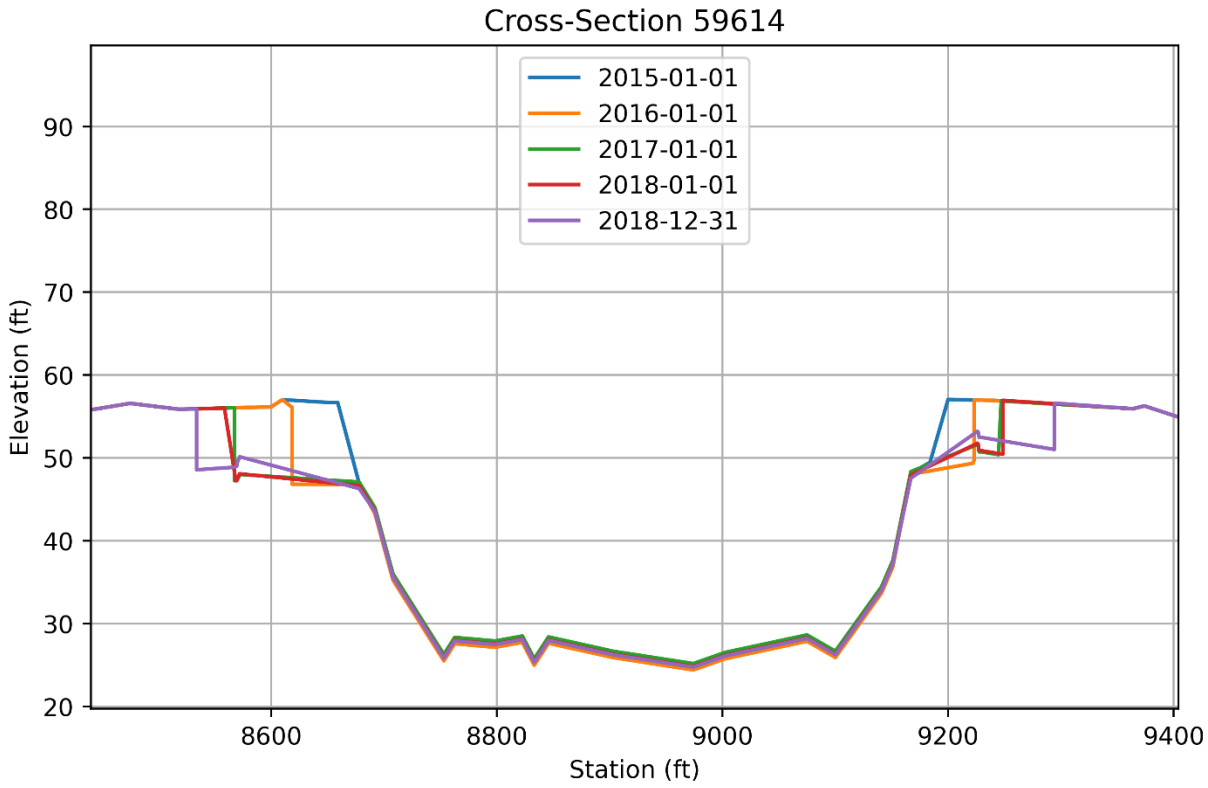

Figure 3-52: Annual change in cross-section form for Lower Model cross-section 59614, with mobile bed sediment transport and BSTEM analysis active.

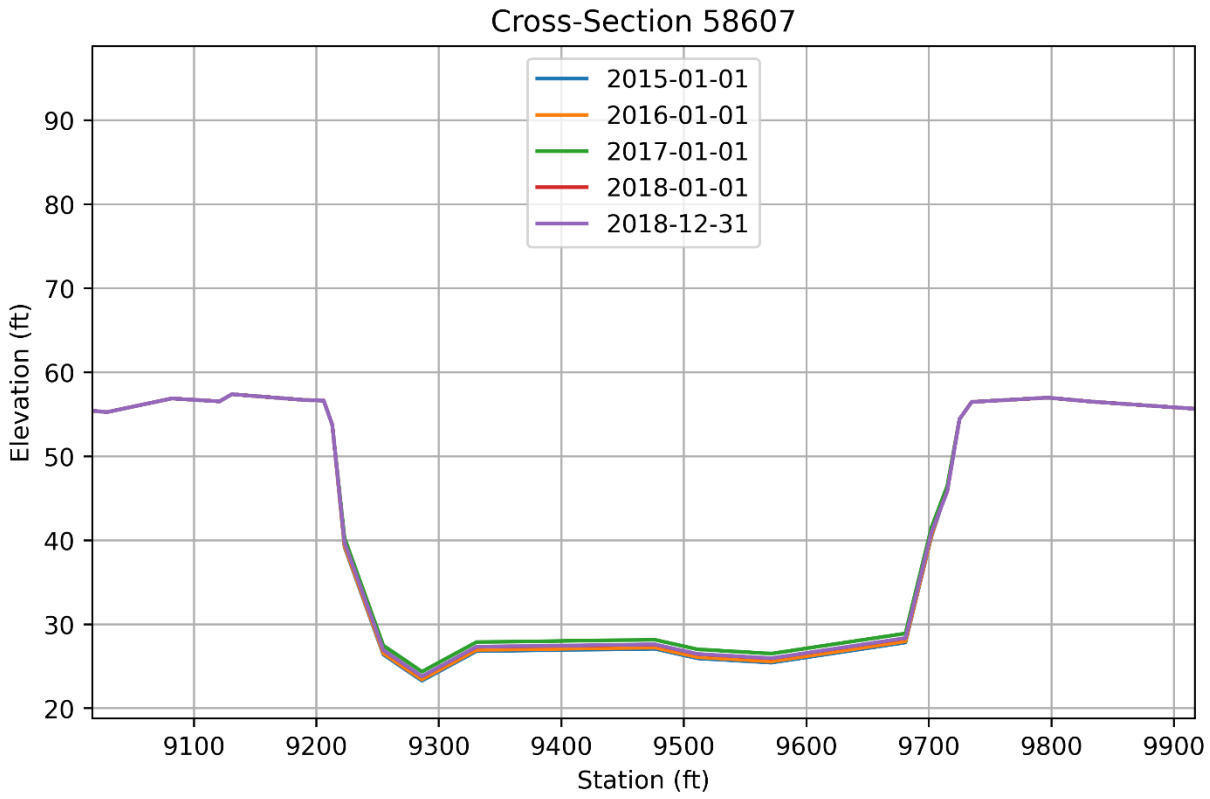

Figure 3-53: Annual change in cross-section form for Lower Model cross-section 58607, with mobile bed sediment transport analysis active.

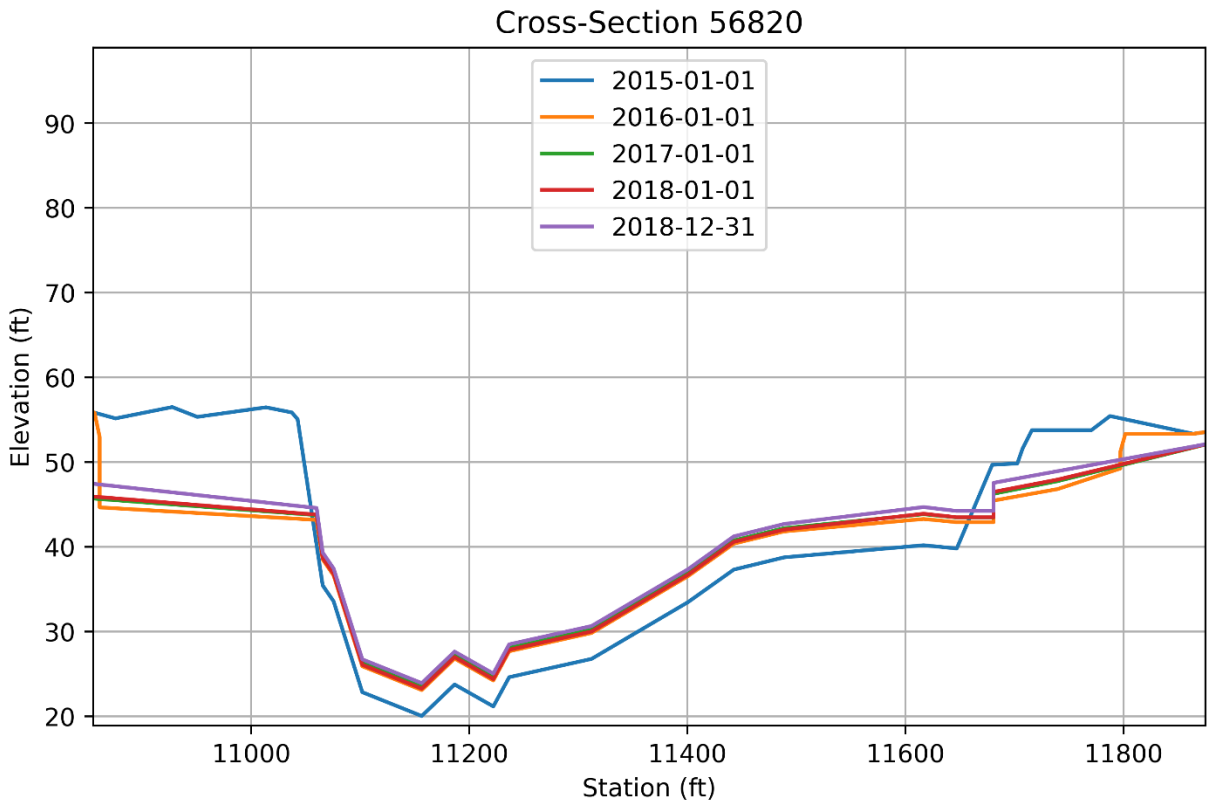

Figure 3-54: Annual change in cross-section form for Lower Model cross-section 56820, with mobile bed sediment transport and BSTEM analysis active.

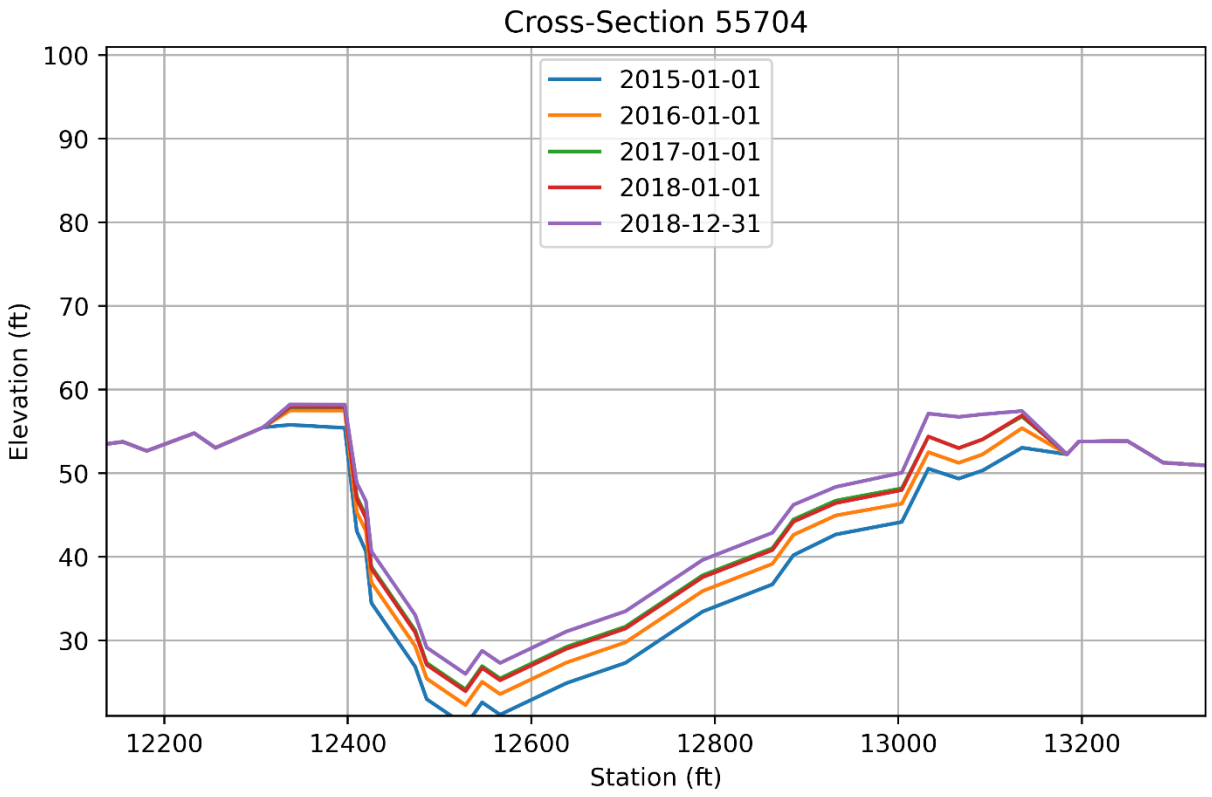

Figure 3-55: Annual change in cross-section form for Lower Model cross-section 55704, with mobile bed sediment transport analysis active.

3.6 *Sediment modeling status and next steps*

In the next phase of the model, we will need to update 1D sediment transport model options and upstream boundary condition, options and parameters, and calibrate the sediment transport function parameters. Further refinement in future phases could include adding in BSTEM capabilities at cross-sections where data is available. The HEC-RAS user manuals identify a stepwise modeling process that yields a well-calibrated sediment transport model with BSTEM analysis, shown below:

1. Calibrate Hydraulics - *This task is completed for both study sites.*
2. Independently model/calibrate 1D sediment transport with calibrated hydraulics – *This task will be completed in the next phase of the project*
3. Independently model/calibrate BSTEM analysis with calibrated hydraulics and integrate with 1D sediment transport, including any further calibration of the coupled model – *This task could be completed as part of a future phase to extend capabilities of the sediment transport model*

3.6.1 1D Sediment Transport Model – Next Phase

For the 1D sediment transport model, the following options should be evaluated by the project team, and appropriate settings for the science goals of the model should be determined:

- Transport Function
- Sorting Method
- Fall Velocity Method
- Cohesive Transport Options
- Deposition Extent
- Erosion Extent
- Active Layer Options
- Extent of mobile bed
- Erodible Sediment Depth
- Pass-through Node Locations
- Upstream Boundary Condition Type

The sediment transport model upstream boundary condition is currently a rating curve that relates discharge to sediment load and load gradation. This rating curve should be vetted by the project team and should be tested in simulations with different short-term hydrographs to determine the sensitivity of modeled sediment transport at the study-site cross-sections to the rating curve characteristics. The rating curve calibration is expected to be the primary component of the 1D sediment transport model calibration.

3.6.2 BSTEM Model – Possible Future Phase

The project team may decide, in future phases of the project, that they want to use HEC-RAS BSTEM capabilities to investigate bank erosion and migration at certain locations. For the BSTEM model options, the following should also be evaluated by the project team and appropriate settings for the science goals of the model should be determined:

- Locations where BSTEM analysis is active
- Number of Failure Plane Computation Nodes
- Number of Time Steps Between Bank Failure Calculations
- Grain Shear Correction
- Cohesive Toe Scour Algorithm Threshold
- Cohesionless Toe Scour Transport Function
- Toe Scour Mixing Method
- Bank Failure Method
- Ground Water Method

The BSTEM analysis results are also extremely sensitive to the user-defined top of toe and edge of bank station locations. A thorough investigation of the effect of the current cross-section geometry and the selection of these two locations within that geometry should be performed by the project team to identify a consistent method for doing so that yields reasonable results. Once adequate locations have been identified, the project team should calibrate BSTEM parameters at each cross-section, using bank failure or bank migration observed data.

4 References

Brotherson, J.D., Rushforth, S.R., Evenson, W.E., Johansen, J.R. & Morden, C. (1983). Population dynamics and age relationships of 8 tree species in Navajo National Monument, Arizona. Journal of Range Management 36(2), 250-256.

Daly, E.R., Fox, G.A., Miller, R.B., and A.T. Al-Madhhachi. (2013). A scour depth approach for deriving erodibility parameters from Jet Erosion Tests. St. Joseph, Michigan: ASABE. Trans. ASABE 56(6): 1343 - 1351. doi: 10.1303/trans.56.10350.

[EPA] Environmental Protection Agency. (2020). Environmental and Compliance History Online. Retrieved from: https://echo.epa.gov/. Accessed: April, 2020.

Hayes, T.D. (2018). Riparian productivity along the Middle Trinity River. Texas Parks and Wildlife Department Contract No. 490954; Texas Water Development Board Contract No. 1348311645.

Hayes, T.D. & Baker, D. (2019). Riparian productivity in the Brazos, Guadalupe, and Trinity River Basins, Texas: Final Report. Texas Parks and Wildlife Department Contract Nos. 490954 & 492283; Texas Water Development Board Contract Nos. 1348311645 & 1600011933.

Hinchman, V.H. & Birkeland, K.W. (1995). Age prediction based on stem size for riparian cottonwood stands. The Southwestern Naturalist 40(4), 406-409. Retrieved from www.jstor.org/stable/30055147

Howe, W.H. & Knopf, F.L. (1991). On the imminent decline of Rio Grande cottonwoods in central New Mexico. The Southwestern Naturalist 36(2), 218-224.

Irvine, J.R. & West, N.E. (1979). Riparian tree species distribution and succession along the lower Escalante River, Utah. Southwestern Naturalist 24(2), 331-346.

Lichvar, R.W., Banks, W.N. Kirchner & Melvin, N.C. (2016). The National Wetland Plant List: 2016 wetland ratings. Phytoneuron 2016(30), 1-17.

Lichvar, R.W., Melvin, N.C., Butterwick, M.L. & Kirchner, W.N. (2012). National Wetland Plant List Indicator Rating Definitions. (ERDC/CRREL TN-12-1). Hanover, NH.: U.S. Army Corps of Engineers, Engineer Research and Development Center, Cold Regions Research and Engineering Laboratory.

Mangham, W., Osting, T.D., & Flores, D.F. (2015). LiDAR Acquisition and Flow Assessment for the Middle Trinity River. Report produced for: Trinity and San Jacinto Rivers and Galveston Bay Stakeholder Committee through the Texas Water Development Board. Contract No. 1400011696.

Mangham, W., Osting, T., & Flores, D. (2017). Evaluation of Adopted Flow Standards for the Trinity River, Phase 2. Report produced for: Trinity and San Jacinto Rivers and Galveston Bay

Stakeholder Committee through the Texas Water Development Board. Contract No. 1600011940.

Rosgen, D. L. (1996). Applied river morphology. Pagosa Springs, Colorado: Wildland Hydrology.

[RPS] RPS Group. (2016). Water Quality Model of the Middle Trinity River. Texas Water Development Board, Contract No.: 1348311642. Austin, Texas: TWDB.

Teck, R.M. & Hilt, D.W. (1991). Individual tree-diameter growth model for the Northeastern United States. Res. Pap. NE-649. Radnor, PA: US. Department of Agriculture, Forest Service, Northeastern Forest Experiment Station. 11p.

[TRA] Trinity River Authority. (2017a). Evaluation of Adopted Flow Standards for the Trinity River, Phase 2. Texas Water Development Board, Trinity and San Jacinto Rivers and Galveston Bay Stakeholder Committee. Contract No. 1600011940. Austin, Texas: TWDB.

[TRA] Trinity River Authority. (2017b). Quality Assurance Project Plan. Arlington, Texas: Trinity River Authority. (p.211). Retrieved from www.trinityra.org/default.asp?contentID=97. Accessed: April, 2020.

[TRA & RPS] Trinity River Authority & RPS Espey. (2013). Trinity River Reconnaissance Survey, 2011. Arlington, Texas: Trinity River Authority.

[TRA & RPS] Trinity River Authority of Texas & RPS Espey Consultants Inc. (2013). Trinity River Long-Term Study. Arlington: Trinity River Authority of Texas.

[TSJ] Trinity and San Jacinto and Galveston Bay Basin and Bay Area Stakeholder Committee with support of the Basin and Bay Expert Science Team. (2012). Work Plan Report. April 24, 2012. Austin, Texas: TWDB.

[USGS] United States Geologic Survey. (2020). USGS 08065000 Trinity River near Oakwood, Texas. Website: https://waterdata.usgs.gov/nwis/dv/?site_no=08065000&PARAmeter_cd=00060 Accessed April 1, 2020.

5 Appendices

Appendix 1. Water Quality Grab Sample Results

								00078	00020	72053	00061	89835	01351	00010	00400	00094	00300	NA	NA	00310	00620	00615	70507	70300	00530	00535	00610	00665	00625	32211	00680	
Tag	Station	Date	Time	Sample Depth (m)	Probe Chlorophyll (ug/L)	Probe BGA (ug/L)	Turbidity (NTU)	Secchi Depth (m)	Air Temp (C)	Days Since Rain	Flow (cfs)	Method	Flow Severity	Water Temp (C)	pH (SU)	Sp Cond (uS/cm)	DO (mg/L)	20 Day Biochemical Oxygen Demand	7 Day Biochemical Oxygen Demand	BIOCHEMICAL OXYGEN DEMAND (MG/L, 5 DAY - 20DEG C	NITRATE NITROGEN, TOTAL (MG/L AS N)	NITRITE NITROGEN, TOTAL (MG/L AS N)	ORTHOPHOSPHATE PHOSPHORUS,DISS,MG/L,FILTER >15MIN	RESIDUE,TOTAL FILTRABLE (DRIED AT 180C) (MG/L)	RESIDUE, TOTAL NONFILTRABLE (MG/L)	RESIDUE, VOLATILE NONFILTRABLE (MG/L)	NITROGEN, AMMONIA, TOTAL (MG/L AS N)	PHOSPHORUS, TOTAL, WET METHOD (MG/L AS P)	NITROGEN, KJELDAHL, TOTAL (MG/L AS N)	CHLOROPHYLL-A UG/L SPECTROPHOTOMETRIC ACID. METH	CARBON, TOTAL ORGANIC, NPOC (TOC), MG/L	Volatile Organic Carbons MG/L
TR0043M	10919	6/29/18	10:06	0.3	22.9	1.05	23.3	0.105	29	18	825	1=Gage	3=Norm	31.2	8.51	868	8.23	24.02	5	NA	7.64	<0.05	0.75	576	130	<20	<0.02	1.02	0.583	97*	6.4	ND
TR0044M	10920	6/29/18	11:05	0.3	19.4	0.87	12.7	0.125	31	18	860	1=Gage	3=Norm	30.8	8.65	891	8.67	23.44	5	NA	8.31	0.08	0.8	544	60	<10	<0.02	1	1.09	78*	7	ND
TR0048M	16998	7/18/18	13:16	0.3	NA	NA	7.48	0.5	28.9	3	1250	1=Gage	2=Low	30.66	8.4	353	8.17	11	3	<2	<0.04	<0.04	***LE***	208	14	5	<0.1	***LE***	***LE***	18	6.3	ND
TR0047M	10896	7/19/18	9:05	0.3	NA	NA	14.7	0.3	26.3	4	1310	1=Gage	2=Low	31.08	8.36	347	8.55	10	3	2	<0.04	<0.04	0.09	206	23	8	<0.1	0.12	***LE***	27	5.8	ND
TR0046M	10895	7/19/18	9:55	0.3	NA	NA	17.7	0.21	27.1	4	NR	NR	2=Low	31.11	7.95	351	7.25	10	3	2	<0.04	<0.04	0.07	204	34	8	<0.1	0.09	***LE***	17	5.5	ND
TR0050M	10919	8/8/18	8:15	0.3	11.1	0.49	29.2	0.125	27	1	566	1=Gage	3=Norm	29.99	8.25	897	6.42	NA	***LE***	<2	7.41	<0.05	0.81	563	86	<14	0.05	1.02	1.08	41	5.8	ND
TR0051M	10920	8/8/18	10:15	0.3	9.9	0.41	26.2	0.11	30.6	1	726	1=Gage	2=Low	30.537	8.33	905	7.2	NA	***LE***	<2	9.44	0.05	1.06	542	72	<10	<0.02	1.21	1.02	41	6.7	ND
TR0054M	16998	8/13/18	11:05	0.3	NA	NA	4.98	0.63	29.1	<1	1250	1=Gage	2=Low	29.37	7.99	393	7.79	9	2	<2	0.06	<0.04	0.13	194	9	3	0.1	0.42	0.51	10	6.1	ND
TR0053M	10896	8/13/18	9:32	0.3	NA	NA	12.8	0.22	28.1	1	1390	1=Gage	2=Low	29.1	8.23	380	8.27	11	4	<2	<0.04	<0.04	0.09	196	23	7	<0.1	0.34	0.53	42	6	ND
TR0052M	10895	8/13/18	10:07	0.3	NA	NA	17.4	0.21	28.9	1	NR	NR	2=Low	29.7	8.08	386	7.77	11	4	2	<0.04	<0.04	0.1	206	39	8	<0.1	0.38	0.59	22	6	ND
TR0055M	10919	9/17/18	11:31	0.3	1.4	0.12	50	0.04	31	2	1310	1=Gage	3=Norm	28.36	7.58	421	6.53	7	NA	<2	1.8	<0.05	0.2	306	272	39	0.03	0.56	0.94	8	4.5	ND
TR0056M	10920	9/17/18	12:28	0.3	4.3	0.26	45.3	0.07	31	2	2320	1=Gage	3=Norm	28.98	7.7	557	7.03	9	NA	3	4.12	0.17	0.39	367	171	25	<0.02	0.61	0.95	18	5.1	ND
TR0059M	16998	9/25/18	13:17	0.3	NA	NA	3.71	0.58	25.3	2	NR	NR	2=Low	27.6	8	416	8.18	6	<2	<2	0.18	<0.04	0.11	220	2	<2	<0.1	0.15	0.2	20	5.5	ND
TR0058M	10896	9/25/18	11:28	0.3	NA	NA	16.7	0.31	24.6	2	1040	1=Gage	2=Low	27.3	7.85	388	7.92	6	<2	<2	0.2	<0.04	0.08	206	18	4	<0.1	0.12	0.43	19	5.5	ND
TR0057M	10895	9/25/18	12:12	0.3	NA	NA	18	0.25	26.3	2	NR	NR	2=Low	28	8.06	392	8.58	7	2	<2	0.13	<0.04	0.1	207	30	6	<0.1	0.13	0.48	28	5.3	ND

* - Lab Error, Sample filtered 1 day out of hold time, results still valid

LE - Lab Error, invalid data

Appendix 2. Daily Flow from USGS gage 08065000

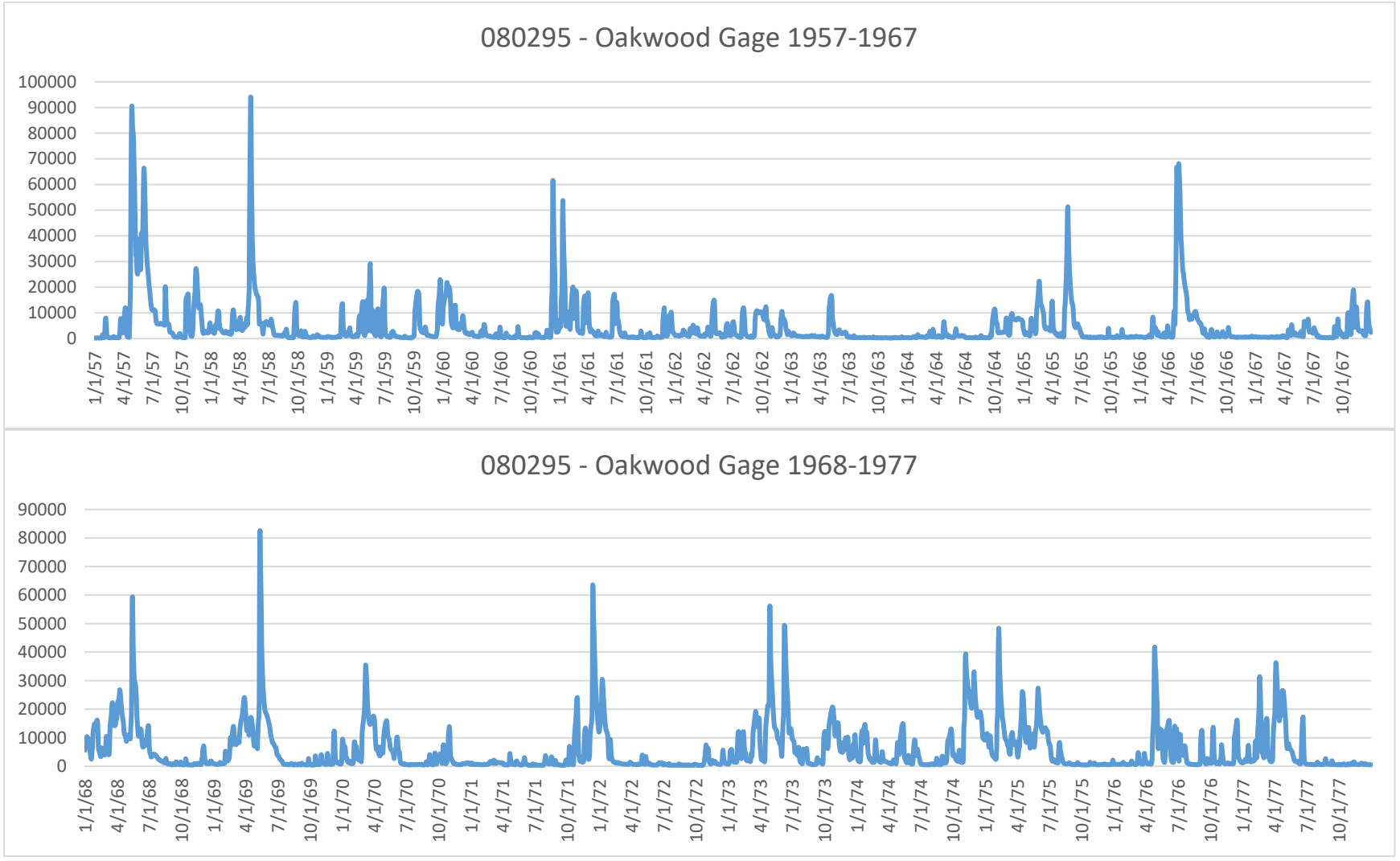

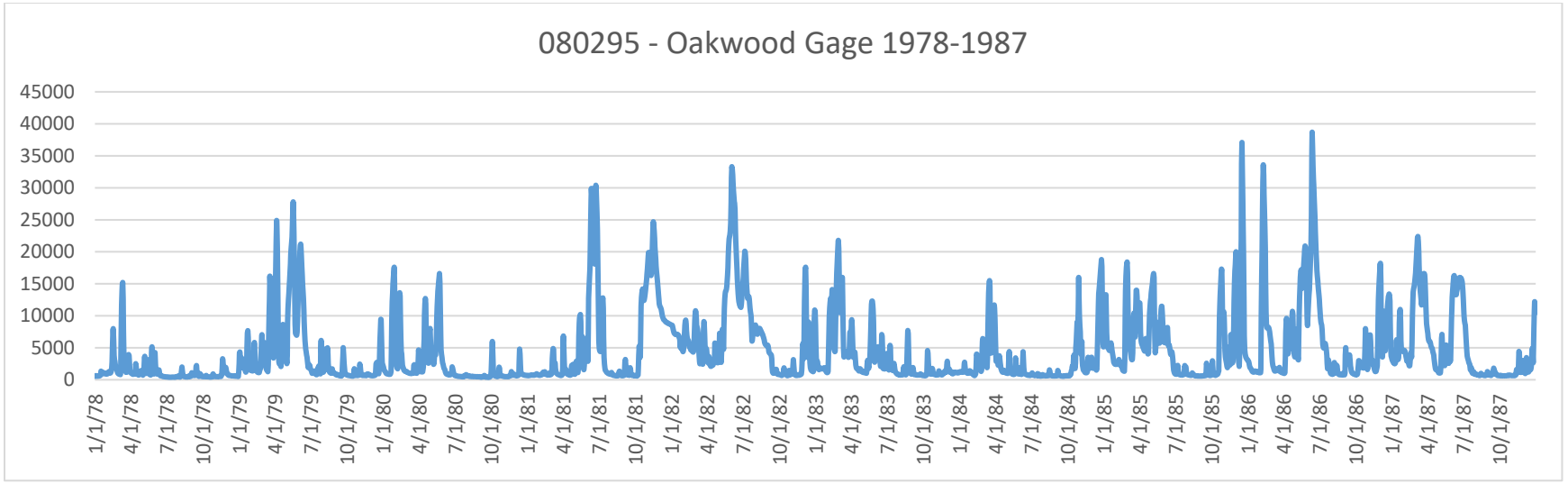
080295 - Oakwood Gage 1978-1987
45000
40000
35000
30000
25000
20000
15000
10000
5000
0
1/1/78
4/1/78
7/1/78
10/1/78
1/1/79
4/1/79
7/1/79
10/1/79
1/1/80
4/1/80
7/1/80
10/1/80
1/1/81
4/1/81
7/1/81
10/1/81
1/1/82
4/1/82
7/1/82
10/1/82
1/1/83
4/1/83
7/1/83
10/1/83
1/1/84
4/1/84
7/1/84
10/1/84
1/1/85
4/1/85
7/1/85
10/1/85
1/1/86
4/1/86
7/1/86
10/1/86
1/1/87
4/1/87
7/1/87
10/1/87

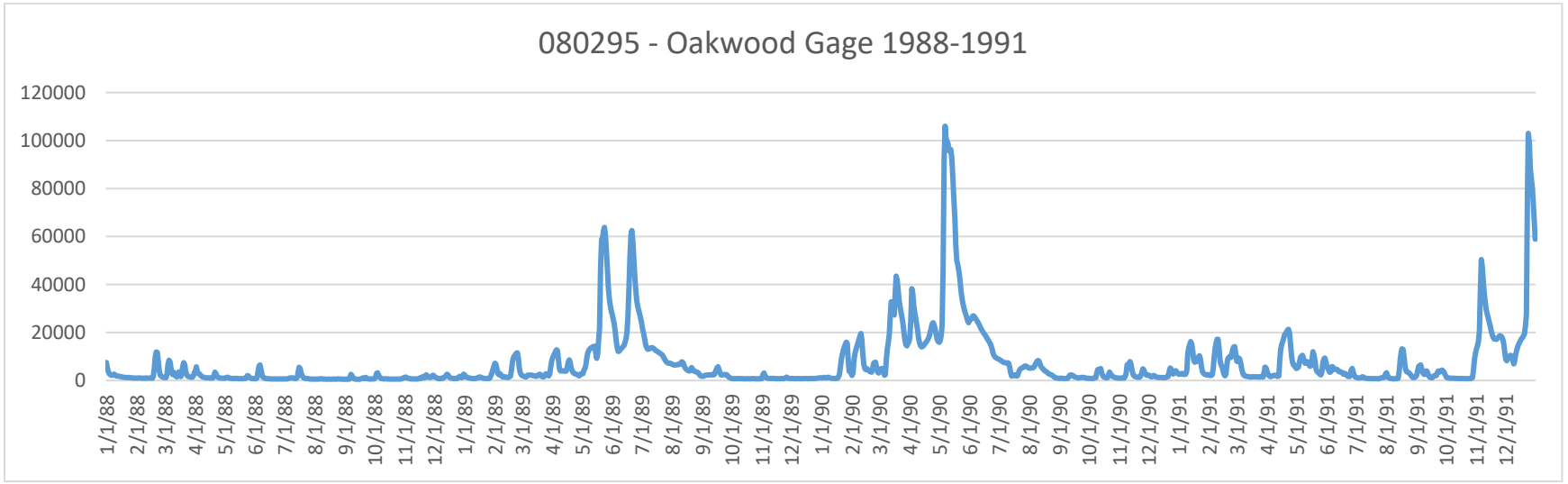
080295 - Oakwood Gage 1988-1991
120000
100000
80000
60000
40000
20000
0
1/1/88
2/1/88
3/1/88
4/1/88
5/1/88
6/1/88
7/1/88
8/1/88
9/1/88
10/1/88
11/1/88
12/1/88
1/1/89
2/1/89
3/1/89
4/1/89
5/1/89
6/1/89
7/1/89
8/1/89
9/1/89
10/1/89
11/1/89
12/1/89
1/1/90
2/1/90
3/1/90
4/1/90
5/1/90
6/1/90
7/1/90
8/1/90
9/1/90
10/1/90
11/1/90
12/1/90
1/1/91
2/1/91
3/1/91
4/1/91
5/1/91
6/1/91
7/1/91
8/1/91
9/1/91
10/1/91
11/1/91
12/1/91

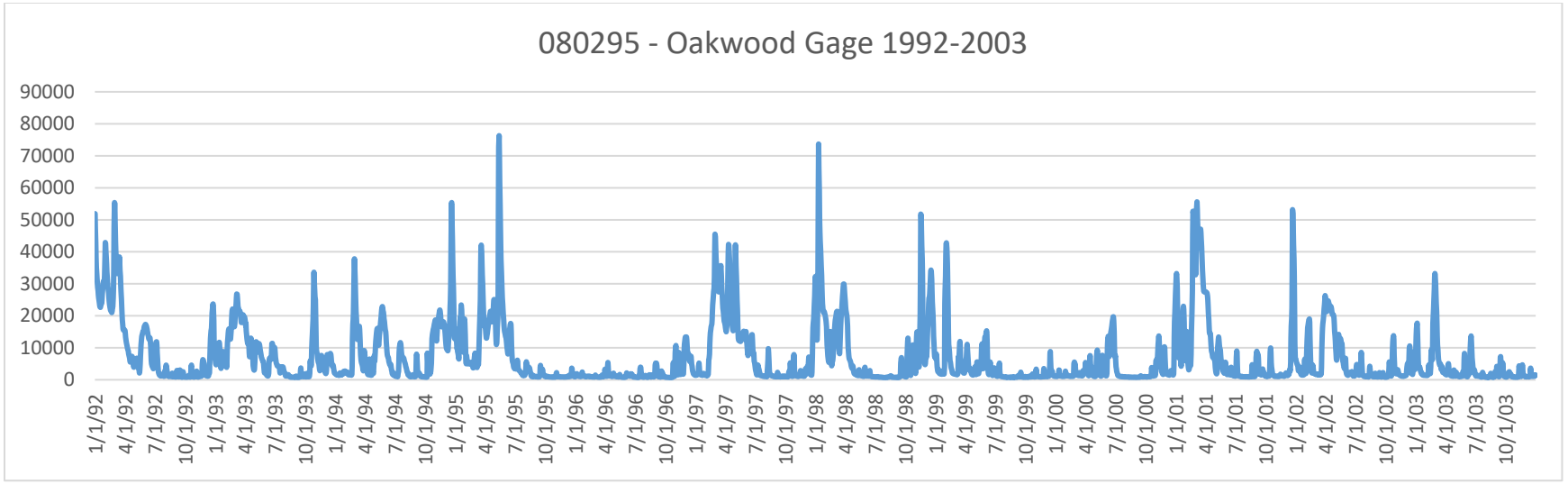
080295 - Oakwood Gage 1992-2003
90000
80000
70000
60000
50000
40000
30000
20000
10000
0
1/1/92
4/1/92
7/1/92
10/1/92
1/1/93
4/1/93
7/1/93
10/1/93
1/1/94
4/1/94
7/1/94
10/1/94
1/1/95
4/1/95
7/1/95
10/1/95
1/1/96
4/1/96
7/1/96
10/1/96
1/1/97
4/1/97
7/1/97
10/1/97
1/1/98
4/1/98
7/1/98
10/1/98
1/1/99
4/1/99
7/1/99
10/1/99
1/1/00
4/1/00
7/1/00
10/1/00
1/1/01
4/1/01
7/1/01
10/1/01
1/1/02
4/1/02
7/1/02
10/1/02
1/1/03
4/1/03
7/1/03
10/1/03

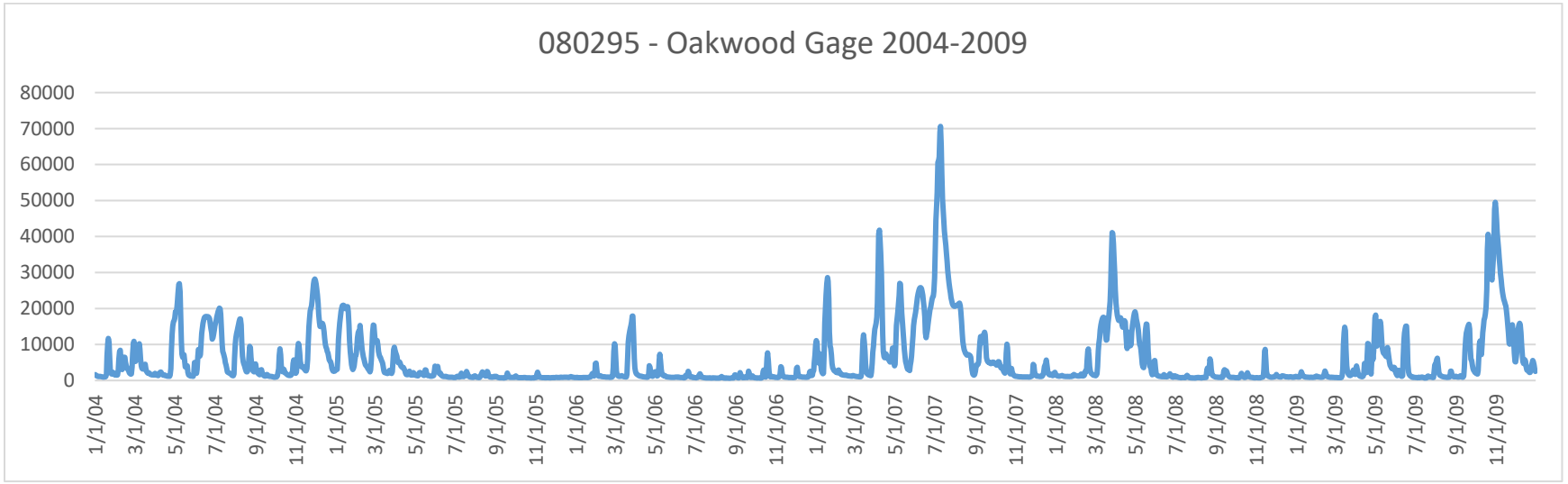
080295 - Oakwood Gage 2004-2009
80000
70000
60000
50000
40000
30000
20000
10000
0
1/1/04
3/1/04
5/1/04
7/1/04
9/1/04
11/1/04
1/1/05
3/1/05
5/1/05
7/1/05
9/1/05
11/1/05
1/1/06
3/1/06
5/1/06
7/1/06
9/1/06
11/1/06
1/1/07
3/1/07
5/1/07
7/1/07
9/1/07
11/1/07
1/1/08
3/1/08
5/1/08
7/1/08
9/1/08
11/1/08
1/1/09
3/1/09
5/1/09
7/1/09
9/1/09
11/1/09

Appendix 3. Tree Core Data from 2017, 2018, and 2019 (Age Adjusted to 2019)

Type	Tag No.	DBH (in)	Age (yrs)	5-Year Age Class (yrs)	Flood Inundation Stage (cfs)
Green Ash	351	5	10	10	11800
Boxelder	376	5	12	10	16500
Boxelder	390	4.5	13	15	11800
Green Ash	333	8	15	15	11800
Green Ash	305	2.75	16	15	16500
Hickory (Pecan)	334	8	17	15	11800
Green Ash	349	8.5	17	15	11800
Green Ash	356	5.5	17	15	11800
Green Ash	392	8.6	17	15	11800
Green Ash	394	7.7	18	20	10000
Green Ash	325	2.5	19	20	10000
Green Ash	350	11.5	19	20	11800
Green Ash	396	9.1	19	20	16500
Green Ash	304	2.75	20	20	21000
Green Ash	393	8.6	20	20	10000
Green Ash	399	9.4	20	20	7000
Boxelder	318	5	21	20	10000
Green Ash	322	4	21	20	10000
Green Ash	398	8.3	21	20	11800
Green Ash	335	6.5	22	20	11800
Green Ash	336	8	22	20	10000
Green Ash	400	8.2	22	20	10000
Boxelder	320	7	23	25	10000
Green Ash	347	6	23	25	21000
Green Ash	306	4.25	25	25	21000
Green Ash	321	6	25	25	10000
Green Ash	324	5	25	25	10000
Green Ash	359	7.5	25	25	11800
Green Ash	360	11	25	25	11800
Green Ash	309	8.5	26	25	21000
Green Ash	380	10	26	25	11800
Green Ash	201	8.1	26	25	30000
Green Ash	323	9.5	27	25	21000
Boxelder	345	6.5	27	25	10000
Hickory (Pecan)	330	11	27	25	6180
Green Ash	346	3.25	28	30	21000
Green Ash	381	14	29	30	11800

Green Ash	202	13.2	29	30	21000
Green Ash	344	6.5	30	30	21000
Green Ash	384	12	31	30	16500
Green Ash	361	13.5	32	30	6180
Green Ash	386	9	32	30	21000
Green Ash	340	5	33	35	21000
Green Ash	385	10	33	35	16500
Green Ash	391	13.6	33	35	16500
Green Ash	308	9.5	34	35	21000
Green Ash	342	8.5	34	35	21000
Green Ash	200	15.6	34	35	21000
Black Willow	303	11	35	35	16500
Green Ash	363	10	35	35	11800
Green Ash	337	10.25	36	35	16500
Green Ash	397	18.3	36	35	6180
Green Ash	307	10	37	35	21000
Green Ash	341	7.75	37	35	21000
Green Ash	383	23	37	35	16500
Green Ash	377	17.5	38	40	11800
Green Ash	374	12.5	39	40	16500
Green Ash	310	11.5	40	40	30000
Green Ash	366	24.25	40	40	16500
Green Ash	367	6.5	40	40	16500
Green Ash	343	15	41	40	21000
Green Ash	357	8.75	41	40	11800
Green Ash	339	15.75	42	40	16500
Green Ash	368	16.5	42	40	16500
Green Ash	369	16.75	42	40	16500
Green Ash	311	11.75	44	45	30000
Green Ash	358	15.5	44	45	11800
Green Ash	364	18.5	45	45	16500
Green Ash	372	10.5	49	50	16500
Green Ash	338	15	50	50	16500
Green Ash	371	10.5	50	50	16500
Green Ash	373	8.75	50	50	16500
Green Ash	389	16.5	50	50	16500
Green Ash	388	18.2	51	50	16500
Green Ash	375	18	63	65	16500
Green Ash	395	26.7	63	65	16500

Appendix 4. Geotechnical results from the field and Baylor University sediment laboratory.

Sample No. Lab	**1**	**2**	**3**	**4**	**5**	**6**
Site	**80295**	**80295**	**80295**	**80075**	**80075**	**80075**
Location	**XS2**	**XS3**	**X1**	**XS4**	**XS1**	**XS2**
River Mile	**295.15**	**294.79**	**295.35**	**73.75**	**75.2**	**74.6**
Bank	**R**	**R**	**R**	**L**	**L**	**L**
Wet Weight	2573	2450	2425	2386	2434	2186
Tare - Humboldt core	586	586	586	586	586	586
BulkDensity(g/cm3)	2.074	1.946	1.920	1.879	1.929	1.670
Lab Vane(kpa)	17.88	7.45	75.245	4.47	29.055	41.72
Field Vane (kpa) (large vane #*.1*.2*98.0665)	17.65	9.41	11.96	0.00	3.33	19.61
Field Vane (Dial Reading)(large)	9	4.8	6.1	No Data	1.7	10.0001
Penetrometer Average (Kg/Cm^2)	2.66	0.78	4.05	2	1.49	2
Penetrometer Average (Kg.)	4.8	1.4	7.3	3.6	2.5	3.6
Pen1	*2.95*	*0.85*	*11.0001*	*3.9*	*2.4*	*3.2*
Pen2	*4.05*	*1.2*	*11.0001*	*4.05*	*2.9*	*3.425*
Pen3	*5*	*1.05*	*11.0001*	*3.9*	*3.2*	*3.5*
Pen4	*3.8*	*1.92*	*3.35*	*3.7*	*2*	*3.9*
Pen5	*7.4*	*1.9*	*3.425*	*2.9*	*2.4*	*3.5*
Pen6	*5.4*	*1.2*	*4.2*	*2.95*	*1.9*	*4.05*
Jet Time (Minutes)	**Scour Depth (mm)**					
0	40	34	35	36	32	32
5	45	112	37	44	65	41
10	47	121	40.5	91	72	55
20	49	128	44	115	88	66
30	52	>130.0	44	123	125	70
40	57		44.5	122	>130.0	79
50	63		45	123		90
60	72		45	124		95
Head	5.46	3.72	3.69	3.75	3.71	5.49
Nozzle	0.125	0.125	0.125	0.125	0.125	0.125
Lab Moisture	0.1461	0.2599	0.2173	0.1296	0.1476	0.4111
Moisture Core	0.2	0.23	0.29	0.21	0.222	0.512
Field % Moisture	0.4	0.48	0.53	0.279	0.35	0.68
Lab Result	Sandy Clay Loam	Sandy Clay Loam	Clay Loam	Sand	Loamy Sand	Clay
Field Observation	Silty Clay	Sandy Loam	Clay	Sand	Sandy Loam	Clay

Appendix 5. Percent finer from laboratory analysis of core samples from site 080295 and 080075.

SUMMARY OF LABORATORY TEST RESULTS

LABORATORY TESTING SERVICES

Trinity River Authority

Sample Identication	Visual Description & Unified Soil Classification (ASTM D-2487/ D-2488)		Moisture Content (%)	Liquid Limit	Plastic Limit	Plasticity Index	Grain Size Analysis (Percent Finer)												Notes
							U.S. Sieve Sizes								Hydrometer (mm)				
							#4	#10	#20	#40	#60	#80	#100	#200	0.0625	0.016	0.008	0.004	
TRA 73.80	Tan and gray poorly graded sand with silt	SP-SM	21.0	Non-Plastic			100	100	100	96.8	59.8	28.6	14.3	6.0	5.5	5.3	5.0	4.8	
TRA 74.65	Gray fat clay	CH	51.2	101	36	65	100	100	100	100	99.8	99.5	99.3	98.4	97.5	92.9	92.5	90.3	
TRA 75.25	Gray slity sand	SM	22.2	Non-Plastic			100	99.6	99.2	96.7	66.1	51.5	44.2	20.7	17.0	8.6	8.2	7.8	
TRA 294.79	Brown clayey sand	SC	23.4	32	17	15	100	100	100	100	98.9	90.7	78.1	42.8	37.8	25.0	23.6	23.0	
TRA 295.15	Brown and gray sandy lean clay	CL	20.0	44	16	28	99.5	97.7	94.4	91.2	85.6	74.3	67.1	54.3	51.9	38.1	35.0	32.3	
RM 295.32	Dark brown and gray fat clay with sand	CH	29.0	53	25	28	100	100	99.4	98.7	97.6	96.6	95.5	73.5	69.0	46.6	40.0	36.2	

Appendix 6. Hydraulics and Water Quality Modeling Input Scenarios – Upper Model.

Hydraulics

Scenario	HEC-RAS Plan	Title (from RPS/ASI Report)	Dates		Geometry File	Flow File	Hydraulic Boundary Conditions							Notes
			Begin	End			US Boundary Condition	Added flow at 1513706	Lateral flow at 1003153	Lateral flow at 892973	Lateral flow at 843230	Lateral flow at 273136	DS Boundary Condition	
A	WQ_RunA	A	1-Jun-14	30-Sep-14	Final_Upper_Trinity_Geometry_ASI_2020	RunA	USGS (Rosser)	--	--	--	--	--	Stage Hydrograph (RPS/ASI HEC-RAS model)	No lateral inflows
B1	WQ_RunB1	B	1-Jun-14	30-Sep-14	Final_Upper_Trinity_Geometry_ASI_2020	RunB		37.1	1.5	5.3	2.7	1.8	Stage Hydrograph (RPS/ASI HEC-RAS model)	RPS/ASI model had higher 1513706 (WWTP) additional flow input for Runs B1/B2, but for ASI 2020 model defaulted to permitted values based on discussion with Tim. Model was calibrated on this run.
C	WQ_RunC	C	1-Jun-14	20-Sep-14	Final_Upper_Trinity_Geometry_ASI_2020	RunC	USGS (Rosser)	37.1	1.9	4.4	2.2	1.5	Stage Hydrograph (RPS/ASI HEC-RAS model)	
D	WQ_RunD	D	1-Jun-14	20-Sep-14	Final_Geometry_ASI_2020_RunD_RunE	RunD	Constant headwater at 75cfs	37.1	1.9	4.4	2.2	1.5	Stage Hydrograph (RPS/ASI HEC-RAS model)	The geometry file used in these runs was altered: (i) incoming tributaries from Cedar Creek were deleted (ii) interpolated cross sections were added throughout the model to decrease cross section spacing to 1,000-ft minimum.
E	WQ_RunE	E	1-Jun-14	20-Sep-14	Final_Geometry_ASI_2020_RunD_RunE	RunE	Constant headwater at 160cfs	37.1	1.9	4.4	2.2	1.5	Stage Hydrograph (RPS/ASI HEC-RAS model)	
F	WQ_RunF	F	1-Jun-14	30-Sep-14	Final_Upper_Trinity_Geometry_ASI_2020	RunF	Constant headwater at 250cfs	37.1	1.9	4.4	2.2	1.5	Stage Hydrograph (RPS/ASI HEC-RAS model)	
G	WQ_RunG	G	1-Jun-14	30-Sep-14	Final_Upper_Trinity_Geometry_ASI_2020	RunG	Constant headwater at 450cfs	37.1	1.9	4.4	2.2	1.5	Stage Hydrograph (RPS/ASI HEC-RAS model)	
H	WQ_RunH1	H	1-Jun-11	31-Aug-11	Final_Upper_Trinity_Geometry_ASI_2020	RunH1	USGS (Rosser)	37.1	1.9	4.4	2.2	1.5	Stage Hydrograph (RPS/ASI HEC-RAS model)	
I	WQ_TI1_2018_JUN19-SEP30	--	19-Jun-18	30-Sep-18	Final_Upper_Trinity_Geometry_ASI_2020	2018_JUN19-SEP30	USGS (Rosser)	18.4	1.4	2.3	1.4	1.1	Stage Hydrograph from USGS Riverside Gauge	Lateral flows from WWTPs taken from average loadings from 'WWTP_Inputs_Upper'

RAS Model	\16008_TRA\2020_WQ_Model\H&H\HEC-RAS\Upper_Model\1-ASI_2020_TRA_Upper_Model_Rosser_Oakwood

Souce Data Files

Water Quality Timeseries data	\16008_TRA\2020_WQ_Model\Handoff_FES_2_JB\MODEL\Upper_Model\ObservedWQ\Observed_WQ_Upper.xlsx
Meteorology Files	\16008_TRA\2020_WQ_Model\H&H\Data\Met_Model_Update
WWTP Loadings	\16008_TRA\2020_WQ_Model\Handoff_FES_2_JB\MODEL\Upper_Model\ObservedWQ\WWTP_Inputs_Upper.xlsx
Observed Flows	\16008_TRA\2020_WQ_Model\H&H\HEC-RAS\FLOWS_Upper_Model.xlsx
Obs WQ from TRA	\16008_TRA\2020_WQ_Model\H&H\Data\Received_Data\From_Web_20200901

Water Quality

Scenario	HEC-RAS WQ Plan	Title (from RPS/ASI Report)	Dates		WQ Boundary Conditions																								Notes
					US - Trinity / TRA Ten Mile				Freestone Power (1003153)				TDCJ Coffield (892973)				TDCJ Beto (843230)				TDCJ Ferguson (273136)				Cedar Creek (US Trib)				Cedar Creek (DS Trib)				
			Begin	End	Temp	DO	CBOD	NH4	Temp	DO	CBOD	NH4	Temp	DO	CBOD	NH4	Temp	DO	CBOD	NH4	Temp	DO	CBOD	NH4	Temp	DO	CBOD	NH4	Temp	DO	CBOD	NH4	
A	RunA	A	1-Jun-14	30-Sep-14	USGS (Rosser)	USGS (Rosser)	5	0	N/A	N/A	N/A	N/A	N/A	N/A	N/A	N/A	N/A	N/A	N/A	N/A	N/A	N/A	N/A	N/A	USGS (Rosser)	5.5	0	0	USGS (Rosser)	5.5	0	0	No WWTP loading
B	RunB1	B	1-Jun-14	30-Sep-14	USGS (Rosser)	USGS (Rosser)	1	0.3	30	7.54	0	0	30	7.05	2.4	0	30	6.98	2.63	0	30	4.67	2.1	0.36	USGS (Rosser)	5.5	0	0	USGS (Rosser)	5.5	0	0	
C	RunC	C	1-Jun-14	20-Sep-14	USGS (Rosser)	USGS (Rosser)	10	3	30	7.54	0.0	0.0	30	5.0	10.0	2.0	30	6.0	10.0	2.0	30	4.0	7.0	2.0	USGS (Rosser)	5.5	0	0	USGS (Rosser)	5.5	0	0	Full permitted amounts; model was calibrated on this run
D	RunD	D	1-Jun-14	20-Sep-14	USGS (Rosser)	USGS (Rosser)	10	3	30	7.54	0.0	0.0	30	5.0	10.0	2.0	30	6.0	10.0	2.0	30	4.0	7.0	2.0	USGS (Rosser)	5.5	0	0	USGS (Rosser)	5.5	0	0	Full permitted amounts
E	RunE	E	1-Jun-14	20-Sep-14	USGS (Rosser)	USGS (Rosser)	10	3	30	7.54	0.0	0.0	30	5.0	10.0	2.0	30	6.0	10.0	2.0	30	4.0	7.0	2.0	USGS (Rosser)	5.5	0	0	USGS (Rosser)	5.5	0	0	Full permitted amounts
F	RunF	F	1-Jun-14	30-Sep-14	USGS (Rosser)	USGS (Rosser)	10	3	30	7.54	0.0	0.0	30	5.0	10.0	2.0	30	6.0	10.0	2.0	30	4.0	7.0	2.0	USGS (Rosser)	5.5	0	0	USGS (Rosser)	5.5	0	0	Full permitted amounts
G	RunG	G	1-Jun-14	30-Sep-14	USGS (Rosser)	USGS (Rosser)	10	3	30	7.54	0.0	0.0	30	5.0	10.0	2.0	30	6.0	10.0	2.0	30	4.0	7.0	2.0	USGS (Rosser)	5.5	0	0	USGS (Rosser)	5.5	0	0	Full permitted amounts
H	RunH1	H	1-Jun-11	31-Aug-11	USGS (Rosser)	USGS (Rosser)	10	3	30	7.54	0.0	0.0	30	5.0	10.0	2.0	30	6.0	10.0	2.0	30	4.0	7.0	2.0	USGS (Rosser)	5.5	0	0	USGS (Rosser)	5.5	0	0	Full permitted amounts
I	TI1_2018_JUN19-SEP30	N/A	19-Jun-18	30-Sep-18	USGS (Rosser)	USGS (Rosser)	1.0	0.16	30	0	0	0	30	6.0	3.5	0.1	30	6.3	3.0	0.1	30	6.0	2.7	0.1	USGS (Rosser)	5.5	0	0	USGS (Rosser)	5.5	0	0	Taken from average of 06/30/2018 through 09/30/2018 entries in 'WWTP_Inputs_Upper' spreadsheet

Appendix 7. Hydraulics and Water Quality Modeling Input Scenarios – Lower Model

Hydraulics

Scenario	HEC-RAS Plan	Dates		Hydraulic Boundary Conditions		Notes
		Begin	End	US Boundary Condition	DS Boundary Condition	
A	WQ_Jun1_Oct15_2018	1-Jun-18	15-Oct-18	USGS (Romayor)	Normal Depth (S = 0.000213)	Used slope condition from email from Tim on 20200722
B	WQ_RunB	1-Jun-18	15-Oct-18	Constant Headwater at 200 cfs	Normal Depth (S = 0.000213)	
C	WQ_RunC	1-Jun-18	15-Oct-18	Constant Headwater at 700 cfs	Normal Depth (S = 0.000213)	
D	WQ_RunD	1-Jun-18	15-Oct-18	Constant Headwater at 575 cfs	Normal Depth (S = 0.000213)	
E	WQ_RunE	1-Jun-18	15-Oct-18	Constant Headwater at 1150 cfs	Normal Depth (S = 0.000213)	

Water Quality

Scenario	HEC-RAS Plan	Dates		WQ Boundary Conditions			
		Begin	End	Temp, C	DO, mg/L	CBOD	NH4
A	WQ_Jun1_Oct15_2018	1-Jun-18	15-Oct-18	TRA Grab Series			
B	WQ_RunB	1-Jun-18	15-Oct-18	TRA Grab Series			
C	WQ_RunC	1-Jun-18	15-Oct-18	TRA Grab Series			
D	WQ_RunD	1-Jun-18	15-Oct-18	TRA Grab Series			
E	WQ_RunE	1-Jun-18	15-Oct-18	TRA Grab Series			

Appendix 8. Water Quality Calibration and Modeling

Calibration typically involves varying model parameters within ranges of values that conform to the observed site characteristics until predicted values match observed values to the extent that it is possible given limitations of the model and any model input data. The primary water quality constituent goals to be assessed with this model are temperature and dissolved oxygen and, accordingly, these are the two primary constituents that guided the calibration. Other nutrients that are included in the model for which we have input data from TCEQ SWQM observations (Algae, NH4, NO2, NO3, OrgN, OrgP, and OPO4) are secondary constituents used to guide model calibration.

In determining what constituted a satisfactory model calibration, two limitations of the model inputs had to be taken into consideration. First, the model does not consider intervening inflows from watershed inputs between the upstream boundary of the model and the downstream boundary of the model. In the real system, watershed inputs have a considerable impact on water quality constituent concentrations, either decreasing or increasing constituent concentrations and temperature depending on what their own temperature and constituent loadings are relative to those of the water in the Trinity mainstem. Second, model inputs at the upstream boundary for nutrients other than dissolved oxygen are either from TCEQ SWQM data or estimated based on TCEQ SWQM data. For the Upper model, TCEQ SWQM observations are only available for a single point in time on a date within the model time period (7/14/2014) and two dates that are just outside of the model time period (5/20/2014 and 10/21/2014). For the Lower model, TCEQ SWQM observations are only available for two dates within the model time period (7/12/2018 and 9/20/2018) and two dates that are well outside of the model time period (3/20/2018 and 12/18/2018). These dates are used as inputs for nutrient constituents Algae, ON, NH4, NO2, NO3, OP and OPO4 at the upstream boundary, with HEC-RAS linearly interpolating between these observations to provide input values for all other dates in the model time period. It is likely that a significant amount of variation in the concentrations of constituents other than dissolved oxygen and temperature at the upstream boundary is not captured in the TCEQ SWQM datasets. It is important to consider these facts in assessing the calibration of the model because constituent concentrations to a large extent govern the nutrient, dissolved oxygen and temperature dynamics of the modeled system. These limitations have predictable consequences for the model's ability to reproduce observed temperature and dissolved oxygen values at the sites chosen for comparison. Model inputs that affect temperature are only the upstream boundary inflow temperature, air temperature and solar radiation datasets. Accordingly, the model is not able to predict any rapid increases or decreases in air temperature at the comparison sites that are not represented in the upstream boundary inflow dataset. Additionally, some of the spikes or dips in observed dissolved oxygen values are likely caused by either i) watershed inputs of nutrients that are not included in the model or ii) variation in nutrient loadings at the upstream boundary that are not captured in TCEQ SWQM data. As a result, the model is not able to predict any rapid increases or decreases in dissolved oxygen caused by variation in constituent concentrations that are not represented in the upstream boundary inflow dataset.

Model calibration goals were established that accounted for the limitations of model input data. The calibration of modeled temperature was considered satisfactory when broad, weekly to biweekly-scale trends in predicted temperature matched those of observed values. The calibration of modeled dissolved oxygen was considered satisfactory when the average dissolved oxygen value predicted by the model approached that of the observed values and the amount of diurnal variation in predicted values approached that of observed values. For the Upper model, the Oakwood site was considered higher priority in the calibration. For the Lower model, the site at River Station 58607 was considered higher priority in the calibration than the site at River Station 12927.

Upper Model Calibration and Validation

The previous iteration of the Upper water quality model from RPS, 2015 has been calibrated on model Run B, which includes historic WWTP average monthly loadings and historic flows from USGS streamgages for 2014 as boundary condition inputs. The model was recalibrated using this same run to incorporate the effects of refined model hydraulics and the inclusion of additional nutrient parameters from TCEQ SWQM data and TRA sonde deployment data on model results. To calibrate the model, results from Run B were compared with observed values at Oakwood and Crockett study sites, and model parameters were adjusted iteratively until a satisfactory calibration was achieved according to the calibration goals stated above. Model coefficients were adjusted based upon on-site conditions and calibration of predictions to observations, and are shown in Table 5-1. The theta values listed alongside parameters are used to account for temperature dependence of parameters and were not changed from HEC-RAS defaults during model calibration. Temperature results from calibrated Run B are provided in Figure 5-1 and Figure 5-2. Dissolved oxygen results from calibrated Run B are provided in Figure 5-3 and Figure 5-4. Box and whisker plots of temperature and dissolved oxygen, shown in Figure 5-5 and Figure 5-6, compare the range of values simulated for the ten-day lowest stable flow period (B1: 8/23/2014 – 8/31/2014) and the observation period (B2: 8/27/2014 – 9/27/2014) to that of observations. Results of the calibrated Upper model for all other nutrients are included at the end of this section.

Table 5-1: Calibrated water quality model coefficients for Upper Model from Run B.

Parameter	Value	Theta
Algae		
Biomass Chl-a ratio	11.1 ugCha/mgA	
Biomass Nitrogen Fraction	0.07 mgN/mgA	
Biomass Phosphorous Fraction	0.005 mgP/mgA	
Maximum Growth Rate	1.2 day^{-1}	1.047
Maximum Growth Rate Formulation	Multiplicative	
Growth Limitation (light)	4 W m^{-2}	
Growth Limitation (N)	0.01 mgN/L	
Growth Limitation (P)	0.01 mgP/L	
Light Limitation Formulation	Half-Saturation	
Light Extinction (non-algal)	0.03 m^{-1}	
Light Extinction (linear algal)	0.007 $m^{-1}(ugCh/L)^{-1}$	
Light Extinction (non-linear algal)	0.05 $m^{-1}(ugCh/L)^{-2/3}$	
Respiration Rate	0.25 day^{-1}	1.047
Nitrogen Preference	1	
Settling Rate	0.75 m day^{-1}	1.024
Dissolved Oxygen		

Parameter	Value	Theta
Production per unit algal growth	1.4 mgO/mgAp	
Uptake per unit algal respired	1.6 mgO/mgAp	
Production per unit benthic algal growth	1.4 mgO/mgAb	
Uptake per unit benthic algal respired	1.6 mgO/mgAb	
Uptake per unit NH4 oxidized	3 mgO/mgN	
Uptake per unit NO2 oxidized	1 mgO/mgN	
Atmospheric Reaeration	1 day^{-1}	1.24
Sediment Demand	0.6 day^{-1}	1.06
CBOD		
Decay Rate	0.02 day^{-1}	1.047
Settling Rate	0 day^{-1}	1.024
Nitrogen		
OrgN -> NH4	0.05 day^{-1}	1.047
NH4 -> NO2	0.2 day^{-1}	1.083
NO2 -> NO3	0.2 day^{-1}	1.047
Org-N Settling Rate	0.001 day^{-1}	1.024
NH4 Benthos Source Rate	0 mgN m^{-2} day^{-1}	1.074
Nitrification Inhibition Factor	0.6 mg/L	
Phosphorus		
OrgP -> InorgP	0.005 day^{-1}	1.047
Org-P Settling Rate	0.01 day^{-1}	1.024
Benthos Source Rate	0.01 mgP m^{-2} day^{-1}	1.074
Benthic Algae		
Biomass Chl-a ratio	5 ugChab/mgAb	
Biomass Nitrogen Fraction	0.07 mgN/mgAb	
Biomass Phosphorous Fraction	0.01 mgP/mgAb	
Maximum Growth Rate	0.3 day^{-1}	1.047
Maximum Growth Rate Formulation	Multiplicative	
Growth Limitation (light)	6276 W m^{-2}	
Growth Limitation (N)	0.01 mgN/L	
Growth Limitation (P)	0.001 mgP/L	
Benthic Light Limitation Formulation	Half- Saturation	
Respiration Rate	0.01 day^{-1}	1.047
Death Rate	0 day^{-1}	1.047
Nitrogen Preference	0	
Bottom Area Fraction	0	

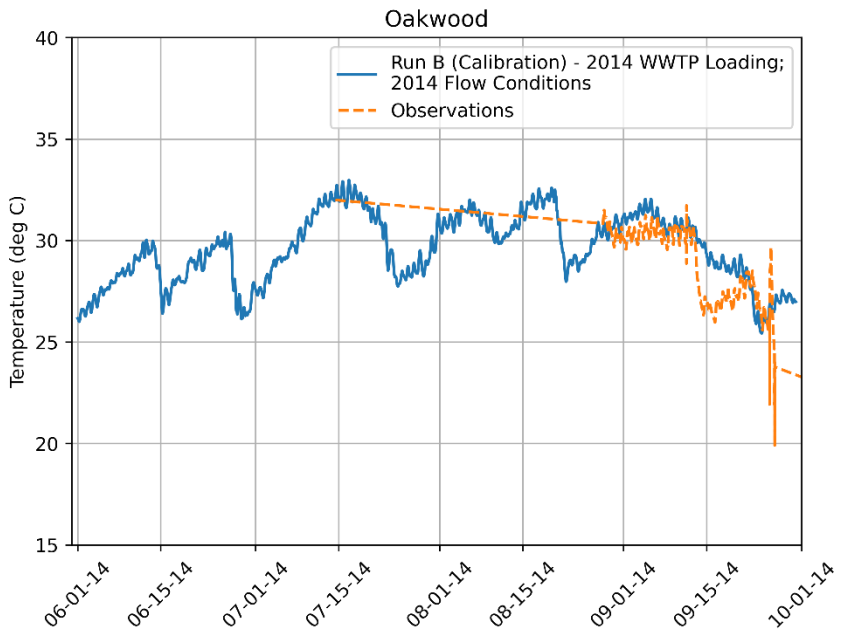

Figure 5-1: Run B predicted and observed temperature at Oakwood study site.

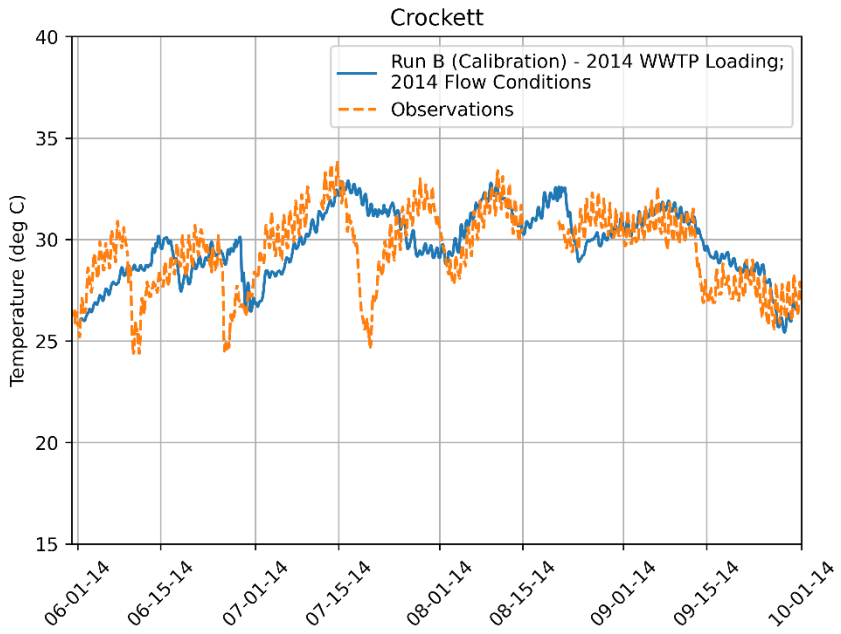

Figure 5-2: Run B predicted and observed temperature at Crockett study site.

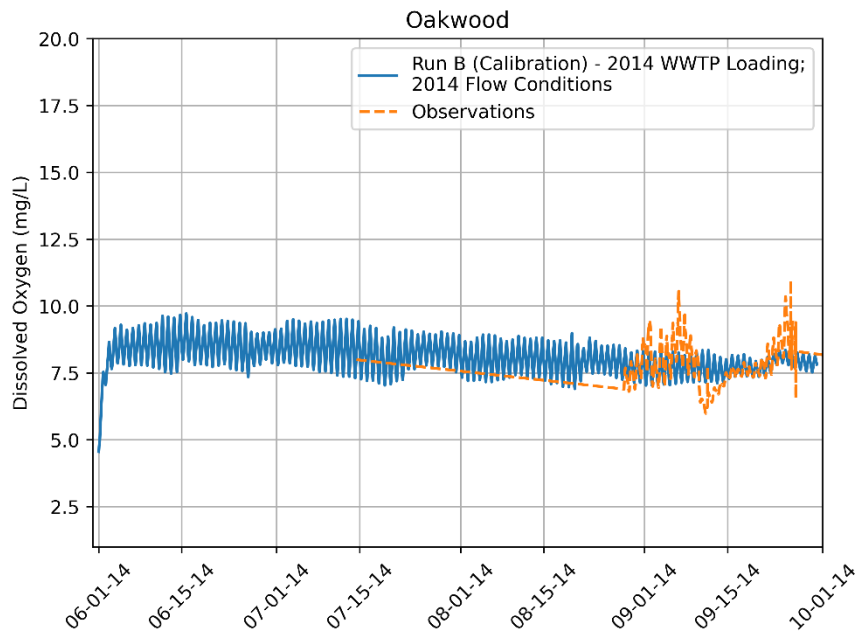

Figure 5-3: Run B predicted and observed dissolved oxygen at Oakwood study site.

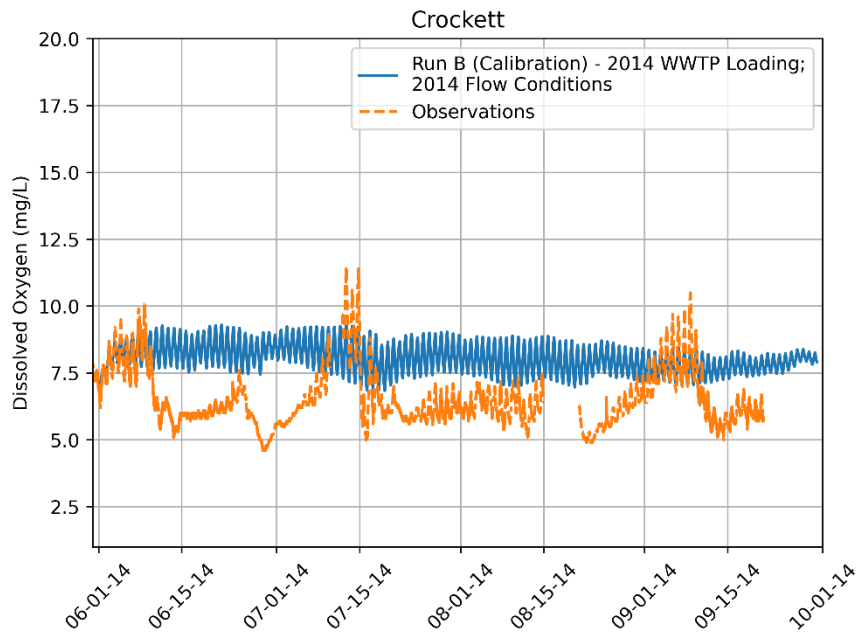

Figure 5-4: Run B predicted and observed dissolved oxygen at Crockett study site.

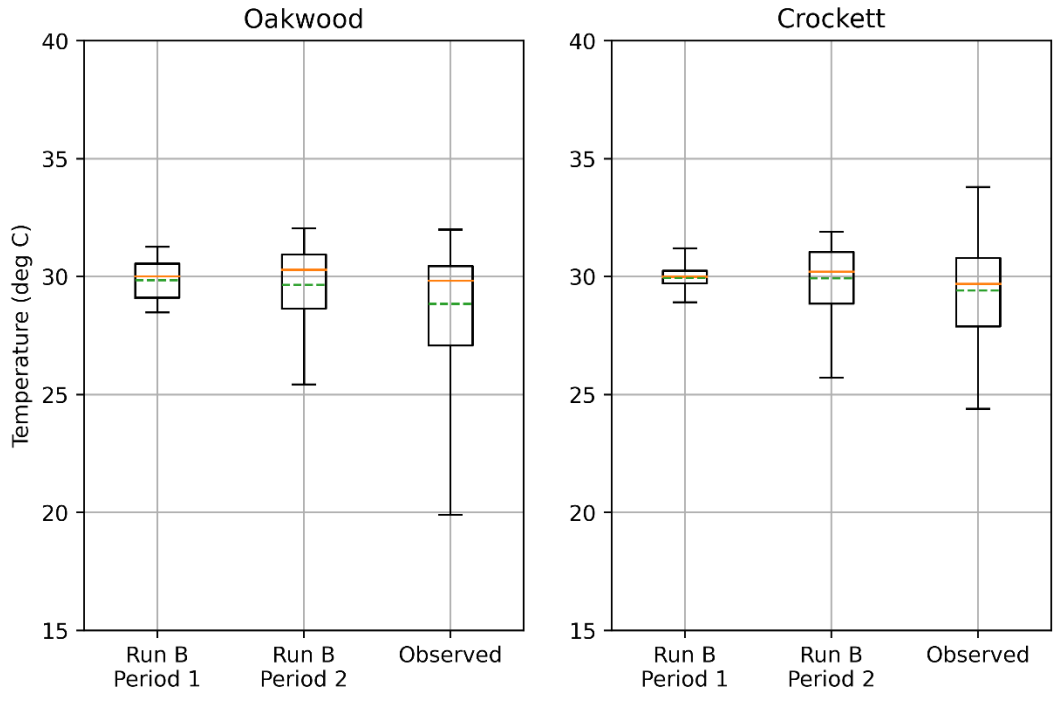

Figure 5-5: Box and whisker plots of Run B temperature results for the ten day lowest stable flow period (B1) and the observation period (B2) and observed temperature. Orange lines represent sample medians, green dashed lines represent sample averages, boxes represent interquartile range (25th percentile – 75th percentile) and whiskers represent sample maximum and minimum.

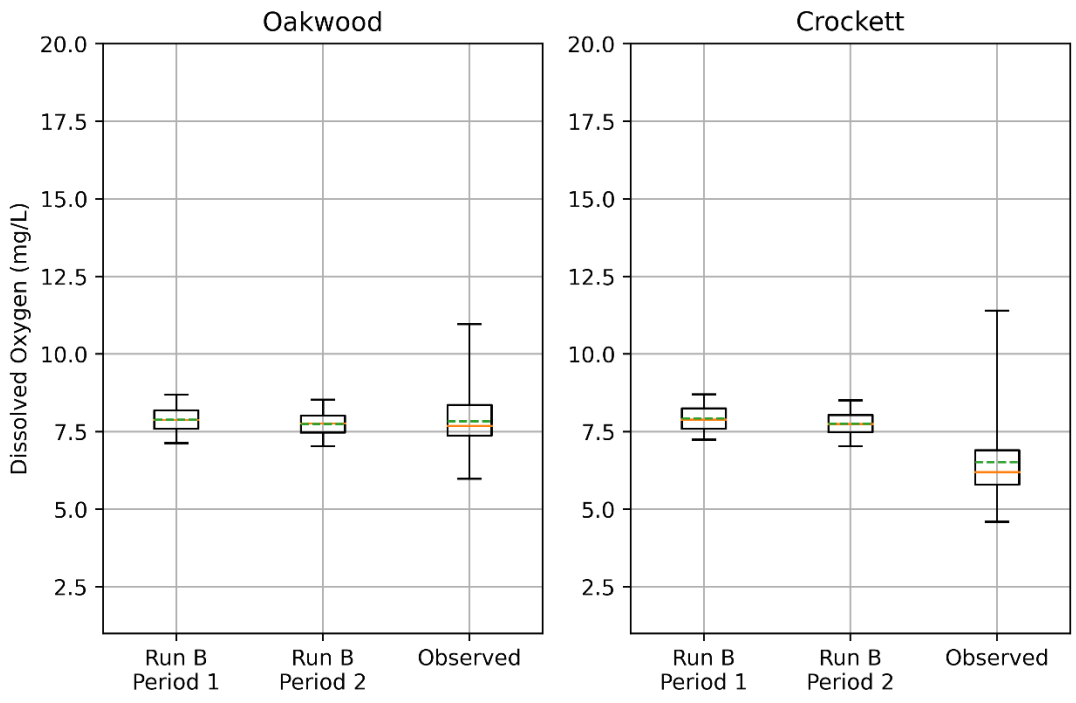

Figure 5-6: Box and whisker plots of Run B dissolved oxygen results for the ten day lowest stable flow period (B1) and the observation period (B2), and observed dissolved oxygen. Orange lines represent sample medians, green dashed lines represent sample averages, boxes represent interquartile range (25th percentile – 75th percentile) and whiskers represent sample maximum and minimum.

As part of this project, new water quality data was collected in 2018 by TRA to be used as observation data for 2018 model simulation Run I, intended to validate the calibration of the model. Temperature results for the model validation run are provided in Figure 5-7 and Figure 5-8. Dissolved oxygen results for the model validation run are provided in Figure 5-9 and Figure 5-10. Box and whisker plots of temperature and dissolved oxygen, shown in Figure 5-11 and Figure 5-12, compare the range of values simulated for the observation period (I1: 6/26/2018 – 7/12/2018) and the full simulation period (I2: 6/1/2018 – 9/30/2018) to that of observations. The results of the model validation indicated that the calibration of the model for temperature and dissolved oxygen achieved the stated calibration goals across a range of flow conditions and time periods.

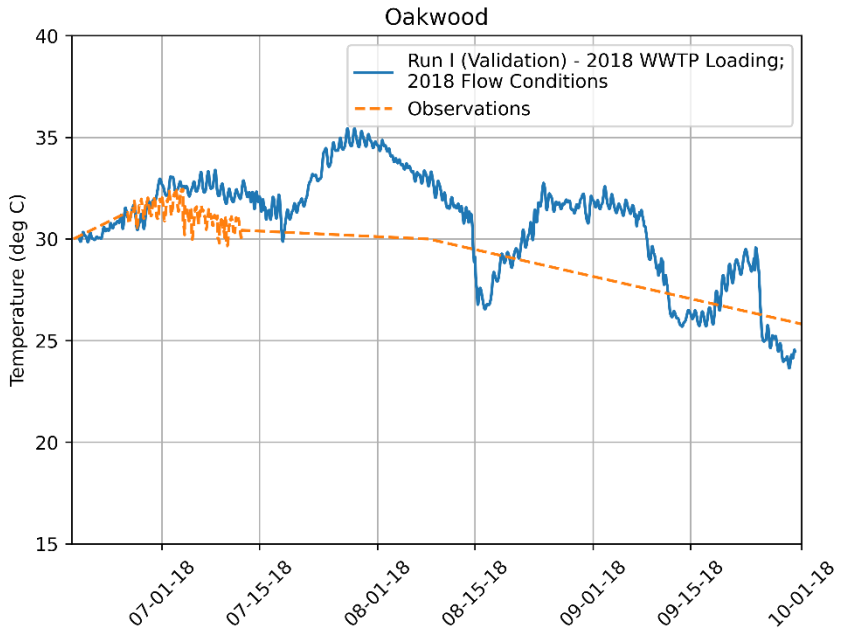

Figure 5-7: Run I predicted and observed temperature at Oakwood study site.

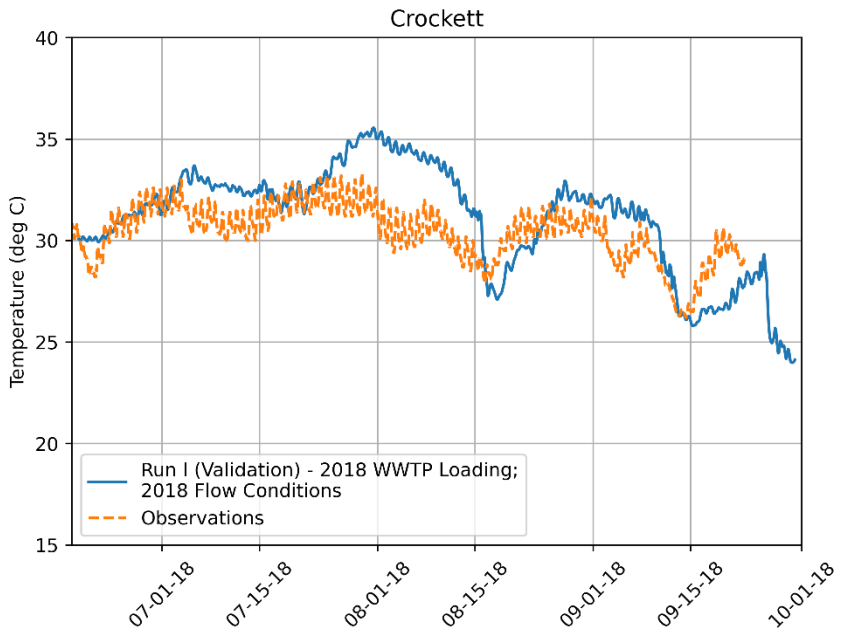

Figure 5-8: Run I predicted and observed temperature at Crockett study site.

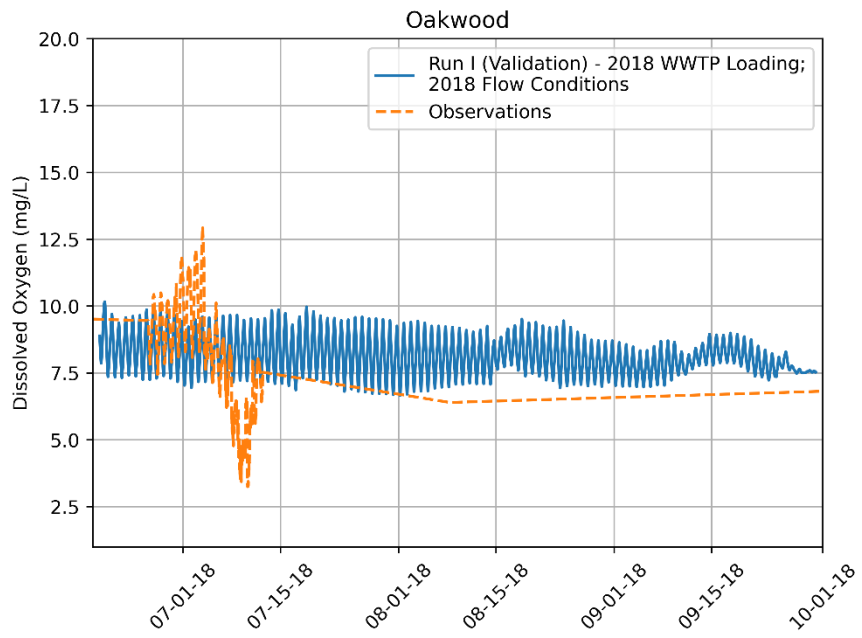

Figure 5-9: Run I predicted and observed dissolved oxygen at Oakwood study site.

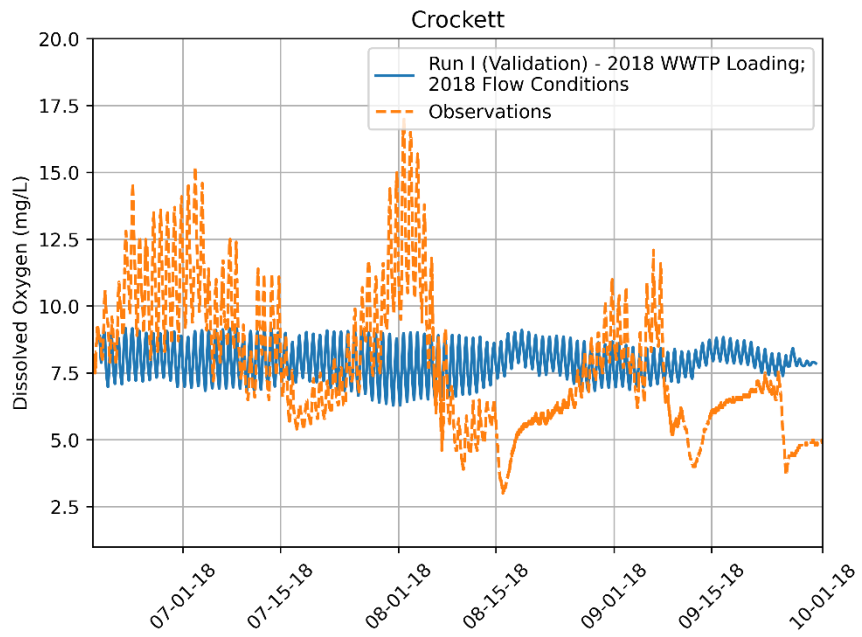

Figure 5-10: Run I predicted and observed dissolved oxygen at Crockett.

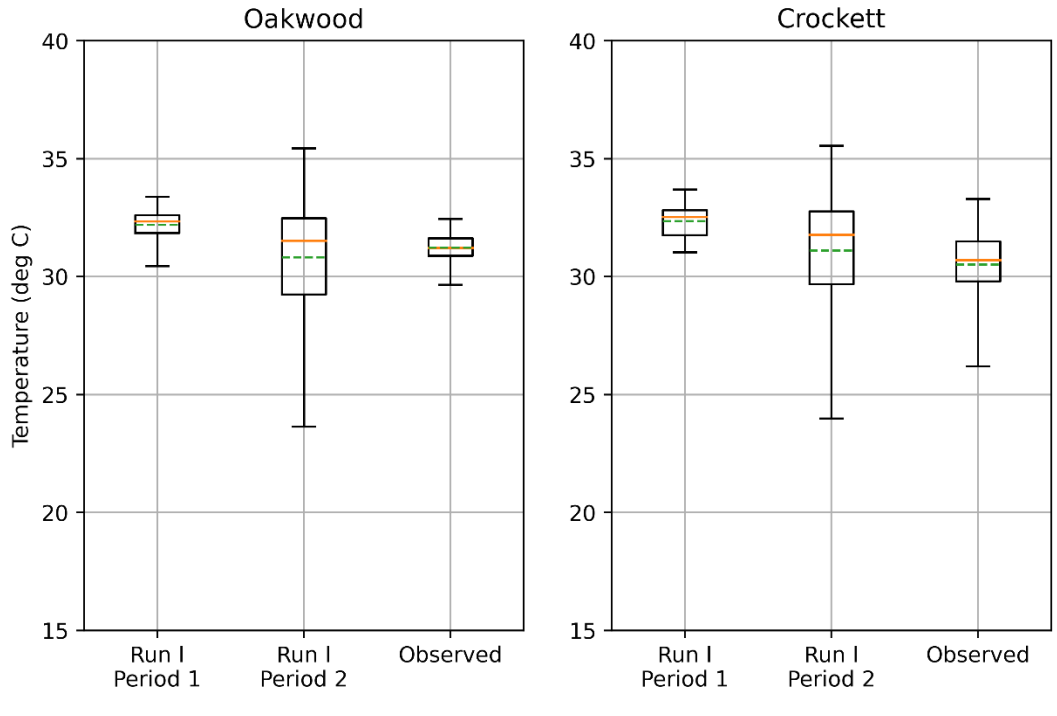

Figure 5-11: Box and whisker plots of Run I temperature results for the observation period (I1) and the full simulation period (I2) and observed temperature. Orange lines represent sample medians, green dashed lines represent sample averages, boxes represent interquartile range (25th percentile – 75th percentile) and whiskers represent sample maximum and minimum.

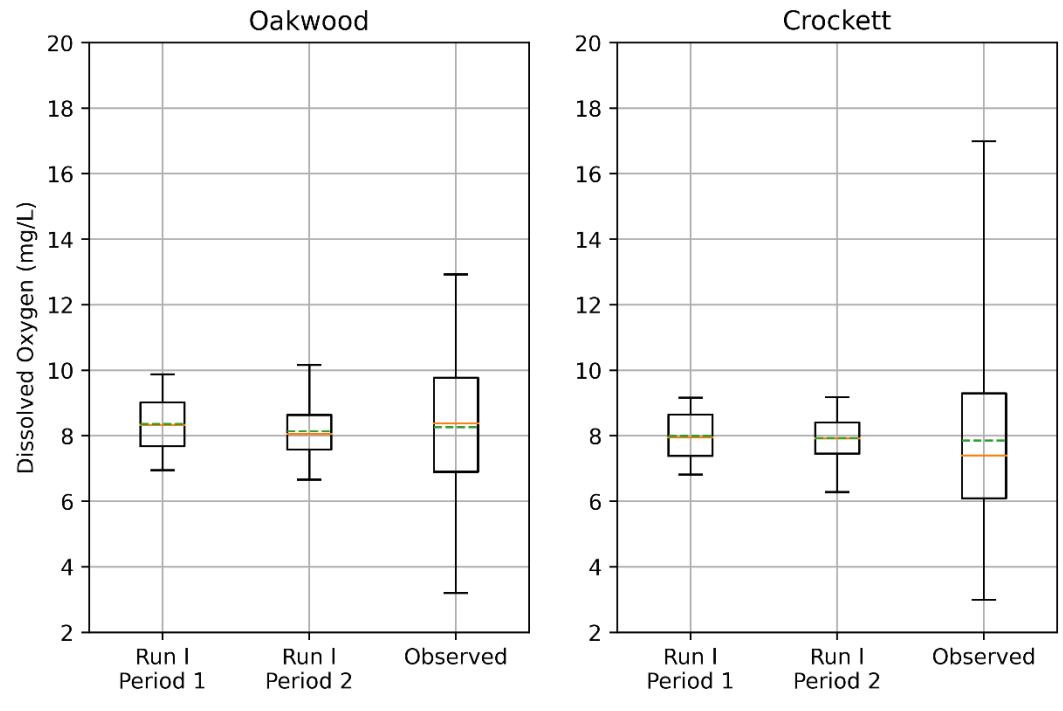

Figure 5-12: Box and whisker plots of Run I dissolved oxygen results for the observation period (I1) and the full simulation period (I2) and observed dissolved oxygen. Orange lines represent sample medians, green dashed lines represent sample averages, boxes represent interquartile range (25th percentile – 75th percentile) and whiskers represent sample maximum and minimum.

Lower Model Calibration

Prior to the onset of this project, no water quality model was available for the Lower Trinity as it was in the case of the Upper Model. A new hydraulic model was created as part of this project and calibrated from scratch using the same inputs and calibration goals as the Upper model. To calibrate the model, results from Run A were compared with observed values at the study site within the reach (RS 58607) and at SH105 near the downstream end of the model (RS 12927), and model parameters were adjusted iteratively until a satisfactory calibration was achieved according to the calibration goals stated above. Model coefficients were adjusted based upon on-site conditions and calibration of predictions to observations, and are shown in Table 5-2. The theta values listed alongside parameters are used to account for temperature dependence of parameters and were not changed from HEC-RAS defaults during model calibration. Temperature results from calibrated Run A are provided in Figure 5-13 and Figure 5-15. Dissolved oxygen results from calibrated Run A are provided in Figure 5-14 and Figure 5-16. Box and whisker plots of temperature and dissolved oxygen, shown in Figure 5-17 and Figure 5-18, compare the range of values simulated for the observation period (A1: 7/10/2018 – 7/27/2018) and the full simulation period (A2: 6/1/2018 – 10/15/2018) to that of observations. Results of the calibrated Lower model for all other nutrients are included in figures at the end of this section.

Table 5-2: Calibrated water quality model coefficients for Lower Model from Run A.

Parameter	Value	Theta
Algae		
Biomass Chl-a ratio	11.1 ugCha/mgA	
Biomass Nitrogen Fraction	0.07 mgN/mgA	
Biomass Phosphorous Fraction	0.005 mgP/mgA	
Maximum Growth Rate	1.5 day^{-1}	1.047
Maximum Growth Rate Formulation	Multiplicative	

Parameter	Value	Theta
Growth Limitation (light)	4 W m^{-2}	
Growth Limitation (N)	0.0485 mgN/L	
Growth Limitation (P)	0.007 mgP/L	
Light Limitation Formulation	Half-Saturation	
Light Extinction (non-algal)	0.03 m^{-1}	
Light Extinction (linear algal)	0.007 $m^{-1}(ugCh/L)^{-1}$	
Light Extinction (non-linear algal)	0.05 $m^{-1}(ugCh/L)^{-2/3}$	
Respiration Rate	0.05 day^{-1}	1.047
Nitrogen Preference	1	
Settling Rate	0.1 m day^{-1}	1.024
Dissolved Oxygen		
Production per unit algal growth	1.4 mgO/mgAp	
Uptake per unit algal respired	1.6 mgO/mgAp	
Production per unit benthic algal growth	1.4 mgO/mgAb	
Uptake per unit benthic algal respired	1.6 mgO/mgAb	
Uptake per unit NH4 oxidized	3 mgO/mgN	
Uptake per unit NO2 oxidized	1 mgO/mgN	
Atmospheric Reaeration	1 day^{-1}	1.24
Sediment Demand	0 day^{-1}	1.06
CBOD		
Decay Rate	0.1 day^{-1}	1.047
Settling Rate	0 day^{-1}	1.024
Nitrogen		
OrgN -> NH4	0.02 day^{-1}	1.047
NH4 -> NO2	0.3 day^{-1}	1.083
NO2 -> NO3	0.2 day^{-1}	1.047
Org-N Settling Rate	0.001 day^{-1}	1.024
NH4 Benthos Source Rate	0 mgN m^{-2} day^{-1}	1.074
Nitrification Inhibition Factor	0.6 mg/L	
Phosphorus		
OrgP -> InorgP	0.01 day^{-1}	1.047
Org-P Settling Rate	0.001 day^{-1}	1.024
Benthos Source Rate	0.001 mgP m^{-2} day^{-1}	1.074
Benthic Algae		
Biomass Chl-a ratio	5 ugChab/mgAb	
Biomass Nitrogen Fraction	0.07 mgN/mgAb	
Biomass Phosphorous Fraction	0.01 mgP/mgAb	
Maximum Growth Rate	0.3 day^{-1}	1.047
Maximum Growth Rate Formulation	Multiplicative	
Growth Limitation (light)	6276 W m^{-2}	
Growth Limitation (N)	0.01 mgN/L	
Growth Limitation (P)	0.001 mgP/L	
Benthic Light Limitation Formulation	Half- Saturation	
Respiration Rate	0.01 day^{-1}	1.047
Death Rate	0 day^{-1}	1.047
Nitrogen Preference	0	
Bottom Area Fraction	0	

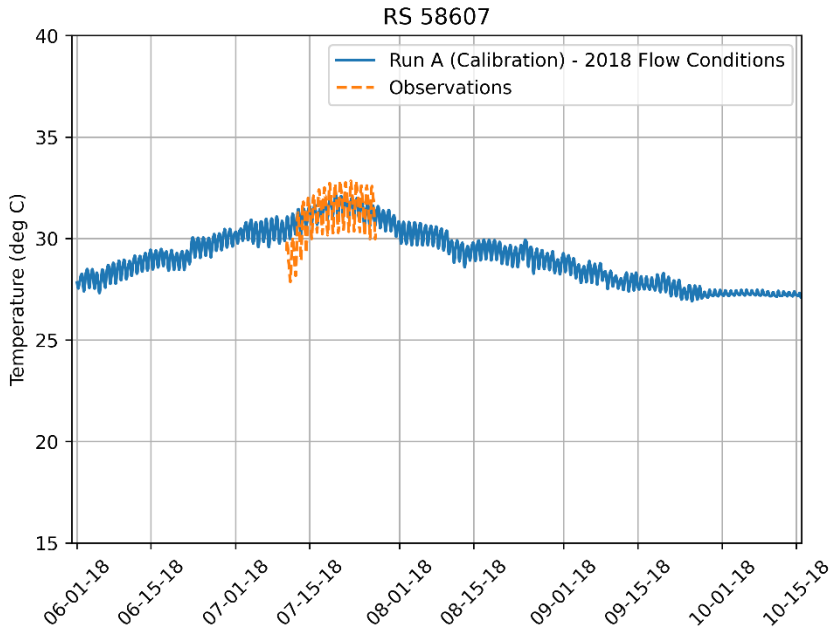

Figure 5-13: Run A predicted and observed temperature at study site downstream of Romayor gage.

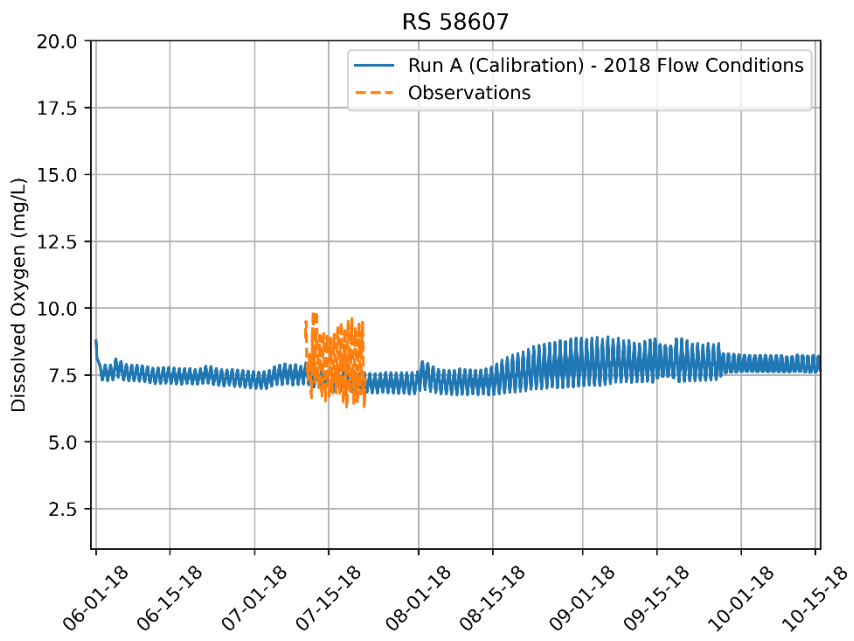

Figure 5-14: Run A predicted and observed dissolved oxygen at study site downstream of Romayor gage.

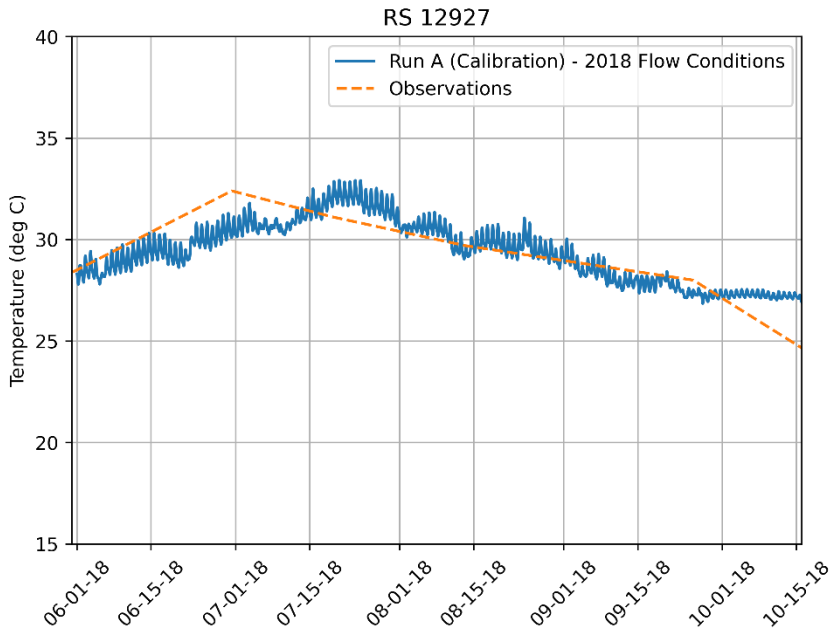

Figure 5-15: Run A predicted and observed temperature at SH 105 near downstream end of model.

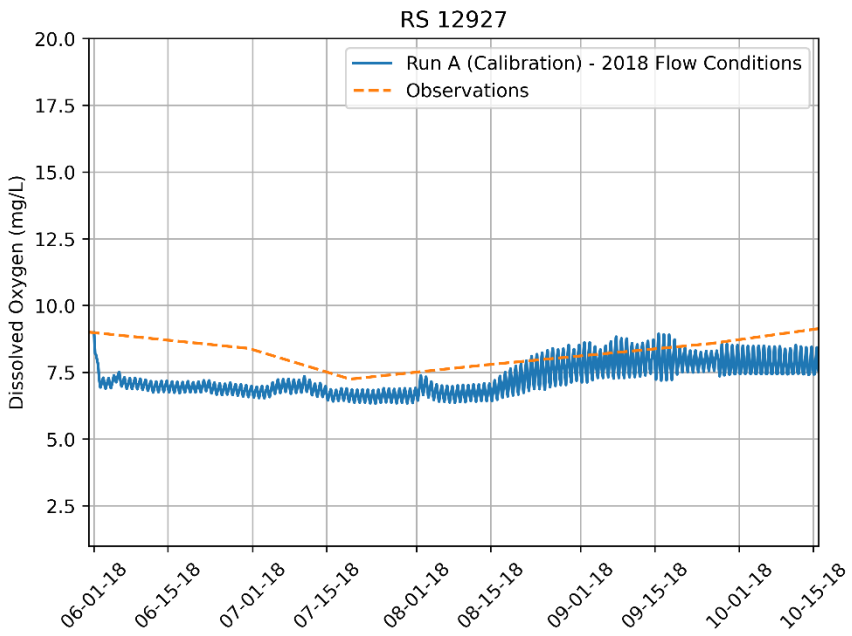

Figure 5-16: Run A predicted and observed dissolved oxygen at SH 105 near downstream end of model.

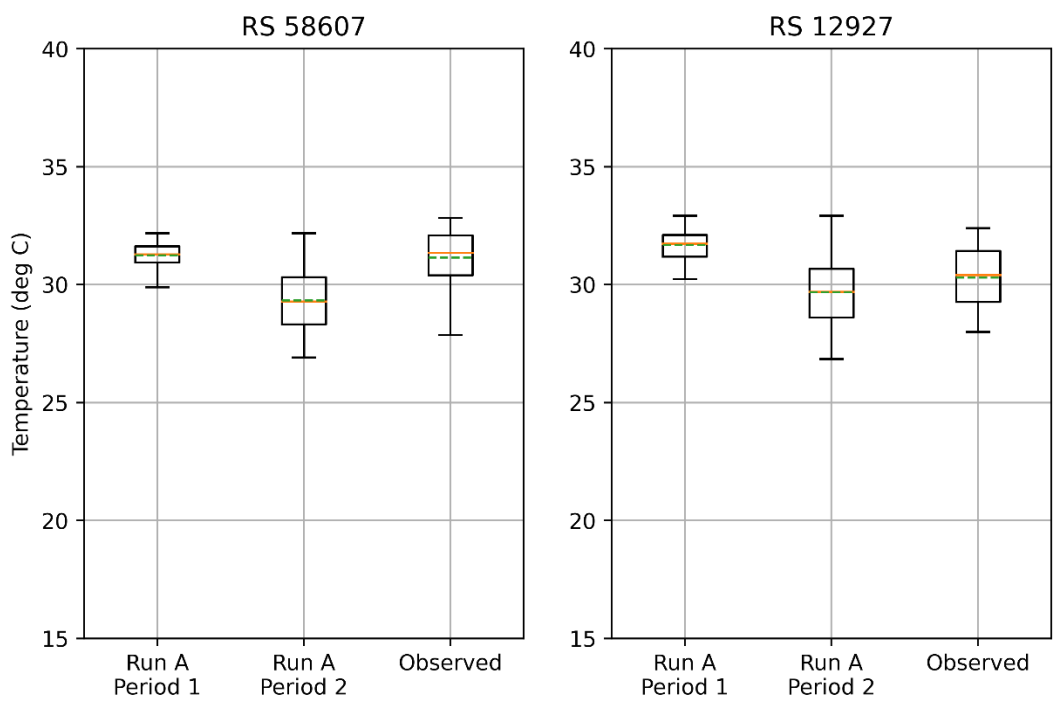

Figure 5-17: Box and whisker plots of Run A temperature results for the observation period (A1) and the full simulation period (A2) and observed temperature. Orange lines represent sample medians, green dashed lines represent sample averages, boxes represent interquartile range (25th percentile – 75th percentile) and whiskers represent sample maximum and minimum.

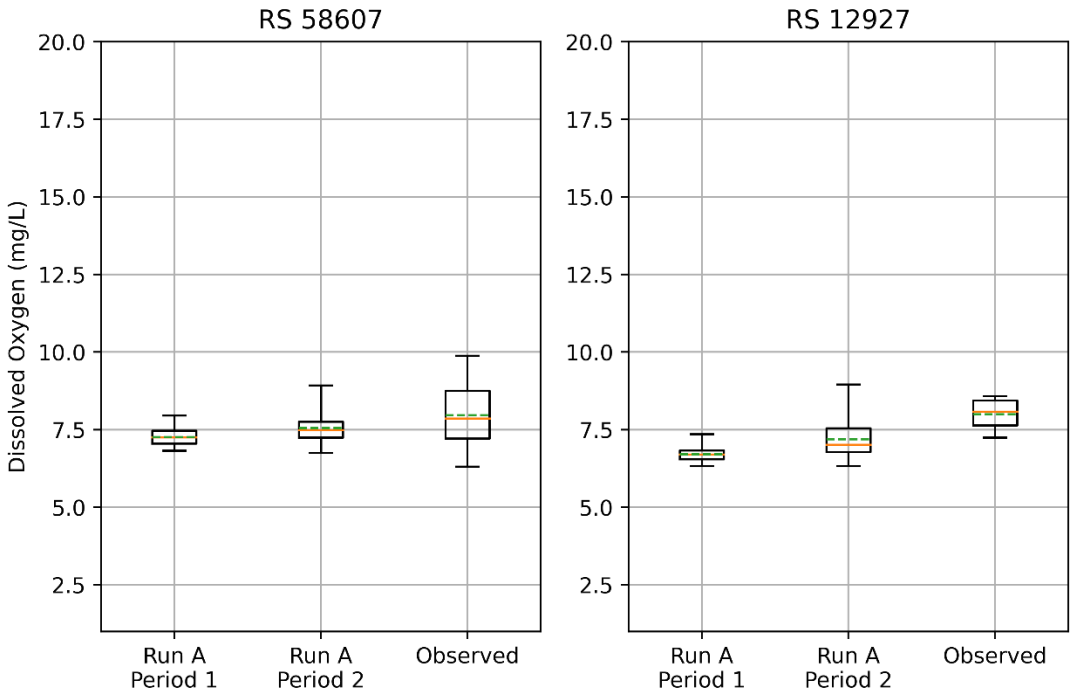

Figure 5-18: Box and whisker plots of Run A dissolved oxygen results for the observation period (A1) and the full simulation period (A2) and observed dissolved oxygen. Orange lines represent sample medians, green dashed lines represent sample averages, boxes represent interquartile range (25th percentile – 75th percentile) and whiskers represent sample maximum and minimum.

Additional water quality nutrient constituent results for calibrated Run B at Oakwood and Crockett sites - Upper Model

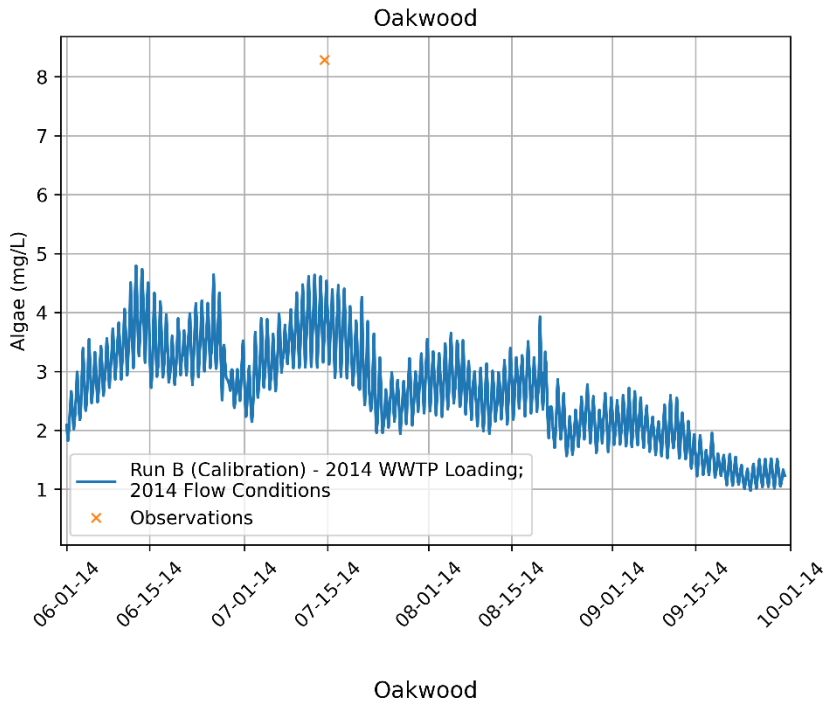

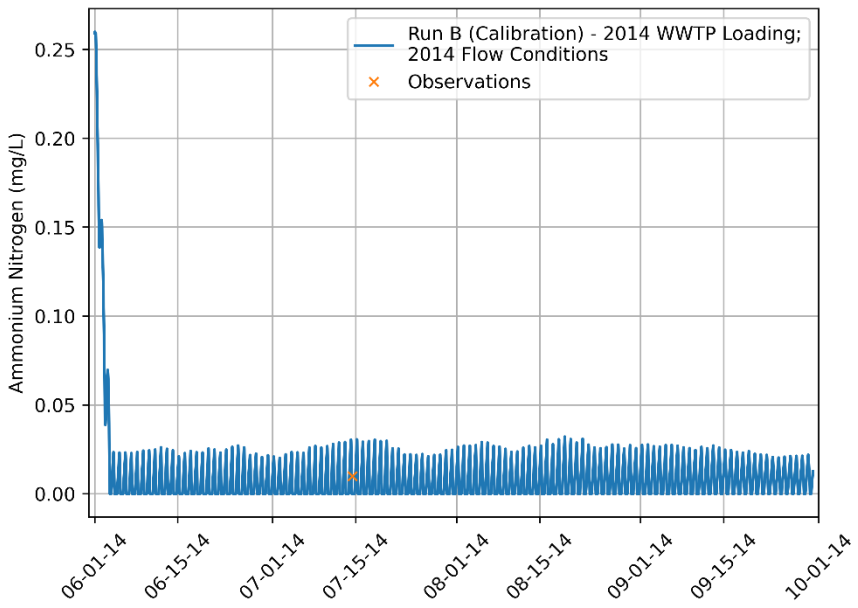

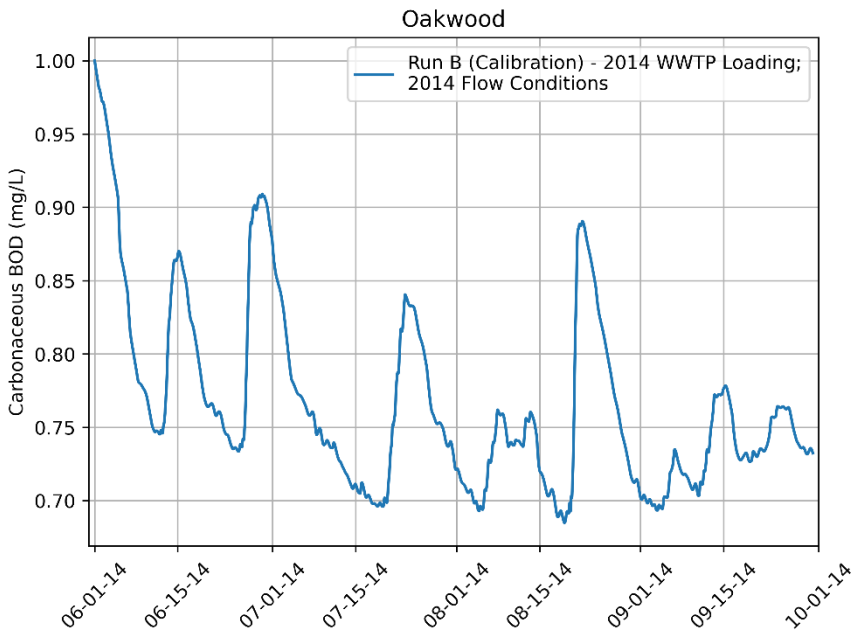

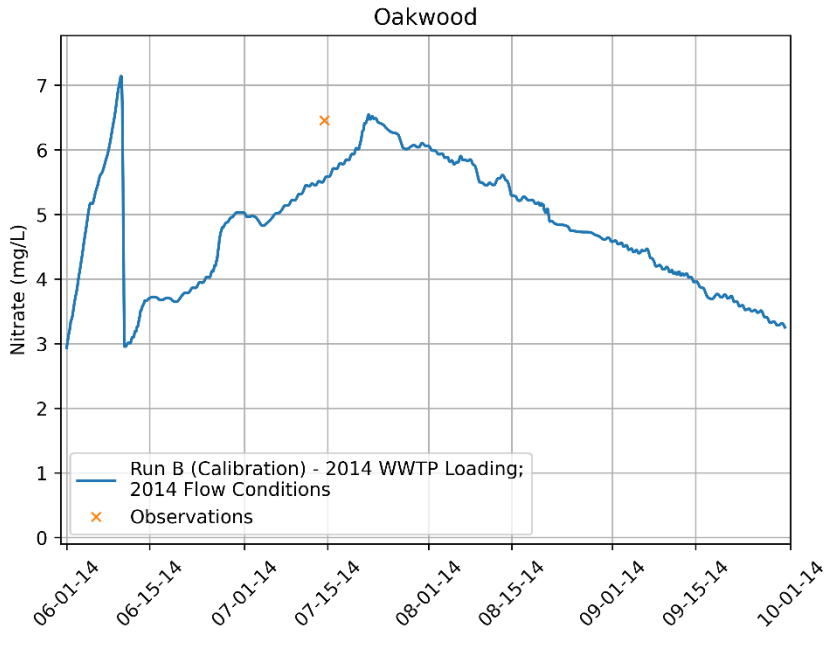

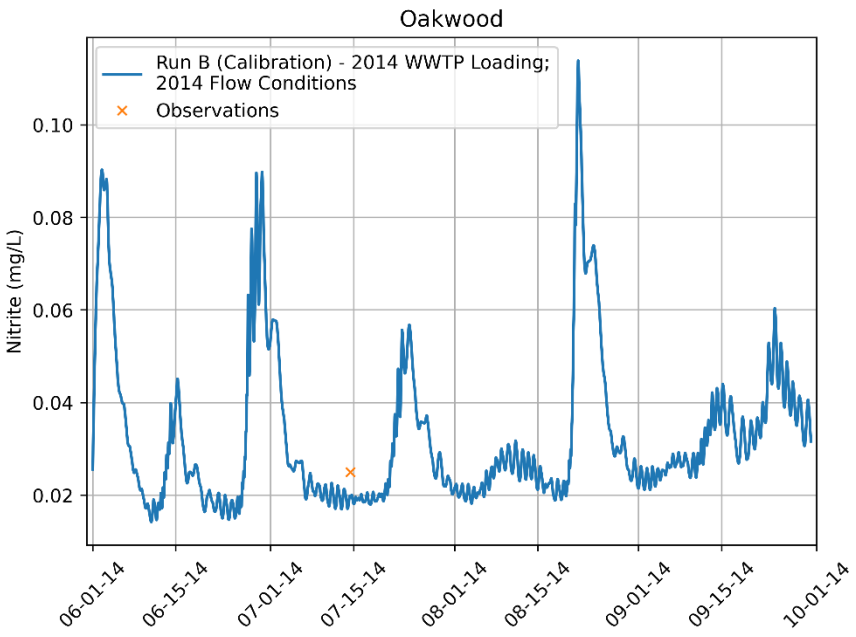
Oakwood
Run B (Calibration) - 2014 WWTP Loading; 2014 Flow Conditions
Observations
Nitrite (mg/L)
0.10
0.08
0.06
0.04
0.02
06-01-14
06-15-14
07-01-14
07-15-14
08-01-14
08-15-14
09-01-14
09-15-14
10-01-14

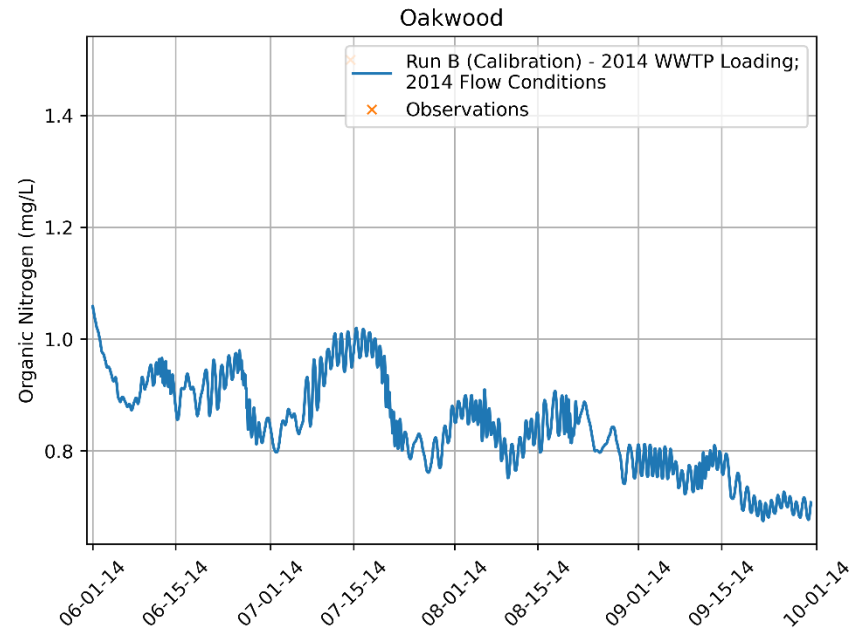
Oakwood
Run B (Calibration) - 2014 WWTP Loading; 2014 Flow Conditions
Observations
Organic Nitrogen (mg/L)
1.4
1.2
1.0
0.8
06-01-14
06-15-14
07-01-14
07-15-14
08-01-14
08-15-14
09-01-14
09-15-14
10-01-14

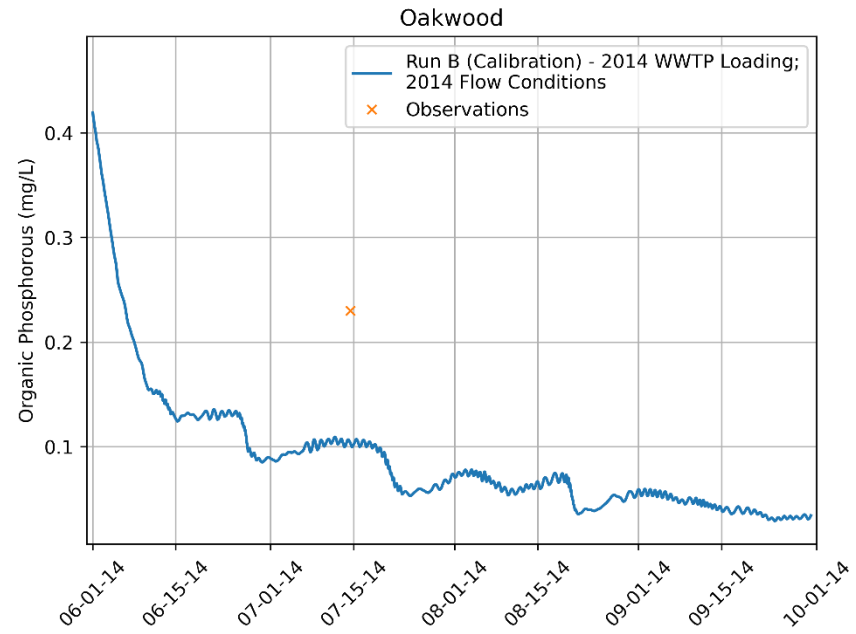
Oakwood
Run B (Calibration) - 2014 WWTP Loading; 2014 Flow Conditions
Observations
Organic Phosphorous (mg/L)
0.4
0.3
0.2
0.1
06-01-14
06-15-14
07-01-14
07-15-14
08-01-14
08-15-14
09-01-14
09-15-14
10-01-14

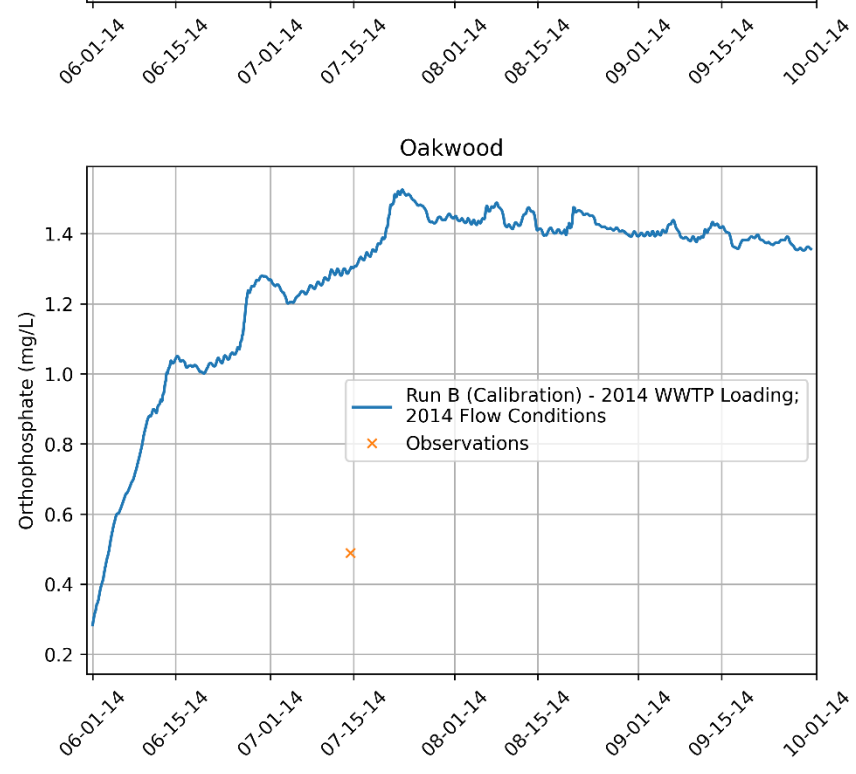
Oakwood
Run B (Calibration) - 2014 WWTP Loading; 2014 Flow Conditions
Observations
Orthophosphate (mg/L)
1.4
1.2
1.0
0.8
0.6
0.4
0.2
06-01-14
06-15-14
07-01-14
07-15-14
08-01-14
08-15-14
09-01-14
09-15-14
10-01-14

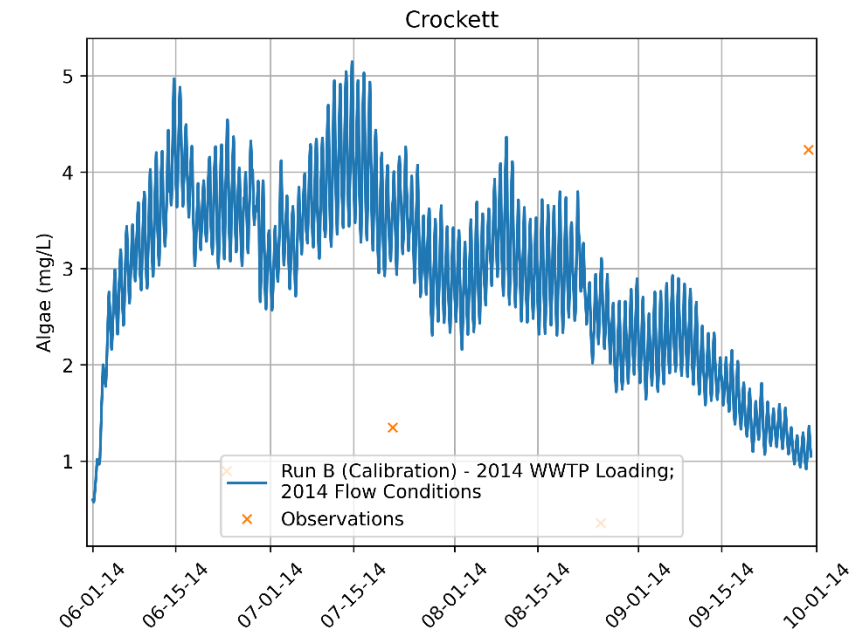
Crockett
Algae (mg/L)
1
2
3
4
5
Run B (Calibration) - 2014 WWTP Loading; 2014 Flow Conditions
Observations
06-01-14
06-15-14
07-01-14
07-15-14
08-01-14
08-15-14
09-01-14
09-15-14
10-01-14

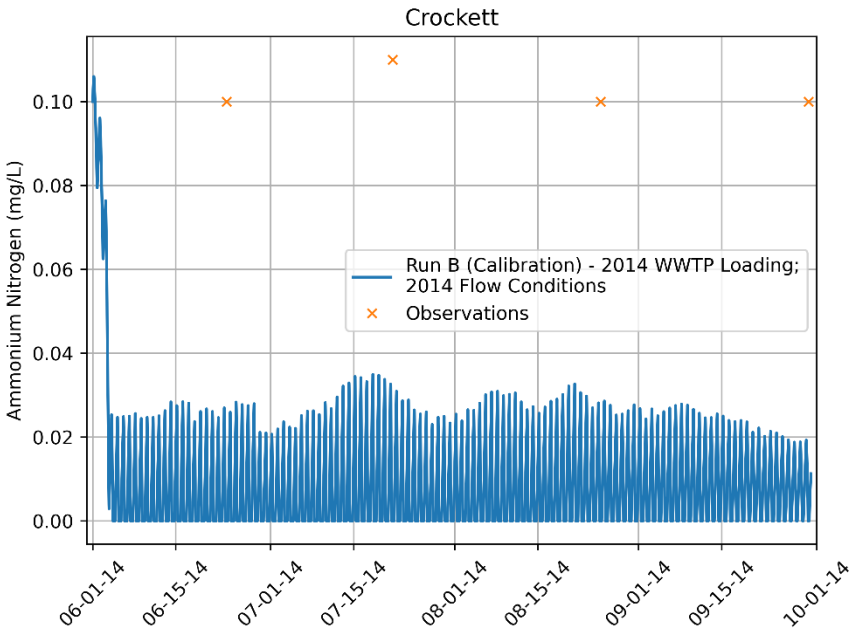
Crockett
Ammonium Nitrogen (mg/L)
0.00
0.02
0.04
0.06
0.08
0.10
Run B (Calibration) - 2014 WWTP Loading; 2014 Flow Conditions
Observations
06-01-14
06-15-14
07-01-14
07-15-14
08-01-14
08-15-14
09-01-14
09-15-14
10-01-14

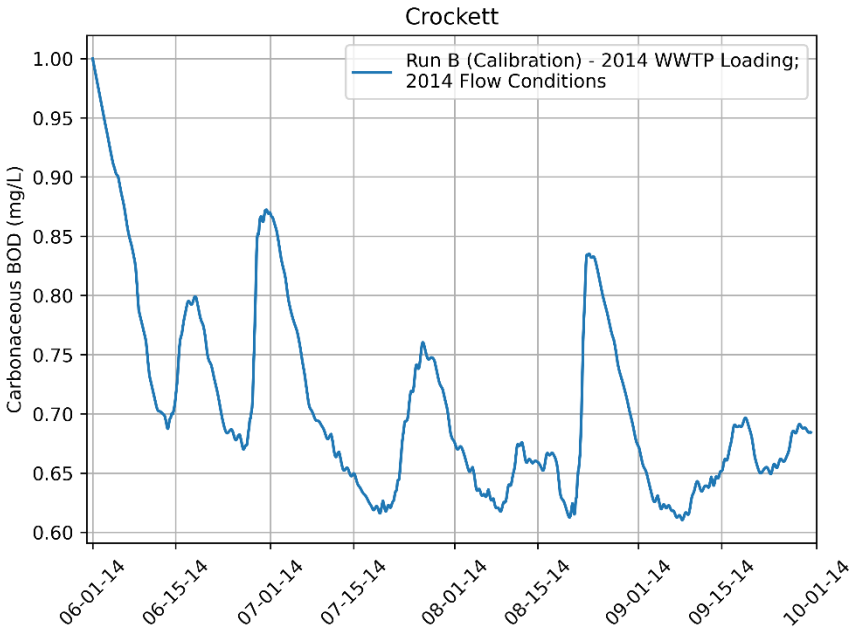
Crockett
Carbonaceous BOD (mg/L)
0.60
0.65
0.70
0.75
0.80
0.85
0.90
0.95
1.00
Run B (Calibration) - 2014 WWTP Loading; 2014 Flow Conditions
06-01-14
06-15-14
07-01-14
07-15-14
08-01-14
08-15-14
09-01-14
09-15-14
10-01-14

Crockett
Nitrate (mg/L)
2
3
4
5
6
7
Run B (Calibration) - 2014 WWTP Loading; 2014 Flow Conditions
Observations
06-01-14
06-15-14
07-01-14
07-15-14
08-01-14
08-15-14
09-01-14
09-15-14
10-01-14

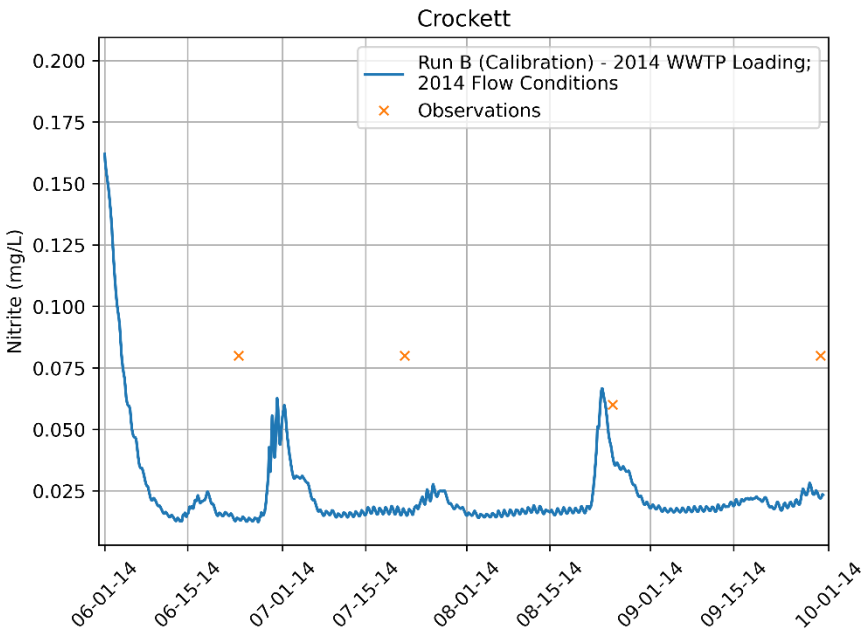
Crockett
Run B (Calibration) - 2014 WWTP Loading; 2014 Flow Conditions
Observations
Nitrite (mg/L)
0.200
0.175
0.150
0.125
0.100
0.075
0.050
0.025
06-01-14
06-15-14
07-01-14
07-15-14
08-01-14
08-15-14
09-01-14
09-15-14
10-01-14

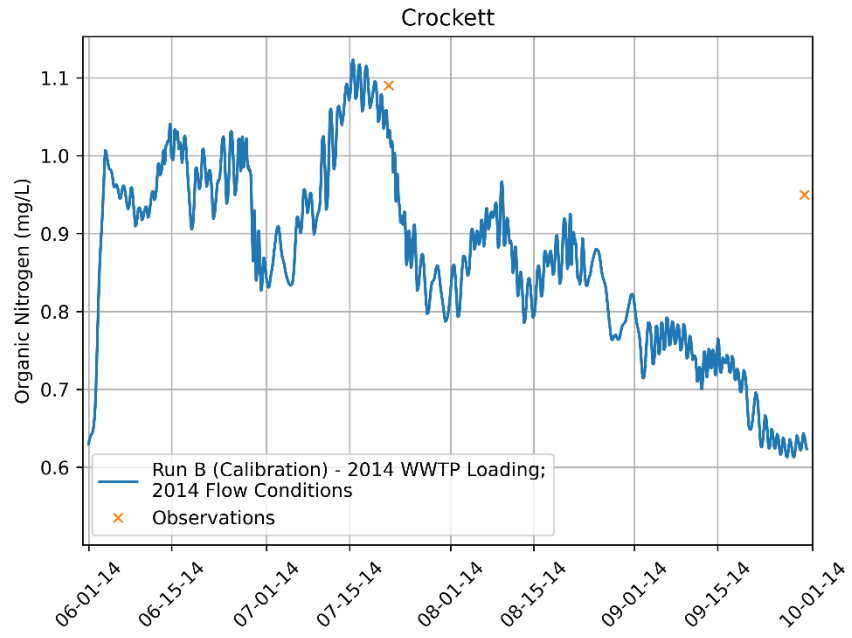
Crockett
Run B (Calibration) - 2014 WWTP Loading; 2014 Flow Conditions
Observations
Organic Nitrogen (mg/L)
1.1
1.0
0.9
0.8
0.7
0.6
06-01-14
06-15-14
07-01-14
07-15-14
08-01-14
08-15-14
09-01-14
09-15-14
10-01-14

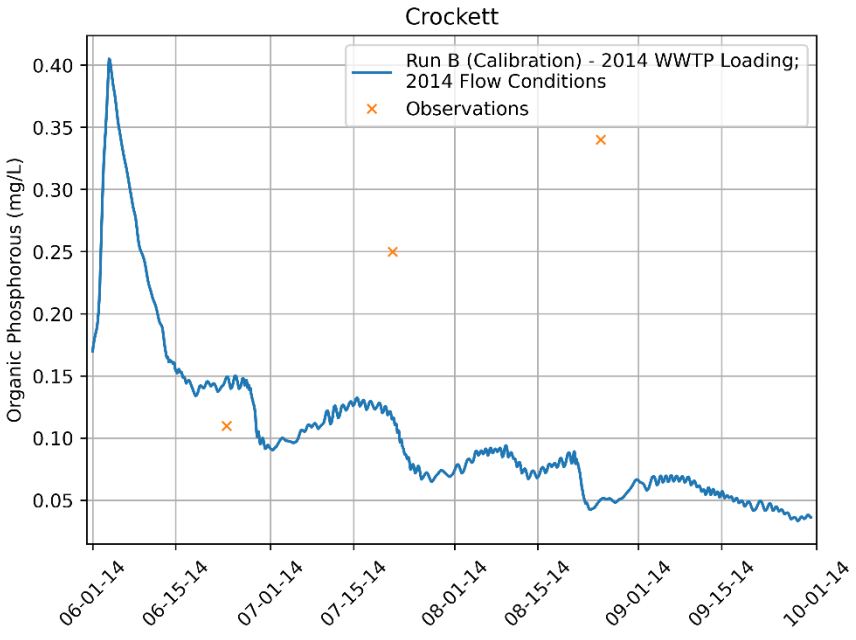
Crockett
Run B (Calibration) - 2014 WWTP Loading; 2014 Flow Conditions
Observations
Organic Phosphorous (mg/L)
0.40
0.35
0.30
0.25
0.20
0.15
0.10
0.05
06-01-14
06-15-14
07-01-14
07-15-14
08-01-14
08-15-14
09-01-14
09-15-14
10-01-14

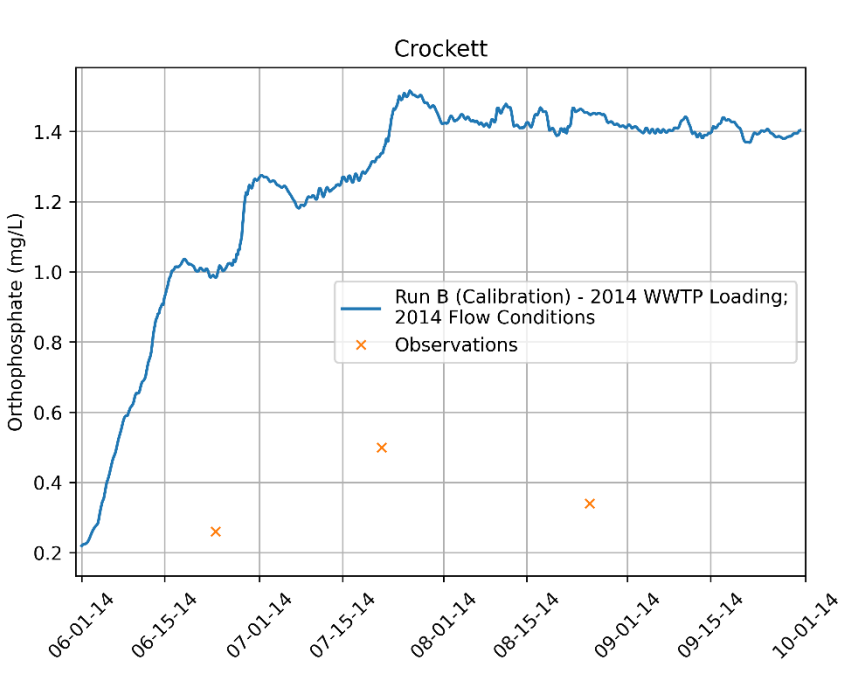
Crockett
Run B (Calibration) - 2014 WWTP Loading; 2014 Flow Conditions
Observations
Orthophosphate (mg/L)
1.4
1.2
1.0
0.8
0.6
0.4
0.2
06-01-14
06-15-14
07-01-14
07-15-14
08-01-14
08-15-14
09-01-14
09-15-14
10-01-14

Additional water quality nutrient constituent results for calibrated Run A at RS 58607 and RS 12927 sites - Lower Model

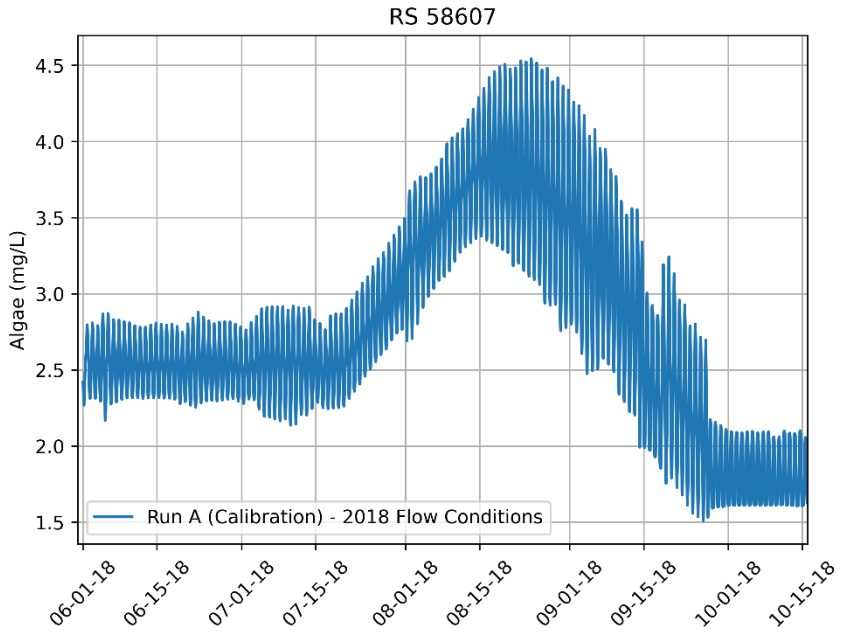

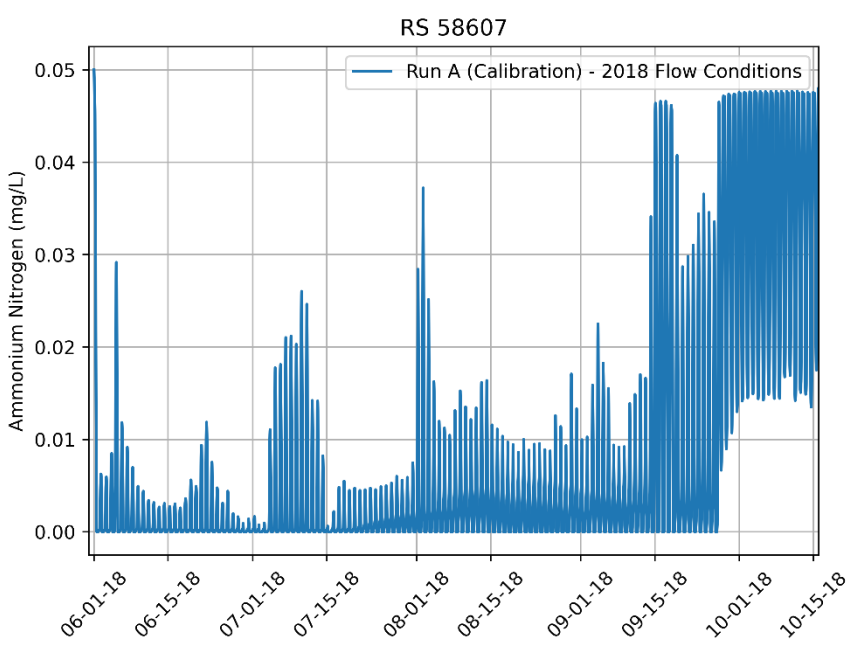

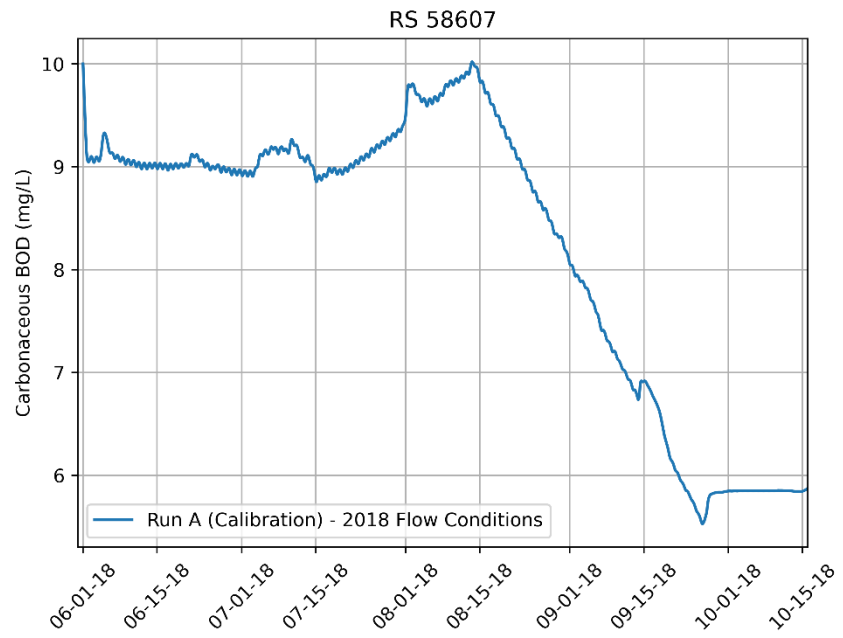

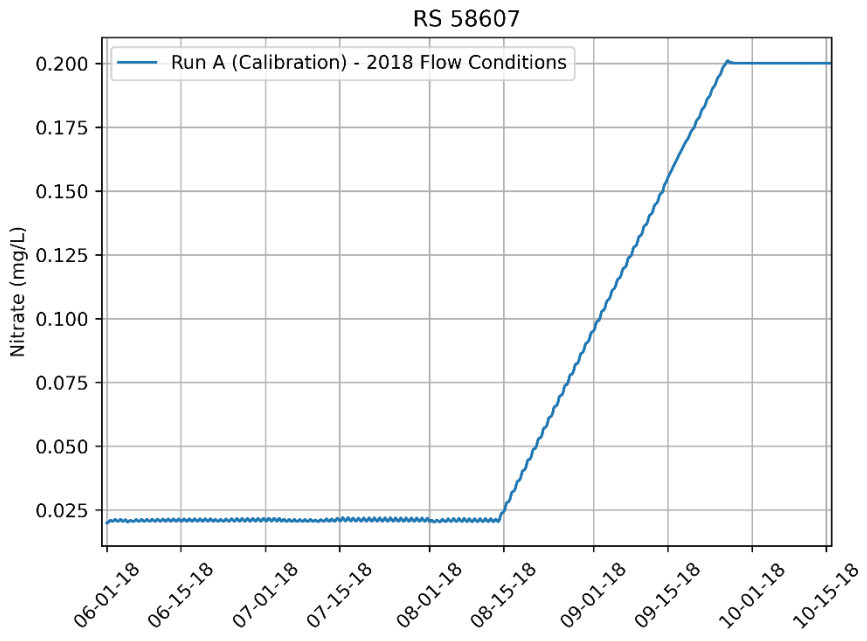
RS 58607
Run A (Calibration) - 2018 Flow Conditions
Nitrate (mg/L)
0.200
0.175
0.150
0.125
0.100
0.075
0.050
0.025
06-01-18
06-15-18
07-01-18
07-15-18
08-01-18
08-15-18
09-01-18
09-15-18
10-01-18
10-15-18

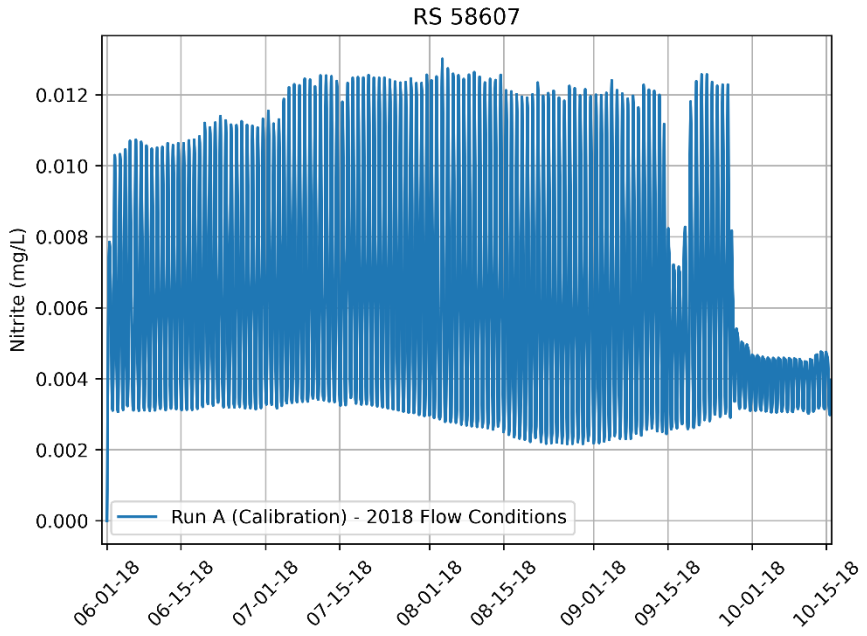
RS 58607
Nitrite (mg/L)
0.012
0.010
0.008
0.006
0.004
0.002
0.000
Run A (Calibration) - 2018 Flow Conditions
06-01-18
06-15-18
07-01-18
07-15-18
08-01-18
08-15-18
09-01-18
09-15-18
10-01-18
10-15-18

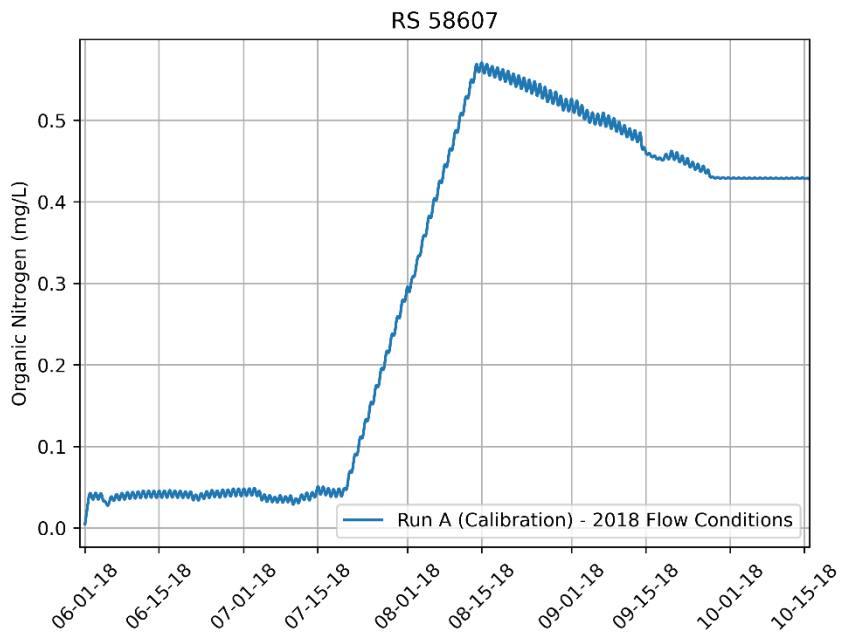
RS 58607
Organic Nitrogen (mg/L)
0.5
0.4
0.3
0.2
0.1
0.0
Run A (Calibration) - 2018 Flow Conditions
06-01-18
06-15-18
07-01-18
07-15-18
08-01-18
08-15-18
09-01-18
09-15-18
10-01-18
10-15-18

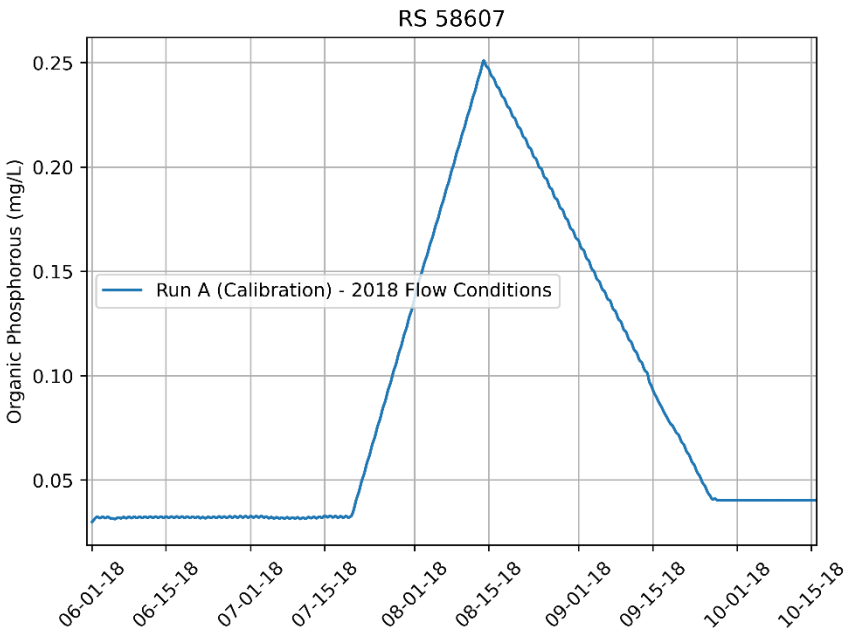
RS 58607
Organic Phosphorous (mg/L)
0.25
0.20
0.15
0.10
0.05
Run A (Calibration) - 2018 Flow Conditions
06-01-18
06-15-18
07-01-18
07-15-18
08-01-18
08-15-18
09-01-18
09-15-18
10-01-18
10-15-18

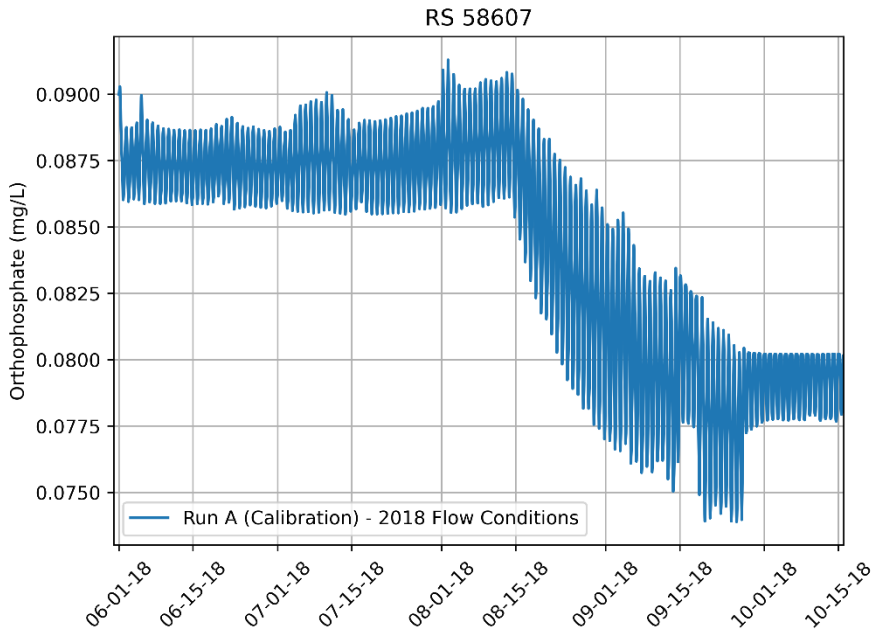
RS 58607
Orthophosphate (mg/L)
0.0900
0.0875
0.0850
0.0825
0.0800
0.0775
0.0750
Run A (Calibration) - 2018 Flow Conditions
06-01-18
06-15-18
07-01-18
07-15-18
08-01-18
08-15-18
09-01-18
09-15-18
10-01-18
10-15-18

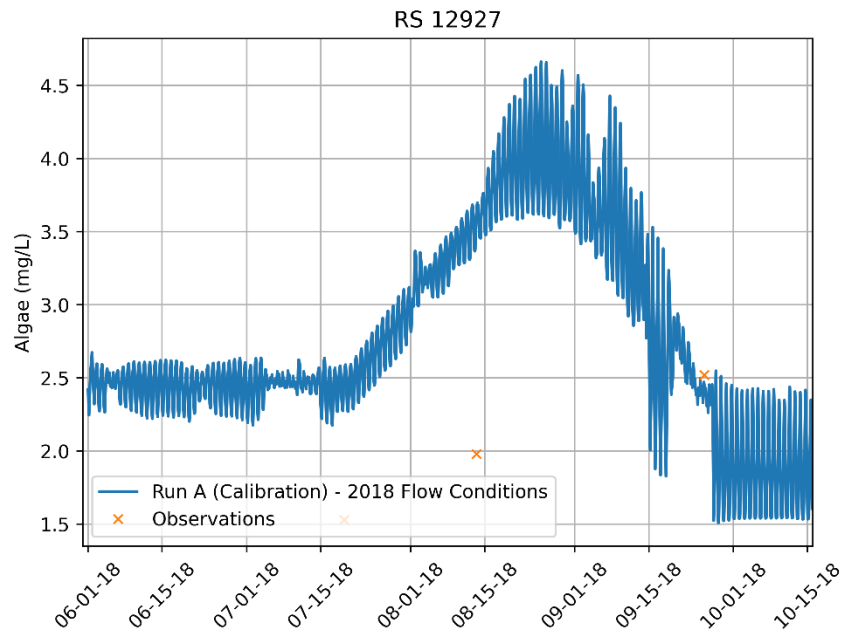
RS 12927
Algae (mg/L)
4.5
4.0
3.5
3.0
2.5
2.0
1.5
Run A (Calibration) - 2018 Flow Conditions
Observations
06-01-18
06-15-18
07-01-18
07-15-18
08-01-18
08-15-18
09-01-18
09-15-18
10-01-18
10-15-18

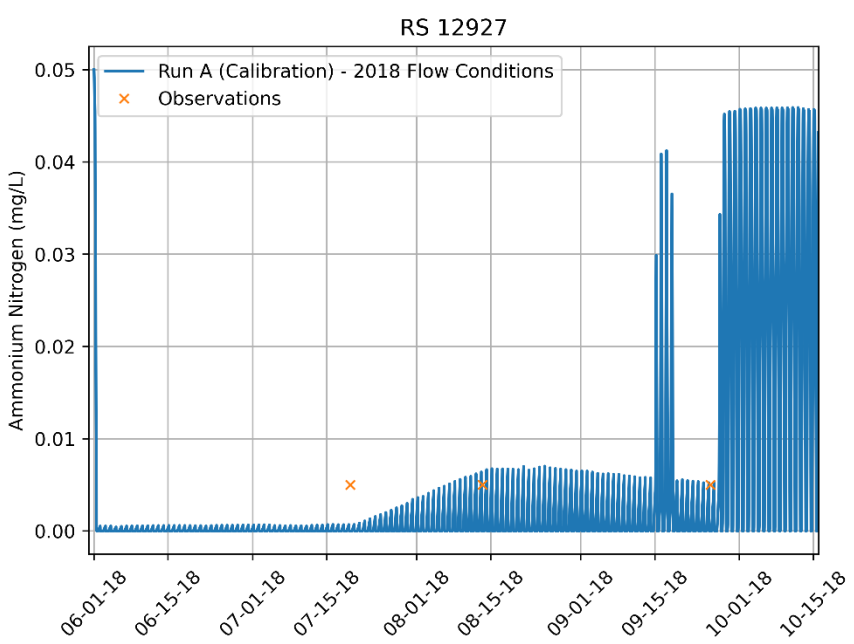
RS 12927
Ammonium Nitrogen (mg/L)
0.05
0.04
0.03
0.02
0.01
0.00
Run A (Calibration) - 2018 Flow Conditions
Observations
06-01-18
06-15-18
07-01-18
07-15-18
08-01-18
08-15-18
09-01-18
09-15-18
10-01-18
10-15-18

RS 12927
Carbonaceous BOD (mg/L)
10
9
8
7
6
5
Run A (Calibration) - 2018 Flow Conditions
06-01-18
06-15-18
07-01-18
07-15-18
08-01-18
08-15-18
09-01-18
09-15-18
10-01-18
10-15-18

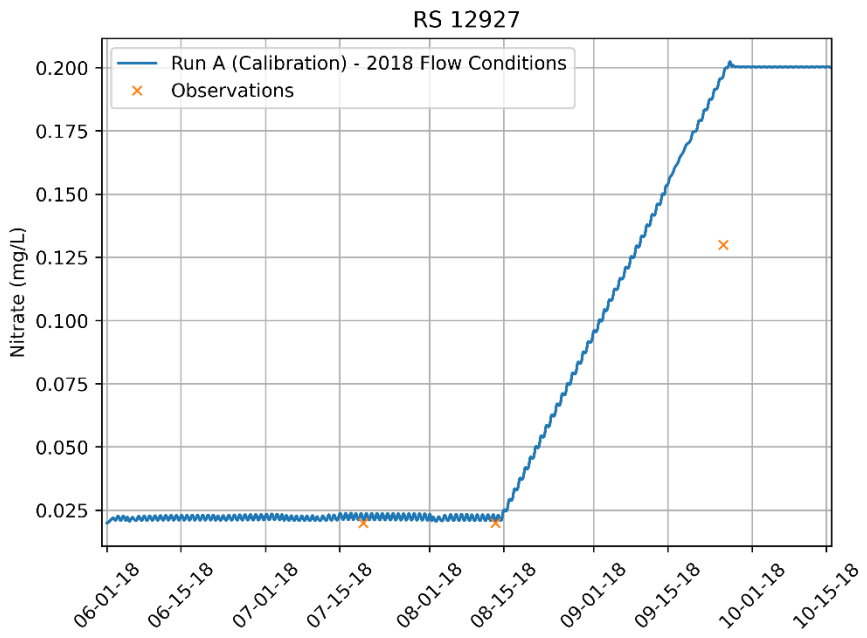
RS 12927
Run A (Calibration) - 2018 Flow Conditions
Observations
Nitrate (mg/L)
0.200
0.175
0.150
0.125
0.100
0.075
0.050
0.025
06-01-18
06-15-18
07-01-18
07-15-18
08-01-18
08-15-18
09-01-18
09-15-18
10-01-18
10-15-18

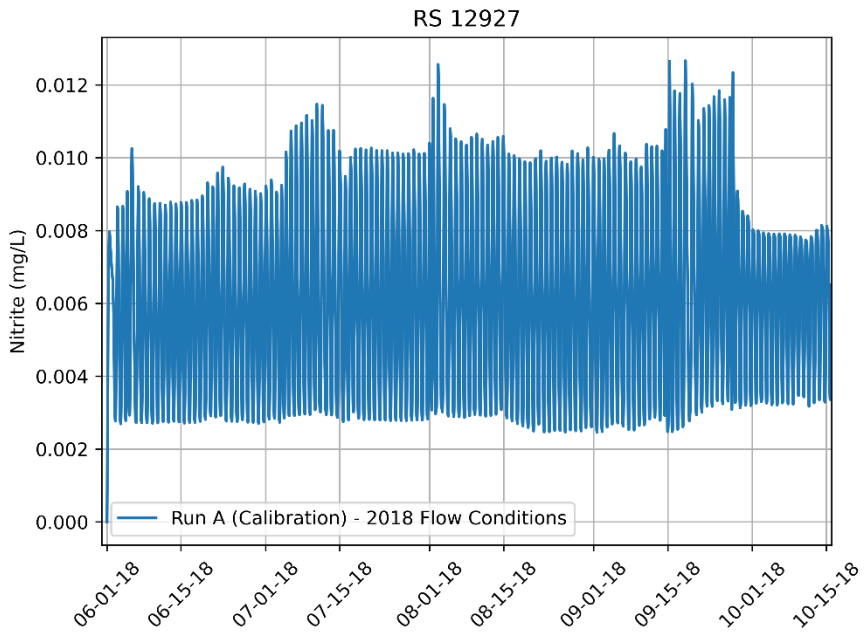
RS 12927
Nitrite (mg/L)
0.012
0.010
0.008
0.006
0.004
0.002
0.000
Run A (Calibration) - 2018 Flow Conditions
06-01-18
06-15-18
07-01-18
07-15-18
08-01-18
08-15-18
09-01-18
09-15-18
10-01-18
10-15-18

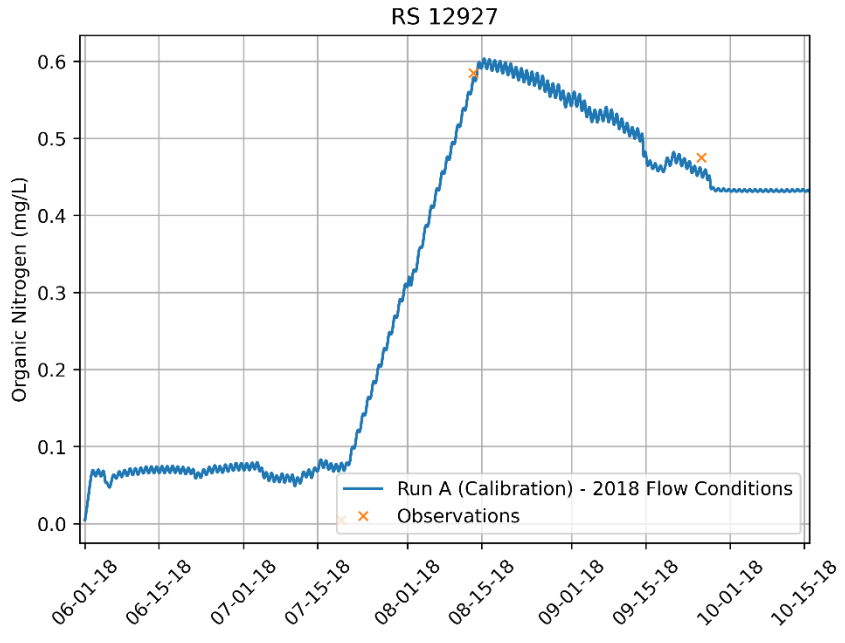
RS 12927
Organic Nitrogen (mg/L)
0.6
0.5
0.4
0.3
0.2
0.1
0.0
Run A (Calibration) - 2018 Flow Conditions
Observations
06-01-18
06-15-18
07-01-18
07-15-18
08-01-18
08-15-18
09-01-18
09-15-18
10-01-18
10-15-18

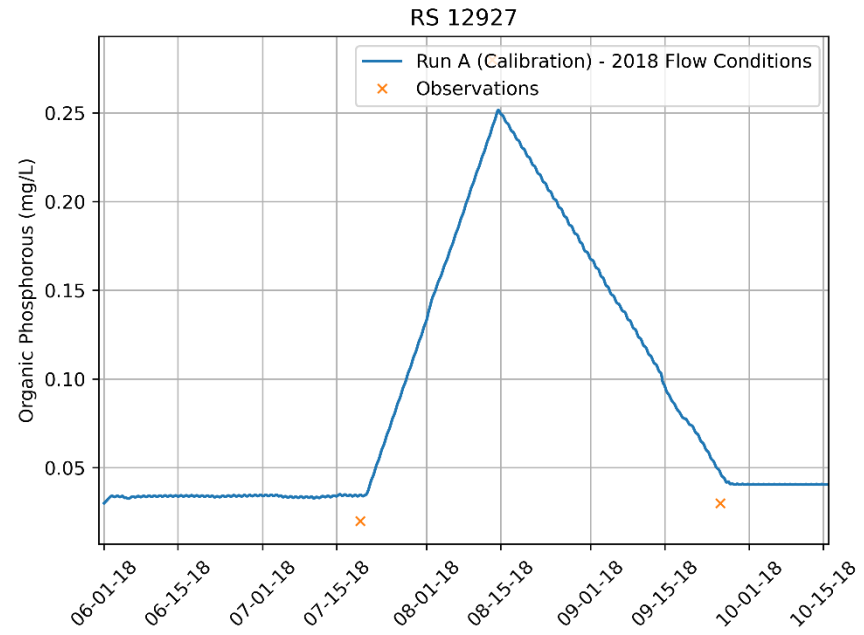
RS 12927
Run A (Calibration) - 2018 Flow Conditions
Observations
Organic Phosphorous (mg/L)
0.25
0.20
0.15
0.10
0.05
06-01-18
06-15-18
07-01-18
07-15-18
08-01-18
08-15-18
09-01-18
09-15-18
10-01-18
10-15-18

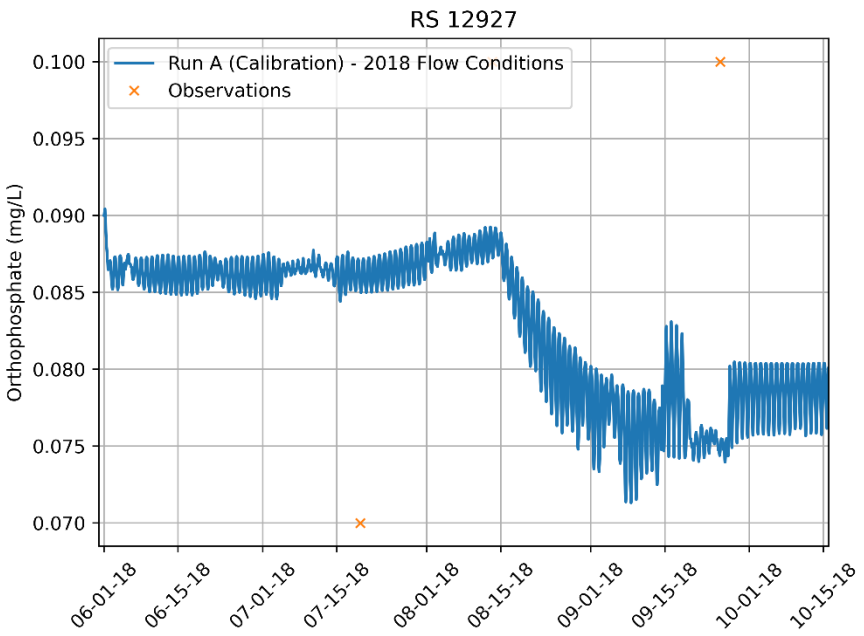
RS 12927
Run A (Calibration) - 2018 Flow Conditions
Observations
Orthophosphate (mg/L)
0.100
0.095
0.090
0.085
0.080
0.075
0.070
06-01-18
06-15-18
07-01-18
07-15-18
08-01-18
08-15-18
09-01-18
09-15-18
10-01-18
10-15-18